

**Characterization of the protein export steps at the
parasite-host cell interface of the human malaria
parasite *Plasmodium falciparum* (Welch, 1897)**

**Dissertation with the aim of achieving a doctoral degree at the
Faculty of Mathematics, Informatics and Natural Sciences**

**Department of Biology
of the University of Hamburg**

submitted by Paolo Mesén-Ramírez

2016

in Hamburg

Day of oral defense: June 10th, 2016

The following evaluators recommend the admission of the dissertation

Prof. Dr. Thorsten Burmester

Dr. Tobias Spielmann

Language certificate

I am a native speaker, have read the present PhD thesis and hereby confirm that it complies with the rules of the English language.

Hamburg, April 11 th, 2016

A handwritten signature in blue ink, appearing to read "Erica T. Lilleodden", written over a horizontal line.

Prof. Erica T. Lilleodden, Ph.D.

Declaration on oath

I hereby declare, on oath, that I have written the present dissertation by my own and have not used other than the acknowledged resources and aids.

A handwritten signature in blue ink, appearing to read 'Paolo Mesén-Ramírez', is written over a horizontal line. The signature is stylized and cursive.

Hamburg, April 11 th, 2016

Paolo Mesén-Ramírez

Summary

Malaria parasites develop within red blood cells (RBC) in a compartment termed parasitophorous vacuole (PV) surrounded by the PV membrane (PVM). To survive within this unique niche the parasites export a large repertoire of proteins into their host cell. These proteins are involved in nutrient uptake, cytoadherence and immune evasion. Protein export is hence crucial for the survival and virulence of intracellular *P. falciparum* blood stage parasites.

Different types of soluble and TM exported proteins with diverse localizations in the RBC have been identified in malaria parasites. All types of exported proteins need to cross the PVM to reach their final destination in the RBC and this step is dependent on unfolding and translocation by a protein complex at the PVM termed *Plasmodium* translocon or PEXEL proteins (PTX). However, up to now there is no demonstration of direct translocation by this complex and the identity of the protein-conducting channel through which polypeptides are threaded into the host cell remains unknown. It is also intriguing how the same type of protein translocons at the PVM mediates the passage of proteins with different export signals and structures. In contrast to soluble proteins, the export pathway for TM proteins is even more enigmatic. The succession of translocation events between the parasite plasma membrane (PPM) and the PVM for these proteins is still elusive and the individual translocation steps have not been demonstrated yet.

To address these questions, a conditional redox sensitive foldable domain termed BPTI was exploited in the present work to gain insights into the export of TM proteins beyond the PPM. Fused to exported proteins, this domain will become folded only in the oxidizing conditions of the PV. Using these constructs it was demonstrated that TM proteins require two unfolding dependent translocation steps to reach the host cell: they are first extracted out of the PPM, released transiently into the PV and further translocated at the PVM in an export step shared with soluble proteins. Depending on the length of the region between the TM domain and the C-terminally fused BPTI (spacer), these steps occurred in a different fashion, suggesting that in proteins with long spacers PPM and PVM translocation may be coupled whereas proteins with short spacers are transiently released into the PV before translocation at the PVM.

Moreover, fusion proteins containing a foldable domain named mDHFR were generated in this PhD thesis. This made possible to conditionally block export at the PVM or PPM by ligand-induced prevention of unfolding of the fusion domain and this was used to dissect the

trafficking events that exported proteins undergo in the parasite periphery. The corresponding fusion proteins revealed that all classes of exported proteins are dependent on unfolding to be exported and hence, translocation is a common mechanism of export in malaria parasites.

Among the newly generated mDHFR fusion proteins several showed a behavior differing from previously published constructs. These fusion proteins remained stably arrested in the translocon when their unfolding was prevented and this hampered the export of all other classes of exported proteins. This indicated that these constructs jammed a common type of translocons, an effect that was in this thesis termed a 'co-block'. The use of different constructs and the identification of their exact localization using protease protection assays in selectively lysed infected RBC indicated that the site of arrest of these intermediates was at the PVM. This indicated that all classes of exported proteins cross the PVM through a common type of protein-conducting channels to reach the host erythrocyte. Prompted by these results, these intermediates were also exploited to generate a global block of protein export which led to an arrest of parasite growth, demonstrating that protein export is essential for parasite development in the RBC.

Similarly to BPTI fusions, the length of the spacer in these constructs affected how they were translocated, and influenced their capacity to induce a co-block. Again, proteins with long spacers appeared to engage the PVM translocon and caused a co-block whereas proteins with a short spacer remained in the PPM and did not induce a co-block.

Furthermore, taking advantage of the stable translocation intermediates, the function of EXP2, the PTEX component proposed to be the membrane spanning pore at the PVM, was investigated using co-immunoprecipitation assays. These experiments revealed that substrates stuck in translocation, but not PPM arrested proteins, are in a complex with EXP2 at the PVM but not with the PTEX component HSP101. This provides evidence that EXP2 may be the protein-conducting channel through which exported proteins are delivered into the infected RBC. This supports a link between translocation activity and the PTEX component.

Taken together conditionally foldable domains enabled to investigate the transport processes across membranes at the parasite periphery in *P. falciparum* parasites. This study provides mechanistical insights into the series of trafficking events that take place at the parasite host-cell interface and reveals overlapping translocation steps for the different types of exported proteins.

Zusammenfassung

Plasmodium falciparum ist ein intrazellulärer Parasit, der die tödlichste Form der menschlichen Malaria verursacht. Die ungeschlechtlichen Blutstadien des Malariaerregers entwickeln sich innerhalb der roten Blutzellen (RBC) in einer parasitären Vakuole (PV), die von der PV-Membran (PVM) umgeben ist. Um innerhalb dieser einzigartigen Nische zu überleben, muss der Parasit ein großes Repertoire an Proteinen in seine Wirtszelle exportieren, um Nährstoffaufnahme, Zytoadhärenz und Immunevasion zu gewährleisten. Der Proteinexport ist daher von entscheidender Bedeutung für das Überleben und die Virulenz von intrazellulären *P. falciparum* Parasiten.

Verschiedene Arten von exportierten Proteinen mit unterschiedlichen subzellulären Lokalisierungen wurden in Malaria-Parasiten identifiziert. Alle exportierten Proteine scheinen zumindest teilweise einen gemeinsamen Exportweg zu haben. Transportierte Proteine müssen die PVM überwinden, um ihren endgültigen Bestimmungsort in der RBC zu erreichen. Dieser Schritt wird möglicherweise durch einen Proteinkomplex in der PVM, Plasmodium Translokon von PEXEL-Proteinen (PTEX) genannt, vermittelt. Dieser Komplex entfaltet die zu translozierenden Polypeptide für den Transport über die PVM. Allerdings gibt es bisher noch keinen Beweis, dass dieser Komplex wirklich Translokationsaktivität hat und die Identität des Kanals, durch den die Polypeptide in die Wirtszelle transportiert werden, ist unklar. Faszinierend ist, wie eine einzige Art von Translokon den Export löslicher und membranständiger Proteine mit unterschiedlichen Exportsignalen und Domain-Architekturen vermitteln kann. Im Vergleich zu löslichen Proteinen ist der Exportweg für die Membranproteine noch rätselhaft. Die Abfolge der Translokationsereignisse zwischen der PPM und der PVM ist zurzeit unklar und schwer zu erfassen und die einzelnen Translokationsschritte sind noch nicht nachgewiesen worden.

Um diese Fragen zu klären, wurden in dieser Dissertation Fusionsproteine erzeugt, die eine redox –sensitive, faltbare Domäne, BPTI genannt, enthalten. Fusioniert mit einem exportierten Protein faltet sich die Domäne nur unter den oxidierenden Umständen der parasitären Vakuole. Die Versuche mit diesen Fusionsproteinen zeigten, dass integrale Membranproteine zwei von der Entfaltung abhängige Schritte benötigen, um die Wirtszelle zu erreichen. Diese Proteine werden erst aus der PPM extrahiert (1. Schritt) und in die PV freigelassen, wo sie durch einen mit löslichen Proteinen gemeinsamen Schritt über die PVM transloziert werden (2. Schritt). Dieser Mechanismus ist abhängig von der Länge der Region

zwischen der TM Domäne und dem C-terminal fusionierten BPTI (Spacer genannt). Bei Proteinen mit einem langen Spacer scheinen die Translokationsschritte in der PPM und PVM gekoppelt zu sein, während Proteine mit kurzem Spacer zwischenzeitlich in die PV freigelassen werden.

Um konditionell den Export eines Proteins an der PVM oder der PPM zu blockieren, wurden Fusionsproteine hergestellt, die eine induzierbare, faltbare Domäne namens mDHFR enthalten. Die Fusionsdomäne wird hierbei an der Entfaltung gehindert, was die Translokation des mit der Domäne verbundenen exportierten Proteins an der Parasitenperipherie blockiert. Aus diesen Daten wurde geschlossen, dass alle Klassen der exportierten Proteine entfaltet werden müssen, um in die rote Blutzelle zu gelangen. Dies deutet darauf hin, dass Translokation ein gemeinsamer Mechanismus für den Export aller Klassen von Proteinen ist.

Zudem verhielten sich die untersuchten mDHFR Fusionsproteine wie stabile Translokationssubstrate, die während der Translokation aufgehalten werden. Dies verstopfte die Translokons und führte zu einer globalen Exportblockade aller Arten von exportierten Proteinen an der Parasitenperipherie, ein Effekt, der hier 'Co-block' genannt wird. Verschiedene Konstrukte und Protease Protection Assays mit selektiv permeabilisierten infizierten RBC deuteten drauf hin, dass die Translokationssubstrate ein Translokon an der PVM verstopfen. Dies zeigte erstens, dass alle Proteinklassen beim Transport in die Wirtszelle beim Exportschritt über die PVM am gleichen Typ Kanal konvergieren. Zweitens konnte dadurch die Wichtigkeit des Protein-Exports für die Entwicklung des Parasiten gezeigt werden, da eine globale Exportblockade die Parasitenentwicklung hemmte. Ähnlich wie bei den BPTI Fusionsproteinen beeinflusste die Länge des Spacers, wie integrale Membranproteine transloziert werden und in der Folge ihre Fähigkeit, einen Co-block zu verursachen. Proteine mit langem Spacer erreichen und verstopfen das PVM Translokon, während Proteine mit kurzem Spacer in der PPM verbleiben und keinen Co-block verursachen.

Darüber hinaus wurde die Funktion von EXP2, einer PTEX-Komponente, die als die Membran-durchspannende Pore in der PVM angenommen wird, untersucht. Die Ergebnisse zeigten, dass Substrate, die in dem Translokon in der PVM stecken geblieben waren, in einem Komplex mit EXP2 sind. Dies liefert einen Hinweis darauf, dass EXP2 Teil des Protein-leitenden Kanals sein könnte, durch den die Proteine in die infizierte RBC exportiert werden. Dies unterstützt eine Verbindung zwischen Translokationsaktivität und dieser PTEX-Komponente.

Zusammengefasst ermöglichen konditionell faltbare Domänen, die Transportprozesse durch die Membranen in der Parasitenperipherie bei *P. falciparum* zu untersuchen. Diese Studie liefert Einblicke in eine Reihe von Transportereignissen, die sich an der Parasiten-Wirtszellen-Grenze bei den verschiedenen Arten von exportierten Proteinen abspielen und beschreibt überschneidende Translokationswege für alle Klassen von exportierten Proteinen, einschliesslich löslicher Proteine und integraler Transmembranproteine.

Table of contents

LANGUAGE CERTIFICATE	FEHLER! TEXTMARKE NICHT DEFINIERT.
SUMMARY	IV
ZUSAMMENFASSUNG	VI
LIST OF FIGURES.....	X
ABBREVIATIONS.....	XII
CHAPTER 1. INTRODUCTION.....	7
1.1 MALARIA.....	7
1.1.1 <i>The causative agent: taxonomy and description of human infecting species</i>	7
1.1.2 <i>Epidemiology: Distribution and prevalence</i>	9
1.1.3 <i>Clinical disease</i>	11
1.1.4 <i>Malaria pathogenesis</i>	12
1.1.5 <i>Malaria control</i>	13
1.2 PLASMODIUM BIOLOGY.....	18
1.2.1 <i>The life cycle of Plasmodium parasites</i>	18
1.2.2 <i>Parasite organelles</i>	25
1.2.3 <i>Host cell modifications</i>	31
1.3 PROTEIN EXPORT IN MALARIA PARASITES	36
1.3.1 <i>Export signals: PEXEL proteins and PNEPs</i>	36
1.3.2 <i>Current model of export for soluble and TM proteins in P. falciparum</i>	39
1.3.3 <i>Plasmodium Translocon of Exported Proteins (PTEX)</i>	41
1.4 PROTEIN TRANSLOCATION ACROSS MEMBRANES	44
1.4.1 <i>General mechanisms of protein translocation</i>	44
1.4.2 <i>Approaches to study protein translocation</i>	46
1.5 AIMS OF THIS PHD THESIS.....	48
CHAPTER 2. MATERIALS.....	49
2.1 TECHNICAL DEVICES	49
2.2 CHEMICALS	51
2.3 LAB WARE AND DISPOSABLES	53
2.4 KITS.....	54
2.5 DNA- UND PROTEIN LADDERS	54
2.6 SOLUTIONS, MEDIA AND BUFFERS.....	55
2.6.1 <i>Media, buffers and other solutions for microbiologic culture</i>	55
2.6.2 <i>Solutions and buffers for molecular biology analyses</i>	56
2.6.3 <i>Media and solutions for parasite culture and cell biology experiments</i>	57

2.6.4	<i>Buffers and solutions for protein analyses</i>	60
2.7	ENZYMES	61
2.8	ANTIBODIES	62
2.8.1	<i>Primary antibodies</i>	62
2.8.2	<i>Secondary antibodies</i>	63
2.8.3	<i>Antibody coupled beads</i>	63
2.9	OLIGONUCLEOTIDES	64
2.10	PLASMIDS	65
2.11	COMPUTER SOFTWARE	66
2.12	BIOINFORMATIC TOOLS AND DATA BASES	66
CHAPTER 3. METHODS		67
3.1	MOLECULAR BIOLOGY METHODS	67
3.1.1	<i>Polymerase chain reaction (PCR)</i>	67
3.1.2	<i>Purification of PCR products and digested vectors</i>	68
3.1.3	<i>Digestion of PCR products and vectors</i>	68
3.1.4	<i>DNA ligation</i>	68
3.1.5	<i>Screening PCR to detect bacterial clones</i>	68
3.1.6	<i>PCR to verify genome integration</i>	69
3.1.7	<i>Sequencing of plasmids</i>	70
3.1.8	<i>Agarose gel electrophoresis</i>	70
3.1.9	<i>DNA precipitation</i>	71
3.1.10	<i>Isolation of genomic <i>P. falciparum</i> DNA</i>	71
3.2	MICROBIOLOGICAL METHODS	71
3.2.1	<i>Rubidium chloride method for preparation of chemo-competent bacterial cells</i>	71
3.2.2	<i>Transformation of <i>E.coli</i> chemo competent cells</i>	71
3.2.3	<i>Cultivation and storage of <i>E. coli</i> transgenic cells</i>	72
3.2.4	<i>Plasmid purification (Mini Prep and Midi Prep)</i>	72
3.3	CELL BIOLOGICAL METHODS	72
3.3.1	<i>Culture of <i>P. falciparum</i></i>	72
3.3.2	<i>Blood smears, Giemsa staining and determination of parasitemia</i>	73
3.3.3	<i>Freezing and thawing of asexual <i>P. falciparum</i> parasites</i>	73
3.3.4	<i>Sorbitol method for synchronization of <i>P. falciparum</i> infected RBCs</i>	73
3.3.5	<i>Differential purification of <i>P. falciparum</i> infected erythrocytes in a Percoll gradient</i>	74
3.3.6	<i>Transfection of <i>P. falciparum</i> ring stages by electroporation</i>	74
3.3.7	<i>Transfection of <i>P. falciparum</i> merozoites</i>	74
3.3.8	<i>Export arrest assays by ligand (WR) induced prevention of unfolding in parasites expressing mDHFR fusion proteins</i>	75
3.3.9	<i>Saponin lysis for selective permeabilization of <i>P. falciparum</i> infected RBCs</i>	75
3.3.10	<i>Tetanolysin lysis</i>	76
3.3.11	<i>Proteinase K assay</i>	76

3.3.12	<i>Reversible Cross-Link Immuno-Precipitation (ReCLIP) for Mass spectrometry analyses</i>	77
3.3.13	<i>Co-immunoprecipitation assays to identify interaction between proteins.....</i>	79
3.4	BIOCHEMICAL METHODS	80
3.4.1	<i>SDS-polyacrylamide gel electrophoresis (SDS-PAGE)</i>	80
3.4.2	<i>Western blot analysis</i>	80
3.4.3	<i>Silver staining</i>	81
3.5	MICROSCOPY	81
3.5.1	<i>Live cell imaging.....</i>	81
3.5.2	<i>Immunofluorescence assays (IFAs) with acetone fixed iRBCs.....</i>	81
CHAPTER 4. RESULTS.....		82
4.1	DISSECTION OF THE TRANSLOCATION PATHWAY FOR TM PROTEINS IN THE PARASITE PERIPHERY	82
4.1.1	<i>Approaches to characterize translocation of TM proteins at the parasite periphery</i>	82
4.1.2	<i>Redox sensitive folding as an approach to characterize translocation</i>	87
4.1.3	<i>TM proteins are extracted out of the PPM and undergo translocation at the PVM.....</i>	88
4.1.4	<i>Redox sensitive folding arrest is dependent on the distance between TM domain and fused BPTI.....</i>	90
4.1.5	<i>PEXEL TM proteins are translocated in a similar two-step process</i>	92
4.2	TRANSLOCATION INTERMEDIATES ARREST GLOBAL PROTEIN EXPORT IN <i>P. FALCIPARUM</i> BY JAMMING A SHARED TRANSLOCON AT THE PVM	94
4.2.1	<i>PNEP TM –mDHFR constructs co-block export of an exported control protein without mDHFR domain.....</i>	94
4.2.2	<i>The stable translocation intermediates are arrested in the PV</i>	97
4.2.3	<i>Stable translocation substrates co-block export of all types of exported proteins</i>	100
4.2.4	<i>A soluble PEXEL protein can block export of TM proteins.....</i>	104
4.2.5	<i>Co-blocking properties of a TM mDHFR construct are related to the length of the region between the TM and the mDHFR domain.....</i>	106
4.3	PARASITE GROWTH IS DEPENDENT ON PROTEIN EXPORT.....	108
4.4	INSIGHTS INTO A ROLE OF EXP2 IN PROTEIN EXPORT.	111
4.4.1	<i>Tagging of endogenous EXP2 and identification of interacting partners</i>	112
4.4.2	<i>Translocation intermediates stuck in translocation at the PVM are in a complex with EXP2</i>	116
4.4.3	<i>PPM arrested mDHFR constructs do not interact with EXP2</i>	122
CHAPTER 5. DISCUSSION		124
5.1	MAJOR FINDINGS	125
5.1.1	<i>Translocation pathway for TM proteins at the parasite periphery</i>	125
5.1.2	<i>Evidence of translocation based export for other TM proteins.....</i>	133
5.1.3	<i>Exported proteins are translocated through the same type of protein-conducting channels at the PVM</i>	134
5.1.4	<i>Essentiality of protein export on parasite development.....</i>	139

5.1.5	<i>Conditionally arrested substrates link PTEX with translocation activity</i>	141
5.1.6	<i>Conclusions</i>	144
REFERENCES		146
ACKNOWLEDGEMENTS		164
LIST OF PUBLICATIONS AND MANUSCRIPTS		164
APPENDIX 1 TABLE S1. CLONING STRATEGIES FOR CONSTRUCTS IN THIS STUDY		165
APPENDIX 2		167

List of figures

Introduction

FIGURE 1. 1 GEOGRAPHICAL DISTRIBUTION OF MALARIA.....	10
FIGURE 1. 2 THE LIFE CYCLE OF <i>PLASMODIUM</i> PARASITES.....	19
FIGURE 1. 3 INVASION EVENTS DURING ERYTHROCYTIC DEVELOPMENT.....	22
FIGURE 1. 4 <i>PLASMODIUM</i> ERYTHROCYTIC DEVELOPMENT.....	23
FIGURE 1. 5 ORGANELLES AND INTRACELLULAR SECRETORY TRANSPORT IN <i>P. FALCIPARUM</i> BLOOD STAGES.	26
FIGURE 1. 6 HOST CELL MODIFICATIONS INDUCED BY <i>P. FALCIPARUM</i> IN IRBCS .	35
FIGURE 1. 7 CURRENT MODEL OF EXPORT PATHWAY IN <i>P. FALCIPARUM</i>	42
FIGURE 1. 8 <i>PLASMODIUM</i> TRANSLOCON OF EXPORTED PROTEINS (PTEX).....	43

Results

FIGURE 4. 1 MDHFR CONSTRUCTS ARE ARRESTED IRREVERSIBLY IN THE PARASITE PERIPHERY.....	85
FIGURE 4. 2 N-TERMINAL FUSIONS OF FOLDABLE DOMAINS.	86
FIGURE 4. 3 FUSION WITH BPTI BLOCKS PROTEIN EXPORT IN THE PV BY REDOX SENSITIVE FOLDING.	88
FIGURE 4. 4 TM PROTEINS ARE TRANSLOCATED IN A TWO STEP PROCESS AT THE PARASITE PERIPHERY.	89
FIGURE 4. 5 THE EXPORT OF THE TM PNEPS SBP1 AND MAHRP1 IS INSENSITIVE TO FUSION WITH BPTI..	90
FIGURE 4. 6 LENGTH OF THE C-TERMINUS OF EXPORTED TM PROTEINS INFLUENCES REDOX SENSITIVE EXPORT ARREST.	91
FIGURE 4. 7 IN THE PARASITE PERIPHERY PEXEL TM PROTEINS ARE TRANSPORTED IN A TWO -STEP TRANSLOCATION PROCESS INTO THE HOST CELL.....	93
FIGURE 4. 8 MDHFR FUSIONS JAM A SHARED TRANSLOCON AND CO-BLOCK THE EXPORT OF OTHER PROTEINS.....	95
FIGURE 4. 9 THE EXPORT BLOCK OF THE REX2MCHERRY CONTROL DEPENDS ON THE EXPRESSION OF THE MDHFR FUSION PROTEIN.....	96
FIGURE 4. 10 SBP1-MDHFR-GFP CONSTRUCTS ARE ARRESTED IN THE PV (A).....	98
FIGURE 4. 11 SBP1-MDHFR-GFP CONSTRUCTS ARE ARRESTED IN THE PV.	99
FIGURE 4. 12 DIFFERENTS TYPES OF EXPORTED PROTEINS PASS THROUGH THE SAME TPE OF TRANSLOCONS.	101
FIGURE 4. 13 SKIP PEPTIDE (2A) ENABLES EFFICIENT POLYCISTRONIC EXPRESSION COMPARABLE TO DOUBLE TRANSFECTION..	102
FIGURE 4. 14 ENDOGENOUS EXPORTED PROTEINS ARE CO-BLOCKED BY MDHFR TRANSLOCATION INTERMEDIATES.	103
FIGURE 4. 15 PEXEL PROTEINS CAN BLOCK THE EXPORT OF A PNEP TM PROTEIN	105
FIGURE 4. 16 LENGTH OF THE SPACER DETERMINES THE CAPACITY OF A MDHFR TM CONSTRUCT TO INDUCE A CO-BLOCK.....	107

FIGURE 4. 17 ENDOGENOUS TAGGING OF SBP1 WITH MDHFR-GFP.....	109
FIGURE 4. 18 ENDOGENOUS SBP1-MDHFR-GFP AS AN APPROACH TO INDUCE GLOBAL EXPORT ARREST IN <i>P. FALCIPARUM</i>	110
FIGURE 4. 19 PAN-EXPORT BLOCK DELAYS PARASITE GROWTH AND ARRESTS PARASITES AS YOUNG TROPHOZOITES.	111
FIGURE 4. 20 ENDOGENOUS TAGGING OF EXP2 IN <i>P. FALCIPARUM</i>	113
FIGURE 4. 21 ENDOGENOUS FLUORESCENT TAGGING OF EXP2 IN <i>P. FALCIPARUM</i>	114
FIGURE 4. 22 RECLIP OF ENDOGENOUS EXP2 PURIFIES KNOWN PTEX COMPONENTS AND POTENTIAL FURTHER INTERACTING PARTNERS.....	116
FIGURE 4. 23 MDHFR INTERMEDIATES ARRESTED IN TRANSLOCATION CO-LOCALIZED WITH EXP2.	117
FIGURE 4. 24 MDHFR INTERMEDIATES ARRESTED IN TRANSLOCATION ARE IN A COMPLEX WITH EXP2. ...	118
FIGURE 4. 25 ENDOGENOUS TAGGING OF HSP101 IN <i>P. FALCIPARUM</i>	120
FIGURE 4. 26 MDHFR INTERMEDIATES ARRESTED IN TRANSLOCATION ARE NOT IN DIRECT CONTACT WITH HSP101.	121
FIGURE 4. 27 ONLY CO-BLOCKING MDHFR INTERMEDIATES ARRESTED IN TRANSLOCATION ARE IN A COMPLEX WITH EXP2..	123

Discussion

FIGURE 5. 1 MODEL OF TRANSLOCATION EVENTS FOR EXPORTED PROTEINS AT THE PARASITE HOST-CELL INTERFACE.	126
FIGURE 5. 2 MODEL OF TRANSLOCATION FOR TM PROTEINS AT THE PARASITE PERIPHERY BASED ON BPTI REDOX SENSITIVE FOLDING.....	131
FIGURE 5. 3 MODEL OF CO-BLOCK INDUCED BY ARRESTED MDHFR TM INTERMEDIATES AT THE PARASITE PERIPHERY.....	138

Abbreviations

3D	Three-dimensional
ACT	Artemisinin combination therapy
AMA	Apical Membrane Antigen
ATP	Adenosine triphosphate
bp	Base pairs
BPTI	Bovine pancreatic trypsin inhibitor
C-	Carboxy
Co-IP	Co-immunoprecipitation
CRT	Chloroquine Resistance Transporter
CSP	Circumsporozoite Surface Protein
DAPI	4'6-Diamino-2-phenylindol
DDT	Dichlordiphenyltrichlorethan
DIC	Differential interference contrast
DMSO	Dimethylsulfoxide
DNA	Desoxyribonucleicacid
DSP	Dithiobis [succinimidyl propionate
DTT	Dithiotreitol
EBA	Erythrocyte binding antigen
EM	Electron microscopy
ER	Endoplasmic Reticulum
et al.	et alii
ETRAMP	Early transcribed membrane protein
EXP 1-2	Exported protein 1-2
GAP	Genetically attenuated sporozoites
GAPDH	Glyceraldehyde-3-phosphate dehydrogenase
GFP	Green Fluorescent Protein
GPI	Glycosylphosphatidylinositol
HBsAg	Hepatitis B surface antigen
HC	Host cell
hDHFR	Human Dihydrofolate Reductase
HRP	Histidine rich protein or Horse radish peroxidase
HSP	heat shock protein
HT	Host targeting

IFA	Immunofluorescence assay
IMC	Inner membrane complex
IP(ed)	Immunoprecipitation (Immunoprecipitated)
IPP	Isopentenyl pyrophosphate
iRBC	infected red blood cell
LSA	Liver stage Antigen
MAHRP	Membrane Associated Histidine Rich Protein
MC	Maurer's clefts
mDHFR	Murine (Mouse) Dihydrofolate Reductase
mRNA	Messenger ribonucleic acid
MSP	Merozoite Surface Protein
N-	Amino-
OD	Optical density
PAGE	Polyacrylamide gel electrophoresis
PBS	Phosphate buffer solution
PCR	Polymerase chain reaction
PEXEL	Plasmodium export element
PfEMP1	<i>Plasmodium falciparum</i> erythrocyte membrane protein 1
PHIST	<i>Plasmodium</i> helical interspersed subtelomeric
PI3P	Phosphatidylinositol 3-phosphate
PM5 (PMV)	Plasmepsin V
PNEP	PEXEL negative exported protein
PPM	Parasite plasma membrane
PTEX	Plasmodium Translocon for exported proteins
PTP1	PfEMP1 trafficking protein 1
PV	Parasitophorous vacuole
PVM	Parasitophorous vacuole membrane

RBC	Red blood cell
ReCLIP	Reversible cross linking immunoprecipitation
REX	Ring exported protein
Rh	Reticulocyte Binding Protein Homologues
RON	Rhoptry neck protein
RPMI	Roswell Park Memorial Institute
SBP	Skeleton Binding Protein
SDS	Sodium dodecylsulfate
SERA	Serine repeat antigen
SERP	Serine Rich Protein
SP	Signal peptide
STEVOR	Subtelomeric variable open reading frame
TCA	Trichloroaceticacid
TM (D)	Transmembrane (Domain)
T3SS	Type III Secretion systems
TVN	Tubo-vesicular network
WHO	World Health Organization
WPC	Whole parasite-based vaccine
Wt	Wild type

Chapter 1. Introduction

1.1 Malaria

Malaria is a vector borne tropical disease caused by apicomplexan protozoan parasites of the genus *Plasmodium*. Clinical syndromes suggestive of malaria have been recorded since antiquity in Rome and Greece as well as by the 15th century in Europe (Bruce-Chwatt and de Zulueta, 1988; Sherman, 1998). However, the causative agent was only identified in 1880 when Alphonse Charles Laveran described microscopically the parasites for the first time in the blood of soldiers in Algeria suffering a febrile disease considered to be caused by 'bad air' (mala aria in Italian). Laveran observed black granules of pigment and mobile filaments emerging from a spherical body (Laveran, 1880) in fresh blood of patients with intermittent fever. His drawings demonstrated that he had seen all stages of *P. falciparum* (Sherman, 1998). Years later it was demonstrated that these parasites were transmitted by *Anopheles* mosquitoes (Ross and Grassi, 1898).

Currently malaria is endemic in tropical and sub-tropical countries. Numerous intervention strategies and extensive research on parasite biology have contributed to considerably reduce the number of reported malaria cases and associated deaths; nevertheless the disease continues to be a huge socio-economical burden in developing countries in terms of mortality, morbidity and economic consequences. The climatic change, the emergence of parasite and mosquitoes resistance against available antimalarial drugs and insecticides and population movements hamper the efforts to control and eradicate the disease.

1.1.1 The causative agent: taxonomy and description of human infecting species

The phylum Apicomplexa comprises unicellular obligate parasites whose invasive motile stages possess an evolutionarily unique apical complex (Morrison, 2008) that enables parasite to actively invade the host cell. This phylum, together with ciliates and dinoflagellates, belongs to the Chromoalveolata (Alveolata), free-living and parasitic organisms that share the presence of flattened membranous vesicles (termed alveoli) that underlie the plasma membrane (Kono et al., 2012). Dinoflagellates and all apicomplexans except for *Cryptosporidium* (Keeling et al., 2010) contain a plastid which derived from a process of secondary endosymbiosis, in which a heterotrophic eukaryote engulfed a red photosynthetic alga (Adl et al., 2005; Keeling, 2008, Janouskovec et al., 2010). Apicomplexan parasites are subdivided into coccidians, gregarines, haemosporidian and

piroplasmides (Morrison, 2008; Adl et al., 2012). Most Apicomplexans are pathogens of animals and humans with medical and veterinary importance and might be unifyingly defined by the hallmarks of obligate parasitism and the capacity for gliding motility (Templeton and Pain, 2016).

The genus *Plasmodium* belongs to the Haemosporidia (Danilewsky 1885) and *Plasmodium* species infect a wide range of different reptile, bird and mammalian species (Zilversmit & Hartl, 2005). The life cycle of *Plasmodium* parasites switches between a vertebrate host where the parasite undergoes asexual replication and an invertebrate host where the sexual development and sexual mating takes place (See 1.2.1 for cycle). Different species of female *Anopheles* mosquitoes are the only known definitive host and vector in nature.

Only five *Plasmodium* species are known to infect humans: *Plasmodium falciparum*, *P. vivax*, *P. ovale*, *P. malariae* and *P. knowlesi*. The different species show differences in morphology, in their life cycle, the clinical outcomes, their geographical distribution and vector species. In contrast to the first four species *P. knowlesi* is the first and only described zoonotic *Plasmodium* specie which infects naturally macaque monkey species (Singh et al., 2004).

Plasmodium falciparum (Welch, 1987) is the specie that causes the most severe form of human malaria. The parasite causes what sometimes is referred to as ‘malaria tropica’ in which fever attacks show no periodicity (Bartoloni and Zammarchi, 2012). The ability of this species to induce cytoadhesion and sequestration of the infected erythrocyte distinguishes it from other species (Greenwood et al., 2008) and is a main contributor to the exceptional virulence of this species (See Section 1.1.4).

Plasmodium vivax (Grassi and Feletti, 1890) is the second specie in terms of importance. It has a wider geographical distribution than *P. falciparum* as it can also be found in temperate regions (Greenwood et al., 2008). This specie infects reticulocytes and the clinical disease is termed malaria tertiana due to the periodicity of febril episodes every 48 hours which coincides with the synchronous rupture of the schizont during the blood development. *P. vivax* and *P. ovale* are the unique human species that form hypnozoites, dormant hepatic stages able to relapse at three weeks intervals or in temperate countries after 8–10 months between primary infection and first relapse (White et al., 2011). Despite the lack of RBC sequestration and lower parasite biomass compared to *P. falciparum*, *P. vivax* is now considered to be cause of several and fatal malaria (Anstey et al., 2009).

Plasmodium ovale (Stephens, 1922) share similarities with *P. vivax* in terms of biology. Both species cause malaria tertian, infect only reticulocytes and relapses can occur from hypnozoites latent parasites in the liver (Collins and Jeffery, 2005).

Plasmodium malariae (Grassi and Feletti, 1890) causes the quartan malaria due to its 72-hour developmental cycle in red blood cells and there is no evidence for hypnozoites in the liver (Collins and Jeffery, 2007), although it is believed to be able to persist as blood stage forms that can lead to relapses up to 50 years after initial infection. The severity of the disease is mild and the parasitemias are low compared to other species and cronical asymptomatic infections have been described in untreated patients (Collins et al., 1989; Vinetz et al., 1998).

Plasmodium knowlesi is found in nature in long-tailed and pig-tailed macaques (Singh and Daneshvar, 2013). First human cases were diagnosed in 2004 (Singh et al., 2004) and it was likely before misdiagnosed as *P. malariae*. *P. knowlesi* infection shows daily (quotidian) fever episodes, coinciding with its 24-hour erythrocytic cycle. Most cases of knowlesi malaria respond to treatment, however, complicated and fatal cases have been reported (Singh & Daneshvar, 2013). The vectors are forest-dwelling mosquitoes that belong to the *Anopheles leucosphyrus* group and *A. latens* (Tan et al., 2008) and *A. balacensis* (Collins et al., 1971) and appear to be involved in monkey-to-human, human-to-human and human-to-monkey transmission.

1.1.2 Epidemiology: Distribution and prevalence

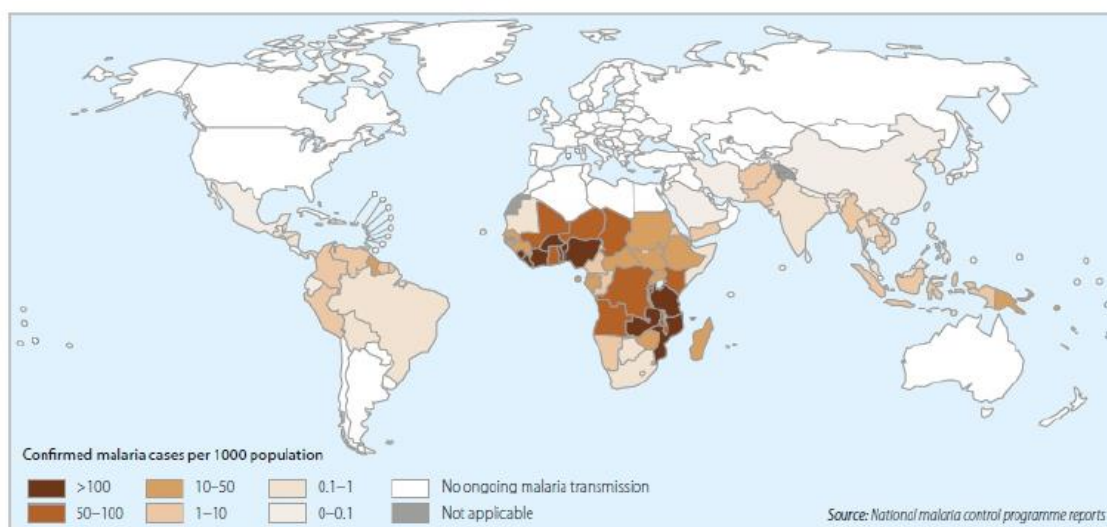
It is estimated that globally around 3.3 billion people are at risk of being infected with malaria of which 1.2 billion are at high risk. According to the most recent WHO Malaria Report, 214 million malaria cases were reported in 2015 (WHO, 2015). Most cases in 2015 were registered in African (88%), followed by South-East Asia (10%) and the Eastern Mediterranean Region (2%). A recent study estimated a decline of malaria cases in Africa by 40% from 321 per 1,000 persons per annum in 2000 to 192 per 1,000 persons in 2015 (Bhatt et al., 2015) (Figure 1.1). Thirty three countries are estimated to have achieved the milestone of fewer than 1000 cases in 2015 and 16 endemic countries reported zero indigenous cases (WHO, 2015). In 2015, 438 000 deaths were reported of which 90% occurred in sub-Saharan Africa, principally in children under five years of age (White et al., 2014; WHO, 2015). In areas of stable endemic transmission about 25% of all-cause mortality in children aged 0 to 4 years has been attributed directly to malaria (Sachs & Malaney, 2002).

The transmission of the disease is restricted to tropical and subtropical countries. Malaria parasites cease development in the mosquito at temperatures below 16 °C, and many anopheline species suspend biting activity at low temperatures, reducing the stability of malaria transmission in temperate regions (Sachs & Malaney, 2002). *P. vivax* can develop in the anophelin vector at lower environmental temperatures than *P. falciparum* and hence can

survive in cooler climates and at higher altitudes; this explains its broader distribution. (Greenwood et al., 2008; WHO, 2014)

Transmission intensity affects all aspects of malaria epidemiology such as incidence, community prevalence, age-profile of infection, type of disease syndrome and total malaria mortality (Ghething et al., 2011; Hay et al., 2008). This intensity varies geographically in endemic countries since it is influenced by factors like temperature, rainfall and humidity (Guerra et al., 2008).

A



B

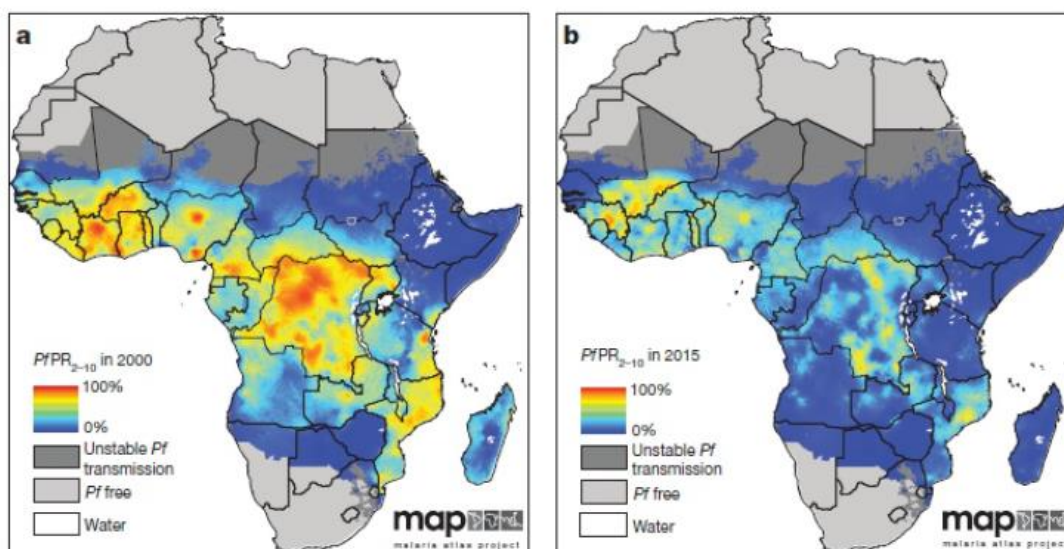


Figure 1. 1 | Geographical distribution of malaria (A) Countries worldwide with ongoing malaria transmission in 2014. Number of cases is indicated as a continuum of brown colors. Dark brown depicts countries with a higher number of confirmed cases. World Health Organization, World Malaria Report 2014 **(B)** Changes in *P. falciparum* prevalence in African countries from 2000 to 2015. The reduction in the number of cases is indicated from 2000 (a) to 2015 (b). Gray zones depict *P. falciparum* free areas and blue zones areas with a low prevalence. Red zones depict areas with the highest prevalence. Modified from Bhatt et al., 2015.

Plasmodium falciparum is the specie that causes around 80% of all malaria infections and the one responsible of the vast majority of deaths (Greenwood et al., 2008). *P. falciparum* causes 98% of the malaria infections in African countries and 65 % of the infections in tropical countries outside Africa. While *P. falciparum* is mainly endemic in Africa, it is largely hypoendemic outside African countries (Guerra et al., 2008).

In Asia, Oceania, Central and South America and the horn of Africa *P. vivax* malaria is the major cause of morbidity (White, 2011). Due the absence of the Duffy blood group antigen (a receptor required for *P. vivax* invasion) in most of the African populations, the endemic areas of *P. vivax* coincide with those of *P. falciparum* only in tropical countries outside of Africa. In most of Asia and South and Central America, where transmission is mainly low and seasonal, *P. falciparum* and *P. vivax* malaria have roughly equal prevalences (Gething et al., 2010). *P. vivax* is more difficult to control and eliminate than *P. falciparum* because of its tendency to relapse after resolution of the primary infection, resulting in an important source of malaria transmission (White, 2011). *P. ovale*, the other species causing tertian malaria, is naturally distributed in sub-Saharan Africa and islands of the western Pacific (Lysenko and Bejaev, 1969; Collins and Jeffery, 2005) but the specie has been also introduced in Southeast Asia.

P. malariae is widespread throughout sub-Saharan Africa, much of Southeast Asia, into Indonesia, and on many islands of the western Pacific. The endemicity of *P. malariae* coincides in general with that of *P. falciparum* and mixed infections are frequent (Collins and Jeffery, 2007). This species was prevalent in a recent past in Europe and in southern parts of the United States.

Human infections with *P. knowlesi* are rare but transmission has been reported in all the countries in Southeast Asia except Laos. Most of the human knowlesi malaria cases have been detected in Sarawak and Sabah, Malaysian Borneo (Singh & Daneshvar, 2013).

1.1.3 Clinical disease

Malaria is a febril, often disabling and life-threatening syndrome that results from the asexual replication of *Plasmodium* parasites within the red blood cells (RBCs). The intracellular replication in liver cells and the sexual development (gametocytes) in RBCs are clinically silent (Schofield and Grau, 2005; Sherman, 1998).

The incubation period of the disease is on average 12-14 days (White, 2014) in *P. falciparum*, *P. vivax* and *P. ovale* infections. In *P. malariae* the incubation period can take 16-59 days (Collins and Jeffery, 2007). First symptoms are non-specific and similar between all malaria species. Fever is one of the key features (Bartoloni and Zammarchi, 2012). Other typical symptoms include nausea, chills, vomiting, malaise, headache, muscle aches and sweating. No combination of symptoms distinguishes malaria from other causes of fever (WHO, 2015). Splenomegaly and hepatomegaly may be present and hematological alterations may include anemia, thrombocytopenia and leucopenia (reviewed in Bartoloni and Zammarchi, 2012). The severity of the clinical manifestations depends on the infecting species, patient age, immunity status and intercurrent infections (Miller et al., 2002; Hunt et al., 2006).

P. falciparum causes the severest clinical outcomes, leading to the complications of cerebral malaria, placental malaria, hypoglycaemia, metabolic acidosis and respiratory distress and severe anemia (Miller et al., 2002). Severe anaemia, hypoglycemia and cerebral malaria are more common in children, whereas acute pulmonary edema, acute kidney injury, and jaundice are more common in adults (White, 2014). The symptoms of cerebral malaria range from confusion or stupor to obtundation and deep coma (Medana and Turner, 2006). *P. falciparum* infection during pregnancy leads to complications such as maternal anemia, low birth weight and premature labor (Desai et al., 2007).

1.1.4 Malaria pathogenesis

Malaria disease results from a combination of pathophysiological processes which are a direct outcome of parasite multiplication and development within the erythrocytes, parasite induced RBC alterations, microcirculatory abnormalities and local and systemic immune reactions (Buffet et al., 2011). In contrast the initial hepatic phase of parasite development is asymptomatic since only few hepatocytes are infected (Bartoloni and Zammarchi, 2012).

The development of the parasite in erythrocytes leads to a destruction of infected RBCs (iRBCs) as new invasive parasite stages egress. This causes hemolysis and the release of parasite antigens such as polymerised hemoglobin degradation products (hemozoin) and other bioactive molecules such as glycosylphosphatidylinositol (GPI) which stimulates a proinflammatory reaction characterized by the release of Th-1 type cytokines like TNF, IFN- γ , IL-1, IL-6 and IL-12 (Sherry et al., 1995; Naik et al., 2000; Schofield and Grau, 2005). This cytokine profile is involved in the characteristic signs and symptoms of the febrile attacks typical for malaria. As a result of the massive destruction of iRBCs the hematocrit may

decline, resulting in mild to severe anemia which is also aggravated by an increased spleen clearance and accelerated destruction of uninfected cells (Buffet et al., 2011). Both *P. falciparum* and *P. vivax* can cause severe anaemia, but only *P. falciparum* causes the many complications of severe malaria (Miller et al., 2002).

One of the main differences between *P. falciparum* and other human malaria species is its ability to induce cytoadherence of the infected RBC (Miller et al., 2002). In contrast to unparasitized RBC, *P. falciparum* iRBC are poorly deformable, highly rigid, and display the propensity to adhere to vascular endothelial cells (Barnwell, 1989). This leads to the sequestration of iRBCs in capillaries to avoid circulation in peripheral blood (Maier et al., 2009). This is essential to the survival of later stage parasite as the iRBCs otherwise would be recognised and cleared in the spleen. Adhesion of iRBCs to each other (auto-agglutination), host leukocytes or platelets or to uninfected red cells (rosetting) (Dumbo et al., 2009) may also lead to microaggregates that are less able to pass through the microcirculation (Rogerson et al., 2004). The sequestration of iRBCs in small vessels in various organs including heart, lung, brain, liver, kidney, subcutaneous tissues and placenta is one of the main contributors to the development of a severe malaria syndrome.

iRBCs sequestered in small blood vessels injure endothelial cells, cause obstruction and interfere with microcirculatory flow, metabolism and the functioning of vascular endothelium, leading to a impaired perfusion of the involved organs, tissue hypoxia and lactic acidosis (Miller et al., 2013). The pathogenesis of cerebral malaria is a complex combination of pathological events in the brain (reviewed in Hunt et al., 2006). Sequestration causes damage of the microvascular endothelium (Combes et al., 2010; Ponsford et al., 2012), leading to an increase of the permeability of the blood brain barrier. CD8 T-cell mediated damage leads to leakage of cytokines, malaria antigens and harmful molecules across the blood brain barrier to the cerebral parenchyma (Hunt et al., 2006), contributing to cerebral edema and axonal injury (Medana and Turner, 2006). Cytokine-driven changes in the brain metabolism as well as the vascular obstruction- induced local reduction of oxygen consumption also play central roles in the pathology of cerebral malaria (Hunt et al., 2003; Ponsford et al., 2012).

1.1.5 Malaria control

1.1.5.1 Treatment and available drugs

Malaria control requires an integrated approach that includes prevention (vector control) and prompt treatment of patients with effective antimalarial agents (WHO, 2015). Malaria treatments have the goal to reduce parasite burden, disease complications and deaths,

serve as profilaxis, eliminate latent hepatic stages and kill gametocytes to block transmission (Delves et al. 2012).

The discovery and development of different antimalarial compounds that target essential processes in different stages of the parasite life cycle has contributed to a significant reduction in the number of cases and a better management of infected patients. The most important antimalarial compounds currently recommended for the treatment of malaria are quinine and its derivatives, artemisine derivatives and antifolates. Due the capacity of the parasite to become resistant to available drugs combination therapies are today recommended and there is a constant need for new antimalarial drugs (Miller et al., 2013).

Quinoline-containing antimalarial drugs are alkaloids extracted from the cinchona tree (Folley and Tilley, 1998) and are the first-line therapy for uncomplicated malaria for *P. vivax*, *P. ovale*, *P. malariae* and *P. knowlesi* (WHO, 2015). Most of the quinine derivatives (4-aminoquinolines) exert their action at trophozoite and schizont stages (Delves et al., 2012) through interference with the heme metabolism and its detoxification (the polymerization of the heme group into hematin crystal leading to hemozoin formation) in the food vacuole. The heme group is toxic for the parasite, causing membrane damage and cell lysis (Folley and Tilley, 1998; Miller et al., 2013; Pulcini et al., 2015). In contrast to many other drugs, the 8-aminoquinolines (primaquine) are active on the relapse causing “hypnozoite” liver forms of *P. vivax* (Campo et al., 2015). The use of these drugs in *P. falciparum* control has been hampered by the emergence and spread of resistance in most of the strains circulating in African countries. *P. falciparum* parasites developed resistance to most of the quinine derivatives due a mutations in the chloroquine resistance transporter (Pfcr) a protein localized in the food vacuole membrane that allows the efflux of the the drug from the food vacuole and its accumulation (Fidock et al., 2000; Ecker et al., 2012; Pulcini et al., 2015).

The second group of compounds are folate inhibitors (sulfonamides and pyrimethamine), compounds that mimic the folate molecule and inhibit enzymes of the *de novo* folate pathway in the parasite, namely the dihydrofolate reductase (DHFR) and dihydropteroate synthase (DHPS). This results in decreased levels of tetrahydrofolate, a necessary cofactor in important one-carbon transfer reactions in the purine, pyrimidine, and amino acid biosynthetic pathways (Olliaro, 2001; Gregson & Plowe, 2005). These drugs are active against all growing stages of the asexual erythrocytic cycle and on young gametocytes; their toxic effect reaches a peak in the late erythrocytic schizont stage, precisely when DNA synthesis peaks (Olliaro, 2001; Gregson and Plowe, 2005; Delves et al., 2012). Resistance to DHFR and DHPS inhibitors is conferred by single point mutations of the gene encoding for the respective enzyme (Gregson and Plowe, 2005; Nzila, 2006).

Since the emergence of resistance to almost all quinolone and antifolate drugs, successful treatment of *P. falciparum* uncomplicated malaria is now highly dependent on artemisinin-based combination therapies (ACT) (Müller and Hyde, 2010; Petersen et al., 2011). ACTs are recommended by the WHO as first –line therapy against falciparum malaria in all areas in which malaria is endemic. ACTs combine artemisinin derivatives with a slow clearing partner drug with different mechanism of action to prevent or delay the spread of drug resistance (WHO, 2015). Artemisinin is isolated from the *Artemisia annua* plant (Chinese wormwood) and has been used in China to treat fevers for many centuries. The active compound is a sesquiterpene lactone with an endoperoxide bridge and its semi-synthetic derivatives (artemether, artesunate, and dihydroartemisinin) are used clinically. The principal advantage of using artemisinins rather than other antimalarial drugs is that they have a very high parasite clearance rate and also show a notable gametocytocidal activity (Dondorp et al., 2009). In addition, the drugs display a short plasma half-life which reduces the risk for resistance to develop. The mechanism of action of artemisinin drugs is not fully understood (Petersen et al., 2011; Wang et al., 2016), but the prevailing theory is that the endoperoxide bridge of the artemisinin derivatives is cleaved or activated by parasite derived heme, leading to the formation of reactive carbon radicals that subsequently trigger oxidative stress and promiscuously damage cellular macromolecules, including parasite membrane components, proteins, and neutral lipids (Bray et al., 2005; Straimer et al., 2015, Wang et al., 2016).

Despite its favourable pharmacokinetic properties, the efficacy of ACT and artesunate monotherapy has declined in Southeast Asia (Cambodia, Thailand, Vietnam, and Myanmar) (Dondorp et al., 2009; Phyo et al., 2012) and the emergence of *P. falciparum* resistance to artemisinin derivatives threatens the world's malaria control and elimination efforts. Artemisinin resistance is associated with mutations in the gene coding for a Kelch propeller domain protein. The normal function of this protein is still unknown and how the effect of various mutations might protect parasites from the lethal effects of artemisinin-induced oxidative damage remains elusive (Ariey et al., 2014; Straimer et al., 2015).

Antibiotics like doxycyclin can be used by travelers for malaria prophylaxis and in conjunction with other drugs are effective for treatment of uncomplicated malaria (Tan et al., 2011). There are also further drugs in the pipeline, for instance new antimalarials termed spiroindolones with a new mechanism of action based on the inhibition of the PfATP4 have shown efficacy in treatment of falciparum and vivax malaria, including patients with artemisinin-resistant *P. falciparum* infection (Rottmann et al., 2010; Spillman et al., 2013; White et al., 2014b). The WHO recommends adherence to full treatment course and the administration of combination therapies (such as ACTs) to reduce the risk of developing resistance. Ideally, new drug

combinations should contain drugs against asexual blood stages and transmission-blocking components (WHO, 2015).

1.1.5.2 Vector control

Vector control through indoor residual spraying (IRS) and insecticide treated nets (ITN) is one of the most effective measures to prevent malaria transmission. At least 12 different insecticides have been widely used in the control of malaria transmitting mosquitoes in the last decades, including dichlorodiphenyltrichloroethane (DDT) and pyrethroids (WHO, 2011; van den Berg, 2009). The disease was eliminated in the US through a campaign that included residual household spraying of DDT (Zucker et al., 1996)

Due the persistence of DDT in the environment and its effect on human health and wildlife, the use of this molecule has been strongly debated. It is nevertheless still used for IRS in many developing countries (Turusov et al., 2002; van den Berg, 2009). Synthetic pyrethroids are potent, broad-spectrum insecticides that in contrast to DDT show rapid dissipation and degradation (Maund et al., 2012). Pyrethroids act rapidly and have both a repellent and a killing function. They are relatively safe for use in close proximity to humans and are easy to formulate and relatively cheap to produce (Hemingway, 2014). Their use for ITN have had the largest effect in the reduction of infection prevalence and case incidence, reducing malaria deaths by a third (Bhatt et al., 2015).

Since the introduction of DDT for mosquito control in 1946, DDT resistance has been reported in anopheline mosquitoes wide spread (Hemingway and Ranson, 2000). Resistance to pyrethroids is now widespread in both *An. gambiae* and *An. funestus* and currently no African country has fully pyrethroid susceptible malaria vectors (Ranson et al., 2011; Hemingway, 2014). DDT and pyrethroids have a common mode of action, binding to the sodium channels in the insect neuronal cell membranes causing repetitive paralysis and eventual death of the insect (Davies et al., 2007). Mutations on the sodium channel confer cross resistance and insects with these alleles withstand prolonged exposure to insecticides (Ranson et al., 2011). Another mechanism described is the overexpression of cytochrome 450 enzymes (Djouaka et al., 2008) or glutathione N-transferases (Kostaropoulos et al., 2001) which favours detoxification of both chemicals.

1.1.5.3 Malaria vaccine approaches

In spite of extensive research and many clinical trials, there is up to now no effective commercial vaccine against malaria. The presence of multiple parasite stages across the complex life cycle, the evasion of the immune system, parasite polymorphisms and antigenic diversity have hindered the development of a vaccine. The difficulty faced for a malaria

vaccine is reflected in the fact that no sterile immune response exists in humans even after multiple natural infections.

Different approaches to achieve a vaccine have been attempted such as the induction of antigen specific protective antibodies or T cells that could act against the sporozoite and/or liver stages (pre-erythrocytic stages), against the asexual erythrocytic stages or the sexual erythrocytic and mosquito stages. Vaccine strategies focus on reducing the morbidity and mortality by reducing the rate at which individuals become infected and/or reducing asexual erythrocytic stage multiplication. Some are aimed to reduce or prevent transmission to mosquitoes, the so-called transmission blocking vaccines (TBV) (Alonso et al., 2011; Hoffman et al., 2015)

One of the most promising candidates for a vaccine is the RTS,S. This vaccine targets the Pf circumsporozoite protein (CSP), a protein displayed on the sporozoite surface expressed by early liver forms and involved in the initial invasion of hepatocytes (Coppi et al., 2011). The RTS,S vaccine consist of the amino acids 207–395 of CSP fused to the hepatitis B surface antigen (HBsAg) as carrier matrix. A multicenter phase III trial conducted from 2009 to 2012 in African children revealed a 56 % reduction in acquisition of clinical malaria and a 47 % reduction of progression into severe malaria 12 months after the vaccination (RTS,S Clinical Trials Partnership 2012). During 4 years of follow-up, RTS,S/AS01E was associated with 29.9% and 16.8% efficacy against first and all episodes of *P. falciparum* clinical malaria and efficacy declined over time and with increasing malaria exposure (Olotu et al., 2014). RTS,S/AS01 prevented a substantial number of cases of clinical malaria over a 3-4 year period in young infants and children when administered with or without a booster dose (RTS,S Clinical Trials Partnership, 2015). While this vaccine is now brought forward for commercial use, its efficacy still falls short of other commercially available vaccines. As the first vaccine effective against a human parasite it is nevertheless considered a milestone.

Another approach tested for vaccination is the use of attenuated whole parasites (sporozoite challenge model) to induce a highly effective pre-erythrocytic immunity. Volunteers immunized by exposure to the bites of mosquitoes carrying radiation attenuated *P. falciparum* sporozoites (RAS) were effectively protected from malaria infection (Clyde et al., 1973). Mice immunized with RAS showed also a high-grade protection (Nussenzweig et al., 1967). Protection induced by RAS appears to be based primarily on the induction of T cell responses but antibodies responses were also detected.

Based on these findings, SANARIA® developed an injectable product composed of radiation attenuated, aseptic, purified and cryopreserved sporozoites that can be safely administered intravenously (Seder et al., 2013) and high-level protection can be achieved by four to six

doses. Challenges regarding the manufacture, delivery, administration and long-term immunogenicity with such a vaccine are still debated (Richie et al., 2015).

Genetically attenuated sporozoites (GAS) are a second alternative for the sporozoite challenge model. GAS are made out of parasites that harbour genetic deletions that arrest parasite development during hepatocyte infection (Müller et al., 2005; Van Buskirk et al., 2009; Spring et al., 2013). Sanaria® generated recently the vaccine PfSPZ-GA1 which consists of purified, aseptic, cryopreserved *P. falciparum* sporozoites genetically attenuated by removal of the b9 and slarp genes that are required for liver development (van Schaijk et al., 2014). It is intended to move into clinical trials in 2016.

A third approach for pre-erythrocytic vaccine development is the attempt to induce high protective cellular and humoral immunity using subunit vaccine platforms. Heterologous prime boost with DNA encoding a selected pre-erythrocytic stage protein or recombinant viral vectors (Richie et al., 2012; Ewer et al., 2013; Sedegah et al., 2014) have been tested using different parasite protein combinations with the aim to stimulate cellular responses. However, to date no effective protection has been demonstrated with this type of vaccine (Hoffman et al., 2015).

Transmission-blocking vaccines (TBV) target sexual erythrocytic and early mosquito stage antigens as the parasite passes from a human host to the mosquito. Efforts are now focused on establishing vaccines delivered to humans that can induce functional antibodies that reduce mosquito infections, for example targeting gametocyte proteins such as Pfs25 (Malkin et al., 2005; Jones et al., 2013). Used in combination with vector control measures TBVs could play a key role in finally breaking the transmission of malaria parasites and leading to eradication of the disease (Greenwood et al., 2008). However, for ethical reasons, such a vaccine can only be administered together with a second component providing a benefit for the vaccinated individual.

1.2 *Plasmodium* Biology

1.2.1 The life cycle of *Plasmodium* parasites

Plasmodium species have a complex life cycle where extracellular and intracellular parasite stages switch between a definitive invertebrate host (female *Anopheles* mosquitoes) and an intermediary host (humans) (Figure 1.2). During a blood meal the *Anopheles* female inoculates infective parasite stages termed 'sporozoites' into the dermis of the human host. The sporozoites reach the hepatocytes via the blood stream and invade the hepatic cells to

initiate the clinically silent exo-erythrocytic schizogony, where the parasite replicates asexually, generating thousands of 'merozoites' (see section 1.2.1.1). The merozoites are released into the blood stream in membraneous sacs termed merozoites. After rupture of the merozoite the merozoites actively invade erythrocytes, beginning the erythrocytic asexual development (see section 1.2.1.2). During this phase parasites develop and replicate within RBC and release up to 32 new merozoites which invade new RBCs, forming the basis for the continued multiplication in the host. Some of these merozoites are committed to develop into male or female gametocytes, sexual precursor stages that will be taken up by mosquitoes during a blood meal (see section 1.2.1.3). After reaching the mosquito midgut, fertilization takes place and the resulting zygote develops into a motile ookinete which undergoes meiosis followed by the generation of hundreds of sporozoites. The sporozoites migrate to and penetrate into the salivary glands of the mosquito from where they can be further transmitted to humans with the next blood meal.

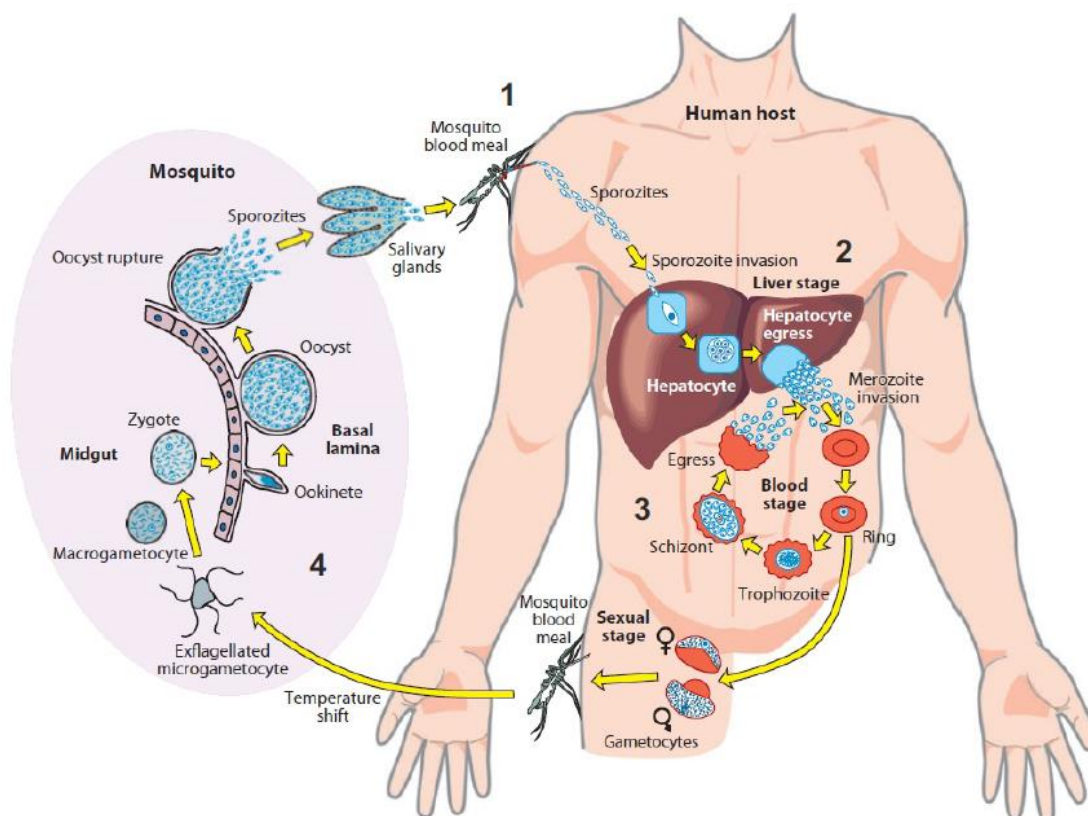


Figure 1. 2 | The life cycle of *Plasmodium* parasites (1) Sporozoites are inoculated during the blood meal of female *Anopheles* mosquito starting the infection. (2) Exoerythrocytic schizogony. Liver stage development ending in release of thousands of merozoites packed in merozoites. (3) Erythrocytic schizogony. Parasites develop from the ring, via the trophozoite, to the schizont stage. Some parasites develop into sexual forms and are taken up during a blood meal. (4) Sexual development in the *Anopheles* mosquito. Fertilization generates motile ookinetes that penetrate the midgut epithelium and develop into oocysts on the basal lamina. Oocysts rupture releases thousands of sporozoites that migrate to salivary glands to be further transmitted to the next host.

1.2.1.1 Parasite development in the liver

On average 100 infective sporozoites are inoculated into the human dermis by infected anophelines (Jin et al., 2007). Once in the skin, sporozoites display random motility (Amino et al., 2006) and once they reach a small blood vessel, penetrate it and are carried away in the blood stream (Ejigiri and Sinnis, 2009). Sporozoites can migrate through cells, a process required for their exit from the dermis and to penetrate cell barriers in the liver (Amino et al. 2008) since there sporozoites first need to cross the sinusoidal barrier to access the hepatocytes. Heparin sulfate proteoglycan expressed on hepatocytes activates sporozoites to an invasive mode (Coppi et al., 2007) and the CSP mediates this first interaction (Rathore et al., 2002). Activated sporozoites migrate through hepatocytes (transmigration) (Mota et al., 2002) and initially traverse cells inside non-replicative transient vacuoles. Sporozoites use pH sensing and a perforin –like protein 1 (PLP1) to exit these vacuoles and finally invade a hepatocyte where they establish a replication competent parasitophorous vacuole (PV) (Risco-Castillo et al., 2015). Surrounded by the PVM, the parasite replicates asexually generating a hepatic schizont that contains thousands of merozoites. During this step *Plasmodium* parasites are able to interfere with central mechanisms of the infected hepatocyte, such as protein synthesis or the expression of genes involved in inflammation (Singh et al., 2007). Membranous structures such as the liver stage tubovesicular network (TVN) have been characterized and parasite proteins may be exported to the host hepatocyte (reviewed in Ingmundson, 2014), although so far only two proteins have been shown to localize to the cytosol of *P. berghei* infected hepatocytes: circumsporozoite protein (CSP) (Singh et al., 2007) and liver-stage specific protein 2 (LISP2) (Orito et al., 2013). A recent study in *P. berghei* showed that indeed proteins exported to the erythrocyte were not translocated into the host hepatocytes and essential components for protein export were absent from the PV in liver stages. It suggests hence that the role of protein export may differ between liver and RBC development (Kalanon et al., 2016).

In *P. falciparum* after 5-7 days (Prudencio et al., 2008) the first-generation merozoites are released from the hepatocytes into the blood vessel as merozoites (Sturm et al., 2006), which represent packets of hundreds of parasites surrounded by host cell membrane. Each infected cell releases multiple merozoites and this step ensures both the migration of parasites into the bloodstream and their protection from host immunity (Sturm et al., 2006; Baer et al., 2007; Vaughan et al., 2012).

P. vivax and *P. ovale* show to some extent a different life cycle since some sporozoites do not develop immediately into schizonts, but remain as uninucleate hypnozoites (Galinski et al., 2013). These stages ensure parasite survival in periods of poor transmission and as such

have to be taken into account for eradication efforts and hence are currently the target of intense research efforts (Hulden and Hulden, 2011).

1.2.1.2 Invasion and blood stage development

After rupture of the merozoite in the circulation, the first -generation merozoites invade RBCs in a highly coordinated process. Merozoites are small non-motile stages that make the initial contact to the host RBC via interaction between proteins located on their surface and erythrocyte receptors. A prominent example for a parasite protein involved in this phase is the merozoite surface protein 1 (MSP1) (Holder, 1988; Blackman et al., 1990; Lin et al., 2014). After this initial contact, the merozoite re-orientates its apical end towards the RBC membrane (See Figure 1.3) and apical organelles, termed micronemes, rhoptries and dense granules (See Section 1.2.2.3) discharge their content, providing proteins to assist invasion. Two protein families termed adhesins, the erythrocyte binding-antigens (EBA) and reticulocyte binding-like homologues (PfRh), which localize to the micronemes and rhoptries respectively, stabilize the initial contact through interaction with erythrocyte receptors (Sim et al., 1992; Rayner et al., 2000; Triglia et al., 2001; Cowman et al., 2012). These adhesins display phenotypical variation which allows the parasite to invade using alternative host receptors. In *P. falciparum*, most members of the EBA proteins interact with erythrocyte glycoprotein proteins, such as EBA175 to glycoprotein (GP) A or EBA140 to GPC (sialic-acid-dependent invasion). PfRh4 binds to complement receptor 1 (Tham et al., 2010) and PfRH5 binds basigin on the RBC surface (Crosnier et al., 2011) (sialic acid independent pathway). These interactions appear to induce changes in the erythrocyte cytoskeleton and trigger the further release of proteins from the apical organelles and downstream invasion events.

Next a set of rhoptry neck proteins (the RON complex) is secreted and inserted into the erythrocyte together with the micronemal Apical Membrane Antigen 1 (AMA1) (See Section 1.2.2.3) to form an electron dense area of close apposition between both cells termed the tight or moving junction (reviewed in Besteiro et al., 2011). The tight junction has been suggested to act as the bridging molecular link binding the parasite surface and both its motor complex and the host cell.

Merozoites possess an actin-myosin motor which provides the force that drives invasion (Baum et al., 2006). The junction moves rearwards along the parasite driven by substrate-dependent gliding which is powered by the actin-myosin motor. The merozoite pushes itself into the host cell and also potentially induces local clearing of cytoskeletal elements and RBC membrane wrapping (Dasgupta et al., 2014). The rhoptries secrete lipids and proteins to establish the parasitophorous vacuole membrane (PVM) together with material from the invaginated RBC membrane. The nascent PVM fuse to seal the invasion process and the

PVM surrounds the parasite in a parasitophorous vacuole (PV) (Reviewed in Cowman et al., 2012; Koch and Baum, 2016)

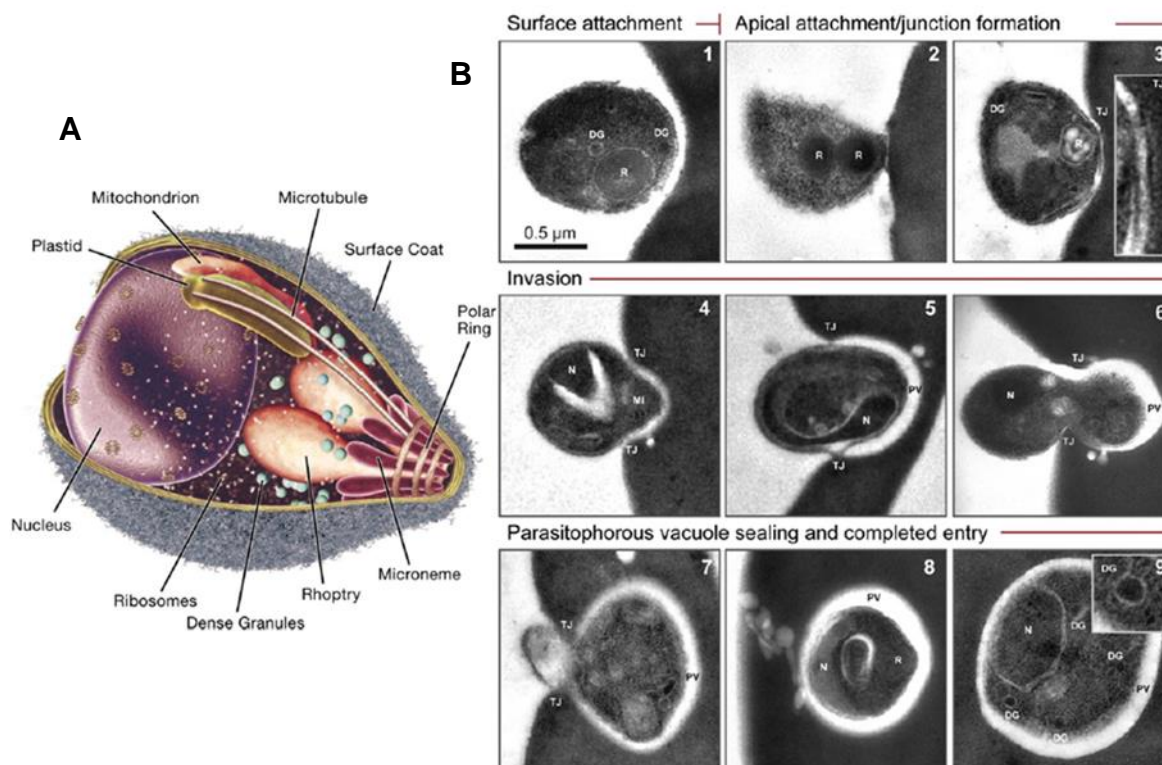


Figure 1. 3 | Invasion events during erythrocytic development (A) Diagram of a *Plasmodium* merozoite highlighting secretory organelles and cellular structures involved in invasion. Modified from Crabb and Cowman, 2006. **(B)** Transmission electron microscopy images showing the steps of invasion of a RBC by merozoites. Modified from Riglar et al., 2011.

Once within the PV, the parasite progresses for 48 hours through different morphological and physiological stages, culminating in the rupture of the host cell and release of new invasive merozoites (See Figure 1.4). Immediately after invasion, the infecting merozoite turns into the so-called ‘ring stage’, a low metabolically active stage, that is mobile in the host cell and shows dynamic changes in shape, switching between amoeboid and disc-shaped forms (Grüning et al. 2011). During the ring stage expression of parasite proteins exported into the host cell peaks (Marti et al., 2004) and it is assumed that this phase is a slow growth “lag” phase (0-18 h.p.i) during which the parasite creates a suitable niche for growth and establishes numerous host cell modifications required for survival of later stages (Spielmann et al., 2006). Membranous vesicular structures termed Maurer’s clefts are by electron microscopy detected in the iRBC from the late ring stage onwards (Bannister et al., 2004) but recent studies show that they appear early (1,5-3 h.p.i) after invasion (Grüning et al., 2011; McMillan et al., 2013).

The trophozoite stage takes around 14 hours, from approximately 18 to 36 hours post invasion. In this phase the parasite grows steadily, occupying a half or two thirds of the iRBC

imaged over 32 hours starting with a late ring stage (12-16 hours post- invasion). The appearance of hemozoin (black pigment inside the parasite) marks the transition to trophozoite and further hemozoin accumulates during the trophozoite and schizont stage. The schizont stage occupies almost the entire RBC and during egress releases infective merozoites able to infect adjacent blood cells (new infection indicated by white arrow). The size bar indicates 2 μm . **(B)** Development of *P. falciparum* in human RBCs (modified from Maier et al., 2009). Schematic representation of the different stages across the erythrocytic development and parasite –induced host cell modifications.

Around 36 hours post invasion the parasite turns into a so called ‘schizont’. In this phase the new merozoites are formed by a process termed schizogony (repeated mitosis without cell division to create a syncytium followed by fission of the daughter cells). The mitotic nuclear division begins in the late trophozoite stage. The parasite undergoes three to four rounds of DNA synthesis, mitosis and nuclear division to produce a syncytial schizont with 8 to 32 new nuclei. *P. falciparum* mitosis differs from the traditional mitosis known from other organisms. *P. falciparum* chromosomes do not appear to condense during mitosis and the nuclear membrane divides into separate daughter genomes while the cell does not divide until several cycles of mitosis have produced a multinuclear cell (Gerald et al., 2011). Mitochondria and apicoplast are also replicated (Van Dooren et al., 2005) and the apical complex required for invasion is established in every single daughter merozoite.

Merozoites exit from their enclosing PVM and erythrocyte membrane in a highly regulated calcium dependent event called egress where cysteine proteases are involved (Salmon et al., 2001; Glushakova et al., 2013; Withers-Martinez et al., 2014; Das et al., 2015). Daughter merozoites are released in circulation and immediately invade new RBCs, initiating the next round of blood-stage development.

1.2.1.3 Sexual blood stages and development in the mosquito

During the asexual blood stage cycle a fraction of parasites differentiates into male or female gametocytes. Commitment to sexual development occurs prior to schizogony, when all merozoites within a mature schizont will either differentiate into gametocytes or continue asexual development (Bruce et al., 1990; Josling and Llinàs, 2015). All merozoites derived from a committed schizont become either male or female gametocytes (Smith et al., 2000). Once that gametocytogenesis has been triggered, subsequent gametocyte development in *P. falciparum* lasts approximately 8–12 days (Sinden, 2009) and is divided into five stages (I–V) that can be distinguished microscopically and by molecular markers (Pradel, 2007).

Macrogametocytes and microgametocytes are ingested by the female *Anopheles* during a blood meal. The drop in temperature in the arthropod, the pH change and the presence of xanthurenic acid (Billker et al., 1997; Billker et al., 1998) in the mosquito midgut signal the maturation into gametes. During this process, gametocytes are released out of the RBC and

female gametocytes are ready for fertilization. In contrast male gametocytes undergo rapidly three rounds of DNA replication, leading to eight nuclei. In addition, eight flagelles are assembled and male gametes are released in a process termed exflagellation. Fertilization takes place in the midgut where haploid male gametes fuse with female gametes, resulting in a diploid zygote (Sinden, 2009; Josling and Llinás, 2015). The parasite immediately returns to a haploid organization by meiotic recombination (Sinden et al., 1985) and the resulting motile ookinete traverses the midgut epithelial cell wall to reach the extracellular space between the midgut epithelium and the basal lamina. The ookinete transforms into an oocyst and undergoes mitotic divisions over a period of 9–20 days to form 2000–8000 sporozoites (Sinden, 2009). Sporozoites are finally released and migrate through the haemocoel to the salivary glands, from where they are delivered to the next human host.

1.2.2 Parasite organelles

As eukaryote protozoa like *Plasmodium* harbour most of the typical eukaryotic organelles. All parasite stages are assumed to contain an endoplasmic reticulum (ER), a mitochondrion and an unusual unstacked Golgi (Bannister et al., 2000; Van Dooren et al., 2005, Struck et al., 2005). Eukaryotic organelles like the peroxisomes are absent in *Plasmodium* (Schlüter et al., 2006). The complex life cycle involving transmission between different hosts by specialised cell-invasive stages (Blackman and Bannister, 2001) and its intracellular growth impose a serie of challenges to the parasite which has led to the evolution of specialized unique organelles, most of them shared only with other apicomplexan parasites. These include the apicoplast, the inner membrane complex (IMC), the food vacuole and the apical complex and its constitutive secretory organelles, rhoptries, micronemes and dense granules.

1.2.2.1 Basic eukaryotic organelles in *Plasmodium* parasites

The endoplasmic reticulum (ER) and the molecular organization of the secretory pathway have been only partially characterized in *Plasmodium*. The ER appears in young blood stages as a perinuclear envelope with two protrusions or horn –like extensions followed by transformation into a more reticulated network as the parasite grows (Van Dooren et al., 2005; Struck et al., 2005) (Figure 1.5). A ‘classical’ secretory pathway is thought to be present in the parasite as a number of trafficking components homologous to other eukaryotes have been identified (reviewed in Deponte et al., 2012). The *P. falciparum* ER has a Sec61 translocation complex and a signal peptidase complex (Couffin et al., 1998; Sharma et al., 2005) and many proteins involved in vesicle budding, docking and fusion (Adisa et al., 2002; Ayong et al., 2007) have also been characterized.

Proteins destined for the extracellular environment or for secretory organelles are translocated into the ER prior to being delivered by transport vesicles to downstream compartments. In eukaryotic cells, vesicle budding and transport of proteins from the ER membrane to the cis-side of the Golgi complex occurs at specialized ER sub-domains devoid of ribosomes known as transitional ER (tER) and is mediated by a complex of cytoplasmic coat proteins, termed the COPII coat (Bonifacino and Glick, 2004; Lee and Miller, 2007; Lee et al., 2008, Struck et al., 2008). Five core proteins comprise this coat: the small GTPase Sar1 that regulates coat recruitment, the Sec23/Sec24 heterodimer that selects cargo proteins for capture into a nascent vesicle, and the Sec13/Sec31 heterotetramer drives the formation of a spherical vesicle. Homologues for each of these components are present in the *Plasmodium* genome and have been localized to the ER (Adisa et al., 2007; Lee et al., 2008, Struck et al., 2008; Deponete et al., 2012).

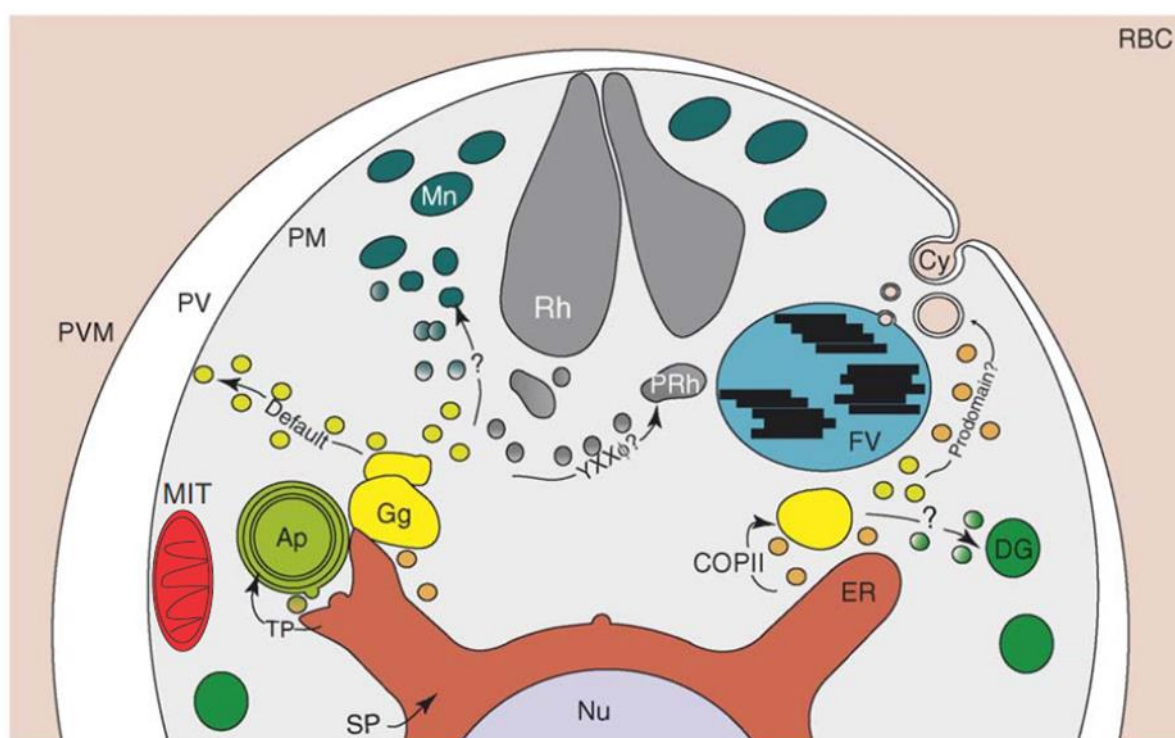


Figure 1. 5 | Organelles and intracellular secretory transport in *P. falciparum* blood stages. The parasite (gray) resides in the PV (white) separated from the RBC cytoplasm (pink) by the PVM. The parasite ER (red) is a simple perinuclear structure (nucleus in blue) with so-called horns protruding from each side. Most secreted proteins require a signal peptide (SP) in order to enter the ER. The Golgi complex (Gg) (yellow) seems to be in a simple unstacked conformation. The apicoplast (light green) has four membranes, and nuclear encoded proteins require a SP and transit peptide (TP) for correct targeting. Haemoglobin is endocytosed by the cytostome (Cy) and trafficked to the food vacuole FV (aqua) in vesicles (orange). FV haemoglobin proteases traffic through the secretory pathway and there is evidence for direct transport to the cytostome (orange vesicles) and through the PV (yellow vesicles). Apical organelles involved in RBC invasion are also synthesised de novo by the secretory pathway. Rhoptries (Rh; grey), micronemes (Mn; dark green) and dense granules (DG; light green). MIT; Mitochondrion. Modified from Tonkin et al., 2006

A typically stacked Golgi apparatus has not been identified in *P. falciparum*, but only a discoid rudimentary cisterna close to the nucleus described as a minimal Golgi apparatus. (Bannister et al. 2000, Bannister, 2004; Struck et al., 2005). This cisterna appears to receive vesicles from the nuclear envelope and generates vesicles that are directed towards the secretory organelles. The *P. falciparum* cis-Golgi is marked by the peripheral membrane protein Golgi re-assembly stacking protein (PfGRASP), which lies in close proximity to the ER marker BiP (Struck et al., 2005). On the trans-face of the Golgi, transport vesicles bud off and traffic their cargo to their final destination. Rab6 has been implicated in the regulation of vesicular intra- and trans-Golgi trafficking and is commonly accepted as a trans-Golgi marker in *P. falciparum* (De Castro et al. 1996; Ward et al., 1997; Struck et al., 2008). The absence of elaborate Golgi stacks in *P. falciparum* might result from a secondary loss of this feature. Since the parasite appears to have a minimal capacity for protein glycosylation, a complex Golgi apparatus seems to be unnecessary (Lee et al., 2008, Dacks et al., 2003).

The mitochondrion in *P. falciparum* appears as a dynamic single crescent-shaped organelle in merozoites that branches out in trophozoites and segregates along with the nucleus and the apicoplast into daughter merozoites in late schizont stage parasites. Contact points between the apicoplast and mitochondrion occur at all times during the erythrocytic life cycle (Van Dooren et al., 2005). In contrast to other eukaryotic cells the mitochondrion in *P. falciparum* blood stages is not a source of ATP. Erythrocytic stages of *P. falciparum* appear to maintain an active mitochondrial electron transport chain only for one metabolic function: regeneration of ubiquinone required as the electron acceptor for dihydroorotate dehydrogenase, an essential enzyme for pyrimidine biosynthesis (Painter et al., 2007). The mitochondrial genome of *Plasmodium* is the smallest known (about 6 kb), encodes no tRNAs and encodes only three proteins (Gardner et al., 2002; Vaidya and Mather, 2009) and all other mitochondrial proteins are nuclear encoded and imported after their synthesis at cytosolic ribosomes (Deponte et al., 2012).

1.2.2.2 The apicoplast

In common with most of apicomplexan parasites, all stages of *P. falciparum* harbor a complex plastid termed apicoplast which evolved through the endosymbiotic uptake of a photosynthetic red alga by a heterotrophic protist (Janouskovec et al. 2010; van Dooren and Striepen, 2013). The apicoplast is surrounded by four membranes and during the course of evolution has lost its ability to perform photosynthesis. In young blood stages, the apicoplast is generally rounded and elongated in shape. During early schizogony the apicoplast elongates, begins to branch and undergoes a process of division and segregation

ensuring that each merozoite obtains an organelle. Like the mitochondrion the apicoplast cannot be generated *de novo* and must be inherited at each cell division (Van Dooren et al., 2005).

The majority of the genes originally encoded by the plastid genome were transferred to the parasite nucleus and consequently apicoplast proteins need to be post-translationally imported to the plastid across the four membranes (Spork et al., 2009; Heiny et al., 2014). Approximately 5%–10% of the *Plasmodium* genome is predicted to encode apicoplast-targeted gene products (Ralph et al., 2004). Protein trafficking to the plastid depends on a bipartite leader peptide which mediates co-translational import into the ER and delivery to the apicoplast. Translocons spanning successive membranes were proposed to act in the further transport of proteins into the stroma of the apicoplast (Agrawal et al., 2013).

Due the prokaryotic origin of the organelle and the presence of essential pathways for the asexual liver and blood development (including the biosynthesis of fatty acids, isoprenoids, haem and iron–sulfur clusters (Ralph et al., 2004; Seeber and Soldati-Favre, 2010), the apicoplast is a potential target for new antimalarials. Nevertheless, the only essential function of the apicoplast during blood-stage growth is the isoprenoid precursor biosynthesis, as parasites that lost the organelle after treatment with antibiotics were able to grow when they were supplemented with isopentenyl pyrophosphate (IPP) (Yeh and DeRisi, 2011).

1.2.2.3 The apical complex

Apicomplexan invasive stages (zoites) possess a series of secretory organelles termed rhoptries, micronemes and dense granules that contain many parasite effectors required for invasion. Among these factors, secreted proteins enable zoites to adhere selectively to host cells, to modify cell membranes during invasion and to establish the parasitophorous vacuole (Blackman and Bannister, 2001). All organelles are present in merozoites and sporozoites but ookinetes are devoid of rhoptries and dense granules (Lal et al., 2009).

Rhoptries are pear-shaped and membrane bound organelles and their bulb and neck appear to form distinct sub-compartments where individual proteins are compartmentalized. To date, more than 30 neck and bulb proteins have been classified as rhoptry proteins in *P. falciparum* (Counihan et al. 2013). *Plasmodium* rhoptry neck proteins (RONs) are predominantly involved in host-cell adhesion and are components of the tight junction complex forming a protein ring during merozoite invasion (Cao et al., 2009; Riglar et al., 2011; Zuccala et al., 2012). *P. falciparum* rhoptry bulb proteins have no homologs in other apicomplexans and play roles in host cell invasion, PV formation, and host-cell modifications. A further rhoptry component is the RhopH complex which is transferred to the host-cell cytoplasm and RBC membrane post-invasion. RhopH1 was associated with the

establishment of the new permeation pathways found in the RBC membrane (Nguitragool et al., 2011). Rhoptries contain a heterologous protein population including soluble proteins, transmembrane, and GPI anchored proteins. This is in contrast to micronemes, for which all of the so far characterized proteins are transmembrane proteins (Kats et al., 2008)

Micronemes are small numerous bottle-like shaped vesicles at the merozoite apex originating from the Golgi apparatus (Bannister et al., 2003). Microneme proteins support several key cellular processes, including gliding motility, active cell invasion and migration through cells (Carruthers and Tomley, 2008). One protein found in micronemes is the Apical Membrane Antigen 1 (AMA1) which is essential for invasion and forms a complex at the tight junction with RON, 2, 4 and 5 (Cao et al., 2009). A well-characterized micronemal protein family in *Plasmodium* merozoites is the erythrocyte-binding antigens (EBA-175, EBA140, EBA181) (Sim et al., 1992). EBAs mediate interaction with erythrocyte receptors during RBC invasion (See Section 1.2.1.2). Micronemal proteins characterized in *Plasmodium* sporozoites are the circumsporozoite protein (CSP) and the thrombospondin-related protein (TRAP) (Blackman and Bannister, 2001).

1.2.2.4 The food vacuole

In contrast to other RBC infecting apicomplexans like *Babesia* and *Theileria*, *Plasmodium* erythrocytic stages display a lysosome-like compartment termed the food vacuole (FV) where ingested hemoglobin is degraded. In contrast to other organelles, such as the mitochondrion or the apicoplast, the FV does not persist throughout the intra-erythrocytic life cycle and is discarded at the end of each cycle (Ehlgen et al., 2012). The organelle appears in blood stages at the end of the ring stage probably by fusion of small vesicles derived from a cytostomal invagination (Abu Bakar et al., 2010).

Hemoglobin is catabolized in the FV by peptidases, providing a source of aminoacids to the parasite (Goldberg et al., 2013; Kolakovic et al., 1997; Klemba et al., 2004). During this process the heme moiety or ferriprotoporphyrin IX (FP) which cannot be metabolized by the parasite and is toxic through membrane damage and peroxidation is released from hemoglobin. Consequently *Plasmodium* trophozoites polymerise the FP into insoluble crystalline hemozoin (Egan et al., 2008), a metabolite that accumulates in the FV. The hemozoin is readily visible by light microscopy ('malaria pigment') and is a distinct feature of trophozoite and schizont parasites. Different models have been proposed to explain how hemoglobin is ingested and transported to the FV (Elliot et al., 2008; Lazarus et al., 2008) but the actual molecular mechanisms remain poorly understood.

1.2.2.5 The parasitophorous vacuole membrane (PVM)

A critical feature for the intracellular development and replication of *P. falciparum* in hepatocytes and RBCs is the establishment of a suitable cellular compartment named the parasitophorous vacuole (PV) surrounded by a membrane, the parasitophorous vacuole membrane (PVM) which differs from endosomal or phagolysosomal compartments (Lingelbach and Joiner, 1998).

The biogenesis of the PV and the PVM begins early during the invasion of the merozoite (See section 1.1.2.1). The secretion of molecules and lipids contained in the apical organelles, predominantly the rhoptries, is believed to contribute components for the PVM (Riglar et al., 2011), which is thought to be generated by invagination of RBC membrane. Erythrocyte proteins such as major integral and cytoskeletal proteins are supposed to be excluded from internalisation during PVM formation (Gratzer and Dluzewski, 1993; Mordue et al., 1999) however glycosylphosphatidylinositol (GPI)-anchored and cytoplasmic host proteins have been detected in the parasite vacuole (Lauer et al., 2000; Haldar et al., 2001). A recent study found that in contrast to *P. falciparum* parasites, *Babesia* parasites internalizes integral membrane RBC proteins such as band 3, glycophorin A and the cytoskeletal protein spectrin into the PVM (Repnik et al., 2015). However, in this parasite the PVM is disintegrated soon after invasion (Rudzinska, 1976; Repnik et al., 2015).

Proteins involved in nutrient uptake, protein trafficking and egress have been identified at the PVM or in the PV, nevertheless the function for most of the PVM resident proteins remain still elusive (reviewed in Spielmann et al., 2012).

Since the PVM forms an interface between the parasite and the host cell cytoplasm (Lingelbach and Joiner, 1998), enclosing the parasite in the PV, it poses two challenges to the parasite. First, the PVM prevents access to host cell nutrients which as a result need to traverse the PVM to be further transported across the PPM. It is believed that a PVM solute channel permeable to molecules up to a size of 1400 Da (Desai et al., 1993 ; Desai and Rosenberg, 1997) mediates the passage, however up to now the molecular identity of this pore is unclear, although a protein termed EXP2 may be involved (Gold et al., 2015). Second, parasite proteins exported to the RBC need to cross the PVM to reach their final destination in the host cell. Components of a protein complex identified at the PVM termed Plasmodium translocon for exported proteins (PTEX) (See Section 1.3.3 for a detailed description of the complex) are essential for protein export across the PVM and for parasite development (Beck et al, 2014; Elsworth et al., 2014a).

A family of PVM resident proteins is the early transcribed membrane proteins (ETRAMPs), comprising 14 members of which several are highly expressed during parasite blood stage

development (Spielmann et al., 2003). ETRAMPs are highly charged TM proteins that form homo-oligomers at the PVM and constitute the most abundant protein component of the blood stage PVM (Spielmann et al., 2003; Spielmann et al., 2006). So far, no data is available about the function of ETRAMPs in blood stages. Hypothesized functions are structural organization of specific membrane domains at the PVM, formation of small vesicles or the generation of the tubovesicular network extending from the PVM (Spielmann et al., 2006; Currà et al., 2012; Spielmann et al., 2012).

EXP-1 was the first integral membrane protein identified at the PVM (Simmons et al. 1987; Kara et al., 1988) and like the ETRAMPs is present as oligomers at the membrane (Spielmann et al., 2006). Attempts to knock the *exp-1* gene out have been unsuccessful so far, suggesting an essential function for it during blood stage development of the parasite (Maier et al., 2008). A recent study indicated that EXP1 shows glutathione transferase activity and is supposed to efficiently degrade cytotoxic hemozoin. Its enzymatic activity is potently inhibited by artesunate and it might be associated with artesunate metabolism and susceptibility in drug-resistant malaria parasites (Lisewski et al., 2014).

A tubovesicular (TVN) network that buds from the PVM to reach into the host cell (Aikawa et al., 1986; Elmendorf and Haldar, 1994; Haldar, 1998; Grützke et al., 2014) has been observed in RBCs during the ring to trophozoite development and in hepatocytes (Grützke et al., 2014). The TVN constitutes together with the MCs the exomembranous system established by the parasite during RBC infection. A role in nutrient import has been proposed for the TVN (Lauer et al., 1997) but to date its function in parasite development is still elusive.

1.2.3 Host cell modifications

RBC infecting parasites like *Plasmodium*, *Babesia* and *Theileria* develop within fully differentiated cells devoid of a nucleus, ribosomes, organelles and any protein trafficking machinery. This adaptation to intracellular parasitism provides a series of advantages but also imposes challenges that the pathogens need to overcome (Leirião et al., 2004).

Erythrocytes do not express the major histocompatibility complex (MHC) molecules on the surface (Scherf et al., 2008) and in contrast to mammalian nucleated cells are not able to present foreign parasite antigens to T cells. Parasites within RBCs therefore partially avoid recognition by the immune system and remain hidden from the host defenses.

In spite of these benefits, erythrocytes are metabolically inert cells, poor in nutrients and metabolic resources (Repnik et al., 2015) containing almost exclusively hemoglobin, what

obliges the parasite to scavenge nutrients or synthesize *de novo* precursors. The lack of endogenous protein trafficking machinery in the RBC also forces the parasite to generate novel structures and compartments in the host cell to transport self-encoded proteins. In addition, RBCs are also filtered and monitored by the spleen; parasites therefore need to evade the passage through the organ to complete the life cycle. In order to circumvent these threats and survive inside the erythrocyte, *P. falciparum* parasites in contrast to other RBC infecting pathogens extensively remodel the host cell across the 48 hour cycle. Some of the best characterized parasite-derived structures are the Maurer's clefts, the knobs and the new permeability pathways at the erythrocyte plasma membrane.

1.2.3.1 The Maurer's clefts (MC)

The Maurer's clefts (MC) are single-membrane flattened disks of about 500-nm width (Hansen et al., 2008a; Tilley et al., 2008) that appear early after invasion in the *P. falciparum* iRBC (Grüning et al., 2011; McMillan et al., 2013). The MCs were described for the first time since 1902 by Georges Maurer, nevertheless their biogenesis, dynamics and actual function remains still enigmatic (Mundwiler-Pachtlatko and Beck, 2013).

Over the years several insights into the function of the MC and numerous MC resident proteins have been identified and characterized. MC are detected in the iRBC cytosol 2 or 4 hours post invasion (Grüning et al., 2011). Studies using live cell imaging over the 48-h life revealed that MCs are highly mobile in ring stages and become fixed with the transition to trophozoite stage (Grüning et al., 2011). At that point MCs become attached to the RBC membrane, probably by proteinaceous tethers (Pachtlatko et al., 2010; McMillan et al., 2013) or host actin cables (Cyrclaff et al., 2011) and their position and number remain unchanged in further development (Grüning et al., 2011; Kilian et al., 2013). MCs are thought to be generated through budding from the PVM (Goldberg and Cowman, 2010; Spycher et al., 2006), however no experimental evidence exists for this at present. Ideas that the MC form a lipid continuum with the PVM (Wickert et al., 2004) were also later disproved (Hanssen et al., 2008).

MCs are considered an intermediate compartment or platform involved in trafficking or sorting of proteins between the parasite and the erythrocyte plasma membrane (Mundwiler-Pachtlatko and Beck, 2013). A growing number of resident integral and peripheral membrane proteins have been identified and characterized in the MCs (Lanzer et al., 2006). Integral proteins include the membrane associated histidine-rich protein-1 (MAHRP1) (Spycher et al., 2003), the skeleton binding protein-1 (SBP1) (Blisnick et al., 2000), the ring-exported protein-2 (REX2) (Spielmann et al., 2006) and PfMC-2TM (Sam-Yellowe et al., 2004) among others. Resident proteins peripherally associated include the ring-exported protein-1 (REX-1)

(Hawthorne et al., 2004) and the merozoite surface related protein- 6 (MSRP6) (Heiber et al., 2013). Soluble proteins localized to the RBC membrane such as PfEMP3 and KAHRP associate transiently with the MC during their export (Waterkeyn et al., 2000; Wickham et al., 2001) and families of TM proteins destined to the erythrocyte membrane such as RIFINs (Khattab et al., 2006) and STEVOR (Kaviratne et al., 2002; Przyborsky et al., 2005) have also been localized to the clefts. The most important *P. falciparum* virulence factor, PfEMP1, is speculated to be transported to the RBC surface via the MC through vesicular transport or along actin filaments, once MCs are attached to the RBC membrane (Cyrklaff et al., 2011).

Knock out studies for some MC resident proteins indicated that they are not essential for the development of the parasite *in vitro* but are required for the stability of the clefts, trafficking of PfEMP1 to the RBC surface, for cytoadherence and for establishing knobs (Maier et al., 2009; Spillman et al., 2015). Deletion of SBP-1 (Cooke et al., 2006; Maier et al., 2007) and MAHRP-1 (Spycher et al., 2008) prevented export of PfEMP1 to the erythrocyte membrane. Deletion or truncation of REX1 caused stacking of the MC lamellae (Hanssen et al., 2008b), indicating a role in determining the ultrastructure of the MC system. In a recent study, the disruption of PfEMP1 trafficking protein 1 (PTP1) (Maier et al., 2008) led to severe alterations in the architecture of Maurer's clefts and PfEMP1 and STEVOR were no longer displayed on the RBC surface, leading to ablation of cytoadherence to host receptors (Rug et al., 2014).

How parasite-encoded proteins reach the MC is still poorly understood (See Section 1.3). The 'nascent cleft' hypothesis proposed that parasite membrane proteins are exported to MC by insertion into nascent clefts at the PVM, linking cleft biogenesis and export (Spycher et al., 2006; Tilley et al., 2008). Recent data contradict this theory since new clefts are not formed during the life cycle and MC membrane proteins steadily reach already formed clefts. This indicates that the major route of export for membrane proteins is not via cleft formation but via alternative pathways such as vesicles or soluble intermediates (Grüring et al., 2011).

1.2.3.2 Knobs and cytoadherence

One of the most fascinating adaptations to the intracellular development is the ability of *P. falciparum* to induce cytoadherence of the infected erythrocyte. In order to evade the passage through the spleen where altered, damaged or infected RBCs are retained and destroyed by phagocytosis or undergo removal of intraerythrocytic bodies (ie. pitting) (Buffet et al., 2015), the parasite sequester on the endothelium of small capillaries. To achieve this, *P. falciparum* parasites export a complex of effectors to the RBC surface. This cytoadherence complex forms electron-dense, cup-shaped structures beneath the RBC membrane that are termed knobs (Luse et al., 1971; Kilejian, 1979). *P. falciparum* erythrocyte membrane protein (PfEMP1) is considered the parasite's main virulence factor, a

multi domain protein which mediates the adhesion of infected RBC to several host receptors (Su et al., 1995) such as ICAM-1 and CD36 on the endothelium (Baruch et al., 1996), to chondroitin sulfate (CSA) on placental syncytiotrophoblast cells (Rogerson et al., 1995; Fried and Duffy, 1996; Viebig et al., 2005) and to complement receptor 1 (Rowe et al., 1997) on uninfected RBCs (rosetting). The protein is encoded by around 60 members of the *var* gene family per genome which are expressed in a mutually exclusive manner by epigenetic mechanisms (Scherf et al., 1998; Voss et al., 2006). This enables parasites to express only one variant at any one time and the “switching” between antigenic variants allows the parasite to decrease or abolish recognition of PfEMP1 by the immune system (Reviewed in Scherf et al., 2008 and Voss et al., 2014).

PfEMP1 proteins have a large extracellular adhesive variable domain and a more conserved cytoplasmic tail, known as the acidic terminal sequence (ATS) (Su et al., 1995). These two domains are separated by a transmembrane domain. PfEMP1 is concentrated on the exterior surface of knobs and embedded in the RBC membrane through the transmembrane helix (Baruch et al., 1995). The protein is anchored to the knob complex via its C-terminal cytoplasmic domain and the external domain binds to receptors on endothelial cells (Baruch et al., 1996; McMillian et al., 2013).

The knobs associated histidine rich protein (KAHRP) is the main component of the knobs (Taylor et al., 1987; Crabb et al., 1997). Genetic disruption of KAHRP led to absence of knobs and reduction of cytoadherence of iRBCs (Crabb et al., 1997). KAHRP interacts with the ATS of PfEMP1 (Waller et al., 1999) and with various cytoskeletal components of the erythrocyte including spectrin, actin, and spectrin-actin band 4.1 complexes (Kilejian et al., 1991; Oh et al., 2000; Pei et al., 2005). The knobs provide a raised platform for display of PfEMP1 molecules that are intracellularly attached to the host-cell cytoskeleton (Wickham et al., 2001; Rug et al., 2006). Two Plasmodium helical interspersed subtelomeric (PHIST)-domain proteins, PFE1605w and PFI1780w, were recently identified at the knob complex where they interact with the intracellular segment of PfEMP1. PFE1605w binds the ATS domain of PfEMP1 with the host cytoskeleton and might ensure mechanical robustness against shear forces exerted by blood flow, thereby allowing strong cytoadherence (Proellocks et al., 2014; Oberli et al., 2014). Consistently, gene disruption and a recent conditional knockdown of PFE1605w strongly reduced adhesion of iRBCs to the endothelial receptor CD36 (Proellocks et al., 2014; Oberli et al., 2016).

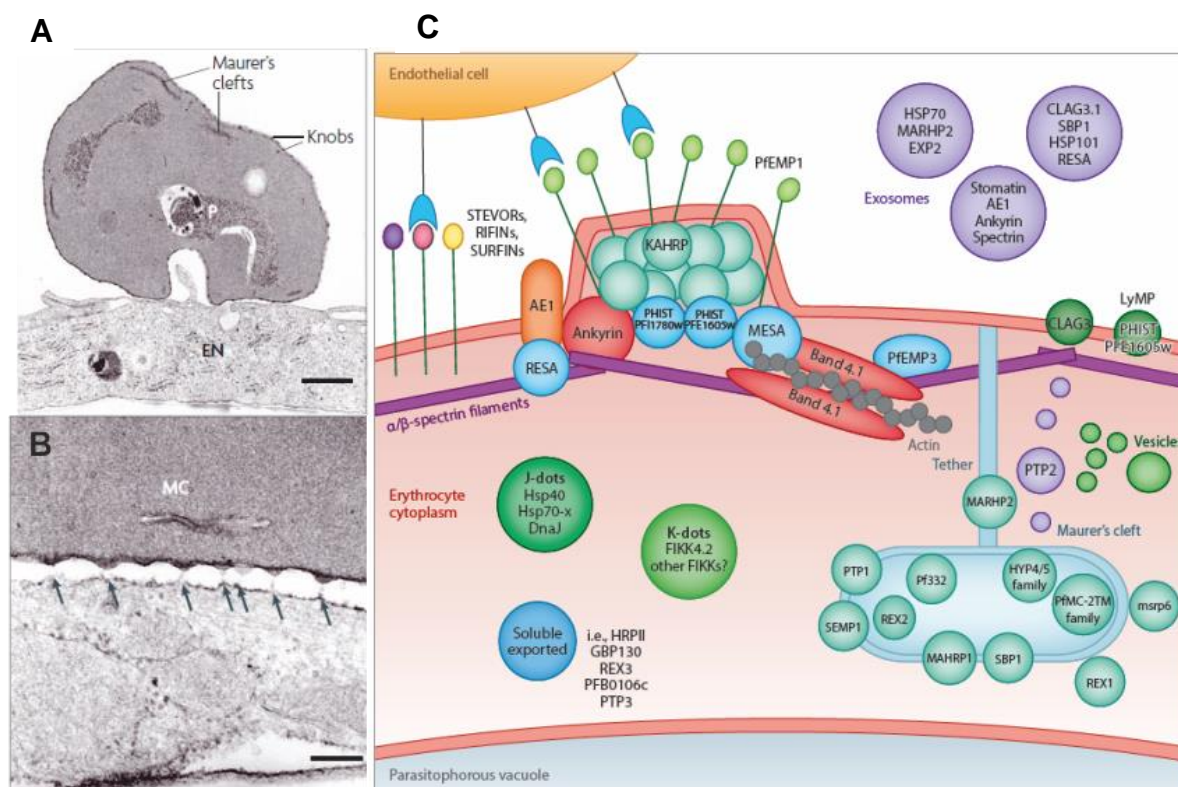


Figure 1.6 | Host cell modifications induced by *P. falciparum* in iRBCs (A) Transmission electron micrograph of an iRBC adhering to the surface of a microvascular endothelial cell (EN). (B) Detail of the interface between an iRBC and an endothelial cell showing strands of electron dense connecting material located at knobs (arrows). MC: Maurer's clefts (modified from Maier et al., 2009). (C) Subcellular localization of exported proteins in the host cell that shows molecular composition of knobs, MC resident proteins, cytoskeleton interacting proteins and erythrocyte surface proteins (modified from Spillmann et al., 2015).

1.2.3.3 New permeation pathways

P. falciparum increases the permeability of the RBC membrane to small structurally unrelated solutes by inducing the so-called new permeation pathways (NPP) or *Plasmodium* surface anion channel (PSAC) (Alkhalil et al., 2004; Staines et al. 2006; Staines et al., 2007). These pathways are supposed to be a single or several anion conducting channels inserted in the erythrocyte membrane at the late ring stage. These permeation pathways mediate the uptake of sugars, amino acids, purines, vitamins and choline and are likely also involved in the exchange of waste products (Desai et al., 2000). CLAG3 is a protein found at the host erythrocyte membrane and is so far the only parasite protein known to be involved in PSAC activation (Nguiragool et al., 2011). The protein is packaged into the rhoptries and secreted into the host erythrocyte upon invasion. Recently it was demonstrated that the trafficking of CLAG3 to the host cell membrane is not dependent on PTEX (See Section 1.3.3) which suggests that the protein is directly delivered into the RBC during invasion (Beck et al., 2014). Nevertheless, PSAC activity was affected when PTEX was conditionally inactivated,

which suggest that other parasite exported proteins might further contribute to it (Beck et al., 2014).

1.3 Protein export in malaria parasites

To ensure successful development in the RBC, *P. falciparum* parasites extensively refurbish their host erythrocytes. To accomplish this process the parasite exports a complex repertoire of soluble and integral proteins to different subcellular localizations in the iRBC. Since the mature RBC lacks any protein synthesis and trafficking machineries, the parasite need to distribute and sorts exported proteins by self –encoded resources. The entire pathway of protein export from the parasite ER beyond the parasite plasma membrane (PPM) and the PVM to the final destination in the RBC continues to be an intriguing field in parasite cell biology (Boddey and Cowman, 2013; Spillman et al., 2015).

1.3.1 Export signals: PEXEL proteins and PNEPs

Two different groups of exported proteins have been identified in malaria parasites: the PEXEL proteins and the so-called PEXEL negative exported proteins (PNEPs). The identification of a five amino acid motif (RxLxE/D/Q) termed *Plasmodium* export element (PEXEL) (Marti et al. 2004) or vacuolar targeting signal (VTS) (Hiller et al., 2004), located 20-30 amino acids downstream of the signal peptide in proteins destined for export, contributed to many aspects of the current understanding of the export pathway in *P. falciparum*. The discovery of the PEXEL allowed the prediction of the exportome, the complement of *Plasmodium* proteins exported to the parasite-infected erythrocyte (Sargeant et al., 2006). Based on the PEXEL prediction it was estimated that the exportome of *P. falciparum* parasites comprises 300–400 different proteins (Marti et al. 2004; Hiller et al., 2004; Sargeant et al., 2006; van Ooij, C. et al. 2008) and of these approximately 75% belong to protein families, leaving ~100 phylogenetically unrelated exported proteins (Sargeant et al., 2006; Heiber et al., 2013).

PEXEL positive proteins enter the secretory pathway via a classical N-terminal hydrophobic signal sequence that is cleaved off in the ER. The PEXEL motif was demonstrated to be cleaved after the leucine (Chang et al., 2008; Boddey et al., 2010; Russo et al., 2010) by an aspartyl protease named Plasmepsin V (PM5) whose active site appears to be on the ER luminal side (Tarr and Osborne, 2015). Processing of the PEXEL is not equivalent to the cleavage of the signal peptide for the entry to the secretory pathway (Boddey et al., 2009; Spielmann and Gilberger, 2010). The PEXEL cleavage by PM5 was thought to be mandatory to license a protein for export, potentially by releasing the N-terminus from the ER membrane

and uncovering the export signal -xE/Q/D, which is further acetylated (Chang et al., 2008; Boddey et al., 2009), although the role in export of the N-acetylation is still unclear (Spillman et al., 2015). Nevertheless, mature PEXEL N termini generated artificially (Grüning et al., 2012) or by a viral protease (Tarr et al., 2013) were trafficked to the host cell, indicating that the PM5 cleavage can be bypassed and that the exposure of the new N-terminus in the ER is sufficient to mediate export (Grüning et al., 2012; Tarr et al., 2013; Spielmann and Gilberger, 2015; Spillman et al., 2015).

The new N-terminus is supposed to direct the mature protein to the PV where proteins are further translocated across the PVM to reach the host cell (Boddey et al., 2009; Boddey and Cowman, 2013) (See sections below). It is still unknown in which step downstream of the export pathway the processed N-terminus is involved but it was hypothesized that the N-terminus mediates substrate recognition for translocation at the PVM (Spielmann and Gilberger, 2010) and enables the distinction of exported proteins (into the iRBC) from proteins destined to remain in the PV (Crabb et al., 2010; Elsworth et al., 2014b).

It was reported that the PEXEL motif binds to phosphatidylinositol-3-phosphate (PI3P) on the luminal side of the ER membrane (Bhattacharjee et al., 2012a) and that this leads exported proteins to a specific export pathway. Contradictory results (Bhattacharjee et al., 2012b; Tarr et al., 2013) and the unusual localization of PI3P on the inner leaflet of the ER raised questions about this model. These doubts were further fostered by a recent publication that indicated that the PEXEL sequence indeed does not bind PI3P, and that this lipid is not concentrated in the ER but on the food vacuole and apicoplast membranes (Boddey et al., 2016) as shown previously (Tawk et al., 2010).

The PEXEL does not appear to be restricted to *Plasmodium* parasites as originally thought (de Koning-Ward et al., 2009). A PEXEL-like signal identified in a series of dense granule proteins (Hsiao et al., 2013) in *T. gondii* undergoes proteolytic cleavage by an aspartyl protease homolog of PM5 (TgASP5) (Curt-Varesano et al., 2015; Hammoudi et al., 2015). This signal is required for protein trafficking to dense granules, to the host cell nucleus and for PVM binding. The identification in *Babesia* and *Cryptosporidium* of a pathway for protein secretion into the host cell functionally related to the PEXEL-dependent export pathway in *Plasmodium* suggests that PEXEL and PEXEL-like motifs coupled to aspartyl proteinase cleavage are ancient trafficking mechanisms shared between apicomplexan parasites (Pellé et al., 2015).

A second group of exported proteins that was initially considered an exception to the PEXEL group are the PEXEL negative exported proteins (PNEPs) (Spielmann and Gilberger, 2010). PNEPs comprise a growing number of exported proteins that lack the PEXEL motif and in fact any predictable sequence or motif for export. The first PNEPs were discovered by

chance and included integral TM proteins without signal peptide that localized to the Maurer's clefts such as for instance REX2 (Spielmann et al., 2006), SBP1 (Blisnick et al., 2000) and MAHRP1 (Spycher et al., 2003) as well as peripheral Maurer's clefts proteins such as MAHRP2 (Pachlatko et al., 2008) and REX1 (Hawthorne et al., 2004). The classical PNEPs lack an N-terminal signal peptide and contain only a single hydrophobic stretch that mediates ER entry and often also is a TM domain (Spycher et al., 2008; Haase et al., 2009; Saridaki et al., 2009; Grüring et al. 2012). The PNEP N-terminus appears to fulfill a comparable role in export with the mature PEXEL N-terminus. The N-termini (the N terminal 20 amino acids) of SBP1, REX1, REX2, MAHRP1 and MAHRP2 were all capable of driving export of a reporter in presence of a PNEP TM (Haase et al., 2009; Saridaki et al. 2009; Grüring et al., 2012; Heiber et al., 2013). This indicated that neither the N terminus nor the TM of PNEPs alone is sufficient for export but that both domains together are necessary for export. In addition, the N-terminal export region was exchangeable with the mature N-terminus of PEXEL proteins, suggesting a shared export mechanism between PNEPs and PEXEL proteins (Grüring et al. 2012).

The export pathway of PNEPs is even more obscure than that of PEXEL proteins. Brefeldin A sensitive ER intermediates have been detected for several PNEPs, indicating that they enter the classical secretory pathway within the parasite and are further trafficked to the parasite periphery (Spycher et al., 2006; Dixon et al., 2008; Haase et al., 2009; Saridaki et al. 2009). PNEPs such as REX2 and SBP1 are not substrates for PM5 in the ER (Boddey et al., 2013), but at least REX2 appears to be N-terminally processed (Haase et al., 2009). Based on the exchangeable properties in the PNEP N-termini and the mature PEXEL motif it was proposed that PNEP and PEXEL export pathways converge (Grüring et al., 2012). Importantly, it was now revealed that this is indeed the case and it occurs at the PVM where both types of proteins are translocated and common trafficking factors are shared (Beck et al., 2014; Elsworth et al., 2014a) (See section 1.3.3).

A comprehensive study revealed that actually PNEPs are not rare in the *Plasmodium* genome (Heiber et al., 2013) and can display different structural organizations, comprising soluble and TM proteins as well as proteins with a classical N-terminal signal peptide (Heiber et al., 2013). A recent study considered only proteins as PEXEL positive if they were processed by PM5 and excluded several proteins with a relaxed or non-canonical PEXEL motif, including PfEMP1 which was reclassified as a PNEP (Boddey et al., 2013). This further increased the number of PNEPs in *P. falciparum*, although some of the proteins with non-canonical PEXEL motifs were later found to be cleaved in a manner typical for PM5 (Schulze et al., 2015).

This indicates that the exportome is larger than predicted and that an unknown number of proteins are missing from the currently predicted exportome (Spielmann and Gilberger, 2010). Non-falciparum species might export a much larger number of proteins than predicted based on the PEXEL motif and this includes a large assortment of PNEPs (Sijwal and Rosenthal, 2010; Bernabeu et al., 2012; Siau et al., 2014).

1.3.2 Current model of export for soluble and TM proteins in *P. falciparum*

How proteins destined to the host cell progress beyond the ER to be exported has not been entirely understood. It remains still unclear whether PNEPs and PEXEL proteins are trafficked separately or within the same cargo environment through the parasite secretory pathway to the parasite periphery (Spielmann and Marti, 2013) but it is generally accepted that both types of proteins reach the parasite boundary through vesicular transport and need to cross the PVM by translocation. Recognition of an exported protein could occur in the ER by chaperones and the protein might be guided via complexes to specific export competent zones at the parasite surface and PV (the so-called regional model). Alternatively, exported proteins may follow the default secretion pathway into the PV by bulk secretory flow and there be recognized by chaperones or directly by PVM spanning translocons (barcode model) (Crabb et al., 2010; Elsworth et al., 2014b) (See Figure 1.7).

The observation that soluble exported proteins are secreted into the PV before reaching the erythrocyte and that their export is ATP-dependent led to the hypothesis that exported proteins might be translocated at the PVM and thus unfolding is necessary (Ansoerge et al., 1996). Years later it was demonstrated that soluble PEXEL (Gehde et al., 2009) and PNEPs (Heiber et al., 2013) require indeed unfolding in the parasite periphery to be exported beyond the PVM. This was established by fusing different soluble exported proteins with the murine dihydrofolate reductase (mDHFR) (Eilers and Schatz, 1986), a protein domain that can be conditionally folded in presence of a small ligand (See Section 1.4.2.1). Proteins fused to this domain were blocked in the PV when mDHFR was arrested in its folded state. This supported translocation as mechanism of export for soluble exported proteins.

Consistent with this mechanistical evidence a protein complex termed PTEX (De Koning-Ward et al., 2009) that satisfies the requirements of a putative protein translocon was identified at the PVM. (See next section). Two components of this complex are essential for the passage of all known types of exported proteins into the host cell, including soluble and TM PEXEL proteins and PNEPs but direct proof of translocation activity is still not available.

It remains also still unsolved how a single translocon can accommodate proteins with different domain architecture and export signals.

It is still unclear how integral membrane proteins can be trafficked across the PVM through the same machinery as soluble proteins (Spielmann and Gilberger, 2015). Exported TM proteins are thought to be trafficked by vesicles to the PPM and after fusion of the vesicle they should remain integral in this membrane. This led to speculate vesicular trafficking as a mechanism of export for these proteins (Trelka et al., 2000; Taraschi et al., 2001; Tilley et al., 2008). Interestingly the fusion of the mDHFR domain to a TM PNEP (REX2) revealed that these proteins are also translocated in an unfolding dependent step excluding vesicular transport as mode of export (Grüring et al., 2012). In contrast to soluble proteins, prevention of unfolding of mDHFR-TM proteins did not cause an arrest in the PV but at the PPM (Grüring et al., 2012). These results suggested therefore that TM proteins need to be first extracted out of the PPM and further translocated at the PVM (Grüring et al., 2012; Spielmann and Marti, 2013). Different molecular arrangements at the parasite boundary have been proposed to explain how embedded TM proteins are first extracted out of the PPM to become translocation competent at the PVM (reviewed in Spielmann and Gilberger, 2015). However, experimental validation of this two-step translocation mechanism for TM proteins is still missing.

Less experimental evidence is available about the sorting and final localization of exported proteins in the RBC. Soluble exported proteins are released into the RBC cytosol after crossing the PVM and by diffusion reach the final destination interacting by specific binding domains (Spielmann and Marti, 2013; Spielmann and Gilberger, 2015). The Maurer's clefts are thought to play a marshalling role in this step as sorting platforms in the host cell with which different exported proteins such as PfEMP1, KAHRP and STEVOR associate transiently along the export pathway. Since a vesicular pathway seems to be unlikely (Grüring et al., 2011) it is also intriguing how Maurer's clefts resident TM proteins are exported from the PVM across the RBC cytosol to their ultimate destination and how these proteins are inserted into the final membrane. TM soluble intermediates have been detected in the RBC cytoplasm (Papakrivos et al., 2005; Grüring et al., 2012) which might be chaperoned complexes comprising HSP40, a parasite-encoded chaperone exported into the erythrocyte (Külzer et al., 2012) and the host chaperone HSP70 (Banumathy et al., 2002). These HSP70/40 complexes in the host RBC have been termed J-dots, mobile foci that are supposed to function as trafficking structures (Külzer et al., 2010).

1.3.3 *Plasmodium* Translocon of Exported Proteins (PTEX)

The discovery of a protein complex localized at the PVM of blood stages that fulfills the features of a protein-conducting channel opened new research lines in *Plasmodium* protein export. The so-called *Plasmodium* *T*ranslocon of *E*xported Proteins (PTEX) contains at least five components: HSP-101, Exported Protein 2 (EXP2), PTEX150, thioredoxin-2 (TRX2) and PTEX-88 (De Koning-Ward et al., 2009) which form a macromolecular complex of > 1.2 KDa and provide the most likely means by which parasite-derived proteins cross the PVM and enter the RBC cytosol. Nevertheless, definitive proof of PTEX functioning as a protein-exporting translocon is currently lacking (Bullen et al., 2012; Spillman et al., 2015). The PTEX components, HSP101, PTEX150 and EXP2 are stored in the dense granules of invasive merozoites and during invasion are secreted from these organelles into the newly formed PVM (Bullen et al., 2012). The complex is organized together in foci that dynamically change their spatial position, which are supposed to be export competent regions (Riglar et al., 2013). PTEX expression is constant across the 48-cycle and its components display little turnover at the PVM (Bullen et al., 2012). PTEX150 together with HSP101 and EXP2 are considered the main constituents and bona fide members of PTEX whereas TRX2 and PTEX are thought to play regulatory or accessory functions (Matthews et al., 2013; Matz et al., 2013).

The PTEX component HSP101 is a ClpA/B-like ATPase from the AAA+ superfamily supposed to perform ATP-driven protein-unfolding and N-terminal substrate recognition (Spillman et al., 2015). Protein members of this family are components of numerous translocon systems and form hexameric ring-shaped complexes that generally translocate proteins through a central pore of the ring core and are involved in unfolding and disaggregation of macromolecules coupled to ATP hydrolysis (Ammelburg et al., 2006; De Koning-Ward, 2009; El Bakkouri et al., 2010). HSP101 is thought to function similarly at the PVM although in the reverse direction to chaperones found in plant and algal chloroplasts used by the Tic/Toc protein translocon system to import proteins into this organelle (Bullen et al., 2012) since this type of chaperones are normally positioned on the *trans* side of the membrane but HSP101 is located at the side *cis* of the PVM (Spillman et al., 2015). A recent study that enabled conditional inhibition of HSP101 by fusion to a destabilization domain revealed its essential and universal function in protein export. After inactivation of HSP101 all types of exported proteins accumulated in the PV and parasites showed a growth arrest at the transition from ring to trophozoite stage (Beck et al., 2014). Knockdown of the protein in *P. berghei* induced similar effects on protein export and parasite growth (Elsworth et al., 2014a).

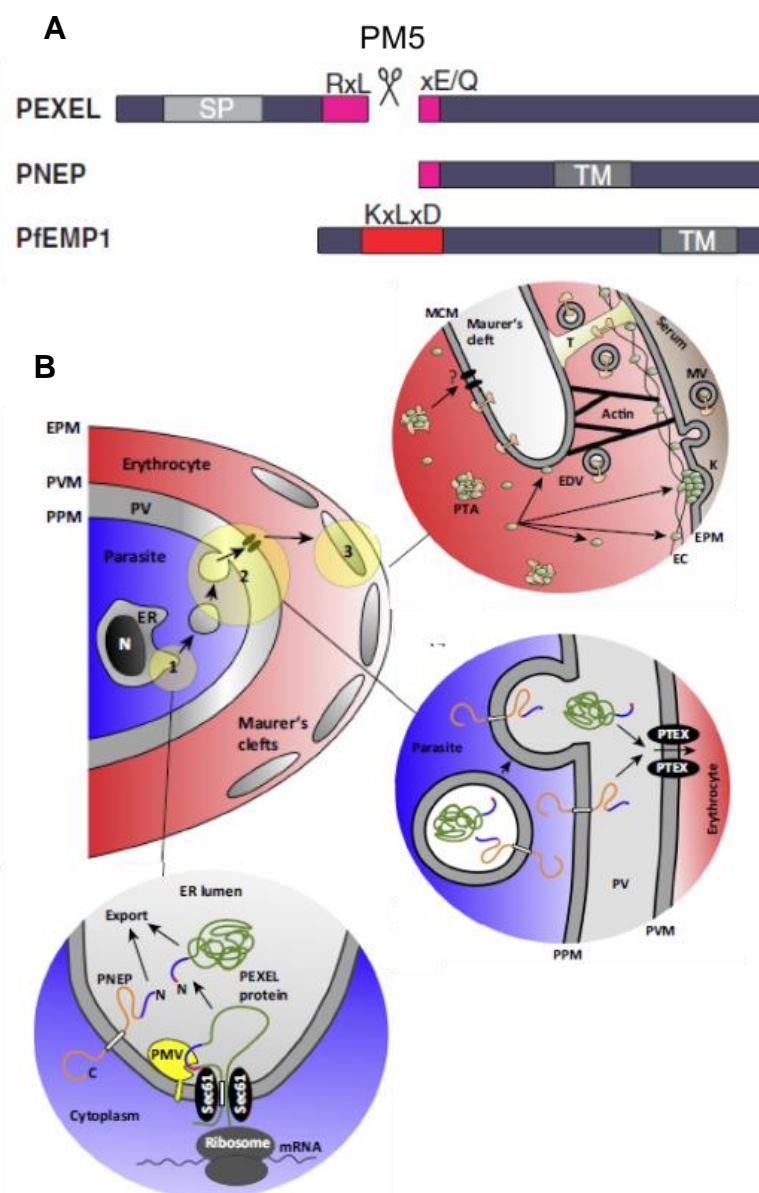


Figure 1. 7 | Current model of export pathway in *P. falciparum* (A) Schematic representation of the different types of exported proteins characterized in *P. falciparum*. PfEMP1 is reclassified as a PNEP since it contains a non canonical PEXEL that is not cleaved by plasmepsin V (PM5). TM: Transmembrane domain (modified from Spielmann and Marti, 2013). (B) Schematic overview of the key steps of the export pathway *P. falciparum* highlighted by yellow circles (1–3) and the general export route signaled with arrows. A soluble PEXEL protein (green) and a TM PNEP (orange) are shown as examples of each group. Circle 1 shows export-relevant events within the parasite's ER. Circle 2 shows events at the parasite periphery. Circle 3 depicts possible sorting mechanisms in the host cell. (1) Exported proteins are co-translationally inserted into the ER where the PEXEL motif (red) is cleaved by PM5, exposing the new N terminus required for further export (blue). PNEPs are inserted into the ER membrane via the TM domain and the export information in their N terminus (blue) together with the TM mediates export. (2) Exported proteins are trafficked by vesicles and fuse with the PPM, releasing the soluble protein (green) into the PV with immediate access to PTEX. The TM protein is delivered to the PPM and requires extraction before it can be transported across PTEX. (3) Sorting events in the host cell after PVM passage. Soluble proteins reach the target site by diffusion and binding to the RBC cytoskeleton (EC), the knobs (Ks), or other structures. Membrane proteins could travel in protein transport aggregates (PTAs) containing chaperones

such as HSP40 and host HSP70 (Modified from Spielmann and Gilberger, 2015). EPM. Erythrocyte plasma membrane; MCM Maurer's cleft membrane

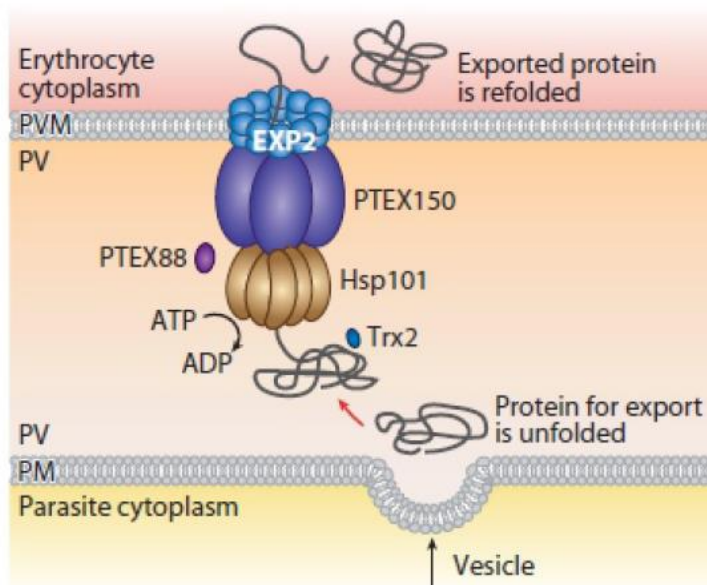


Figure 1. 8 | *Plasmodium* translocon of exported proteins (PTEX). Diagram depicting structural organization of the putative PVM translocon at the parasitophorous vacuole membrane (PVM). EXP2 is the suspected protein-conducting channel in the PVM to which the other components are attached. HSP101 contains an AAA+ ATPase domain and is thought to unfold exported proteins in the PV coupled to ATP hydrolysis and feed them through the complex. PTEX 150 and HSP101 are demonstrated to be essential for protein export. PTEX88 and TRX2 are considered accessory factors of the complex. Proteins are released in the PV by vesicles from the secretory pathway, translocated in an unfolded conformation across PTEX and once in the erythrocyte cytoplasm need to be refolded by host or parasite exported chaperones (modified from Boddey and Cowman, 2013).

EXP2 is a 35 kDa peripheral membrane protein localized to the inner side of the PVM (Johnson et al., 1994; Fischer et al., 1998). The homology of EXP2 with *Escherichia coli*, HlyE (De Koning-Ward et al., 2009), a toxin predicted to form oligomeric pores, led to propose EXP2 as the PTEX component that plays the role of the protein-conducting channel to which the other constituents are associated. Bullen et al., 2012 showed that EXP2 might form higher order oligomers resolvable to an 8-mer with a core dimeric subunit. EXP2 is related to PVM resident dense granule proteins (GRA17 and GRA23) in *Toxoplasma gondii* which function as pores for small molecules at the PVM (Gold et al., 2015). EXP2 was able to complement the function of these proteins in *T. gondii* suggesting a possible dual functionality as nutrient pore and protein channel (Gold et al., 2015). EXP2 was endogenously tagged in *P. berghei* and localized along the parasite periphery to tubular structures of the PV and vesicles in the RBC cytoplasm in blood stages; in liver stages the protein localized to the periphery of the developing parasite (Matz et al., 2015). Intriguingly, HSP101 was not detected at the PVM of liver stages (Kalanon et al., 2016; Matz et al., 2015) and PEXEL reporters were not exported into the hepatocyte, suggesting that EXP2 may

perform functions different than protein export in different stages. There is so far neither functional data nor endogenous tagging that support the role of EXP2 in *P. falciparum* since it appears to be refractory to gene disruption (de Koning-Ward et al., 2009; Matthews et al., 2013; Matz et al., 2013; Matz et al., 2015) likely indicating an essential function in parasite development.

The PTEX component TRX2 belongs to the thioredoxin family and might be involved in the reduction of disulfide bonds and unfolding of substrates in the oxidising environment of the PV to enable passage through PTEX (Matthews et al., 2013; Matz et al., 2013). *trx2* deficient parasites in *P. berghei* displayed a reduced growth and virulence phenotype but the protein was dispensable for development (Matthews et al., 2013; Matz et al., 2013). Previous localization of TRX2 in other organelles such as mitochondria (Boucher et al., 2006) and to unidentified structures within the parasite in addition to the PV (Kehr et al., 2010; Matz et al., 2013) however raises questions about its role in protein export.

The PTEX components PTEX150 and PTEX88 are *Plasmodium* specific proteins with unknown function and no homology to proteins in other organisms (De Koning-Ward et al., 2009; Boddey and Cowman, 2013). A recent conditional knockdown of PTEX150 in *P. falciparum* ablated parasite development and showed that all parasite protein classes destined to the RBC were prevented from crossing the PVM, similar to the phenotype observed when HSP101 was inactivated (Elsworth et al., 2014). Although this indicates a mandatory role of PTEX150 in protein export it is still unknown which function this component performs in the complex.

The function of PTEX88 also still remains elusive but knockout parasites in *P. berghei* showed a striking growth defect (Matz et al., 2013). Interestingly protein export to the host erythrocyte was not affected in PTEX88 knockout parasites but the protein seems to be necessary for tissue sequestration *in vivo* and parasite virulence (Matz et al., 2015).

1.4 Protein translocation across membranes

1.4.1 General mechanisms of protein translocation

Protein translocation is a ubiquitous and essential activity in prokaryotic and eukaryotic cells to export or import polypeptides across cellular membranes. The process is mediated by translocons, complex molecular machineries that consist of a protein conducting channel and an associated motor protein (Tomkiewicz, 2007). Such complexes are directly responsible for the secretion of soluble proteins across membranes as well as the insertion of integral

membrane proteins into and across lipid bilayers (Ulmschneider et al., 2015). Diverse translocons have been described in different organelles and organisms but in general all translocons possess several essential features. First, they contain signal recognition sites that function as docking site for translocation substrates. Proteins destined to be transported across a membrane are usually synthesized with a cleavable N-terminal sequence termed signal-, transit-, or presequences (Blobel and Dobberstein, 1975; Schatz und Dobberstein, 1996; Schulz et al., 2015) recognized by the translocation machinery. Second, translocons form a selective permeable protein-conducting channel that allows the passage of polypeptides from a *cis* (source) compartment to their destination (*trans* compartment) and third they are coupled to a translocation driving force, in most cases protein chaperones which associate with the polypeptide in the *trans* compartment and pull the protein driven by adenosine triphosphate (ATP) or by a pH gradient (Schatz und Dobberstein, 1996; Schnell et al., 2003).

Two classes of translocons can be distinguished: firstly, signal-gated translocons, channels through which an polypeptide is threaded in an unfolded conformation, examples include the Sec 61 translocon in the ER (Rapoport, 2007; Zimmerman et al., 2011) and the translocase of the outer membrane (TOM) in the mitochondria (reviewed in Murcha et al., 2014). Secondly, translocons that transport fully folded and/or oligomeric proteins. These include the TAT translocase in bacteria (Wickner and Schekman, 2005; Lee et al., 2006) and the peroxisome import machinery (Rucktäschel et al., 2011).

For unfolding-dependent translocation systems, proteins need either to be presented to the translocation system in an unfolded state or be unfolded actively. Two models for translocations of polypeptides have been conceived: the power-stroke model and the Brownian ratchet model. In the first model, ATP hydrolysis leads to conformational changes in the motor protein that actively unfolds the protein during the translocation process resulting in movement across the membrane. In the Brownian ratchet model, translocation occurs by diffusion of the unfolded polypeptide through the translocation pore while directionality is achieved by trapping and refolding (Tomkiewicz, 2007).

Motor proteins are found either at the *cis*- side of the membrane such as the SecA in bacteria (de Keyzer et al., 2003) or *trans*-side of the membrane such as BiP in the ER translocon (Rapoport, 2007) or mtHSP70 in mitochondria (Ungermann et al., 1994; Schnell et al., 2003) depending on the availability of the energy source. Cis-acting motors are thought to push, while trans-motors pull on the substrate protein during translocation (Tomkiewicz et al., 2007; Rapoport, 2007).

1.4.2 Approaches to study protein translocation

1.4.2.1 Murine dihydrofolate reductase: Ligand induced prevention of unfolding

The dihydrofolate Reductase (DHFR) is an enzyme of the nucleotide synthesis pathway involved in thymidylate synthesis (Schnell et al., 2004). The murine DHFR (mDHFR) is a system widely used to investigate protein folding dependent translocation (Eilers and Schatz, 1986). In presence of folate analogues, i.e. methotrexate, aminopterin or also WR99210, which bind to the enzyme catalytic site, the protein is highly stabilized in its folded conformation or tertiary structure. The fusion of this domain to cargo proteins therefore represents a valuable tool to conditionally modify the folding state of the cargo protein and analyze the requirement for unfolding at specific transport steps. Chaperones or membrane translocation machineries like pore-complexes are not able to unfold mDHFR in the presence of folate analogues (Backhaus et al., 2004) and the reporter will be arrested in translocation. Hence this is a convenient system for ligand induced prevention of translocation. Methotrexate has a high affinity for mDHFR and its binding stabilizes the moiety in a protease resistant conformation (Rassow et al., 1989; Salvador et al., 2000). The attachment of mDHFR to a protein does not alter the conformation of the substrate protein itself (Eilers and Schatz, 1986) and the most significant advantage of DHFR tagging is its extreme flexibility due to reversible, ligand induced protein folding *in vitro* and *in vivo* by removal and washing of the ligand (Eilers et al., 1988; Rassow, 1989; Salvador et al., 2000; Deponte, 2012). The system was originally tested *in vitro* to characterize protein import in isolated organelles (Eilers and Schatz, 1986) but it can be used *in vivo*, since methotrexate, aminopterin and WR99210 are able to cross membranes. Several studies using mDHFR fusion proteins revealed that the proteins are imported into mitochondria (Eiler and Schatz, 1986; Rassow et al., 1989; Hwang et al., 1991; Wienhues et al., 1991) and lysosomes (Salvador et al., 2000) in an unfolded conformation and it was also employed to identify components of the import machinery interacting with the arrested reporter (Rapaport et al., 1997). In contrast, transport across the chloroplast envelope (Endo et al., 1994) and into glycosomes in trypanosomes (Häusler et al., 1996) does not depend on unfolding. As described in section 1.3.2, the mDHFR system provided evidence that exported proteins in *P. falciparum* required unfolding to be exported (Gehde et al., 2009; Grüning et al., 2012; Heiber et al., 2013) but a systematic dissection of the translocation steps at the PPM and PVM for the different classes of exported proteins have to date not been carried out. In addition, the studies so far did not demonstrate translocation intermediates trapped in the actual translocons and a direct link to the PTEX translocon has remained elusive.

1.4.2.2 Bovine pancreatic trypsin inhibitor (BPTI)

A second approach to characterize translocation is the bovine pancreatic trypsin inhibitor (BPTI), a small protein with three intramolecular disulfide bridges that under oxidizing conditions becomes irreversibly folded. Hence, BPTI represents a model for redox sensitive folding and this has been well characterised (Arolas et al., 2006). Originally tested *in vitro* in mitochondria, the C-terminal fusion of this domain prevented the import of a mitochondrial protein into the matrix (Vestweber and Schatz, 1988) and arrested it across the membrane. A reversible alternative of this system consisting of a mutant BPTI that can be unfolded in presence of reducing agents revealed a sequential translocation across the mitochondrial membranes (Jascur et al., 1992). The system was useful to identify mitochondrial import components (Vestweber et al., 1989) and to investigate folding dependent import in chloroplast (Clark and Theg, 1997).

1.5 Aims of this PhD thesis

The development of *P. falciparum* parasites is dependent on the export of proteins to different destinations in the infected RBC. In spite of a large body of experimental evidence that supports several principles in malaria protein export, the sequence of molecular events that exported proteins follow from the parasite to their final destination in the host cell across several membranes is still unresolved. A key step in protein export is the passage of exported proteins across the PVM, a process supposed to be mediated by translocation of polypeptides through a complex termed PTEX. However, PTEX is still a translocon in concept and direct proof of translocation activity for the complex is still missing. It is also unclear how PTEX can translocate different classes of exported proteins, including soluble as well as integral TM proteins that are embedded in the parasite plasma membrane (PPM). Especially for TM proteins it remains elusive how they can be trafficked across the PPM and the PVM to reach the host cell and many mechanistic questions are still unresolved.

The aim of this thesis is to dissect the translocation steps at the parasite periphery for the export of different classes of exported proteins with a particular focus on the trafficking mechanisms of TM proteins. The individual trafficking steps at the PPM and PVM will be resolved using parasite exported proteins fused with conditionally foldable domains. Potential overlaps in the export mechanisms between the different classes of exported proteins will be assessed with the goal to provide a model for these crucial steps in protein export. Finally, this thesis has the aim to pinpoint parasite effectors involved in these transport steps.

Protein export is a critical and parasite-specific process of *Plasmodium* biology. It is expected that this thesis will inform on crucial aspects of protein export that may lead to a better understanding of this process, and hence will reveal promising targets for new therapeutical interventions.

Chapter 2. Materials

2.1 Technical devices

Device	Specifications	Brand/ Distributor
Agarose gel chamber	Sub Cell GT basic	Bio-Rad, München
Analytical Balance	870	Kern
Blot device Gel holder cassettes Foam pads Electrode assembly Cooling unit	Mini Protean Tetra Cell System	Bio-Rad, München
Centrifuge	Megafuge 1.0R J2- HS Ultracentrifuge Rotor JA-12 Avanti J-26S XP Rotor JA-14	Heraeus, Hannover Beckman Coulter, Krefeld Beckman Coulter, Krefeld
Table centrifuge	Eppendorf 5415 D	Eppendorf, Hamburg
Casting gel stuff Casting stand Casting plates Casting frames 12 –wells combs	Mini Protean	Bio-Rad, München
Developer	Curix 60	AGFA-Gevaert, Mortsel/Belgium
Developer cassette	Cronex Quanta III	Dupont, Neu Isenburg
Electrophoresis chamber	Mini Protean 67s	Bio-Rad, München
Electroporator	Gene Pulser X- Cell	Bio-Rad, München
Electroporator	Nucleofector II AAD-1001N	Amaxa Biosystems, Germany
Ice machine	EF 156 easy fit	Scotsmann, Vernon Hills/USA

Device	Specifications	Brand/ Distributor
<i>P. falciparum</i> cell culture incubator	Heratherm IGS400	Thermo Scientific, Langensfeld
Bacterial incubator	Thermo function line	Heraeus, Hannover
Shaking incubator	Max Q4000	Barnstead, Iowa/ USA
Light Microscope	Axio Lab A1	Zeiss, Jena
Fluorescence Microscope	Axioscope 1	Zeiss, Jena
Microscope digital camera	Orca C4742-95	Hamamatsu Phototonics K.K., Japan
Microwave	Micro 750W	Whirlpool, China
Laboratory scale	Atilon	Acculab Sartorius, Göttingen
PCR Mastercycler	epgradient	Eppendorf, Hamburg
Photometer	BioPhotometer plus	Eppendorf, Hamburg
pH-meter	SevenEasy	Mettler-Toledo, Gießen
Pipettes	1-10/200/1000 µl	Gilson, Middleton, USA
Pipettor	Pipetboy acu	IBS,
Power supply	EV31 Power Source 300 V	Consort, Belgium VWR, Taiwan
Roller mixer	STR6	Stuart
Sterile laminar flow bench	Steril Gard III Advance	Baker, Stanford USA
Thermoblock	Thermomixer compact	Eppendorf, Hamburg
Ultrapure water purification system	Milli Q	Millipore
UV transilluminator	PHEROlum289	Biotec Fischer, Reiskirchen
Vacuum pump	BVC Control	Vacuubrand, Deutschland
Vortexer	Genie 2	Scientific Industries, USA
Waterbath	1083	GFL, Burgwedel

2.2 Chemicals

Reagent	Brand/ Distributor
Acrylamide/Bisacrylamide solution (40 %)	Roth, Karlsruhe
Agar LB (Lennox)	Roth, Karlsruhe
Agarose	Invitrogen, USA
AlbumaxII	Gibco, Life Technologies, USA
Albumin bovine Fraction V (BSA)	Biomol, Hamburg
Ammonium persulfate (APS)	Applichem, Darmstadt
Ampicillin	Roche, Mannheim
Blasticidin S	Invitrogen, USA
Bromophenol blue	Roth, Karlsruhe
Desoxynucleotides (dNTPs)	Thermo Scientific, Lithuania
4',6-diamidino-2-phenylindole (DAPI)	Roche, Mannheim
Dimethyl sulfoxide (DMSO)	Sigma, USA
Dipotassium phosphate	Merck, Darmstadt
Disodium phosphate	Roth, Karlsruhe
DSP	Thermo Scientific, USA
1,4,-dithiothreitol (DTT)	Biomol, Hamburg
Dulbecco's Phosphate Buffered Saline (DPBS)	PAN, Biotech, Aidenbach
Ethanol	Roth, Karlsruhe
Ethidium bromide	Sigma, Steinheim
Ethylenediaminetetraacetic acid (EDTA)	Biomol, Hamburg
Gentamycin	Ratiopharm, Ulm
Giemsa's azure, eosin, methylene blue solution	Merck, Darmstadt
D-Glucose	Merck, Darmstadt
Glycerol	Merck, Darmstadt
Glycine	Biomol, Hamburg

Reagent	Brand/ Distributor
(4-(2-Hydroxyethyl)-1-piperazineethanesulfonicacid) (HEPES)	Roche, Mannheim
Hydrochloric acid (HCl)	Merck, Darmstadt
Hypoxanthin	Sigma, Steinheim
Isopropanol	Roth, Karlsruhe
LB-Medium (Lennox)	Roth, Karlsruhe
Magnesium chloride	Merck, Darmstadt
Manganese(II) chloride	Merck, Darmstadt
Methanol	Roth, Karlsruhe
3-(N-morpholino)propansulfonic acid (MOPS)	Sigma, Steinheim
Milk powder	Roth, Karlsruhe
N, N, N, N-Tetramethylethylenediamin (TEMED)	Merck, Darmstadt
Percoll	GE Healthcare, Sweden
Phenylmethylsulfonylfluorid (PMSF)	Sigma, Steinheim
Potassium chloride	Merck, Darmstadt
Protease inhibitor cocktail ("Complete Mini")	Roche, Mannheim
Rubidium chloride	Sigma, Steinheim
RPMI (Roswell Park Memorial Institute)-Medium	Applichem, Darmstadt
Saponin	Sigma, Steinheim
Sodium acetate	Merck, Darmstadt
Sodium chloride	Gerbu, Gaiberg
Sodium bicarbonate	Sigma, Steinheim
Sodium dodecyl sulfate (SDS)	Applichem, Darmstadt
Sodium dihydrogen phosphate	Roth, Karlsruhe
Sodium hydroxide	Merck, Darmstadt
Sorbitol	Sigma, Steinheim
Tetanolysin	Sigma, Steinheim

Reagent	Brand/ Distributor
Tris base	Roth, Karlsruhe
Trichloroacetic acid	Roth, Karlsruhe
Triton X-100	Biomol, Hamburg
Water for molecular biology (Ampuwa)	Fresenius Kabi, Bad Homburg

2.3 Lab ware and disposables

Labware and disposables	Specifications	Manufacturer
Conical Falcon tubes	50 / 15 ml Material	Sarstedt, Nümbrecht
Pasteur pipette		Brand, Wertheim
Sterile filter	0.22 µm	Sarstedt, Nümbrecht
Disposable pipette tips	1-10/ 20-200/ 100-1000 µl	Sarstedt, Nümbrecht
Filter tips	1-10/ 20-200/ 100-1000 µl	Sarstedt, Nümbrecht
PCR Reaction tubes	Multiply-µStrip Pro 8-Strip	Sarstedt, Nümbrecht
Eppendorf Reaction Tubes	1.5 ml / 2 ml	Sarstedt, Nümbrecht/ Eppendorf Hamburg
Glass slides		Engelbrecht, Edermünde
IFA glass slides	10 wells ER-208B-CE24 6.7 mm	Thermo Scientific, USA
Glass cover slips	24 X 65 mm Thickness 0.13-0.16	R. Langenbrinck, Emmendingen
Transfection cuvettes	0.2 cm	Bio-Rad, München
Cryotubes	1.6 ml	Sarstedt, Nümbrecht
Plastic pipettes	5/ 10/ 25 ml	Sarstedt, Nümbrecht
Chromatography paper		Whatman
Nitrocellulose blotting Membrane Protran	Amersham 0.45 µm	GE Healthcare, Deutschland
Parafilm		Bemis, USA
Petri dishes	5 mL/ 10 ml	Sarstedt, Nümbrecht

Labware and disposables	Specifications	Manufacturer
Culture bottles	50 mL	Sarstedt, Nümbrecht
Medical X-Ray screen film blue sensitive	CEA RP NEW	AGFA Health Care NV, Mortsel, Belgium

2.4 Kits

NucleoSpin. Plasmid	Macherey-Nagel, Düren
NucleoSpin. Extract II	Macherey-Nagel, Düren
QIAamp DNA Mini Kit	Qiagen, Hilden
QIAGEN Plasmid Midi Kit	Qiagen, Hilden
Western Blot ECL-SuperSignal West Pico Chemiluminescent Substrate Detection Kit	Thermo Scientific, Schwerte
Western Blot ECL-Clarity Detection Kit	Bio-Rad, USA
Silver Staining Kit for mass spectrometry	Thermo Scientific, Schwerte

2.5 DNA- und protein ladders

GeneRuler™ 1000 bp ladder	Thermo Scientific, Schwerte
PageRuler™ prestained protein ladder	Thermo Scientific, Schwerte
PageRuler™ unstained protein ladder	Thermo Scientific, Schwerte

2.6 Solutions, media and buffers

2.6.1 Media, buffers and other solutions for microbiologic culture

10X Luria-Bertani (LB) Medium

Stock solution

10 % NaCl

5 % Peptone

10 % yeast extract

in dH₂O/ autoclaved

LB medium working solution (1X)

1 % (w/v) NaCl

0.5 % (w/v) pepton

1 % (w/v) yeast extract in dH₂O

in dH₂O

LB Agar plate solution

1.5 % Agar-Agar

1x LB medium

Ampicillin stock solution

100 mg/mL in 70 % ethanol

Glycerol freezing solution

50 % (v/v) glycerol

in 1 x LB medium

2.6.1.1 Buffers for competent *E. coli* cells

TFBI buffer

30 mM acetic acid

50 nM MnCl₂

100 mM RbCl

10 mM CaCl₂

15 % (v/v) glycerol

pH 5.8 (with 0.2 N Acetic acid)

TFBII buffer	10 mM MOPS
	75 mM CaCl ₂
	10 mM RbCl
	15 % (v/v) glycerol
	pH 7.0 (with NaOH)

2.6.2 Solutions and buffers for molecular biology analyses

2.6.2.1 DNA precipitation

Sodium acetate	3 M, pH 5.2
Ethanol	100%
Tris-EDTA (TE) buffer	10 mM Tris-HCl pH 8.0
	1 mM EDTA

2.6.2.2 DNA electrophoresis

50x TAE-Buffer	2 M Tris base
	1 M Pure acetic acid
	50 mM EDTA
	pH 8.5
6x Loading buffer	40 % Glycerol (v/v)
	2.5 % (w/v) Xylene cyanol
	2.5 % (w/v) Bromophenol blue
	in dH ₂ O

2.6.3 Media and solutions for parasite culture and cell biology experiments

2.6.3.1 *P. falciparum* in vitro culture

RPMI complete medium	1,587 % (w/v) RPMI 1640 12 mM NaHCO ₃ 6 mM D-Glucose 0.5 % (v/v) Albumax II 0.2 mM Hypoxanthine 0.4 mM Gentamycin pH 7.2 sterile filtered
Synchronization solution	5 % (w/v) D-Sorbitol in dH ₂ O, sterile filtered
Transfection buffer (Cytomix)	120 mM KCl 150 μM CaCl ₂ 2 mM EGTA 5 mM MgCl ₂ 10 mM K ₂ HPO ₄ / KH ₂ PO ₄ 25 mM HEPES, pH 7.6, sterile filtered
Amaya transfection buffer	90 mM Na ₂ HPO ₄ 5mM KCl 0.15 mM CaCl ₂ 50 mM HEPES pH 7.3, sterile filtered

Malaria freezing solution (MFS)	4.2 % D-sorbitol 0.9 % NaCl 28 % Glycerol sterile filtered
Malaria thawing solution (MTS)	3.5 % NaCl in H ₂ O sterile filtered
WR99210 stock solution	20 mM WR99210 in 1 ml DMSO sterile filtered
WR99210 working solution	1:1000 dilution of stock solution in RPMI complete medium
Blasticidin S (BSD) working solution	5 mg/ml BSD in RPMI complete medium sterile filtered
Human red blood cells	Blood bank, Universitätsklinikum
Sterile, concentrate; bloodgroup 0+	Eppendorf (UKE), Hamburg

2.6.3.2 Solutions for cell biology and biochemical assays

Parasite lysis buffer	4 % SDS 0.5 % Triton X-100 0.5 x PBS in dH ₂ O
Percoll stock solution	90 % (v/v) Percoll 10 % (v/v) 10 x PBS

80 % Percoll solution	89 % (v/v) Percoll stock solution 11 % (v/v) RPMI compl. medium 4 % (w/v) sorbitol sterile filtered
60 % Percoll solution	67 % (v/v) Percoll stock solution 33 % (v/v) RPMI compl. medium 4 % (w/v) sorbitol
40 % Percoll solution	44 % (v/v) Percoll stock solution 56 % (v/v) RPMI compl. medium 4 % (w/v) sorbitol
Saponin solution for selective membrane permeabilization	Saponin 0.03 % (w/v) in DPBS
Tetanolysin Stock	50 HU / μ l in dH ₂ O
RIPA Buffer	10 mM Tris/HCl pH 7.5 150 mM NaCl 0.1% SDS 1% Triton X-100 1 mM PMSF 2X Protease inhibitor cocktail
Diluting buffer	10 mM Tris/HCl pH 7.5 150 mM NaCl 1 mM PMSF 2X Protease inhibitor cocktail
DSP (Stock solution)	20 mM in DMSO
Quenching buffer	25 mM Tris-HCl in PBS 1X

2.6.4 Buffers and solutions for protein analyses

2.6.4.1 SDS-Page and Western blot

10 x Running buffer	250 mM Tris base 1.92 M Glycine 1 % (w/v) SDS in dH ₂ O
Ammonium persulfate (APS)	10% (w/v) in dH ₂ O
Separating gel buffer	1.5M Tris-HCl, pH 8.8
Stacking gel buffer	1M Tris-HCl, pH 6.8
Stacking gel (for two gels) (5%)	0.75 ml stacking gel buffer 4.35 ml dH ₂ O 750 µl Acryl amide (40%) 60 µl SDS(10%) 60 µl APS (10%) 6 µl TEMED
Separating gel (for two gels) (12%)	2.5 ml running gel buffer 4.2 ml H ₂ O 3 ml Acryl amide (40%) 100 µl SDS (10%) 100 µl APS (10%) 4 µl TEMED

6 x SDS sample buffer (Laemmli Buffer)	375 mM Tris HCl pH 6.8 12 % (w/v) SDS 60 % (v/v) Glycerol 0.6 M DTT 0.06 % (w/v) Bromophenol blue
10 x Western transfer buffer	250 mM Tris base 1.92 M glycerol 0.1 % (w/v) SDS in dH ₂ O
1 x Western-Transfer buffer	10 % 10 x Western transfer buffer 20 % Methanol in dH ₂ O
Silver staining fixing solution	30% ethanol 10% acetic acid 6:3:1 water:ethanol:acetic acid

2.7 Enzymes

2.7.1.1 Polymerases

FirePol. DNA Polymerase [5 U/μl] Solis Biodyne, Taipei, Taiwan

Phusion. High-Fidelity DNA Polymerase [2 U/μl] NEB, Ipswich, USA

2.7.1.2 Restriction enzymes

2.7.1.3 Ligases

T4 DNA-Ligase [3 U/μl] NEB, Ipswich, USA.

2.7.1.4 Proteases

Proteinase K [800 U/ml] NEB, Ipswich, USA.

2.8 Antibodies

2.8.1 Primary antibodies

Antigen	Organism	Dilution		Source
		WB	IFA	
Aldolase	Rabbit	1:4000	-	Nyalwidhe & Lingelbach, 2006 Newly raised
ETRAMP5	Mouse	-	1:400	Spielmann et al., 2006
ETRAMP4	Rabbit	1:1000	-	Spielmann et al., 2003
GAPDH	Mouse	1:4000	-	Daubenberger et al., 2000
GFP	Mouse	1:1000	1:500	Roche, Mannheim
GFP	Rabbit	1:2000	1:500	Thermo Scientific
HSP101	Mouse	1:1000	-	Heiber et al., 2013
Triple hemagglutinin (HA)	Rat	1:2000	1:500	Roche, Mannheim
KAHRP	Rabbit	-	1:500	Prof. Dr. Brian Cooke,
MAHRP-2	Rabbit	-	1:250	Pachlatko et al., 2010
mCherry	Rat	1:1000	-	Chromotek, München
mDHFR	Rabbit	1:1000	-	Abcam, Cambridge, UK
MSRP6 (PF13_192)	Mouse	-	1:250	Heiber et al., 2013
myc	Rabbit	1:500	1:200	Cell Signaling, USA
REX1	Rabbit		1:5000	Hawthorne et al., 2004. Newly raised
REX2	Mouse		1:250	Haase et al., 2009
REX3	Mouse	1:2000		Spielmann et al., 2006a
SERP	Rabbit	1:4000		Ragge et al., 1990. Newly raised

2.8.2 Secondary antibodies

Antigen	Conjugate	Organism	Dilution	Application	Source
Mouse	HRP	Goat	1:3000	Western blot	Dianova, Hamburg
Mouse	Alexa 488	Goat	1:2000	IFA	Life Technologies, USA
	Alexa 594	Goat			
	Alexa 647	Donkey			
Rabbit	HRP	Donkey	1:2500	Western blot	Dianova, Hamburg
Rabbit	Alexa 488	Donkey	1:2000	IFA	Invitrogen, Molecular Probes Leiden
	Alexa 594	Donkey			Life Technologies, USA
	Alexa 647	Goat			
Rat	HRP	Goat	1:3000	Western blot	Dianova, Hamburg
Rat	Alexa 594	Goat	1:2000	IFA	Invitrogen, Molecular Probes

2.8.3 Antibody coupled beads

Antigen	Matrix	Organism	Application	Source
HA	Agarose	Mouse	IP	Thermo Scientific, USA
GFP	Agarose	Camel	IP	Chromotek, München

2.9 Oligonucleotides

All oligonucleotides were synthesized by Sigma-Aldrich (Steinheim). Restriction sites are indicated in lower case and overlapping regions in bold.

Oligonucleotide	Sequence
REX2 Kpn fw	GTCTggtaccTTTATGAAAATGATTTAGCTGAAATTTTTAGTTC
REX2 AvrII rv	TCATcctaggCTAATGTTGTTGTTGATC
REX2 ZnFwt fw	GAAGAGATTTATTAATAAGACAC GCACAAAAAATACATAGTGAAAT actagtCTGAAACCATGTGAAGGCCTTGAGTG
REX2 ZnFwt rv	GTGCGTGTCTTATTAATAAATCTCTTC TTGTA AACATCTATTACATAA TCCACATGGATATGGTTTgctagcTGGAGAAAAATTACTAGATCCTAAAG
REX2 ZnFmut fw	GAAGAGATTTATTAATAAGACCC GCACAAAAAATACATAGTGAAAT actagtCTGAAACCATGTGAAGGCCTTGAGTG
REX2 ZnFmut rv	GTGCGGGTCTTATTAATAAATCTCTTC TTGTA AACATCTATTACATA ATCCACATGGATATGGTTTgctagcTGGAGAAAAATTACTAGATCCTAA G
SBP-1fw(XhoI)	GTCTctcgagATGTGTAGCGCAGCAGCAGCATTG
SBP-1rv(AvrII)	TCCTcctaggGGTTTCTCTAGCAACTGTTTTTGTGTTG
SBP259AvrIIrv	TGATAGcctaggGTTTTGTTCTAGCATTGTTG
SBP1 40rv	GTCTCTGGTACTGCATCCTGTAATTG TGTTGGTTCGTCGGCTAAATC AG
SBP1 211fw	CAATTACAGGATGCAGTACCAGAGACA ACCGAAAAATTGGCCGAAG TAGTTTCGGATGCAGCAATGTCCCCTATTCTTAGAGTACAATTTTTTG C
MAHRP1 Xho fw	GTCTctcgagATGGCAGAGCAAGCAGCAGTACAACCAGAAAG
MAHRP1rvAvrII	TCCTcctaggATTATCTTTTTTTCTTGTCTAATTTTGCTTTTTGGC
REX3 XhoI fw	CGGCctcgagATGCAAACCCGTAAATATAATAAGATGTTG
REX3 AvrII rv	TCCTcctaggTGAAGAACTTGACTTGGTTTAGC
STEVOR XhoI fw	GTCTctcgagATGAAGATGTATAACCTTAAATGTTATTG
STEVOR AvrII rv	CAGTcctaggCTTACATAAATGTTTCTTGCATTCATGTTTC
PTP1 XhoI fw	CTGTctcgagATGGTGAATAAAGATAATAGGAAAATTCATAAGGC
PTP1 rv AvrII	CAGTcctaggTTGGTTTTGTATATTTAAATTGTCATCTTGTTC
PTP1 rv SpeI	CAGTactagtTTGGTTTTGTATATTTAAATTGTCATCTTGTTC
KAHRP Xho fw	CTGTctcgagATGAAAAGTTTTAAGAACA AAAAATACTTTGAGG
KAHRP AvrII rv	TCCTcctaggACCACAGCATCCTCTTTTCTTCTTTTCTTTCC
GFP-PH mut fw BstBI	AGGAttcgaaAGATCCCAACGAAAAGAGAGACC
PH mut rv XmaI	CGAGcccgggTACTTCAGGAAGTCTGCAGCTCC
BPTI fwAvrII	GTCTcctaggTCAACACCAGGTTGTGATACATC
BPTI rvKpnI	TCCTggtaccTAAATTTTCCCATGGACCTATAGCAC
REX2 XhoI fw1	GTCTctcgagTTTATGAAAATGATTTAGCTGAAATTTTTAGTTC
REX2rvAvrII Ext C-t	TCCTcctaggATGCTGCTGCTGATCGTACTGCTC
GFPrv NheI-XmaI	TCCTcccggggctagcTTTGTAGAGCTCATCCATGCCATGTG
mDHFR Spe-Xma rv	TCCTcccgggTTAactagtGTCTTTCTTCTCGTAGACTTCAAACCTTATACTT GATGCC
mDHFR NheI fw	GTCTgctagcATGGTTCGACCATTGAACTGCATCG
mDHFR rv SpeI-XhoI	CTCGAGTTAactagtATGGTTCGACCATTGAACTGCATCGTCC
pARL2 Xhofw	CTTCctcgagCAAAATGAAAAGTTTTATAACAAGAAATAAAACAGC
pARL2-2A-AvrIIrv	TCCTcctaggACTGATTGGTCTGGATTTTCTTCTACATCTCCACATGTT AATAAACTTCTCTTCTTCTCCATAactagtCTTTGAGATTGTCGG
GFPrvSpe	TCCTactagtTTTGTATAGTTCATCCATGCCATGTGTAATCCC
REX3 fw AvrII	CGGCcctaggATGCAAACCCGTAAATATAATAAGATGTTG
REX3 rv KpnI	TCCTggtaccTGAAGA ACTTGACTTGGTTTAGC

Oligonucleotide	Sequence
MSRP6 fw AvrII	AGGAcctaggATGAAAAGCAAAAAATAATATGTTTCATCTTGC
MSRP6 rv KpnI	TCCTggtaccTAATTTCTGTTGGGATTTAAAGC
KAHRP fw AvrII	CTTCcctaggATGAAAAGTTTTAAGAACAAAAATACTTTGAGG
KAHRP rv KpnI	TCCTggtaccACCACAGCATCCTCTTTTCTTCTTTTCTTTCC
STEVOR fw1	CTTTTTGATTAATACTTTGG CTTTGCCACATTATGATAATTATCAAAA TAGCCATTATAATATAAACC
STEVOR fw2 AvrII	AGGAcctaggATGAAAATGTATAATTTGAAAATGTTGTTGTTT ACTTTTT GATTAATACTTTGG
STEVOR rv KpnI	TCCTggtaccCTTGCATAAATGTTTCTTGCATTCATGTTTCC
REX3 fw KpnI	CGGCggtaccATGCAAACCCGTAAATATAATAAGATGTTG
REX3 rv AvrII	TCCTcctaggTGAAGAACTTGACTTGGTTTAGC
MSRP6 fw KpnI	CAGCggtaccAAAAATGAAAAGCAAAAAATAATATGTTTCATCTTGC
MSRP6 rv AvrII	CAGCcctaggTAATTTCTGTTGGGATTTAAAGCTAAGTCC
STEVOR fw KpnI	GTCTggtaccATGAAGATGTATTACCTTAAATGTTATTG
STEVOR rv AvrII	CAGTcctaggCTTACATAAATGTTTCTTGCATTCATGTTTCC
SBP1-Int-check_F	TGTAGCGCAGCTCGAGCATTG
SBP1-Int-check_R	CAAATTCTCATTATTGTTGGCAC
GFP42_rev	CATCACCATCTAATTCAACAAG
GFP272_rev	GAAAAATATAGTTCTTTCCTGTACATAAC
EXP2410 Not fw	CTCGgcgccgcTAATTTAACAATTAAGATATTTATGAACACGG
EXP2HA rv1	CGTACGGGTACATCGTAGCGTAATCTGGAACATCGTATGGGTACAT GGTggtaccTTCTTTATTTTCATCTTTTTTTTCATTTTTAAATAAATCTCC
3xHA-Sallrv2	TCCTgtcgacAGCATAATCTGGAACATCATATGGATACATAGTCGCGTA GTCCGGCACGT CGTACGGGTACATCGTAGCGTAATCTGG
5'EXP2fw	CTTTTATACCACCACTTCCCCTGTGTCATCG
3'EXP2rv	GATTGTTTCTCCATCAGATACTGTAC
pARL55sense	GGAATTGTGAGCGGATAACAATTTACACACAGG
pARL_1_40 rv	CGAATAGCCTCTCCACCCAAG
HSP101fw NotI	CTCGgcgccgcTAATTTAAGAGATTCTGGTATGCCACTTGG
HSP101-HA KpnI rv	TCCTggtaccGGTCTTAGATAAGTTTATAACCAAGTTTTTAGC
HSP101 fw 5'	CCTTGTTTGTGATTTTAGTATGTAATTCGGAAC
HSP101 rv 3'	GGAACACACAAGTAACAATAAATTTACAAATGTG

2.10 Plasmids

pARL1-mCherry

Grüning et al., 2012

_mDHFRGFP in pARL2

Grüning et al., 2012

SLI in pARL1

Birnbaum and Spielmann, unpublished

2.11 Computer software

A plasmid Editor (ApE)	Open Source (http://biologylabs.utah.edu/jorgensen/wayned/ape/)
Axio Vision 40 V 4.7.0.0	Zeiss, Jena
GraphPad Prism 6.0d	GraphPad Software, La Jolla, USA
Microsoft Office 14.4.8 USA	Microsoft Corporations, Redmond, USA

2.12 Bioinformatic tools and data bases

BLAST	http://blast.ncbi.nlm.nih.gov/Blast.cgi
ClustalW	http://www.ebi.ac.uk/Tools/msa/clustalw2/
Compute pi/Mw	http://web.expasy.org/compute_pi/
GenBank	http://www.ncbi.nlm.nih.gov/genbank/
HHpred	http://toolkit.tuebingen.mpg.de/hhpred
MotifScan	http://myhits.isb-sib.ch/cgi-bin/motif_scan
PlasmoDB	http://plasmodb.org/plasmo/
PubMed	http://www.ncbi.nlm.nih.gov/pubmed
ToxoDB	http://www.toxodb.org/toxo/

Chapter 3. Methods

3.1 Molecular biology methods

3.1.1 Polymerase chain reaction (PCR)

Genes of interest were amplified from *Plasmodium falciparum* 3D7 genomic DNA, DNA libraries, isolated plasmids or synthesized genes using Phusion High Fidelity DNA Polymerase (NEB) which has proof-reading activity to avoid undesired mutations. Primers and templates used for every construct can be found in Appendix 1. PCR conditions and reagents are detailed in tables below. Amplification was performed in a final volume of 50 μ L. In those cases where no product was obtained or unspecific products were detected, the annealing temperature was optimized using a temperature gradient. Extension time was dependent on the product length and complexity.

PCR standard mix Phusion Polymerase

Reagent	Volume(μ L)	Final concentration
dH ₂ O	32.4	-
5X Phusion Buffer	10	1X
dNTP's (10 mM)	5	1 mM
Primer forward (10 μ M)	1	0.2 μ M
Primer reverse (10 μ M)	1	0.2 μ M
Template	0.3	<250 ng
Phusion Polymerase (2U/ μ L)	0.3	0.012 U/ μ L

Thermocycling conditions for PCR with Phusion polymerase

PCR-step	Temperature (°C)	Time	Cycles
Initial denaturation	98	1 min	
Denaturation	98	30 s	30 X
Annealing	48-65*	90 s	
Elongation	72	1-3 min**	
Final hold	4	~	

* Optimized depending on primer length and product complexity

**variable depending on amplicon size and template concentration

3.1.2 Purification of PCR products and digested vectors

Amplicons and restricted plasmids or inserts were purified from PCR and digestion reactions respectively using a commercial kit Nucleo Spin Gel and PCR Clean –up (Macherey- Nagel) according to manufacturer's protocol. This guarantees the removal of enzymes (digestion enzymes and polymerases), oligonucleotides, salts and additives and the recovery of up to ~15µg DNA from 50 bp to at least 20 kbp.

3.1.3 Digestion of PCR products and vectors

To generate cohesive ends purified PCR products and vectors were digested with the respective enzymes in a volume of 100 µl with a final enzyme concentration of 0.02 U/µl. Restriction enzymes used for every construct are listed in Appendix 1. Reaction was performed for 1-3 hours at 37°C except for construct SBP1mDHFRGFP-PHmut where a BstBI enzyme only active at 65°C was used. DNA integrity and correct digestion pattern was verified by agarose gel electrophoresis. Digested inserts and plasmids were purified as described above (3.1.2)

3.1.4 DNA ligation

To promote join of cohesive ends between insert and restricted vector a ligation reaction was performed using a molar ratio of 1:3 vector to insert. In a total volume of 10 µl, ~100 ng digested vector were incubated with the respective amount of insert, 1 µL 10x T4 ligase buffer and 400 U T4 ligase (NEB) for 1 hour at room temperature or overnight at 16 °C.

3.1.5 Screening PCR to detect bacterial clones

To screen for bacterial colonies carrying the desired plasmid after transformation (See 3.2.2) a PCR master mix with FIREpol polymerase was prepared using a vector specific primer and an insert specific primer following the composition outlined below. The screening PCR reaction was performed in a volume of 10 µl. From the LB-Amp plate where the transformed cells were smeared, a single colony was picked with a pipet tip, inoculated in a second plate to generate a master plate and placed in a PCR tube containing the master mix. At least 16 colonies were screened for every construct. Thermocycling conditions for screening PCR are detailed above. PCR reactions were analyzed by agarose electrophoresis to identify clones with the expected product size.

PCR standard mix (FIREPol Polymerase)

Reagent	Volume(μ l)	Final concentration
dH ₂ O	6.5	-
10X FIREPol Buffer	1	1X
dNTP's (10 mM)	1	1 mM
Magnesium chloride (25 mM)	1	2.5 mM
Primer forward (10 μ M)	0.2	0.2 μ M
Primer reverse (10 μ M)	0.2	0.2 μ M
FIRE Polymerase (2U/ μ L)	0.1	0.02 U/ μ L

Thermocycling conditions for screening PCR (FIREPol)

PCR-step	Temperature ($^{\circ}$ C)	Time	Cycles
Initial denaturation	95	2 min	
Denaturation	95	40 s	30 X
Annealing	48	90 s	
Elongation	68	1-3 min*	
Final hold	4	~	

*variable depending on amplicon size and template concentration

3.1.6 PCR to verify genome integration

PCR verification of genome integration in *P. falciparum* was performed with FIREpol polymerase on genomic DNA (gDNA) of integrant cell lines and 3D7 in a final volume of 40 μ l according to mix composition detailed below. Three different primer combinations were set up to confirm 5' and 3' integration and disruption of endogenous locus using 3D7 gDNA as control.

5' integration was checked using a primer specific for the region upstream of the modified locus and a vector specific reverse primer. 3' integration was verified using a reverse primer specific for the downstream 3' region and a vector specific forward primer.

Reagent	Volume(μ l)	Final concentration
dH ₂ O	25.5	-
10X FIREPol Buffer	4	1X
dNTP's (10 mM)	4	1 mM
Magnesium chloride (25 mM)	2.4	1.5 mM
Primer forward (10 μ M)	1.6	0.4 μ M
Primer reverse (10 μ M)	1.6	0.4 μ M
FIRE Polymerase (2U/ μ L)	0.4	0.02 U/ μ L
Template (gDNA)	0.5	-

PCR-step	Temperature ($^{\circ}$ C)	Time	Cycles
Initial denaturation	90	1 min	
Denaturation	90	20 s	30 X
Annealing	41	20 s	
Elongation	61-65*	1-4 min**	
Final hold	4	~	

* Optimized by temperature gradient

**variable depending on amplicon size and template concentration

3.1.7 Sequencing of plasmids

To exclude mutations in isolated clones at least 0.8 μ g of a purified plasmid were premixed with a specific primer (20 pmol) and adjusted with water to a final volume of 15 μ l. Primers for sequencing should be ~ 20 base pairs and have binding site 30-60 nucleotides upstream of the start sequence. Samples were shipped to SeqLab (Sequence Laboratories Göttingen).

3.1.8 Agarose gel electrophoresis

DNA fragments (PCR products and digestions) were separated by length in an electric field in an agarose matrix (Garoff and Ansorge 1981). Agarose (Invitrogen) was dissolved in buffer 1X TAE to a final concentration of 1% and cooked in a microwave until agarose melted completely. Ethidium bromide was added to a final concentration of 1 μ g/ml and agarose solution was poured in a gel tray and cooled down until it became solid. Agarose gel was placed in an electrophoresis chamber filled with 1X TAE. Samples were diluted with 6x DNA

loading dye and load into wells next to a DNA ladder to determine size of bands. Separation was performed for 25-30 minutes at 150V.

3.1.9 DNA precipitation

For *P. falciparum* transfection protocol 50-100 µg DNA are required. A volume of isolated plasmid (Midi Preparation) containing 50-100 µg DNA was mixed thoroughly with a 1/10 volume sodium acetate 3M, pH 5.0 and further precipitated with three volumes of absolute ethanol. Precipitated DNA was stored overnight at -20 °C before transfection procedure.

3.1.10 Isolation of genomic *P. falciparum* DNA

To verify genome integration, 5-10 ml culture of a *P. falciparum* transgenic cell line with a parasitemia 5-10% were harvested and centrifuged at 1800 rpm for 5 minutes. Supernatant was discarded and culture pellet was processed with the kit QIAamp DNA Mini Kit according to manufacturer's protocol. Genomic DNA was aliquoted and stored at -20 C.

3.2 Microbiological methods

3.2.1 Rubidium chloride method for preparation of chemo-competent bacterial cells

To enable bacterial cells to take up exogenous DNA (circular plasmids) cell envelope has to be destabilized (Hanahan, 1983) by chemical treatment.

LB medium (10 ml) was inoculated with *E. coli* cells XL-10 Gold (NEB) and incubated overnight with vigorous shaking at 37 °C. The next day 4 ml of the culture were transferred into an Erlenmeyer flask containing 200 ml of prewarmed LB medium. Culture was grown at 37°C to an OD₆₀₀ of 0.5-0.55 and immediately cooled down on ice. Cells were recovered by centrifugation at 4 °C for 20 minutes at 2400 g. Bacterial pellets were gently resuspended in cold TBF1 buffer and kept on ice for 10 minutes. Suspension was centrifuged again and pellet further resuspended with TBFII. Aliquots (100 µl) of the bacterial suspension were pipetted into 1.5 ml tubes and stored at -80 °C.

3.2.2 Transformation of *E.coli* chemo competent cells

The heat shock method was performed to promote the uptake of foreign DNA by *E.coli* chemo competent cells. Competent cells were thawed on ice and incubated together with a volume of ligation (10 µl) or diluted plasmid for 30 minutes on ice. Bacterial cells were placed in a thermoblock at 42 °C for 30 seconds and immediately placed back on ice. Cells were suspended with 1 ml prewarmed LB medium (without ampicillin) and shaken for 1 hour at 37 °C. Bacterial suspension was centrifuged at 16000 rpm for 1 minute, most of the supernatant

was discarded and bacterial pellet was resuspended, pipetted on a prewarmed LB – Amp agar plate and spread with sterile glass beads. Plates were incubated overnight at 37 °C.

3.2.3 Cultivation and storage of *E. coli* transgenic cells

Positive colonies detected with screening PCR were picked with a pipette tip from the master plate (See 3.1.5) and inoculated in 2 ml LB medium under antibiotic pressure (ampicillin). Bacteria were grown overnight with continuous shaking at 900 rpm at 37 °C. Cultures were centrifuged for 1 minute at 11000 g and bacterial pellet suspended in 1 ml Glycerol freezing solution (50 % glycerol in 1X LB medium). Bacteria were stored at -80 °C.

3.2.4 Plasmid purification (Mini Prep and Midi Prep)

For plasmid mini-preparations (<25 µg DNA) 2 ml Eppendorf tubes containing LB-Amp were inoculated with bacteria *E.coli* from a single colony and incubated as described above (3.2.3). Bacterial cultures were centrifuged for 1 minute at 11000 g. After discarding supernatant bacterial pellet was processed according to manufacturer's protocol using the NucleoSpin Plasmid Kit (Macherey Nagel) to isolate plasmids. Plasmids were verified by a test digestion and sequenced to discard undesired mutations (See 3.1.7).

For plasmid preparations with a higher DNA concentration (Midi-Preps) required for *P. falciparum* transfection, a positive colony was picked and inoculated in an Erlenmeyer with 100 ml LB Amp. Cultures were incubated overnight at 37°C with constant shaking at 1200 rpm. Bacterial pellets were obtained by centrifugation at 6000 rpm for 15 minutes at 4 °C. Purification of plasmids was performed with Plasmid Midi Kit (QIAGEN) following the kit protocol. DNA pellet recovered was dissolved in 200 µl TE buffer and absorbance at 260 nm was measured in a spectrophotometer (Eppendorf) to determine DNA concentration.

3.3 Cell biological methods

3.3.1 Culture of *P. falciparum*

Asexual erythrocytic stages of *P. falciparum* parasites were grown in petri dishes (6 and 12 ml) or 50 ml culture bottles according to standard procedures (Trager and Jansen, 1976) using RPMI complete medium and human erythrocytes (blood group O+) at a hematocrit of 5 %. Cultures were maintained at 37 °C in an atmosphere of 1 % O₂, 5 % CO₂ and 94 % N₂. Transgenic cell lines were maintained under drug selection using 10 nM WR99210, 1.5 µg/ml Blasticidin. Every second day cultures were smeared and either diluted or fed depending on the parasitemia. To avoid starvation, cultures were diluted to the required parasitemia when it reached more than 2% trophozoites. For biochemical assays that require a high protein amount parasites were grown to ~10% parasitemia and medium was changed twice a day.

3.3.2 Blood smears, Giemsa staining and determination of parasitemia

To determine parasitemia ~0.5 μ L of culture were dropped on a glass slide and a thin smear was distributed with the help of a second slide tilt in an angle of 45°. Smear blood was air-dried and fixed with methanol in a Couplin jar for ~10 seconds. Slides were placed in a Giemsa solution (10%) and stained for 15 minutes. Slides were washed with water, dried and observed at 100X. Infected and uninfected erythrocytes were counted in 5-10 fields where ~100 red blood cells (RBC) per field were homogeneously distributed. Parasitemia was calculated as percentage of infected RBC.

3.3.3 Freezing and thawing of asexual *P. falciparum* parasites

P. falciparum transgenic cell lines can be frozen and stored at -80°C or in liquid nitrogen. Only ring stages will resist the freezing-thawing procedure, thus a culture with a high percentage of ring stages was harvested for a long term stabilate. For cryopreservation of strains 5-10 mL of culture were centrifuged at 1800 rpm for 5 minutes. After discarding supernatant, RBC pellet was resuspended in 1 ml malaria freezing solution (MFS), transferred into a sterile 2 ml cryotube and placed at -80°C or liquid nitrogen for long-term storage.

To recultivate frozen parasite strains, the cryotube was removed from freezer or liquid nitrogen and placed immediately on ice. Cryotubes were transferred to a water bath at 37 °C and quickly thawed. Cell suspension was transferred to a 15 mL conical tube and centrifuged at 1800 rpm for 5 minutes. Supernatant was discarded and 1 ml of pre-warmed malaria thawing solution (MTS) was added drop by drop to resuspend gently the pellet and once again centrifuged. The resulting pellet was suspended in RPMI medium and placed into a 5 ml dish with fresh blood. The next day medium was changed and selection drug was added.

3.3.4 Sorbitol method for synchronization of *P. falciparum* infected RBCs

Synchronous development of *P. falciparum* from ring stage onwards can be achieved by lysis of mature stages using 5% D-sorbitol (Lambros and Vanderberg, 1979). 5-10 ml of a ring asynchronous culture were spun down at 1800 rpm for 5 minutes and pellet was suspended in 5 pellet volumes of pre warmed 5 % D-sorbitol. Suspension was incubated for 5-10 minutes in a water bath at 37 °C and centrifuged at 1800 rpm for 5 minutes. The resulting pellet was washed once with RPMI medium and further centrifuged. After washing, cells were returned to culture and adjusted to the desired parasitemia. Since the cultures will be enriched in mature stages 24 hours later, medium was changed the next day or the culture was diluted to avoid starvation.

3.3.5 Differential purification of *P. falciparum* infected erythrocytes in a Percoll gradient

A Percoll gradient was performed with aim to purify late parasite stages (trophozoite and schizonts) from uninfected RBCs and ring stages based on differential permeability of cells to sorbitol (Aley et al., 1986). 500 μ L of Percoll 80% were first pipetted in a 2mL tube, followed by 500 μ L of the 60% solution and finally 500 μ L 40% solution were layered carefully on the top. A parasite culture was pelleted, supernatant was discarded and cells were overlaid slowly on the top of the gradient. After centrifugation for 5 minutes at 16000 rpm three different phases were observed. The upper phase containing merozoites and debris was discarded, the middle one containing schizonts and trophozoites was transferred to a fresh 1.5 mL tube and the pellet of uninfected RBCs and ring stages at the bottom was discarded or recultured. Late stages collected were suspended with DPBS, centrifuged for 5 minutes at 16000 rpm and washed twice more. Resulting pellet was processed for biochemical assays.

3.3.6 Transfection of *P. falciparum* ring stages by electroporation

Transfer of circular plasmids into the nucleus of *P. falciparum* ring stages is mediated by electroporation (Wu et al., 1995, Spielmann et al., 2006). Precipitated DNA (See 3.1.9) was centrifuged at 16000 rpm for 10 minutes and pellet washed with ethanol 70%. Under sterile conditions pellet was air dried and suspended in 15 μ L of TE buffer followed by 385 μ L of cytomix buffer. 10 mL culture containing between 5 and 10 % synchronized ring stages was harvested and pelleted at 1800 rpm for 5 minutes. Resulting cell pellet (~500 μ L) was mixed with cytomix-DNA solution and transferred into an electroporation cuvette (BioRad).

The electroporation was conducted with a Gene Pulser Xcell (Biorad; conditions: 310 V, 950 μ F, ∞ Ω). Electroporated cells were placed into a 10 mL petri dish containing warmed RPMI medium and incubated under standard conditions (3.3.1). Medium was changed after 6-12 hours and transfected parasites were set on drug pressure (WR or BSD). Cultures were fed daily during 7 days and after the first week every second day. Weekly a drop of fresh blood was added and parasitemia was monitored by Giemsa smears after two weeks. Transgenic parasites appeared in culture between 20 and 40 days after transfection.

Double transfectants strains were generated by transfecting a pARL2 –mDHFR-GFP plasmid expressing blasticidine deaminase as resistance marker into a WR resistant cell line harbouring pARL1-mCherry constructs with hDHFR as resistant marker. Transfectants were put on BSD selection and WR was added only once a week to avoid loss of pARL1 plasmid.

3.3.7 Transfection of *P. falciparum* merozoites

A second transfection method using tightly synchronized schizonts was performed for some constructs to reduce the long selection time required for episomal expression (Moon et al

2013). 20-50 µg DNA were precipitated and washed as described above (3.1.9; 3.3.6), dissolved in 10 µL of TE buffer followed by 100 µL of Amaxa transfection Buffer. 4 mL of Percoll 60% solution were pipetted in a 15 mL Falcon tube and ~8 mL of a culture containing 5-10% schizonts were layered carefully over the solution. The gradient was centrifuged for 8 minutes at 2000 rpm. The brownish phase between Percoll and medium was collected, transferred to a clean 15 mL tube and suspended with warm RPMI. After centrifugation for 5 minutes at 1800 rpm, most of supernatant was discarded and 10-12 µL of schizont pellet were added to the DNA-buffer solution. The suspension was transferred into an electroporation cuvette and electroporated immediately with a Nucleofector II (Amaxa) using program U-033. Electroporated schizonts were transferred to a 1.5 ml tube containing 500 µL warmed medium and 300 µL fresh blood and incubated for 30 minutes at 37 °C in a thermomixer shaking at 650 rpm. Cell suspension was further transferred into a 10 ml petri dish with RPMI medium and hematocrit was adjusted to 5%. Parasites were cultured under standard conditions and selection drug was added 6-24 hours later. Medium was changed daily during the first five days and after this period every second day. Parasites were detected in Giemsa smears 8-15 days after transfection.

3.3.8 Export arrest assays by ligand (WR) induced prevention of unfolding in parasites expressing mDHFR fusion proteins

Parasite cell lines expressing mDHFR fusion proteins were synchronized with 5% sorbitol (3.3.4) to obtain ring stages before they expressed the transgene. Thereafter parasites were grown for 24 hours in presence or absence (control) of 4 nM WR during which transgene expression occurred. The cells were either directly imaged (3.5.1), processed for immunofluorescence assays (IFA) (3.5.2), lysed for parasite extracts, or processed for solubility or protease protection assays (3.3.10-12).

3.3.9 Saponin lysis for selective permeabilization of *P. falciparum* infected RBCs

Saponin is a detergent that lyses preferentially the RBC and the PVM membrane leaving intact the PPM due different lipid compositions between membranes (Benting et al. 1994, Ansorge et al. 1996). To release parasites from RBCs and eliminate hemoglobin from parasite extracts a saponin lysis was performed. For membrane proteins 5-10 ml parasite culture grown to a parasitemia of 5-10 % trophozoites were harvested and pelleted by centrifugation at 1800 rpm for 5 minutes. Cells were resuspended with 10 pellet volumes of freshly prepared 0.03 % saponin (Sigma)/ 1X PBS and incubated on ice for 10 minutes. Lysate was transferred into Eppendorf tubes and spun down for 5 minutes at 16000 rpm. Pellets containing intact parasites and RBC/ PV membranes were pooled and washed with DPBS until no hemoglobin was observed in supernatant. Final pellet was suspended in 2-5

µl complete protease inhibitor cocktail 25X (Roche) and 50-100 µl of lysis buffer (See 2.6.3.2) were added. Extracts were frozen at -20°C or immediately centrifuged for 5 minutes at 16000 rpm. Carefully, supernatant was collected without disturbing debris pellet, transferred to a new tube and further diluted with 6X SDS buffer.

In case of PV soluble or host cell soluble constructs 5-10 ml parasite culture were harvested, pelleted as described above and purified in a Percoll gradient (3.3.5). After washes iRBC pellet was incubated on ice for 10 minutes with 50-100 µl (depending on the size of the pellet) freshly prepared saponin 0.015%/ 1X PBS followed by centrifugation at 16000 rpm for 5 minutes. Supernatant (containing PV and host cell soluble proteins) was transferred to a new tube and mixed with 25x protease cocktail inhibitor and 6X SDS Buffer. Parasite pellet (containing TM and cytosolic soluble parasite proteins) was resuspended with 2-5 µl complete protease inhibitor cocktail (Roche) and 50-100 µl of lysis buffer. Protein extracts were frozen at -20°C and analyzed by Western blot.

3.3.10 Tetanolysin lysis

Tetanolysin is a pore-forming toxin purified from *Clostridium tetani* able to permeabilize selectively the erythrocyte membrane without disrupting the PVM and parasite plasma membrane. This allows for the release of host cell content and sequential lysis of iRBCs. Infected RBCs from 10 ml culture (5-10% trophozoites) were carefully purified in a Percoll gradient (3.3.5) to avoid the presence of uninfected RBCs, which the tetanolysin will lyse preferentially, thereafter washed twice with RPMI medium, transferred into a tube containing 100 µl of DPBS with 1 HU (hemolytical unit) tetanolysin (Sigma) and incubated at 37°C for 10 min. Cell suspension was observed at the microscope to verify permeabilization of RBC membrane. Parasites should look intact surrounded by a RBC membrane ghost. Incubation time or number of HU must be optimized depending on the activity of the tetanolysin batch. Permeabilised parasites were centrifuged at 6000 rpm for 5 minutes. Tetanolysin supernatant was transferred into a new tube, further centrifuged at full speed, transferred to a fresh tube and diluted with 25x protease cocktail inhibitor and 6X SDS Buffer. Parasite pellet was further processed for proteinase K (3.3.12) or solubility assays.

3.3.11 Proteinase K assay

The selective permeabilization of *P. falciparum* iRBCs together with protease protection assays has been useful to reveal the orientation of TM proteins in Maurer's clefts (MCs) or the PVM. (Spielmann et al., 2006; Saridaki et al., 2009; Grüning et al., 2012)

Tetanolysin-lysed parasite pellet was resuspended with DPBS (150 μ l) , equally divided into three tubes containing either 50 μ l DPBS alone (control), 50 μ l DPBS containing 8 U/ml proteinase K (NEB), or 50 μ l DPBS containing 0.03 % saponin and 8U/ml proteinase K, respectively. Tubes were incubated 30 minutes on ice and immediately reactions were quenched and proteins precipitated by adding trichloroacetic acid 20% to a final concentration of 10 % (100 μ l). Samples were incubated 30 minutes on ice and centrifuged at 16000 g for 20 minutes. The supernatant was discarded and protein pellets were washed twice with 100 % acetone, dried briefly, resuspended in 50 μ l 1x TE buffer and frozen at -20°C. Samples were thawed and mixed with 6X SDS sample buffer. Equal amounts of every fraction and tetanolysin supernatant were subjected to Western analysis.

3.3.12 Reversible Cross-Link Immuno-Precipitation (ReCLIP) for Mass spectrometry analyses

3.3.12.1 In-cell DSP cross-linking of iRBCs

With aim to identify potential binding partners of a target protein, a lysine-reactive crosslinker Dithiobis[succinimidyl propionate] (DSP) was used to preserve labile protein-protein interactions before co-immunoprecipitation with specific antibodies. The tagged protein is pulled down together with the interacting proteins and after the cleavage of the cross-linking with a reducing agent (e.g DTT) interacting proteins are released in the eluate and identified by mass spectrometry (MS).

A cell line expressing a -3XHA/ GFP tagged protein expressed from the endogenous promoter was synchronized with sorbitol (3.3.4) and 100 ml culture were grown to 5 % parasitemia (trophozoites) in 50 ml bottles. Culture was harvested and pelleted at 2000 rpm for 5 minutes. Medium was discarded and cells washed twice thoroughly with DPBS. A solution 20 mM DSP was prepared in DMSO and further diluted in DPBS to 0.5 mM. RBC pellet was resuspended in the DSP solution and incubated for 30 minutes at RT to cross link proximal interacting proteins. After centrifugation supernatant was discarded and 10 ml quenching buffer were added to cells and incubated for 10 minutes at RT.

Cell pellet was layered on a Percoll gradient (3.3.5) prepared in a 50 ml Falcon tube (10 ml of each solution) and centrifuged at 9000 rpm for 10 minutes. Fraction containing trophozoites and schizonts was harvested and washed twice with DPBS.

3.3.12.2 Parasite lysis

After washing, resulting iRBC pellet was resuspended with 1-2 ml RIPA buffer containing 2X protease cocktail inhibitor (Roche) and 1 mM PMSF. After two freeze-thaw cycles at -80 °C, lysates were cleared by centrifugation at 16000 g for 10 minutes at 4 °C.

3.3.12.3 Immunoprecipitation

Supernatant was transferred to a pre-cooled tube and diluted 1:2 with dilution buffer to reduce the detergent concentration before binding. 25-50 μ l of mouse monoclonal anti-HA beads (Pierce) or anti-GFP beads (Chromotek) were equilibrated with RIPA buffer and added to lysate. Samples were incubated for 3 hours at 4 °C with end-over-end rotation. Beads were recovered by centrifugation at 11000 rpm for 30 seconds (anti-HA) or at 2000 rpm for 2 minutes (anti GFP) and washed five times with RIPA buffer.

3.3.12.4 Elution and ReCLIP (Smith et al., 2011)

Washed beads were incubated with 50 μ l of complete RIPA buffer supplemented with 100 mM DTT for 30 minutes at 37 °C with gentle shaking. After centrifugation supernatant (ReCLIPed eluate containing potential binding partners) was transferred carefully into a precooled tube and on ice stored until next step. Beads were incubated shortly with 50 μ l NaOH 50 mM, centrifuged and supernatant was saved (Eluate 2). 10% of every eluate was separated by SDS-PAGE and protein was visualized using Silver Stain for Mass Spectrometry (Pierce) (3.4.3).

3.3.12.5 TCA protein precipitation

Proteins eluted from beads (ReCLIPed eluate and eluate 2) were precipitated with trichloroacetic acid (TCA) in a final concentration of 20%, incubated on ice for 30 minutes and centrifuged at 16000 rpm for 20 minutes at 4 °C. Supernatant was discarded and protein pellets were washed once with 17 % TCA, five times with cold acetone and air-dried. Samples were stored at -80°C and shipped on dry ice to mass spectrometry laboratory for further analyses.

3.3.12.6 Proteomic analyses

TCA Protein pellets were solubilized in lysis buffer (6 M urea, 2 M thiourea, 10 mM HEPES pH 8.0) by sonication for 10 min at 4 °C. Proteins were reduced with 10 mM DTT for 10 min at room temperature and alkylated with 55 mM iodoacetamide for 20 min in the dark. Proteins were digested with 0.5 μ g LysC (Wako) for 3h at room temperature. Samples were then diluted 1:4 with water and subsequently digested with mass-spectrometry grade trypsin (Promega) overnight at 32°C. Tryptic peptides were purified by SPE on a SepPAC-tC18 (Waters) according to the manufacturer's instructions, lyophilized and re-dissolved in 0.1% formic acid and spiked with 20 fmol/ μ L of yeast enolase 1 MassPREPTM protein digestion standard (Waters) prior to LC-MS analysis. Tryptic peptides were analyzed using a nanoscale UPLC system (nanoAcquityUPLC) (Waters) coupled online to a Synapt G2-S HDMS mass spectrometer (Waters). Peptides were separated on a HSS-T3 1.7 μ m, 75 μ m x

250 mm reversed-phase column (Waters) using direct injection mode as described before (Distler et al., 2014). Analysis was performed in positive mode ESI-MS using an ion-mobility enhanced data-dependent acquisition workflow (HD-DDA) described in detail previously (Helm et al., 2014). The data were post-acquisition lock mass corrected using [Glu1]-Fibrinopeptide B. LC-MS data were processed using PEAKS v 7.5 (Bioinformatics Solutions Inc) searching against a combined database consisting of UniprotKB/Swissprot human database (UniProtKB release 2015_02) and UniProt Plasmodium 3D7 Reference Proteome, supplemented with common contaminant proteins, which was concatenated to a reversed decoy database, using the following search criteria for peptide identification: i) trypsin as digestion enzyme ii) up to three missed cleavages allowed iii) fixed carbamidomethylcysteine and variable methionine oxidation as modifications. Precursor and fragment ion mass tolerances were set to 15 ppm for precursors and 0.03 Da for fragment ions. The initial false discovery rate (FDR) for peptide identification was set to 1% in PEAKS based on a reversed decoy database search.

3.3.13 Co-immunoprecipitation assays to identify interaction between proteins

To validate interaction between two putative interacting protein partners, a co-immunoprecipitation assay was performed from parasites expressing two tagged proteins. The immunoprecipitation of a protein should allow for the recovery of the putative binding partner in the eluate and viceversa (reciprocal co-IP).

Parasites were grown, cross-linked and lysed as described above (3.3.14.1-3.3.14.2). Cleared lysates were transferred to a pre-cooled tube and diluted 1:2 with dilution buffer to reduce the detergent concentration before binding. 50 μ l of lysate (input) were saved and diluted with 4 x SDS sample buffer and DTT was adjusted to a final concentration of 100mM DTT. 25-50 μ l of mouse monoclonal anti-HA beads (Pierce) or anti-GFP beads (Chromotek) were equilibrated with RIPA buffer and added to lysate. Samples were incubated for 3 hours at 4 °C with end-over-end rotation. Beads were centrifuged and washed as described in 3.3.14.3. An aliquot of 50 μ l supernatant (post- binding or unbound fraction) was saved and mixed with 4 x SDS sample buffer and DTT. Both samples (input and post binding) were heated at 85°C for 5 minutes. Washed beads were eluted in 50 μ l 4 x SDS sample buffer at 85°C for 5 minutes. Beads were centrifuged and supernatant containing eluted proteins (bound fraction) was saved and transferred to a new tube. Equal volumes of input, post binding extract and bound fractions were subjected to Western analysis. For the quantification of Western blot signals, band intensities were measured with a Chemi Doc XRS imaging system (Bio-Rad) and densitometry analyses were done with Image Lab Software 5.2 (Bio-Rad). Data are representative of three independent experiments.

3.4 Biochemical methods

3.4.1 SDS-polyacrylamide gel electrophoresis (SDS-PAGE)

Sodium dodecyl sulphate polyacrylamide gel electrophoresis under denaturing conditions was performed to separate proteins based on the molecular weight of polypeptides. Separating gels were prepared at a concentration of 12 % acrylamide (2.6.4.1), cast between two glasses in a casting gel stand (Bio-Rad) and polymerized for 30 minutes. Stacking gels were prepared at a concentration of 5% acrylamide and layered over the polymerized separating gel. For silver staining precast gels (Mini Protean TGX Bio-Rad) with a gradient 4-15% acrylamide were used. Samples diluted in 4x Laemmli SDS buffer were heated at 85 °C for 5 minutes, loaded into wells next to a prestained (WB) or unstained (silver staining) protein ladder (Thermo) and run in an electrophoresis chamber (Bio-Rad) filled with SDS Buffer running buffer 1X for ~90 minutes at 150 V or until the dye front reached the end of the gel. Separated proteins were further analyzed by silver staining or WB.

3.4.2 Western blot analysis

Proteins resolved in polyacrylamide gels can be transferred to nitrocellulose membranes in such a way that a replica of the original gel pattern can be further identified with specific antibodies against the immobilized proteins (Towbin et al., 1979). A nitrocellulose membrane (PROTRAN) was thoroughly soaked in Western transfer buffer 1X together with two blotting foams and six Whatman paper. A blotting cassette was sandwiched placing a foam followed by three papers and the membrane. The SDS gel was removed carefully from the glasses and laid over the membrane, and further covered with three additional papers and a blotting foam. Proteins were transferred in a blotting chamber filled with cooled transfer buffer at 4 °C for 1 hour at 100 V or overnight at 15 V. To probe with specific antibodies, membranes were first transferred to a 50 ml tube and blocked with skimmed milk 5% / PBS/1X for at least 30 minutes at RT and thereafter incubated on a roller mixer for at least 2 hours at RT or overnight at 4 °C with the primary antibody diluted in milk 5% / PBS 1X (See 2.8.1 for dilutions). Membrane was washed three times with PBS and incubated for 2 hours at RT with the organism specific HRP-conjugated secondary antibody. After washing three times thoroughly with PBS, nitrocellulose was incubated for 5 minutes with a mixture of equal volumes of luminol/enhancer and peroxide solution from an ECL detection kit (Bio-Rad or Thermo) to detect HRP by chemiluminescence. The membrane was placed in a film cassette between two plastic sheets, bubbles were eliminated and medical x-ray screen blue sensitive films were exposed during different time intervals to record light emission and optimize the better signal. Films were developed in a developer Curix 60 (AGFA). Signals intensities were measured as well with a Chemi Doc XRS imaging system (Bio-Rad) and densitometric analyses were done with Image Lab Software 5.2 (Bio-Rad).

3.4.3 Silver staining

For sensitive detection of proteins in samples from IP assays, eluates were separated by SDS PAGE (3.4.1). Gel was transferred into a clean plastic tray with Milli Q water and washed twice for 5 minutes with constant gentle shaking. Gel was covered with fixing solution and proteins fixed for 15 minutes or overnight at RT. Staining and visualization of resolved proteins was performed with the kit Pierce Silver Stain for mass spectrometry (Thermo) according to manufacturer's instructions. Protein bands were imaged with a Chemi Doc XRS imaging system (Bio-Rad) and Image Lab Software 5.2 (Bio-Rad).

3.5 Microscopy

3.5.1 Live cell imaging

P. falciparum cell lines expressing GFP or mCherry fusion proteins were analyzed on a fluorescence microscopy Zeiss AxioScope M1 equipped with a 100X/1,4 numerical aperture oil immersion lens. A Hamamatsu Orca C4742-95 and the Zeiss Axiovision software were used for collecting pictures. Images were processed in Corel PHOTO-PAINT X6. ~500µL culture were incubated with 1 µg/ml DAPI (Roche) for 5 min at 37 °C to stain nuclei of parasites and centrifuged at 2000 rpm for 1 minute. Supernatant was discarded and a drop (5 µL) of infected erythrocytes was imaged in medium at RT (Grüning and Spielmann, 2012).

3.5.2 Immunofluorescence assays (IFAs) with acetone fixed iRBCs

IFAs were performed for the detection of endogenously expressed parasites proteins under standard and WR export arrest conditions. ~500µL of a culture (~5% parasitemia) were harvested and pelleted at 2000 rpm for 1 minute. Cells were washed twice with PBS1X. and resuspended in 750 µL PBS to obtain a hematocrit of ~3%. 50 µL suspension were pipetted onto a well of a 10 well IFA slide (Thermo) and aspirated again only leaving a thin cell monolayer on the well. Cells on slides were air-dried and fixed in fresh acetone 100 % for 30 minutes. Dry slides were rehydrated and washed twice with PBS 1X and placed into a humid chamber. Antibodies were diluted (See 2.8.1) in BSA 3%/ PBS1X containing 100 µg/ml ampicillin. For co-localization IFAs two antibodies were diluted together in an Eppendorf tube. 50 µL of every dilution were applied to the respective well. Slides were incubated with primary antibodies in a humid chamber for 1 hour at RT. Wells were washed with PBS 1X five times. Alexa 488-594-647 conjugated secondary antibodies against a specific organism were diluted 1:2000 in BSA 3%/ PBS1X. Dilutions (50 µL) were applied to wells and incubated for 1 hour at RT followed by five washes with PBS. Slides were allowed to dry and mounting medium (Dako) was dropped between wells. A coverslip was placed onto the slide and sealed with nail polish. IFAs were directly imaged on a fluorescence microscopy Zeiss AxioScope M1 with a 100X/1,4 numerical aperture oil) immersion lens as described above.

Chapter 4. Results

4.1 Dissection of the translocation pathway for TM proteins in the parasite periphery

4.1.1 Approaches to characterize translocation of TM proteins at the parasite periphery

In a first attempt to characterize translocation of a TM protein, REX2 was fused with the mDHFR domain and GFP (REX2-mDHFR-GFP) (Grüning et al., 2012) (See Section 1.4.2.1). The ligand-induced prevention of unfolding of the fusion domain arrested this construct at the parasite plasma membrane (PPM) (Figure 4.1 A). In contrast to *in vitro* studies in yeast mitochondria (Eilers et al. 1988) it was not possible in living *P. falciparum* parasites to chase the arrested mDHFR reporter by removal of the ligand only, as the system appeared not to be reversible (Gehde et al., 2009). This precluded the characterization of the subsequent export steps of a TM protein after passage of the PPM. To circumvent this drawback and to find a reversible system, different fusion proteins were designed, using several mDHFR arrangements and testing different fusion domains.

4.1.1.1 Assessing the role of GFP in preventing reversibility of mDHFR fusion constructs

Gehde et al. 2009 explained this irreversibility by the folding dynamics of the GFP fused after the mDHFR domain. GFP becomes folded irreversibly after reaching the final localization (Deponate, 2012) consequently it prevents further trafficking after removal of the folate analogue (and unfolding of the mDHFR domain) and only new synthesized protein can be translocated. To test whether this is the reason for the observed irreversibility and to possibly circumvent this problem, a construct where GFP was replaced by a myc-tag (a 10 amino acid small tag unable to fold) was generated (REX2-mDHFR-myc) and expressed in the parasite. IFAs were performed from parasites grown in presence or absence of WR, the stabilizing ligand used in this study that prevents unfolding of the mDHFR domain. Treated parasites were next thoroughly washed to remove the ligand and recultured for five hours without WR. Consistent with previous results (Gehde et al., 2009) the arrested mDHFR-myc construct remained blocked irreversibly at the parasite periphery. Small amounts of the fusion protein were found in the clefts five hours later, likely representing newly synthesized protein (Figure 4.1 B). Hence, REX2-mDHFR-myc was unsuitable as a reversible reporter.

In a second attempt to generate a reporter that can be chased after removal of the ligand, the order of the domains (mDHFR and GFP) in the construct was exchanged to REX2-GFP-mDHFR. The rationale for this was that in this new construct GFP might still be unfolded in the translocon when mDHFR blocks the transport and hence after removing the block, GFP would not prevent further transport and mDHFR potentially would become transport competent again. The corresponding construct was exported to the Maurer's clefts and addition of WR arrested it in the parasite periphery (Figure 4.1 C). Attempts to chase the blocked construct five hours after removal also were unsuccessful. Again low level of fluorescence at the Maurer's clefts suggested that only newly synthesised protein had reached these structures. Of note, this construct showed some differences with the previous REX2-mDHFR-GFP that will be discussed in the section 4.2.1. From the REX2-mDHFR-myc and the REX2-GFP-mDHFR constructs it can be concluded if folding of GFP prevents reversibility at all, it is not the only reason why the mDHFR system is not reversible.

4.1.1.2 Insertion of foldable domains into the N-terminus of exported proteins

TM proteins are thought to be delivered to the PPM with the N-terminus in the PV and the C-terminus facing the parasite cytoplasm. In a further attempt to obtain intermediates arrested after the PPM extraction and to investigate the effect on export of the folding state of the N-terminus, foldable domains were fused N-terminally to exported *P. falciparum* proteins. To this end mDHFR was placed into the N-terminus of REX2 (Figure 4.2 A). The corresponding construct REX2-(N-mDHFR)-GFP accumulated at the ER and was not further exported (Figure 4.2 A). This indicated that the introduction of large exogenous domains into the N-terminus may interfere with the insertion into the ER membrane or led to aggregation and retention in the ER. Hence insertion of mDHFR into the N-terminus of REX2 was not useful to characterize export.

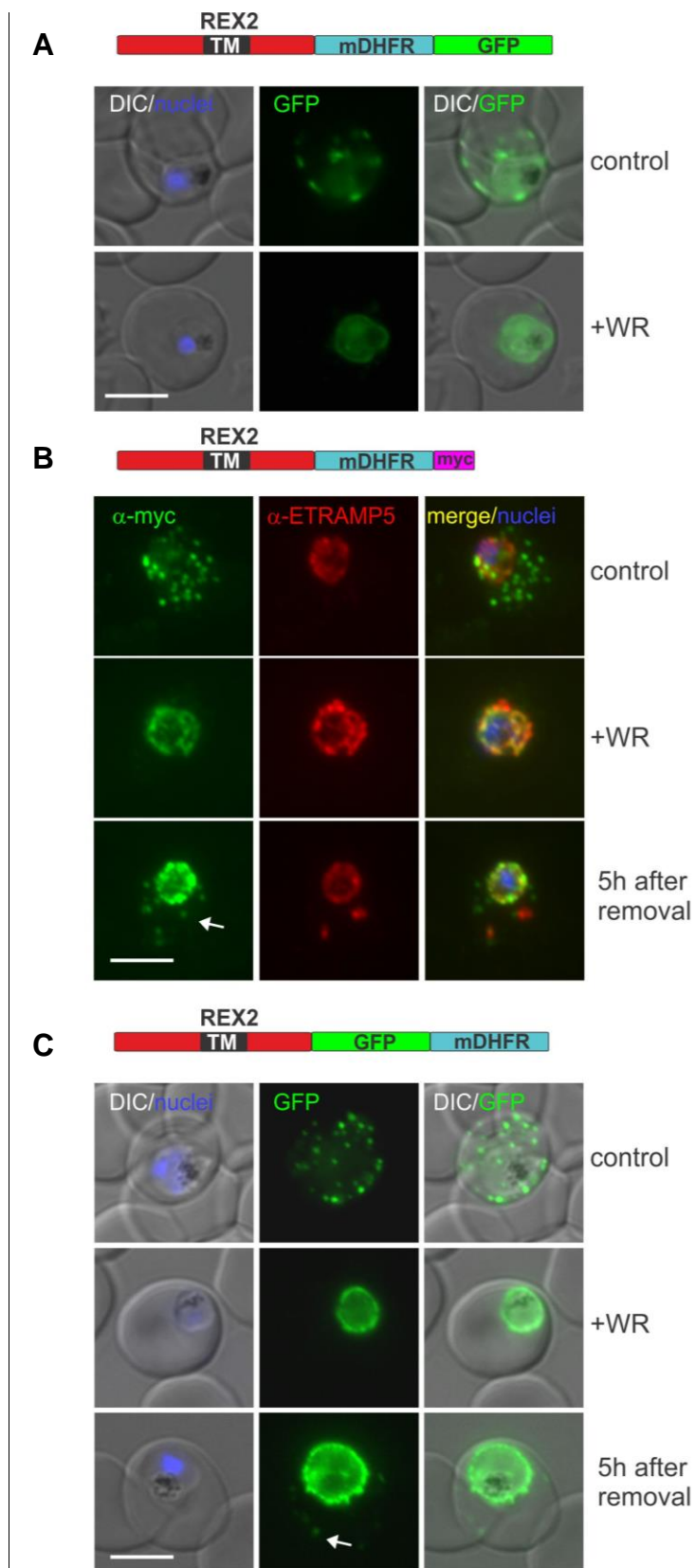


Figure 4. 1 | mDHFR constructs are arrested irreversibly in the parasite periphery. Representative images of live *P. falciparum* parasites expressing REX2-mDHFR-GFP (A) and REX2-GFP-mDHFR (C) or an IFA of parasites expressing REX2-mDHFR-myc detected with anti myc and co-stained with the PVM marker ETRAMP5. (B). The cells shown were grown in presence (+WR), absence of WR (control) and 5 hours after removal of WR, as indicated. Constructs are shown schematically above each panel. Hydrophobic regions (TM, transmembrane domain) are in black. Likely only newly synthesized protein is exported to the MC after removal of the ligand (arrows in B and C) and the blocked construct remains arrested. DIC, differential interference contrast. Nuclei were stained with DAPI. Size bars: 5 μ m.

The zinc finger domains are folded peptide loop structures (Denzer et al., 1995) that can be destabilized by point mutations. It was reasoned that the small size of these domains may be more suitable to insert them into the N-terminus of an exported protein than the large bulky mDHFR domain. For this reason, a wild type (wt) zinc finger domain was inserted into the N-terminus of REX2. The resulting construct REX2-ZnFwt-GFP was exported to Maurer's clefts but also showed some staining in the parasite periphery and within the parasite, likely in the ER (Figure 4.2 B, top panel). In some cells only parasite internal cytoplasmic and/or ER localization was observed (Figure 4.2 B, bottom panel). To test whether these findings were due to folding of the zinc finger domain, a second construct with a mutated unfolded zinc finger was generated. This construct, REX2-ZnFmut-GFP, showed a similar fluorescence pattern to the construct with the wt zinc finger (Figure 4.2 C). This indicated that the limited reduction in export observed with REX2-ZnFwt-GFP was not due to folding of the N-terminal zinc finger domain.

The number of zinc finger in the N-terminus was increased to potentiate possible folding effects expected to block the export. The corresponding constructs, REX2-5XZnFwt-GFP and REX2-5XZnFmut-GFP, containing 5 wt or mutated zinc finger domains, respectively, accumulated in the ER similar to REX2-(N-mDHFR)-GFP (Figure 4.2 D-E), indicating that the extension of the N-terminal region before the TM domain interferes with trafficking, either affecting entry into the ER, aggregation preventing transport, or changed the orientation of the protein in the ER membrane. Based on these results N-terminal fusion of foldable domains was not further pursued to study the translocation of exported proteins into the host cell.

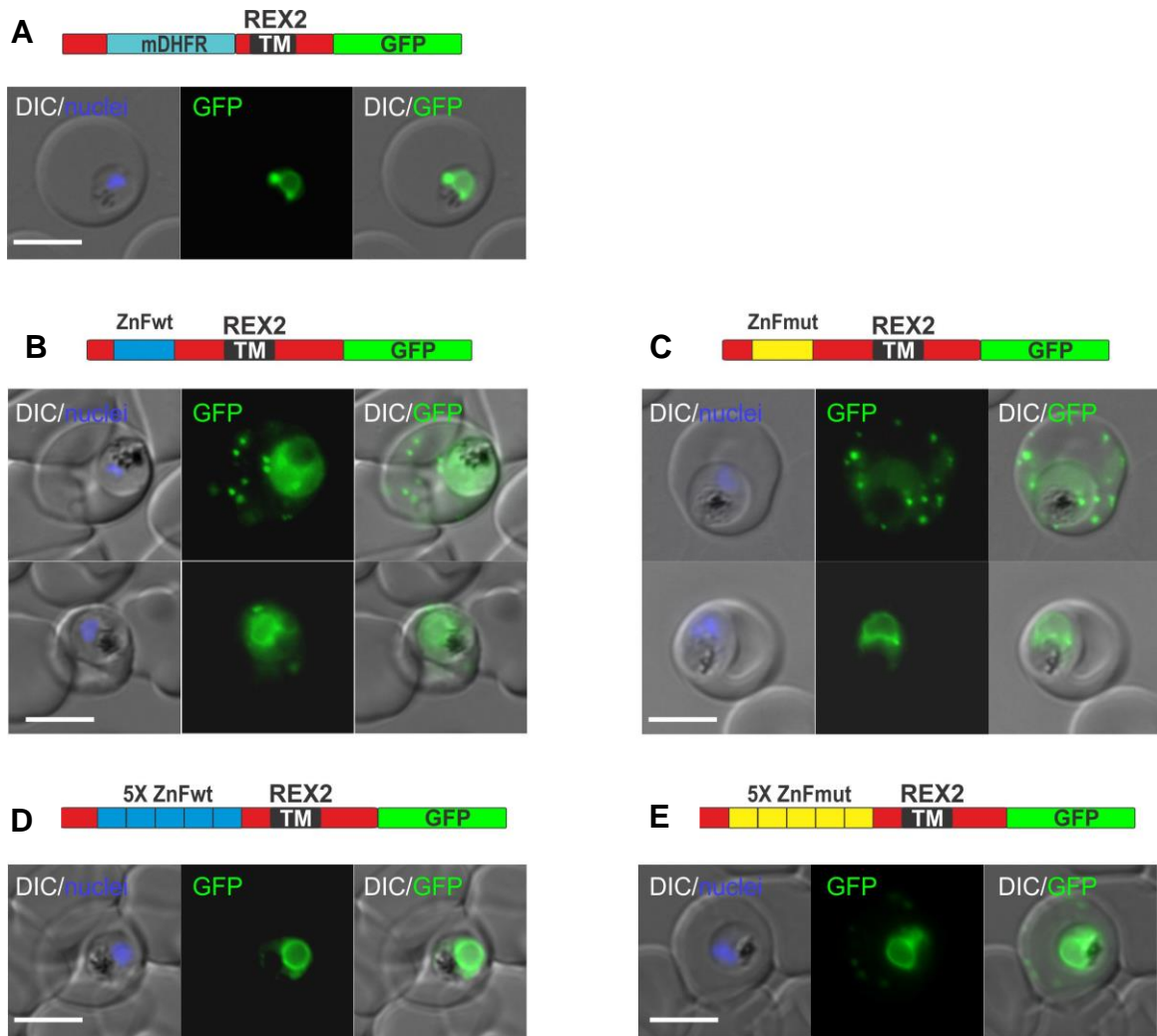


Figure 4. 2 | N-terminal fusions of foldable domains. (A-E) Representative images of live *P. falciparum* parasites expressing the constructs shown schematically above each panel. Hydrophobic regions (TM, transmembrane domain) are in black. Wild type (wt) single zinc fingers (ZnF) are represented by dark blue boxes and mutated (mut) by yellow boxes. DIC, differential interference contrast. Nuclei were stained with DAPI. Size bars: 5 μ m

4.1.2 Redox sensitive folding as an approach to characterize translocation

As all attempts to obtain a reversible system to characterise the translocation after the PPM were unsuccessful, a novel foldable domain was tested to characterize the translocation of a TM protein beyond the PPM. As introduced in section 1.4.2.2, bovine pancreatic trypsin inhibitor (BPTI) is a small domain that becomes folded only under oxidizing conditions (See Section 1.4.2.2). Since the PV is considered to be an oxidizing compartment and the parasite cytoplasm a reducing environment (Kehr et al., 2010; Kasozi et al., 2013; Withers-Martinez et al., 2014) this domain should become folded when it reaches the PV. Thus, if an exported TM protein fused C-terminally with BPTI is released into the PV, oxidative folding of its fusion domain should arrest its further transport as the protein cannot be translocated at the PVM due to the stabilization of the BPTI moiety by the intramolecular disulfide bridges.

To test first whether the PV is actually an oxidizing compartment and also whether the BPTI domain is able to block the translocation at the PVM, the domain was fused C-terminally to REX3, a soluble PEXEL protein that is released directly into the PV before being translocated at the PVM. The construct REX3-BPTI-GFP accumulated in the PV with only partial export into the host cell (Figure 4.3 A). This suggested that the system is suitable to generate translocation incompetent reporters in the PV. To further validate this approach REX3 was fused with a mutated form of BPTI (BPTImut) unable to form disulfide bridges (the cysteine residues were mutated to alanine) (Kowalski et al., 1998). The resulting construct (REX3-BPTImut-GFP) was exported into the host cell with no accumulation in the PV (Figure 4.3 B), indicating that the export arrest seen with REX3 fused to wt BPTI was due the oxidative folding in the vacuole.

Prompted by these results BPTI was fused C-terminally to the exported TM protein REX2 (REX2-BPTI-GFP). The construct showed a strong accumulation in the parasite periphery with only partial export to the Maurer's clefts (Figure 4.3 C). The control construct, REX2-BPTImut-GFP, was fully exported to the clefts (Figure 4.3 D), excluding oxidation unrelated trafficking defects. These results suggest that REX2 is released into the PV after extraction out of the PPM and the subsequent oxidative folding in the vacuole of the fused BPTI domain prevented its translocation across the PVM.

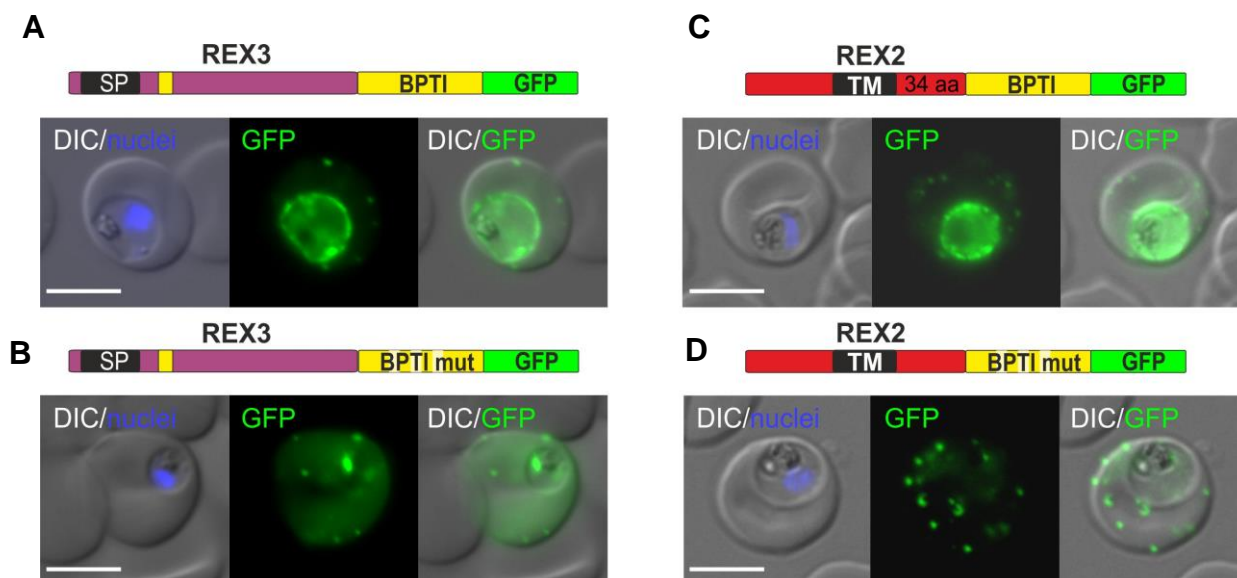


Figure 4. 3 | Fusion with BPTI blocks protein export in the PV by redox sensitive folding. (A-D) Representative images of live *P. falciparum* parasites expressing the constructs shown schematically above each panel. Hydrophobic regions (SP, signal peptide; TM, transmembrane domain) are represented as black boxes, the PEXEL motif in yellow, mutated BPTI (BPTImut) as interrupted yellow box. Length of the C-terminus of REX2 is indicated as number of amino acids (aa). DIC, differential interference contrast. Nuclei were stained with DAPI. Size bars: 5 μ m.

4.1.3 TM proteins are extracted out of the PPM and undergo translocation at the PVM

REX2-mDHFR-GFP arrests in the PPM (Grüning et al., 2012). If BPTI indeed causes oxidation-dependent arrest in the PV, REX2-BPTI-GFP should be found one step further, beyond the PPM. With aim to identify the actual localization of the construct REX2-BPTI-GFP at the parasite periphery, a proteinase K assay was performed from parasites expressing REX2-BPTI-GFP. Three possibilities were considered (Figure 4.4 A): (1) the construct is integral to the PVM, (2) the construct is entirely in the PV after extraction out of the PPM and folding arrest and (3) the construct was arrested at the PPM, which seems to be unlikely, since the parasite cytoplasm is a reducing environment where BPTI should not be folded. Selective permeabilization of the RBC membrane using tetanolysin (Figure 4.4 B) allows the protease to access the N-terminus if the construct is in the PVM (1) and a protected fragment will be observed. If the construct has not yet reached the PVM, situation 2 or 3, it will remain intact. If the localization is as described in (1) and (2), permeabilization of the PVM with saponin would lead to digestion of the construct down to GFP (protease resistant

core) and if it as described in (3) only the N-terminus will be digested and a N-terminally truncated fragment should be detected. To control for differential permeabilisation of the iRBC, REX3 (a parasite exported protein found soluble in the RBC cytosol) was detected to control for proper permeabilization of the RBC membrane, as evident by its release in the tetanolysin supernatant. SERA5 (a soluble parasite protein resident in PV) was detected to control for integrity and permeabilization of the PVM. GAPDH (a cytosolic parasite protein), was detected to show equal loading and as control for integrity of PPM to show that internal parasite proteins were not digested.

As shown in Figure 4.4 C, after permeabilizing the RBC membrane with tetanolysin and addition of protease, only the full length protein and no protected fragment were detected. The degraded GFP observed after permeabilization of the RBC membrane might correspond to the small fraction localized to the Maurer's clefts accessible to the protease (asterisk). When saponin was added, the construct was digested down to GFP and no protected fragment was detectable. This indicates that the construct is entirely in the PV and thus REX2-BPTI-GFP was beyond the PPM (Situation 2) (Figure 4.4 D). These data are consistent with a two-step model of translocation for TM proteins, in which TM proteins are first extracted out of the PPM and released transiently into the PV followed by a translocation step at the PVM.

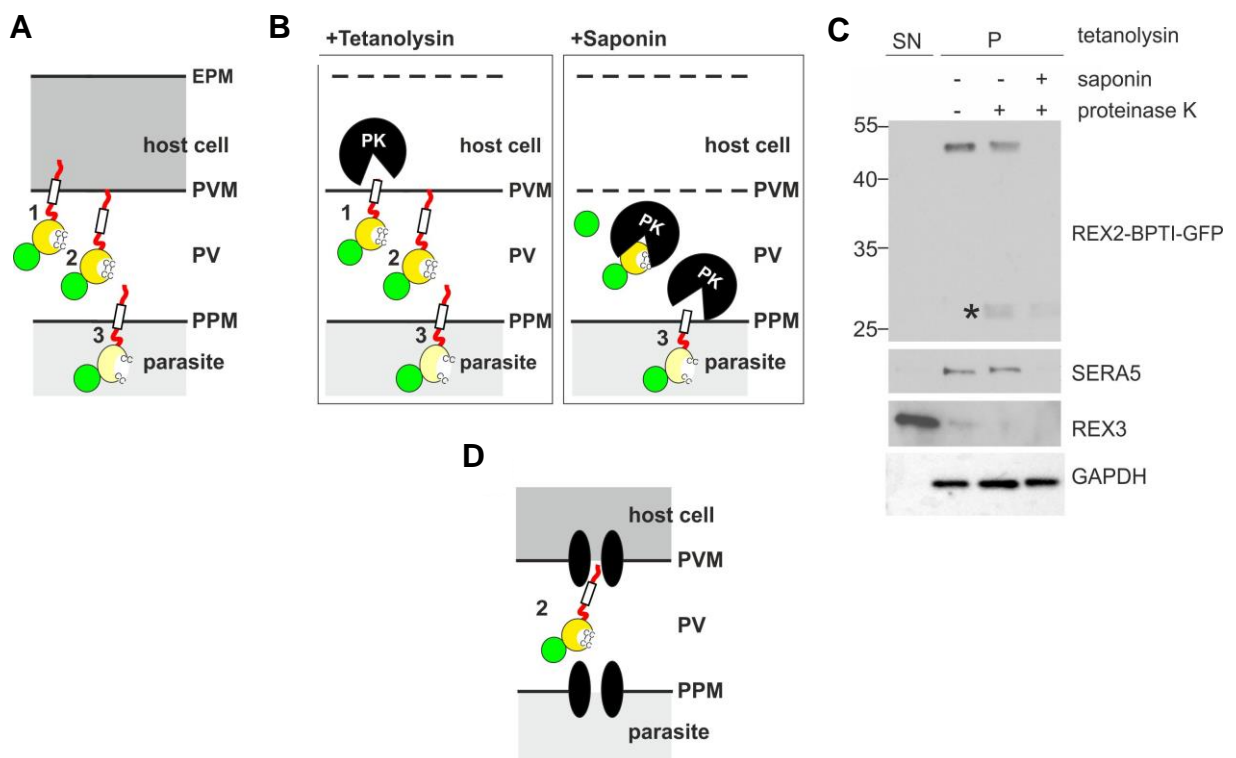


Figure 4. 4 | TM proteins are translocated in a two step process at the parasite periphery. (A) Schematic of an intact iRBC depicting the possibilities for the localization of REX2-BPTI-GFP at the parasite

periphery: (1) protein is integral to PVM; (2) protein is entirely accessible in the PV; (3) protein is integral to PPM. **(B)** Schematic of a proteinase K (PK) protection assay indicating: left panel, permeabilisation of the erythrocyte plasma membrane (EPM) with tetanolysin, only the N-terminus of the construct will be digested if it is in the PVM (1), but it remains intact in situation 2 and 3; right panel, permeabilisation of the PVM with saponin, the construct will be digested if it is in the PVM (1) or the PV (2) but if in the PPM (3), a protected fragment will be generated. Red, exported protein; white box, TM domain; yellow circle, BPTI with double cysteine bonds; green, GFP. **(C)** Western analysis of a protease protection assay according to (B). Digestion is visible only after saponin treatment. As no protected fragment is detectable, the protein is freely accessible in the PV (situation 2). The faint bands (asterisk) represent protein degraded down to GFP (27 KDa). REX2-BPTI-GFP was detected using anti-GFP antibodies. The membranes were reprobbed with anti SERA5 (PV resident) as control for PVM integrity, anti GAPDH (resident in parasite cytoplasm) as control for PPM integrity and as a loading control and anti- REX3 (resident in host cell cytosol) as control for permeabilisation of the EPM. The marker is indicated in kDa. **(D)** Schematic of the location of REX2 based on the protease protection assay shown in (C). Translocation factors are indicated as two black ellipses. Other features are as in (B).

4.1.4 Redox sensitive folding arrest is dependent on the distance between TM domain and fused BPTI

To validate the two-step translocation mechanism for TM proteins two additional Maurer's clefts resident TM PNEPs, SBP1 and MAHRP1, were fused with BPTI. In contrast to REX2 these two constructs were exported to the host cell with no accumulation in the PV (Fig. 4.5 A-B).

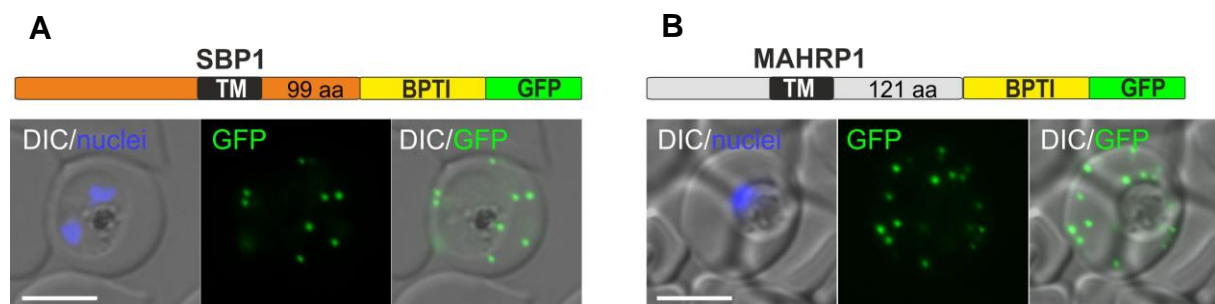


Figure 4. 5 | The export of the TM PNEPs SBP1 and MAHRP1 is insensitive to fusion with BPTI. (A-B) Representative images of live *P. falciparum* parasites expressing the constructs shown schematically above each panel. Hydrophobic regions (TM, transmembrane domain) are represented as black boxes. Numbers refer to length in amino acids (aa) of the sequence between TM domain and BPTI. DIC, differential interference contrast. Nuclei were stained with DAPI. Size bars: 5 μ m.

All these proteins possess a similar structural organization typical for PNEPs (absence of signal peptide, absence of a PEXEL and presence of a single bona fide TM domain) but compared to REX2, SBP1 and MAHRP1 both have larger N- and C-termini. It was reasoned that the length of a TM protein might influence how the protein is translocated at the parasite periphery and that this might affect the folding of BPTI, and hence export.

To test this hypothesis, deletions were generated in SBP1 by removing regions of the N and C terminus previously reported to be dispensable for export of this protein (Saridaki et al., 2009). SBP1 constructs carrying these deletions fused to BPTI-GFP (Δ NSBP1-BPTI-GFP and Δ CSBP1-BPTI-GFP) were then expressed in the parasite. The protein with the shortened N terminus (Δ NSBP1-BPTI-GFP) was not blocked in export (Figure 4.6 A) whereas the deletion of the C-terminus (SBP1 Δ C-BPTI-GFP) led to a clear arrest in the parasite periphery with only partial export to the Maurer's clefts (Figure 4.6 B), comparable to the result obtained with REX2-BPTI-GFP (see Figure 4.3 C). The fusion of Δ CSBP1 with the mutated BPTI (Δ CSBP1-BPTImut) was fully exported (Figure 4.6 C), indicating that the observed block was not due to an export defect introduced by the C-terminal deletion but due to the oxidative folding of BPTI. These results suggest that the length of the C-terminus, specifically the distance between the TM domain and the BPTI, influences the capacity of BPTI to fold in the PV if fused to exported TM proteins. To further confirm this hypothesis the C-terminus of REX2-BPTI was extended by inserting three consecutive REX2 C-termini in order to make it comparable in length with the C-terminus of SBP1. The resulting protein (REX2+3C-BPTI-GFP) was exported to the Maurer's clefts (Figure 4.6 D). This indicates that the observed effect of the C-terminus length is not specific for the protein but likely is solely due to the distance between BPTI and the TM region.

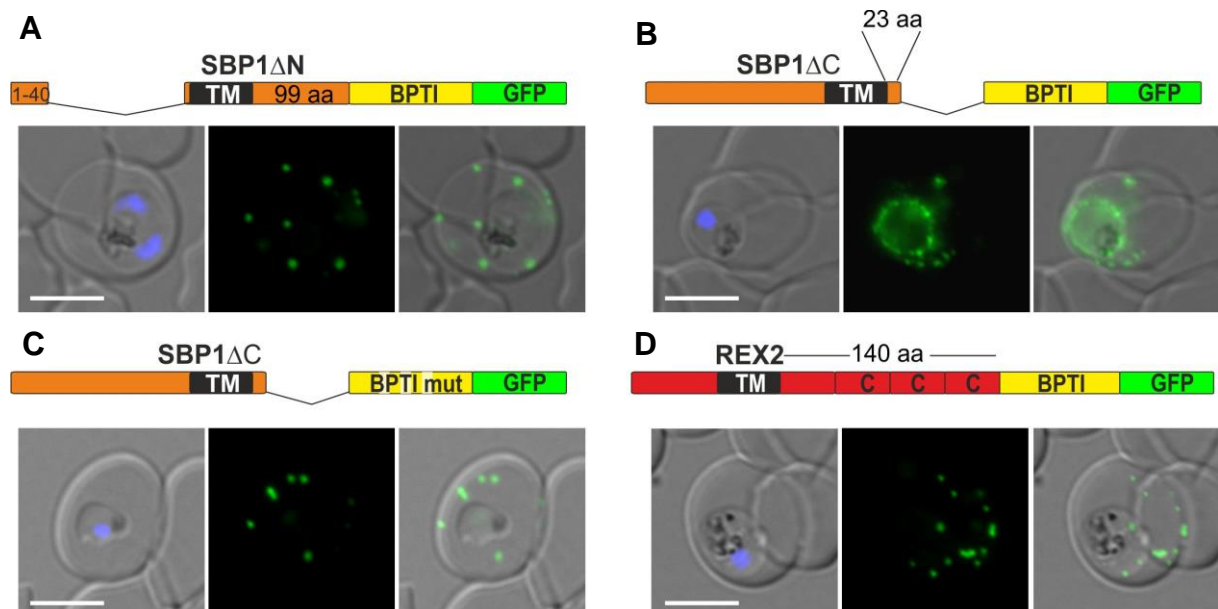


Figure 4. 6 | Length of the C-terminus of exported TM proteins influences redox sensitive export arrest. (A-D) Representative images of live *P. falciparum* parasites expressing the constructs shown schematically above each panel. Hydrophobic regions (TM, transmembrane domain) are represented as black boxes, mutated BPTI (BPTImut) as interrupted yellow box, additional REX2 C-termini as red boxes labelled with 'C'. Numbers refer to amino acids (aa). DIC, differential interference contrast. Nuclei were stained with DAPI. Size bars: 5 μ m.

Taken all together these data suggest that exported TM proteins with a long C-terminus are not sensitive to the BPTI folding and that translocation at the PVM is then not prevented. One explanation for this would be that proteins with long C-termini might engage with the translocon at the PVM while they are being extracted out the PPM which could prevent the release into the PV and thus the oxidative folding. In contrast, in proteins with a short C-terminus the protein is released into the oxidising PV before engaging the PVM translocon, leading to folding of BPTI and transport arrest at the PVM.

4.1.5 PEXEL TM proteins are translocated in a similar two-step process

The fact that TM PEXEL proteins depend on PTEX components to be exported (Beck et al., 2014; Elsworth et al., 2014) suggest that this class of proteins are also translocated to pass from the parasite into the host cell. However, there is so far no demonstration that these proteins indeed require unfolding to be exported. To test this two well-characterized PEXEL TM proteins, PTP1 (Maier et al., 2008; Rug et al., 2014) and STEVOR (PF3D7_0900900), were fused to mDHFR-GFP. The resulting transgenic parasites (parasite cell lines kindly generated and pictures in Figure 4.7 A-C taken by Ferdinand Reinsch) displayed correct localization of the proteins to the Maurers cleft's and upon addition of WR the constructs accumulated in the parasite periphery (Figure 4.7 A-B), confirming translocation as the mode of export for these proteins.

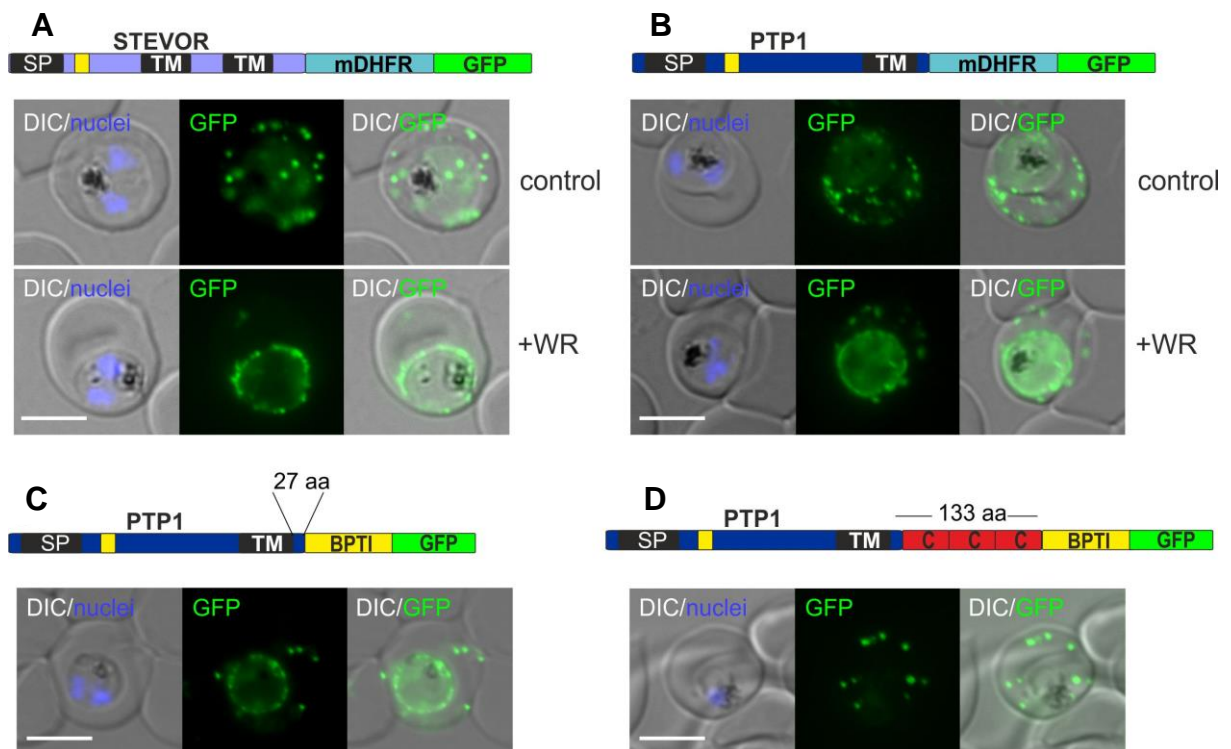


Figure 4.7 | In the parasite periphery PEXEL TM proteins are transported in a two -step translocation process into the host cell. (A-B) Representative images of live *P. falciparum* parasites expressing the mDHFR constructs shown schematically above each panel grown in presence (WR+) or without WR (control). Hydrophobic regions (SP, signal peptide; TM, transmembrane domain) are represented as black boxes, the PEXEL motif in yellow. **(C-D)** Live cell imaging of *P. falciparum* parasites expressing the BPTI constructs shown schematically above each panel. Mutated BPTI (BPTImut) as interrupted yellow box, additional REX2 C-termini as red boxes labelled 'C'. Numbers refer to length in amino acids (aa) of the sequence between TM domain and BPTI. DIC, differential interference contrast. Nuclei were stained with DAPI. Size bars: 5 μ m.

These data together with previous studies (Gehde et al., 2009; Grüning et al., 2012; Heiber et al., 2013) support the hypothesis that all types of exported proteins in *P. falciparum* are translocated in an unfolded conformation in the parasite periphery to reach the host erythrocyte.

Next, to confirm that the two-step translocation process observed with PNEPs is a common export mechanism for PNEP and PEXEL TM proteins, PTP1 was fused to BPTI. This protein was arrested in the parasite periphery, demonstrating sensitivity of the export to BPTI (Figure 4.7 C). The fact that PTP1 has a short C-terminus (27 amino acids), comparable to the C-terminus of REX2 (34 amino acids), may explain its sensitivity to oxidative folding-dependent export arrest. Consistent with the results obtained in section 4.1.4, the extension of the C-terminal region of this construct (PTP1+3C- BPTI GFP) led to full export of the fusion construct to the Maurer's clefts. In conclusion, PNEP and PEXEL TM proteins are

translocated at the PVM and based on the similar behaviour depending on the C-terminal length, appear to share similarities in this trafficking step at the parasite periphery.

4.2 Translocation intermediates arrest global protein export in *P. falciparum* by jamming a shared translocon at the PVM

4.2.1 PNEP TM –mDHFR constructs co-block export of an exported control protein without mDHFR domain

Prompted by the differences observed with SBP1 and MAHRP1 fused to BPTI compared to REX2-BPTI-GFP (see section 4.1.4) and in order to analyze their requirements for unfolding, SBP1 and MAHRP1 were fused to mDHFR-GFP and expressed in a cell line co-expressing REX2-mCherry. This second construct, lacking an mDHFR domain, functions as an internal control to exclude general effects on protein export and provides resistance against WR, as previously done with mDHFR constructs (Grüning et al., 2012; Heiber et al., 2013). Both fusion proteins SBP1-mDHFR-GFP and MAHRP1-mDHFR-GFP were correctly trafficked and co-localized with the internal control REX2-mCherry at the Maurer's clefts. The addition of WR arrested both mDHFR constructs in the parasite periphery, indicating translocation as mode of export for these proteins (Figure 4.8 B-C), similar to REX2 (Grüning et al., 2012; Figure 4.8 A) and PEXEL TM proteins (Figure 4.7 A-B).

Unexpectedly, in contrast to the cell line REX2-mDHFR-GFP (Grüning et al., 2012) (Figure 4.8 A), not only the mDHFR fusion protein was arrested but also the internal control was blocked in export. In addition, these new mDHFR constructs showed two noticeable differences to the phenotype observed with REX2-mDHFR-GFP: the presence of partial export into the host cell (leakiness) and small mobile worm-like protrusions reaching into the host cell (arrows). The construct REX2-GFP-mDHFR (differing to REX2-mDHFR-GFP in the order of the fusion domains, see Section 4.1.1) showed a similar phenotype to SBP1 and MAHRP1 when it was co-expressed with the internal control (Figure 4.8 D).

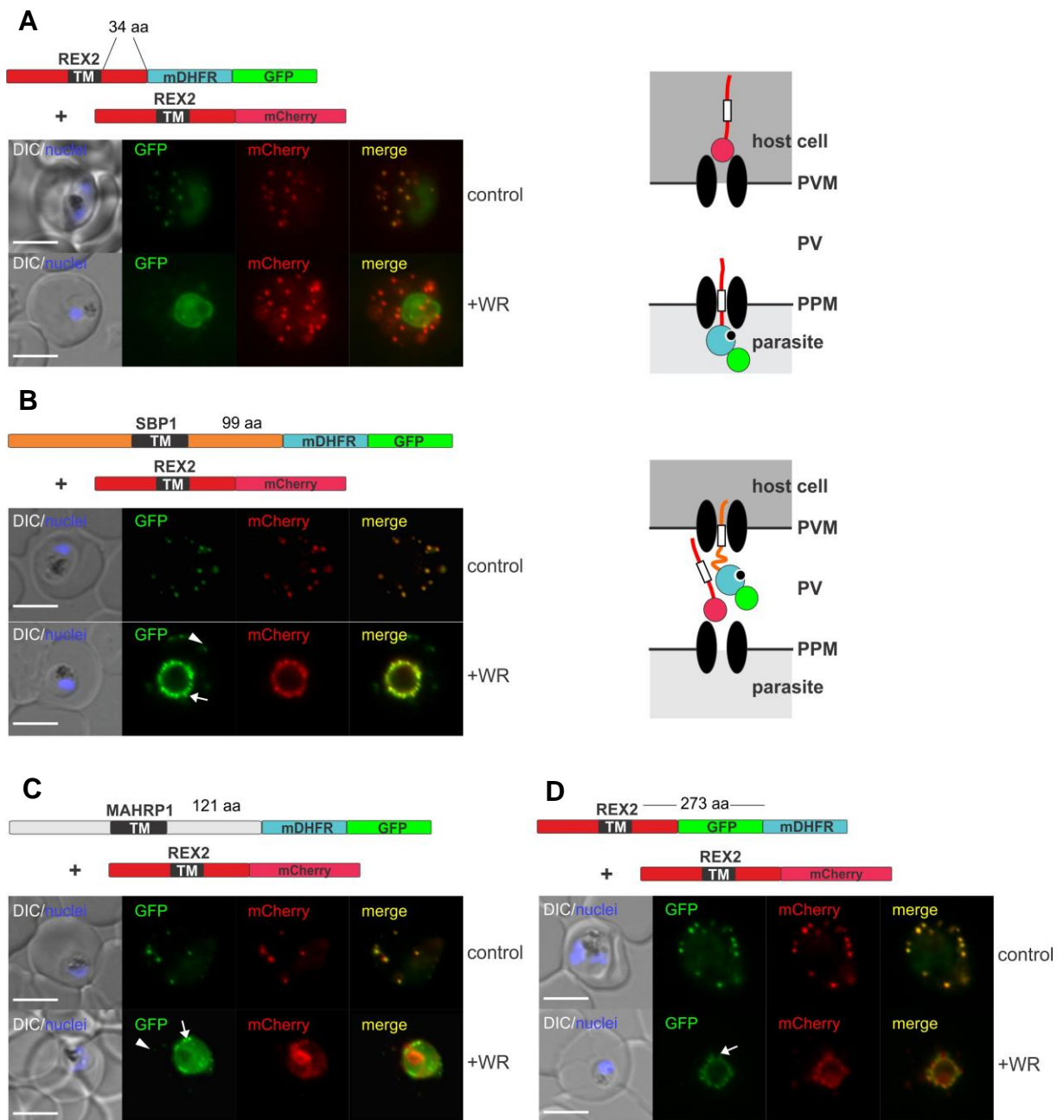


Figure 4. 8 | mDHFR fusions jam a shared translocon and co-block the export of other proteins. (A-D) Representative images of live *P. falciparum* parasites expressing the constructs shown schematically above each panel grown in presence (+WR) or absence of WR (control). Hydrophobic regions (TM, transmembrane domain) are shown as black boxes. Numbers refer to length in amino acids (aa) of the sequence between TM region and mDHFR domain. DIC, differential interference contrast; arrow heads indicate faint signals at the Maurer's clefts; arrows show mobile worm-like protrusions. Size bars: 5 μ m. The schematics of the parasite periphery shown to the right of the figure **A** and **B** depict the potential location of the fusion protein containing the folded WR-bound mDHFR domain (light blue circle with smaller black circle in binding pocket) and the co-expressed REX2 (red line) fused to mCherry (red circle); green circle, GFP; white box, TM.

The possibility that the block in export of the internal REX2-mCherry control was due to an interaction of REX2 with each of the 3 proteins this was observed with (SBP1, MAHRP1 and REX2 itself) was unlikely, especially as it did not occur with the original REX2-mDHFR-GFP (Figure 4.8.A). These results therefore suggested that these new mDHFR constructs, when arrested by folding, became stable translocation intermediates that prevented the passage of the internal control (REX2-mCherry), probably by jamming a shared type of translocon at the PVM (Figure 4.8 B, right). This effect was termed 'co-block' to refer to the block of a translocation competent protein by an arrested mDHFR substrate. This effect was clearly caused by the mDHFR fusion protein, as in a subpopulation of cells not expressing the mDHFR construct (present in the same culture), REX2-mCherry was correctly trafficked to the Maurer's clefts in presence of WR (Figure 4.9). In contrast, REX2-mCherry was always arrested in parasites harbouring the GFP-tagged mDHFR fusion.

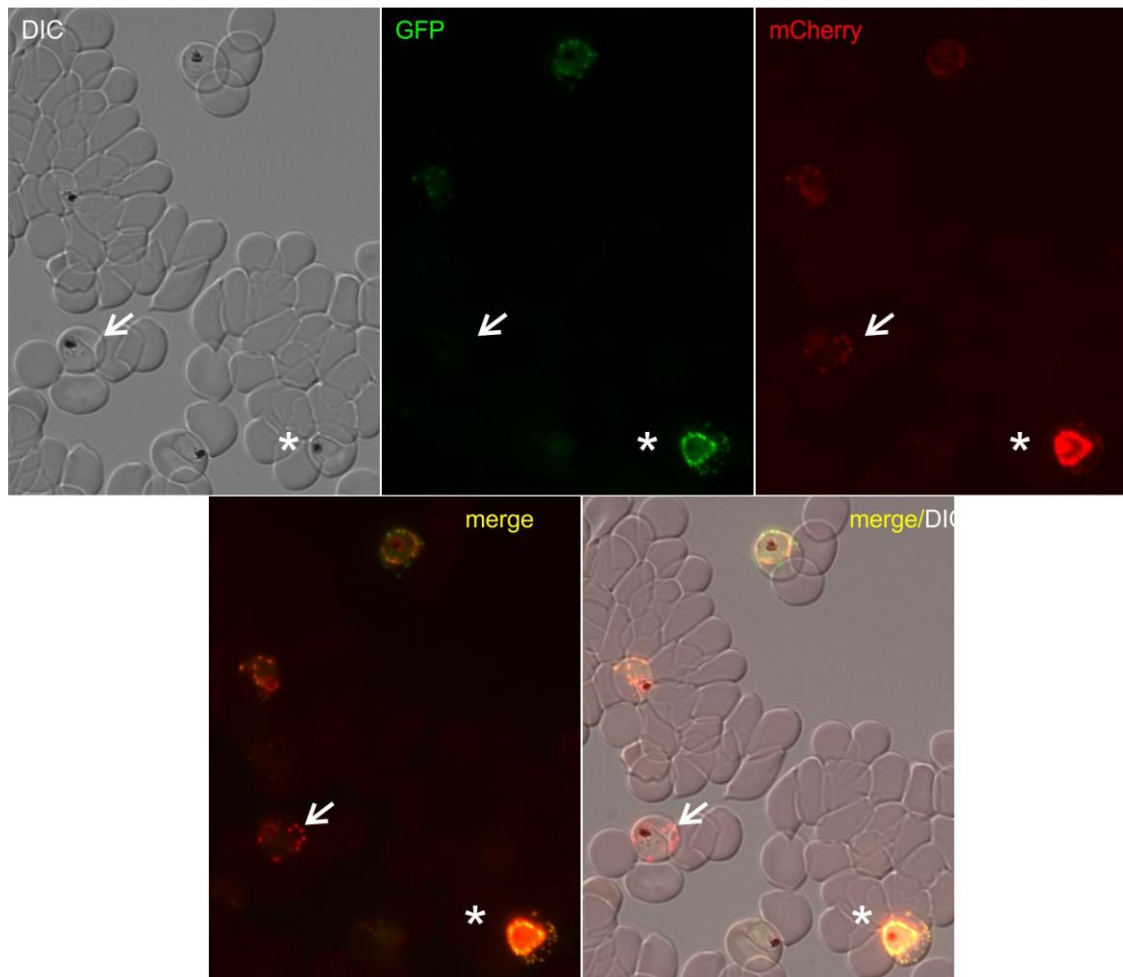


Figure 4. 9 | The export block of the REX2mCherry control depends on the expression of the mDHFR fusion protein. Representative live fluorescence images containing several infected RBCs in a culture of the cell line expressing SBP1-mDHFR-GFP together with the internal control REX2mCherry in the presence of WR. Note that double transgenic cell lines frequently contain a proportion of parasites expressing only one of the

transgenes. REX2-mCherry is fully exported to the Maurer's clefts in a cell expressing only the mCherry construct but not SBP1-mDHFR-GFP (arrow). In contrast, in cells that express SBP1-mDHFR-GFP (asterisk), both proteins are blocked at the parasite periphery. DIC, differential interference contrast.

4.2.2 The stable translocation intermediates are arrested in the PV

REX2-mDHFR-GFP, after prevention of unfolding, was found to be arrested at the PPM (Grüning et al., 2012). Due the differences observed between REX2-mDHFR-GFP (the construct that did not cause co-block) and the co-blocking construct SBP1-mDHFR-GFP, the localization of the export blocked SBP1-mDHFR-GFP was investigated in double transfectant parasites with a proteinase K assay as described above in Section 4.2.3 (Figure 4.10 B).

After RBC permeabilization with tetanolysin the protein remained intact and no protected fragmented was observed (Figure 4.10 B situation 1). However, after saponin permeabilization of the PVM the blocked construct was digested down to the core mDHFR-GFP (the stabilization of the mDHFR domain by the ligand renders it protease-resistant) but no protected fragment was detected. These results suggest that the construct is neither in the PPM nor PVM but in the PV (Figure 4.10 B Situation 2). Nevertheless, due the small size difference between this core and a protected fragment (assuming the protein is inserted up to the mDHFR moiety into the translocon), it could not be concluded from this experiment whether the construct is stuck in the PPM translocon (situation 3 in Figure 4.10 B) or whether it is entirely in the PV (situation 2 in Figure 4.10 A). To control for selective fractionation of the iRBC, REX3 was detected to control for proper permeabilization of the RBC membrane. To control for integrity and permeabilization of the PVM, SERA5 (a soluble parasite protein resident in PV) was detected. Aldolase (a cytosolic parasite protein) was used as loading control and as control for integrity of PPM.

Interestingly the co-blocked REX2-mCherry control was also found in the PV in WR treated parasites (Situation 2, Figure 4.10B), as no protected fragment was observed after permeabilization of the PVM (Figure 4.10 A). The presence of a co-blocked TM protein in the PV affirms that the site of arrest of the co-blocking construct is the PVM and that PPM extraction of REX2-mCherry is not hampered by jamming the PVM translocons. This further supports a two-step model of translocation for TM proteins.

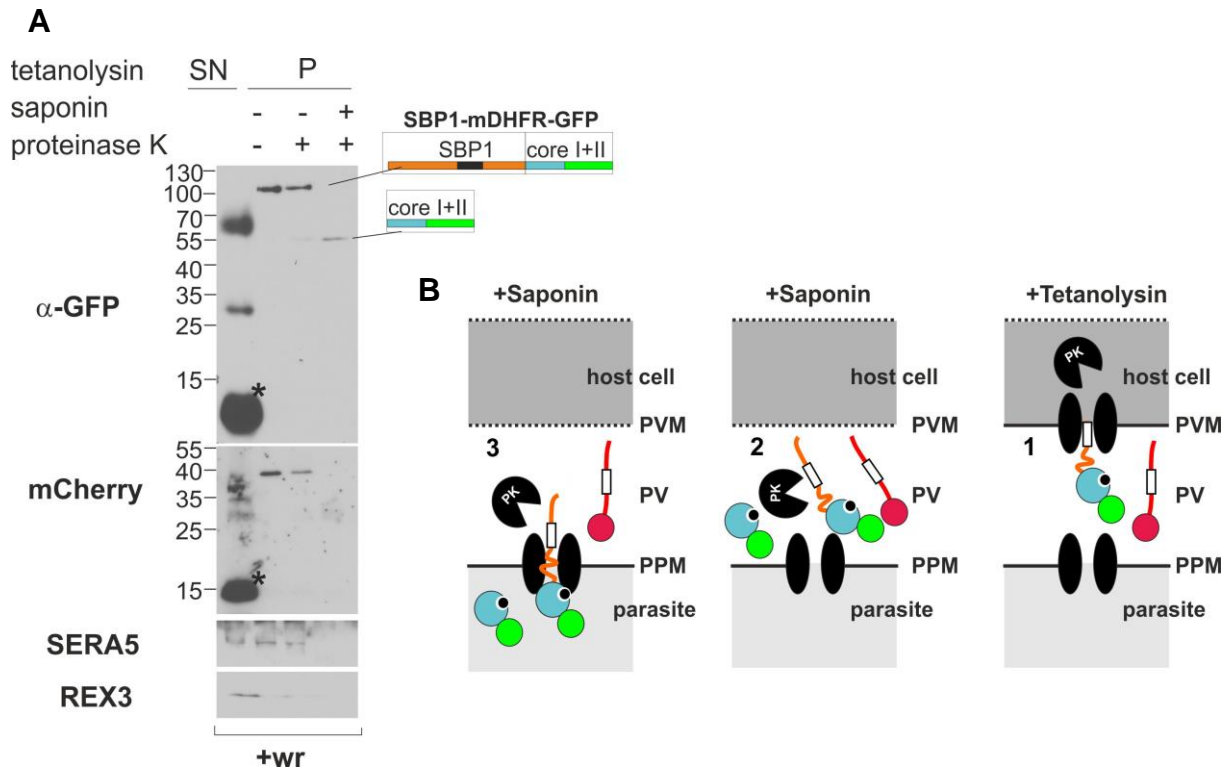


Figure 4. 10 | SBP1-mDHFR-GFP constructs are arrested in the PV (A) Western blot analyses of a representative proteinase K assay with double transfectant parasites expressing SBP1-mDHFR-GFP+ REX2mCherry grown in presence of WR shows digestion of the construct (detected with anti-GFP) down to the core mDHFR-GFP after saponin permeabilization. The same is the case for the co-blocked REX2-mCherry (mCherry is completely digested by the protease and no detectable resistant core remains). Calculated molecular weights are: 85 kDa for the full length construct, 48,9 kDa for core I+II and 21 kDa for core I. **(B)** Schematics of a protease protection assay show the possible locations in the parasite periphery of the fusion protein SBP1-mDHFR-GFP containing the folded WR-bound mDHFR domain (light blue circle with smaller black circle in binding pocket) and the co-expressed REX2 (red line) fused to mCherry (red circle); white box, TM; green circle, GFP; black circle labelled with pk, protease. Controls are as follows: REX3, for release of the host-cell cytosol; SERA5, for release of PV material.

To distinguish these two possibilities a protease sensitive domain [a mutated PH domain (Varnai and Balla, 1998)] was appended to the C-terminus of the construct to increase the size of the potential protected fragment (Figure 4.11 A). If the construct is arrested up to the mDHFR domain into the PPM translocon, a larger protected fragment should be detected after saponin permeabilization of the PVM (situation 3 in Figure 4.11 B) and if the construct is entirely in the parasitophorous vacuole, the construct would be digested down to the protease resistant core (situation 2 in Figure 4.11 B).

The resulting construct SBP1-mDHFR-GFP-PHmut was similarly trafficked to the Maurer's clefts and conditionally arrested at the parasite boundary in presence of WR (Figure 4.11 A). A protease protection assay performed with WR treated parasites showed that after permeabilizing the RBC with tetanolysin, no protected fragment was observed (Figure 4.11

C), excluding situation 1 (Figure 4.11 B). After saponin permeabilization of the PVM, the size of the digested product was consistent with that of the protease resistant core (mDHFR-GFP) and no larger protected fragment was detectable (Figure 4.11 C). This confirms that indeed the construct is fully accessible to the protease in the PV (Figure 4.11 B, situation 2). This series of assays indicates that the blocked SBP1-mDHFR-GFP, after the PPM extraction, is arrested in the vacuole, where it prevents the export of other proteins by jamming a shared type of translocons at the PVM. It can be concluded that the site of arrest for export blocked SBP1-mDHFR-GFP-PHmut is different from that observed for REX2-mDHFR-GFP.

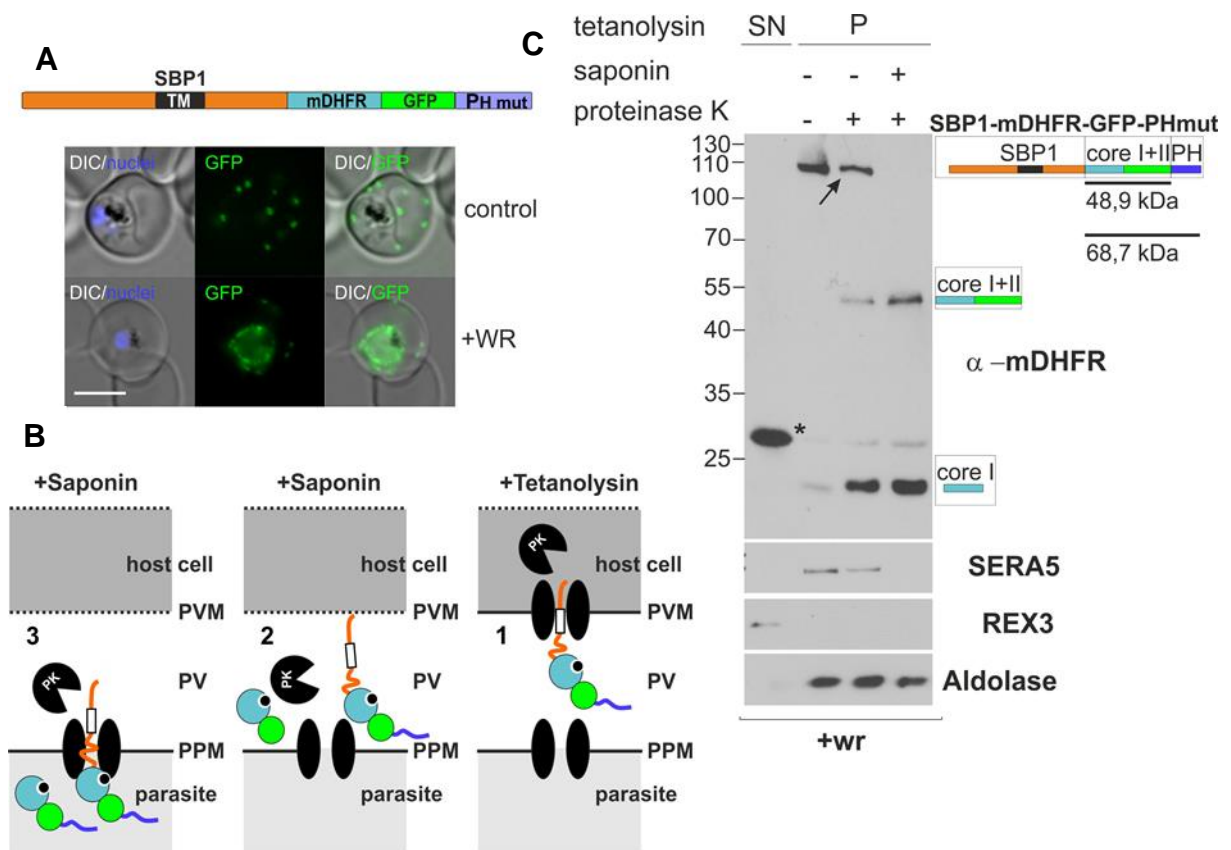


Figure 4. 11 | SBP1-mDHFR-GFP constructs are arrested in the PV (A) Representative live cell images of *P. falciparum* parasites expressing SBP1-mDHFR-GFP-PHmut grown with (WR+) and without WR (control). DIC, differential interference contrast. Nuclei were stained with DAPI. Size bars: 5µm. **(B)** Schematic of a protease protection assay according to features as in (A) shows the likely localizations of the arrested construct SBP1-mDHFR-GFP-PHmut in the parasite periphery and the accessibility of the protease after selective permeabilization with tetanolysin and saponin. Purple line, protease sensitive mutated PH domain. **(C)** Western blot of a representative protease protection assay with WR treated parasites expressing SBP1-mDHFR-GFP-PHmut. The construct (detected with α-mDHFR antibodies) is in the PV, as only full length protein (after permeabilization of the RBC membrane) or protease resistant cores (after saponin treatment) but no larger protected fragment indicative of an intact C-terminus, is detectable. Calculated molecular weights are, 105 kDa for the full length construct, 48,9 kDa for core I+II and 68,7 kDa for I+II+PH and 21 kDa for core I. Arrow indicates full length protein after tetanolysin permeabilization. The asterisk indicates a band likely representing RBC derived

hDHFR. Detected controls are as in A. The marker is indicated in kDa. Controls are as follows: REX3, for release of the host-cell cytosol; SERA5, for release of PV material; parasite aldolase, for integrity of PPM and as loading control.

4.2.3 Stable translocation substrates co-block export of all types of exported proteins

The next important question was to establish whether these new PNEP mDHFR-fusions arrested in translocation co-block also other types of exported proteins besides REX2-mCherry. To this purpose SBP1-mDHFR-GFP was expressed together with mCherry tagged members of each of the different known groups of exported proteins. The co-expressed proteins included the soluble PEXEL proteins REX3 and KAHRP, the soluble PNEP MSRP6, and the TM PEXEL protein STEVOR. In the resulting cell lines both proteins were correctly expressed and trafficked into the host cell (Figure 4.12 A-D). Upon the addition of WR SBP1-mDHFR-GFP was arrested in translocation and in each case the co-expressed mCherry fusion protein was also hindered in export (Figure 4.12 A-D). Similarly REX2-GFP-mDHFR (the domain order that in contrast to REX2-mDHFR-GFP led to a co-block of REX2-mCherry) caused a co-block of the PEXEL protein KAHRP (Figure 4.12 E). In these experiments co-expression was done by expressing two individual proteins from the same open reading frame using a skip peptide (Szymczak et al., 2004; Straimer et al., 2012).

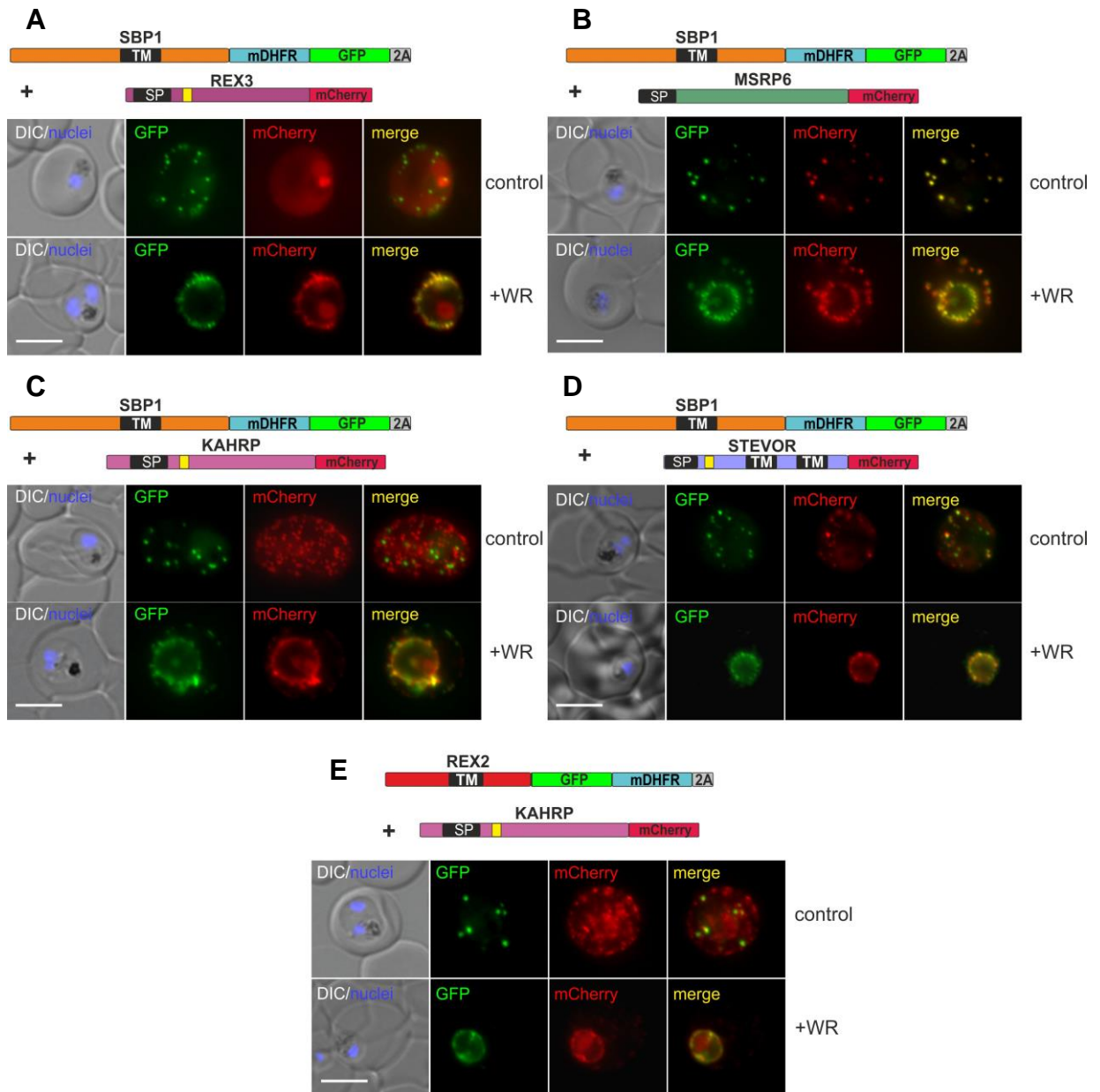


Figure 4.12 | Different types of exported proteins pass through the same type of translocons. (A-E) Representative images of live *P. falciparum* parasites expressing the constructs shown schematically above each panel grown in presence (+WR) or absence of WR (control). Hydrophobic regions (SP: signal peptide; TM transmembrane domain) are indicated as black boxes, PEXEL motif in yellow, the skip peptide is indicated by a grey box labelled 2A. The two proteins expressed from the same open reading frame are shown skipped. DIC, differential interference contrast. Nuclei were stained with DAPI. Size bars: 5µm.

Western blot analysis demonstrated efficient 2A mediated skipping and co-expression of individual proteins (Figure 4.13 C). In addition, to validate the skip peptide approach, some of the protein combinations were also tested using double transfection with two plasmids carrying each one of the co-expressed proteins (Figure 4.13 A-B).

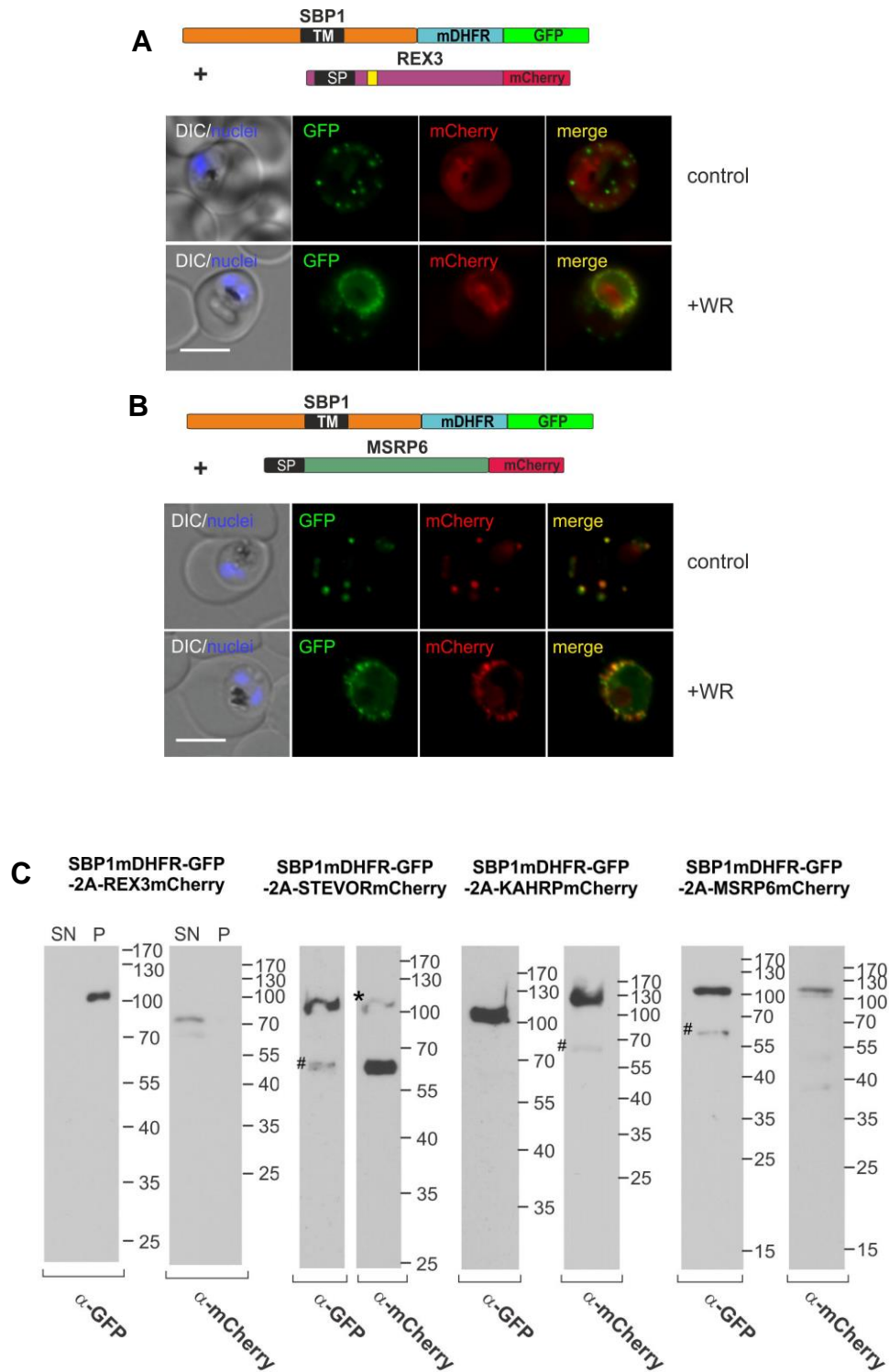


Figure 4. 13 | Skip peptide (2A) enables efficient polycistronic expression comparable to double transfection. (A-B) Representative live cell images of the double transgenic parasites expressing SBP1-mDHFR-GFP with either the PEXEL protein REX3mCherry (A) or the PNEP MSRP6 (B) from a second plasmid show comparable results to the same combinations expressed from a single mRNA using a skip peptide (Figure 4.12 A-B). Hydrophobic regions (SP: signal peptide; TM transmembrane domain) are indicated as black boxes, PEXEL motif in yellow. DIC, differential interference contrast. Nuclei were stained with DAPI. Size bars: 5µm. **(C)** Western blots demonstrate efficient skipping of the 2A containing constructs. Molecular weight standards are indicated (in kDa) on the left. Saponin supernatant (SN) and pellet (P) after Percoll enrichment are shown for the

REX3mCherry expressing cell line as REX3 is found soluble in the host cell cytosol and otherwise would not be detected. The calculated molecular weights are: SBP1-mDHFR-GFP: 87.5 kDa; STEVORmCherry: 60.85kDa; REX3mCherry: 64.5 kDa; MSRP6mCherry: 97.6 kDa; KAHRPmCherry: 98.2 kDa. As typical for many *P. falciparum* proteins, most products show a slower migration than expected. The asterisk indicates anti-GFP signal left over in an anti-mCherry reprobe of the same filter. Hashes indicate weak degradation products.

To confirm the data observed with episomally expressed artificial constructs, endogenous exported proteins were detected in SBP1-mDHFR-GFP by IFA using specific antisera. Under export arrest conditions (WR+), proteins expressed late during the life cycle such as MSRP6 (Heiber et al., 2013) and KAHRP, were consistently co-blocked in the parasite periphery by the mDHFR arrested substrate (Figure 4.14 A). In contrast, proteins expressed earlier in the cycle, such as REX-1 and MAHRP-2, were unaffected (Figure 4.14 B).

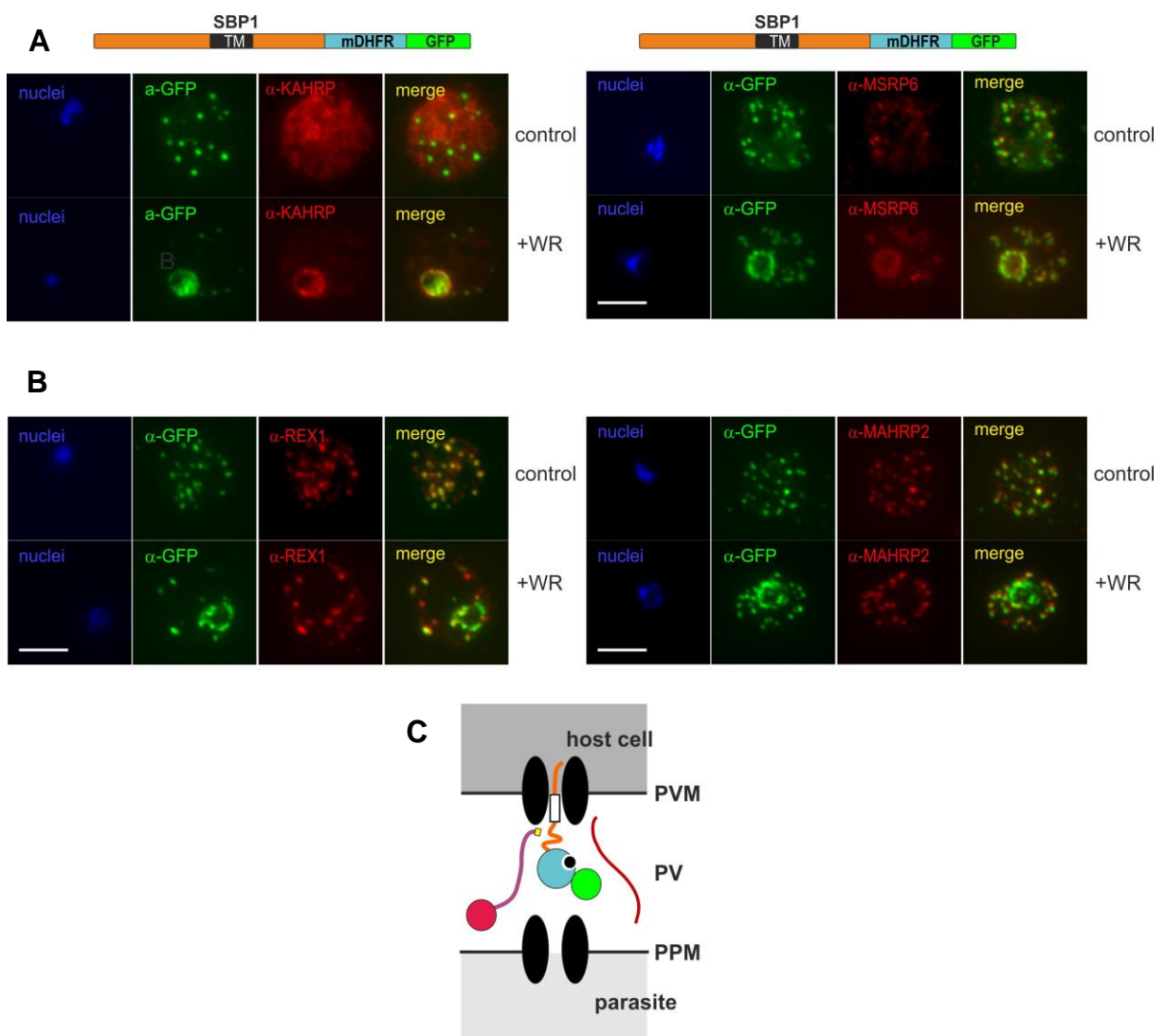


Figure 4. 14 | Endogenous exported proteins are co-blocked by mDHFR translocation intermediates. (A) Co-localization IFAs of parasites expressing SBP1-mDHFR-GFP grown with (WR+) and without WR (control) stained with antibodies against late expressed antigens: anti- KAHRP and anti-MSRP6. (B) Co-localization IFAs with the same cell line but detecting early expressed antigens, REX1 and MAHRP2, shows failure of episomal intermediate to co-block early endogenous protein. The mDHFR intermediate was detected with anti GFP. Nuclei

were stained with DAPI. Size bar: 5µm **(C)** Schematics of the parasite periphery to depict the model of co-block where SBP1-mDHFR-GFP prevented the export of artificial episomal constructs and endogenous proteins. Folded WR-bound mDHFR domain (light blue circle with smaller black circle in binding pocket); co-expressed soluble protein (purple line); mCherry (red circle); endogenous protein (red line); TM (white box); GFP (green circle); the yellow small box indicates the mature PEXEL N-terminus.

These findings correlate with the known expression timing of the episomal SBP1-mDHFR-GFP under the *crt* promoter, which drives expression from late ring stage onwards. Hence only proteins that were expressed after the expression of SBP1-mDHFR-GFP were co-blocked. Fitting with this reasoning, when SBP1-mDHFR-GFP was expressed under the SBP1 endogenous promoter (starting 3-6 hours post-invasion) (an integrant cell line kindly provided by A. Blancke-Soares), early and late antigens were co-blocked (See Section 4.3).

Taken together, these data show that TM PNEPs arrested during translocation hamper the export of all known types of exported proteins. The most likely explanation is that they clog a common type of translocons at the PVM and this supports the idea that all exported proteins cross the PVM through the same protein- conducting channel (Figure 4.14 C).

4.2.4 A soluble PEXEL protein can block export of TM proteins

The results obtained with TM PNEP translocation substrates indicated that all proteins pass the PVM through the same protein- conducting pore at the PVM. If the same type of translocon is involved in the export of all proteins, PEXEL proteins should also be able to hinder the export of TM PNEPs. To confirm these assumptions it was next investigated whether PEXEL protein can form translocation intermediates that induce a co-block. To this end double transfectant cell lines were generated expressing either the soluble PEXEL protein REX3-mDHFR-GFP or the integral TM PEXEL protein PTP1-mDHFR-GFP (Section 4.1.5) alongside the TM PNEP REX2-mCherry. After growing the double transfectant REX3-mDHFR-GFP+REX2-mCherry in presence of WR, the mDHFR construct was arrested at the parasite periphery and induced a co-block of REX2-mCherry as evident by an accumulation of this protein in the parasite periphery (Figure 4.15 A). This indicated that soluble PEXEL proteins are also capable to cause a co-block. Worm-like, mobile protrusions were observed with the fluorescent proteins in this cell line (arrows), similar to the phenotype of the other co-blocking constructs (see Figure 4.8). Since REX3 is a soluble protein directly released from the secretory pathway into the PV, the results obtained with this cell line support the idea that the site of arrest where all proteins converge is a translocon at the PVM (Figure 4.15 A, bottom). Moreover, the fact that a soluble protein can block the export of a TM protein

demonstrates that TM proteins undergo a second translocation step at the PVM, supporting the results obtained with BPTI constructs (Section 4.1.2) and protease protection assays (Section 4.2.2). Finally, these findings also show that the block at the PVM does not affect extraction of exported TM proteins out of the PPM.

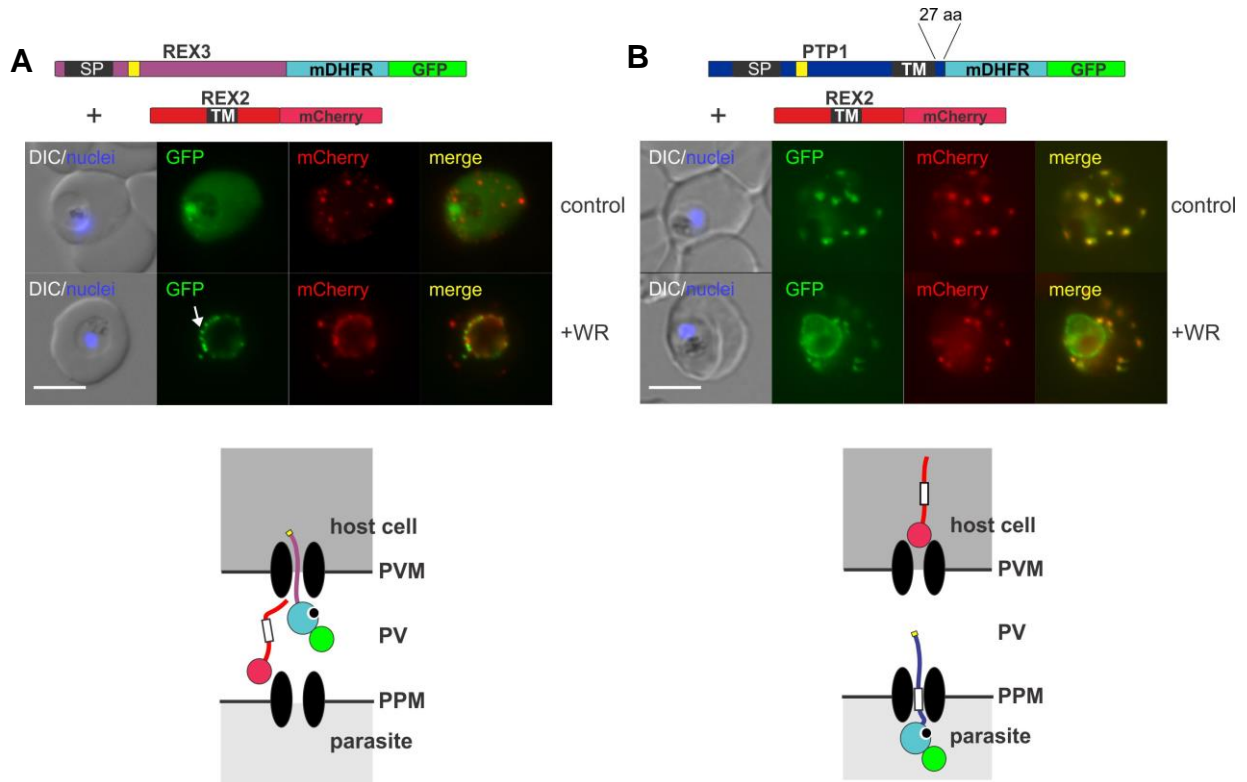


Figure 4. 15 | PEXEL proteins can block the export of a PNEP TM protein (A) Top, representative images of live double transfectant *P. falciparum* parasites expressing REX3-mDHFR-GFP and REX2-mCherry in presence (+WR) or absence of WR (control). Hydrophobic regions (SP: signal peptide; TM transmembrane domain) are indicated as black boxes, PEXEL motif in yellow. Arrows indicate mobile protrusions DIC, differential interference contrast. Nuclei were stained with DAPI. Size bars: 5µm. Bottom, model of co-block where a soluble mDHFR intermediate prevents export of a TM protein without interfering with its PPM extraction. Folded WR-bound mDHFR domain (light blue circle with smaller black circle in binding pocket); REX2 (red line) fused to mCherry (red circle); green circle, GFP; white box, TM; small yellow box, processed PEXEL N-termini. **(B)** Top, representative images of live double transfectant *P. falciparum* parasites expressing PTP1-mDHFR-GFP and REX2-mCherry in presence (+WR) or absence of WR (control). Features as in (A). Bottom, schematic of the parasite periphery that depicts the failure of PTP-1 to induce a co-block as the protein appears to be arrested at the PPM and does not hamper the PVM translocation. Numbers refer to the length in amino acids (aa) of the sequence between TM region and mDHFR domain. Features as in A.

Interestingly, in contrast to REX3-mDHFR-GFP, no co-block was observed with PTP1-mDHFR-GFP (Figure 4.15 B). PTP1-mDHFR-GFP showed a similar phenotype to REX2-mDHFR-GFP (Figure 4.8 A) in WR treated parasites as it did not show worm-like protrusions extending from the PVM but a smooth fluorescence pattern and it did not prevent the export

of the internal control REX2-mCherry. As mentioned in Section 4.1.5, these both proteins have in common a short C-terminus and hence a short distance between the TM region and the mDHFR domain. This suggested that PTP1 behaves similar to REX2, as the protein appears to be arrested at the PPM and does not interfere with the PVM translocation. This may explain the failure to co-block (Figure 4.15 B, bottom and Figure 4.8 A).

4.2.5 Co-blocking properties of a TM mDHFR construct are related to the length of the region between the TM and the mDHFR domain.

The failure of some TM constructs (PTP1 and REX2) to induce a co-block raised questions regarding the differences between co-blocking and no-co-blocking mDHFR substrates and the pathway by which these proteins are translocated at the parasite periphery. It is noteworthy that TM mDHFR constructs that induce a co-block (SBP1, MAHRP1) were not sensitive to the BPTI-induced oxidative folding and those constructs sensitive to BPTI (REX2 and PTP1) did not induce co-block. This led to the hypothesis that the length of the region between the TM domain and the blocking domain (from now on termed 'spacer'), which was found to influence the sensitivity of export to BPTI fusion proteins (see 4.1.4), might also influence the capacity of a TM construct to induce co-block.

To test this correlation the C-terminal region of REX2-mDHFR-GFP was extended by inserting three REX2 C-termini (as described in section 4.1.4) and the resulting construct was expressed in the REX2-mCherry expressing cell line. This extended spacer turned REX2 into a co-blocking molecule (Figure 4.16 A) as evident upon addition of WR. Consistently, when the C-terminus of SBP1-mDHFR-GFP was shortened, Δ CSBP1-mDHFR-GFP, this construct was not anymore able co-block the export of REX2-mCherry (Figure 4.16 B). Of note, the remaining C-terminus (23 amino acids) of Δ CSBP1 after deletion was comparable to the spacer of REX2 and PTP1 (both no-blocking constructs) and the export of the construct Δ CSBP1 was sensitive to BPTI fusion (Figure 4.6 B).

To validate this as a common mechanism for exported TM proteins and not only an effect seen with PNEPs, the importance of the spacer length was tested in the TM PEXEL protein PTP1. The BPTI fusion of this protein was already shown to behave similarly to PNEP TM proteins, displaying a spacer length dependent sensitivity of export to fusion with this domain (see Figure 4.7). To test whether this correlation with PNEPs held also for mDHFR fusions of PTP1, the C-terminus of PTP1-mDHFR-GFP was also extended and expressed together with the internal control REX2-mCherry. The protein (PTP1+3C-mDHFR-GFP) accumulated

at the parasite periphery upon addition of WR and displayed a similar behavior than other constructs with long spacer, hampering the export of REX2-mCherry (Figure 4.16 C).

From these results it can be conceived that the length of the spacer determines both, the capacity of a construct to induce a co-block and the sensitivity to oxidative folding in the PV. The results are summarized in the table 4.16 D, correlating the sensitivity to each foldable domain and the suspected site of arrest for every type of construct.

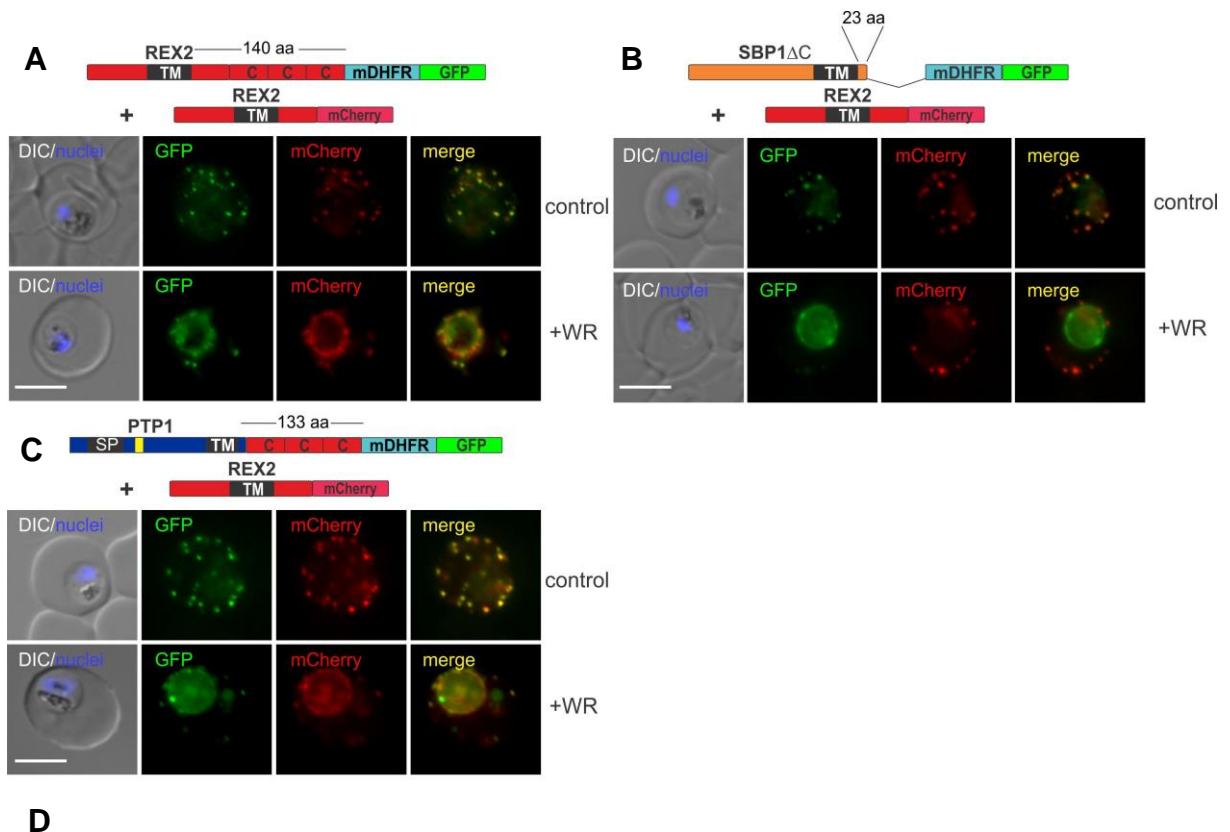


Figure 4. 16 | Length of the spacer determines the capacity of a mDHFR TM construct to induce a co-block (A-C) Representative images of live double transfectant *P. falciparum* parasites expressing the constructs shown schematically above each panel grown in presence (+WR) or absence of WR (control). Hydrophobic regions (SP: signal peptide; TM transmembrane domain) are indicated as black boxes, PEXEL motif in yellow, additional C-termini as red boxes labeled with C. Number refer to length in amino acids (aa) of the spacer between TM region and mDHFR domain. DIC, differential interference contrast. Nuclei were stained with DAPI. Size bars: 5µm. **(D)** Summary of correlation between BPTI and mDHFR constructs indicating the sensitivity to each domain, the observed localization in either parasitophorous vacuole (PV), PV membrane (PVM), parasite plasma membrane (PPM) or the host cell (HC).

4.3 Parasite growth is dependent on protein export

The translocation intermediates described above can be used as a tool to induce a global blockade of protein export in *P. falciparum*. To observe the effect of blocking general protein export, an integrant cell line expressing SBP1-mDHFR-GFP from the endogenous locus was generated (SBP1-mDHFR-GFP^{endo}, kindly provided by Alexandra Blancke Soares). In contrast to episomal expression genome integration ensures that all parasites harbour the blocking construct. SBP1 was chosen because the protein is expressed early in the cycle (Grüring et al., 2011) which allows the export arrest of early expressed proteins. In addition, the protein is not essential for the development of the parasite *in vitro* (Cooke et al., 2006; Maier et al., 2007). Furthermore, its mDHFR version, as shown in Section 4.2.3, was capable to prevent the export of all types of exported proteins.

SBP1-mDHFR-GFP^{endo} was detected in the resulting cell line from young ring stages onwards and trafficked correctly to the Maurer's clefts. Similar to the phenotype observed with the episomal construct the protein was arrested in the periphery of the parasite after WR induced prevention of unfolding (Figure 4.17 A). Genomic DNA from SBP1-mDHFR-GFP^{endo} was analyzed by PCR using genome and plasmid-specific primers to verify correct integration into the *sbp1* locus (PCR analysis kindly carried out by Alexandra Blancke – Soares) (Figure 4.17 B). Western Blot using antibodies specific against SBP1 as well as anti-mDHFR and anti GFP antibodies demonstrated the tagging of the endogenous protein with mDHFR-GFP and the absence of unmodified locus in the integrant cell line (Figure 4.17 C). A 21 KDa band corresponding to the human DHFR was detected in SBP1-mDHFR-GFP^{endo}, since this cell line expresses it as the resistance marker from the integrated plasmid after drug selection, conferring resistance to the folate analogue WR (Figure 4.17 C).

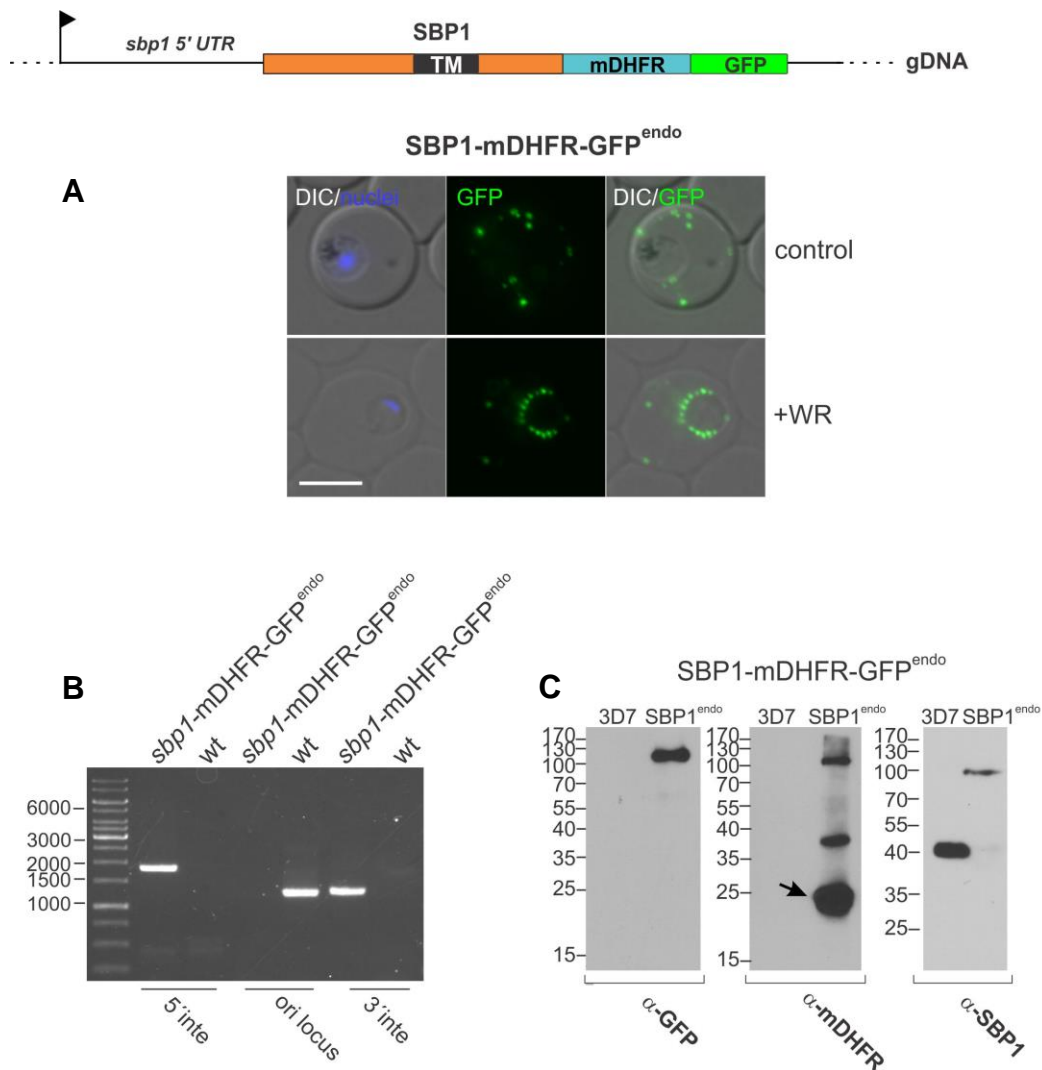


Figure 4. 17 | Endogenous tagging of SBP1 with mDHFR-GFP (A) Representative live fluorescence images of integrant cell line expressing endogenous SBP1 fused to mDHFR-GFP (SBP1-mDHFR-GFP^{endo}) grown with (+WR) and without WR (control). DIC, differential interference contrast. Nuclei were stained with DAPI. Size bar: 5µm. (B) PCR on genomic DNA of SBP1-mDHFR-GFP^{endo} and 3D7 (wt) parasites (as indicated) shows correct integration of the plasmid into the genome, leading to fusion of the endogenous *sbp-1* gene with *mdhfr* and *gfp*. A genome and a plasmid-specific primer were used each to confirm correct 5' and 3' integration. Primers (Table S1) were SBP1-Int-check_F (3 bp after start ATG) with GFP42_rev to demonstrate 5' integration (5'inte, 1815 bp) and SBP1-Int-check_R (23 bp after stop) with pARL55sense to demonstrate 3' integration (3'inte, 1285 bp). Primers SBP1-Int-check_F and SBP1-Int-check_R were used to detect the unmodified original locus (1227 bp). (C) Western blot analysis detects SBP1-mDHFR-GFP (85 KDa) but not unmodified SBP1 (36.3 KDa) in SBP1-mDHFR-GFP^{endo} parasites while 3D7 contains only unmodified SBP1. Anti-mDHFR antibodies also detect the resistance marker (hDHFR) (21 KDa) in SBP1-mDHFR-GFP^{endo} parasites. Molecular weight standard is indicated in kDa.

In contrast to the episomal construct (expressed under *crt* promoter from late ring stage onwards) (4.14 B) early endogenous exported proteins such as REX1, REX2 and MAHRP2 (Figure and 4.18 A-C) in addition to late expressed antigens such as KAHRP (Figure 4.18 D) were co-blocked by SBP1-mDHFR-GFP^{endo} in presence of WR.

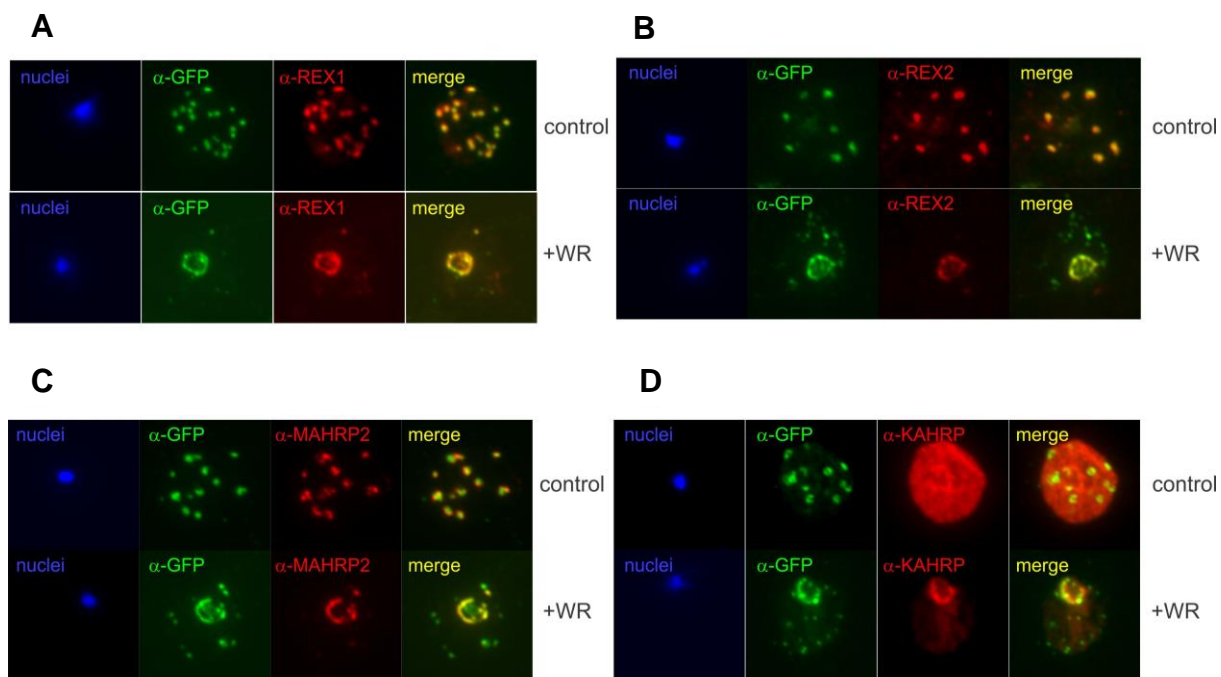


Figure 4. 18 | Endogenous SBP1-mDHFR-GFP as an approach to induce global export arrest in *P. falciparum*. (A-D) Co-localization IFAs of SBP1-mDHFR-GFP^{endo} parasites treated with (+WR) and without (control) WR. Endogenous proteins were detected with anti REX1, MAHRP2, REX2 and KAHRP (A-D), mDHFR construct was detected with anti-GFP. Nuclei were stained with DAPI. Size bar: 5 μ m.

To assess the effect of this pan-export arrest on parasite development the growth of the cell line was compared in presence and absence of WR. The WR -blocked parasites showed a strong growth inhibition compared to control (Figure 4.19 A). Giemsa stained smears showed that after 48 hours WR treated parasites were predominantly in the young trophozoite stage, whereas the control already completed the schizogony, as evident by the presence of schizonts and rings (Figure 4.19 B-C). This indicated a slowed growth with an arrest as young trophozoites in parasites where general protein export was blocked.

The results indicate that arrested translocation intermediates hamper parasite growth probably by preventing the export of parasite effectors required for development *in vitro*.

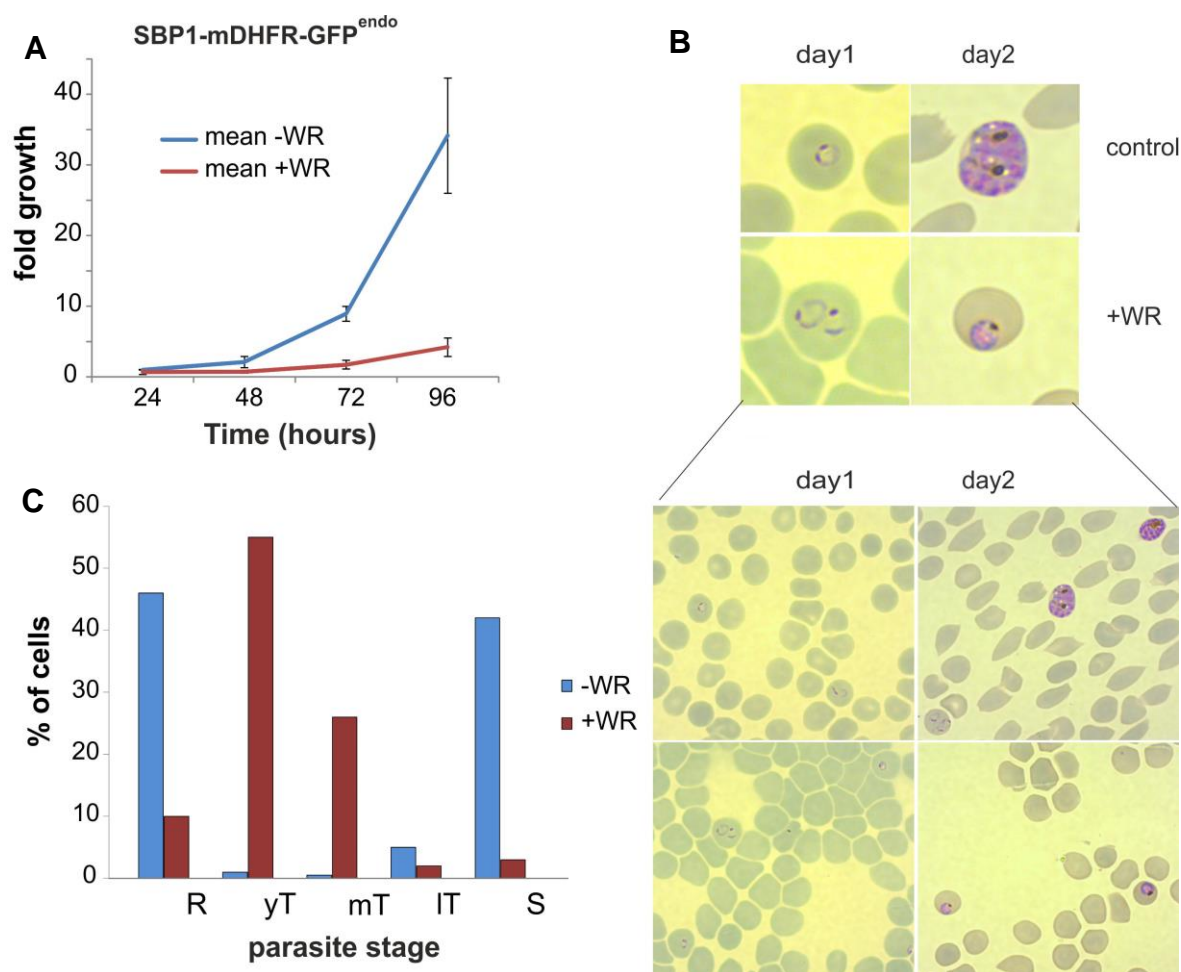


Figure 4.19 | Pan-export block delays parasite growth and arrests parasites as young trophozoites. (A) Fold growth compared to starting parasitemia of SBP1-mDHFR-GFP^{endo} parasites on (+WR) and off WR (control). Mean of $n=3$ independent experiments; error bars represent SD. (B) Giemsa stained smears of SBP1-mDHFR-GFP^{endo} parasites grown in presence (+WR) and without (control) WR after 24 hours (day 1) and 48 hours (day 2) showed a delayed development in WR treated parasites as evident by the accumulation of young trophozoite stages 48 hours after addition of WR. Top, cropped image of larger sections shown at the bottom (C) Graph showing parasite stage distribution in cultures after 2 days on WR (WR+) compared to control (WR-) (one representative of $n = 3$ experiments) R, rings; yT, mT, IT: young, mid and late trophozoites, respectively; S, schizonts.

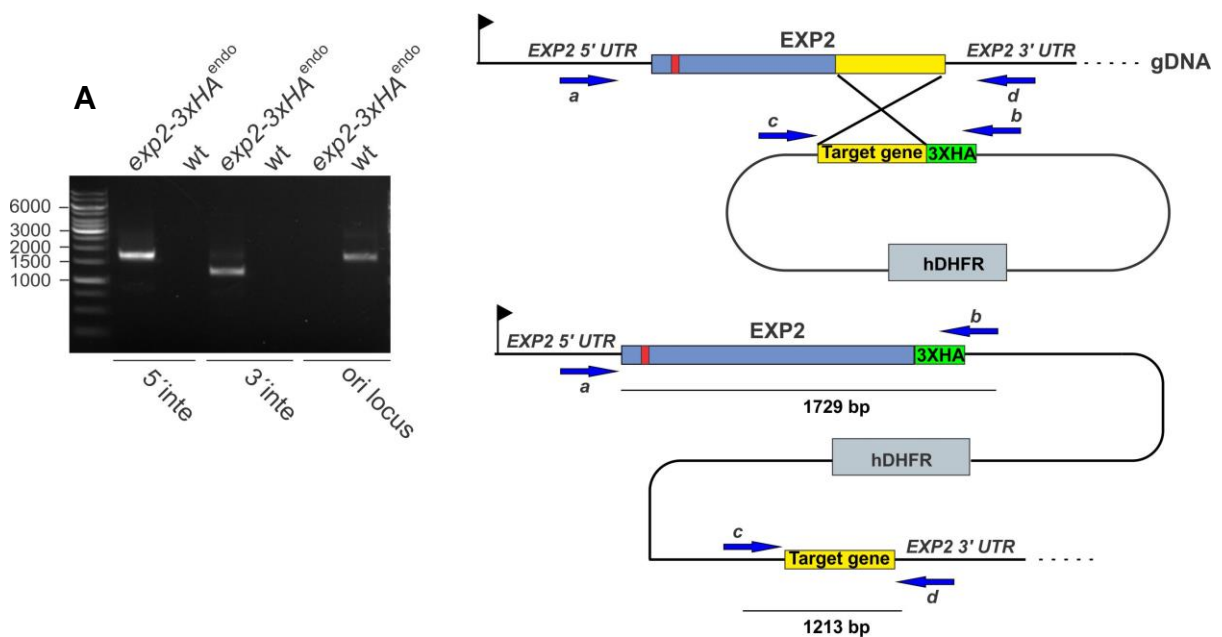
4.4 Insights into a role of EXP2 in protein export.

Although two components of PTEX are essential for the delivery of exported proteins into the RBC, there is so far no direct evidence that this complex actually has protein translocation activity. EXP2 has been proposed as the putative protein conducting pore at the PVM (See Section 1.3.3) but to date no functional data are available in *P. falciparum* that demonstrate its proposed role in protein export. To our knowledge EXP2 has not been endogenously tagged in *P. falciparum*. For these reasons and because it is the supposed membrane spanning pore of the translocon where a partially threaded, export arrested substrate can be

expected to be in contact with, EXP2 was chosen to investigate its interaction with substrates arrested in translocation.

4.4.1 Tagging of endogenous EXP2 and identification of interacting partners

In order to work with the PTEX component EXP2, an integrant cell line was generated, which expresses EXP2 C-terminally fused with a triple hemagglutinin tag (3XHA) from the endogenous locus (Figure 4.20 A). Genomic DNA from the resulting cell line was analyzed by PCR using genome and plasmid-specific primers to verify the correct genomic integration (Figure 4.20 A). IFAs showed the localization of the tagged protein at the PVM as evident from its co-localization with the PVM marker ETRAMP5 (Figure 4.20 B). Western Blot analyses showed a band of the appropriate size, indicating proper tagging of the protein. (Figure 4.20 C).



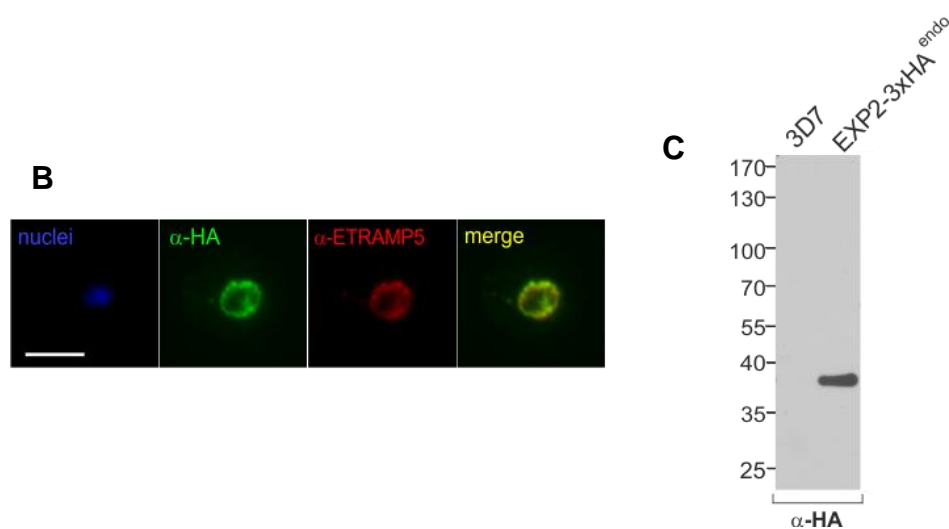


Figure 4. 20 | Endogenous tagging of EXP2 in *P. falciparum*. (A) Left, PCR on genomic DNA of EXP2-3xHA^{endo} and 3D7 (wt) parasites (as indicated) shows correct integration of the plasmid into the genome, leading to fusion of the endogenous *exp-2* gene with a sequence coding for 3 HA tags. A genome (blue arrows a and d) and a plasmid-specific primer (blue arrows c and b) were used each to confirm correct 5' and 3' integration. Primers were 5'EXP2fw (a) (125bp upstream of start ATG) with pARL_1_40rv (b) to demonstrate 5' integration (5'integ, 1729 bp) and 3'EXP2 rv (d) (168 bp downstream of stop) with pARL55sense (c) to demonstrate 3' integration (3'integ, 1213 bp). Primers 5'EXP2fw (a) and 3'EXP2rv (d) were used to detect the unmodified original locus (1696 bp) in 3D7. Right, schematics of genomic integration approach for endogenous tagging of EXP2. (B) Co-localization IFAs of EXP2-3xHA^{endo} parasites using anti HA antibodies to detect the endogenous EXP2 and anti ETRAMP5 antibodies as PVM marker. Nuclei were stained with DAPI. Size bars: 5µm. (C) Western blot analysis using anti-HA antibodies detects triple HA tagged EXP2 in parasite extracts of EXP2-3xHA^{endo} but not in WT parasites. Expected molecular weight of EXP2-3xHA is 39,6 kDa. Molecular weight standard is indicated in kDa.

The endogenous EXP2 was also tagged C-terminally with GFP and the resulting integrant cell line displayed the correct localization from young ring stage onwards for the duration of the cell cycle, consistent with previous studies using EXP2 specific antibodies (Bullen et al., 2012). In contrast to a recent study in *P. berghei* (Matz et al., 2015), no EXP2-GFP positive tubular structures protruding from the PV were observed in the analyzed parasites (Figure 4.21 A). Genetic analysis of EXP2-GFP^{endo} confirmed genomic integration and Western Blot using anti GFP antibodies the fusion of the endogenous EXP2 with GFP (Figure 4.21 B-C)

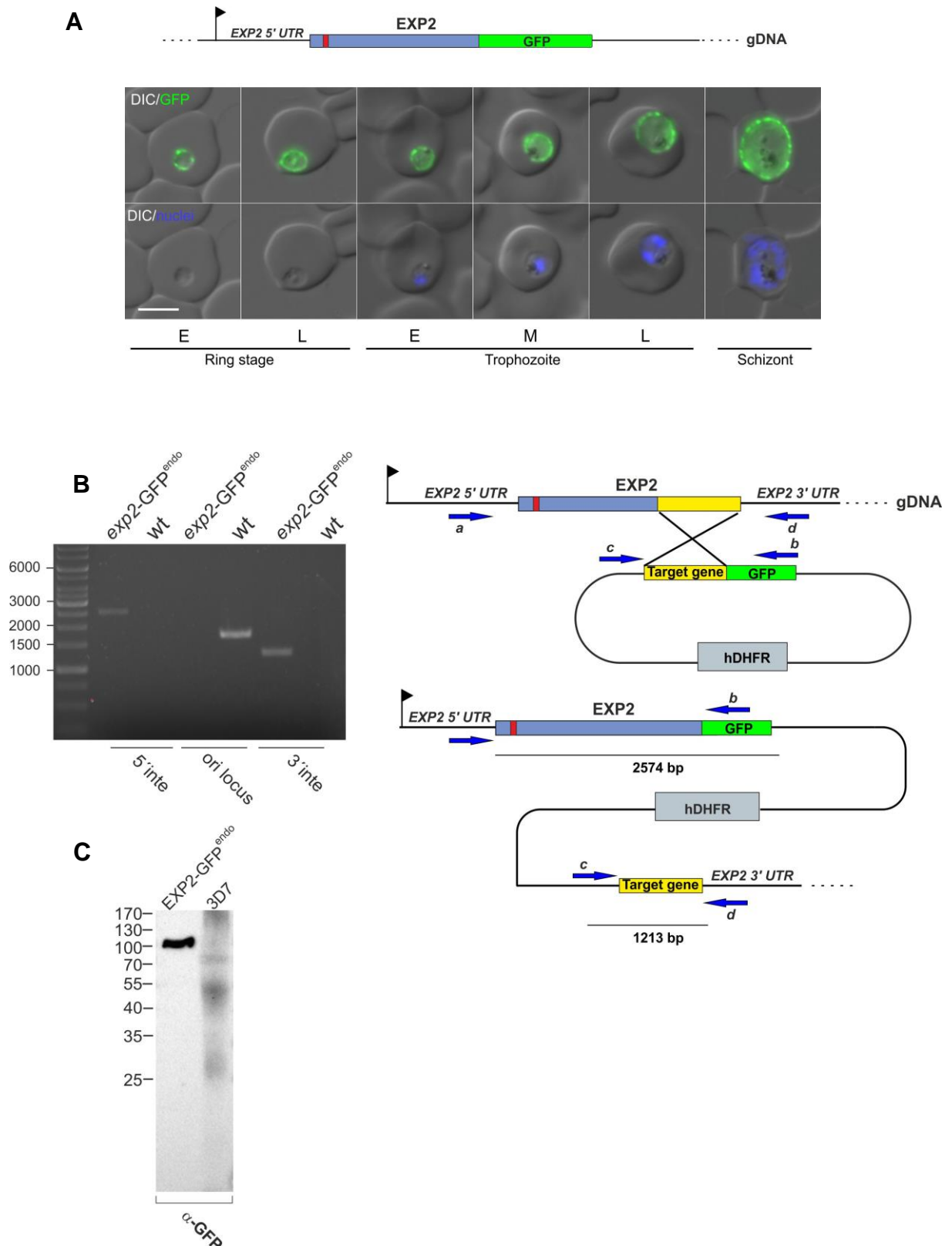


Figure 4. 21 | Endogenous fluorescent tagging of EXP2 in *P. falciparum*. (A) Live cell imaging of different stages of *P. falciparum* parasites across the life cycle expressing endogenous EXP2-GFP show expression of the PTEX component from early ring stages onwards. E, M, L: early, mid and late; DIC, differential interference contrast. Nuclei were stained with DAPI. Size bars: 5 μ m. (B) Left, PCR on genomic DNA of EXP2-GFP^{endo} and 3D7 (wt) parasites (as indicated) shows correct integration of the plasmid into the genome, leading to fusion of the endogenous *exp-2* gene with a sequence coding for GFP. A genome (blue arrows a and d) and a plasmid-specific

primer (blue arrows c and b) were used each to confirm correct 5' and 3' integration. Primers were 5'EXP2fw (a) (125bp upstream of start ATG) with GFPrv272 (b) to demonstrate 5' integration (5'integ, 2574 bp) and 3'EXP2 rv (d) (168 bp downstream of stop) with pARL55sense (c) to demonstrate 3' integration (3'integ, 1213 bp). Primers 5'EXP2fw (a) and 3'EXP2rv (d) were used to detect the unmodified original locus (1696 bp) in 3D7. Right, schematics of genomic integration approach for endogenous tagging of EXP2 with GFP. **(C)** Western blot analysis using anti-GFP antibodies detects GFP tagged EXP2 in EXP2-GFP^{endo} but not in WT parasites. Expected molecular weight of EXP2-GFP is 90,1 kDa. Molecular weight standard is indicated in kDa.

To our knowledge the endogenous EXP2 has not been tagged in *P. falciparum*. To confirm that EXP2-3XHA interacts with other known PTEX components, reversible cross linking immunoprecipitation assays (ReCLIP) (Smith et al., 2011) were performed using anti HA-beads with parasite extracts derived from EXP2-3xHA^{endo} parasites treated with the protein crosslinker DSP. This method is used to preserve labile protein-protein interactions before co-immunoprecipitation with specific antibodies. The tagged protein is pulled down together with the interacting proteins and the crosslinked binding partners are selectively released in a first eluate by cleavage with a reducing agent (e.g DTT) before analysis by mass spectrometry (MS). This allows an efficient recovery with low background. A second eluate was also obtained by chemical elution with NaOH and further analyzed by MS (See section 3.1.12) (Figure 4.22 A).

Consistently with previous studies (De Koning-Ward et al., 2009; Bullen et al., 2012) the immunoprecipitation (IP) of EXP2-3xHA recovered the PTEX components PTEX150, HSP101 and PTEX88 (Figure 4.22 B) as determined by MS analysis of the eluate after the IP (MS analysis was kindly performed by Prof. Stefan Tenzer, Institute for Immunology, University Medical Center, Johannes Gutenberg University, Mainz). (See Appendix 2 for all proteins recovered in MS analysis). Interestingly several other proteins that may include further PTEX interaction partners were also identified (Table 4.22 B). This includes unidentified proteins with unknown function, known PV resident proteins such as PV1 (Chu et al., 2011), PVM resident proteins such as ETRAMP5 and ETRAMP10.2 (Spielmann et al., 2003) as well as exported proteins that may be cargo protein on the way to the host cell which were cross-linked during the procedure.

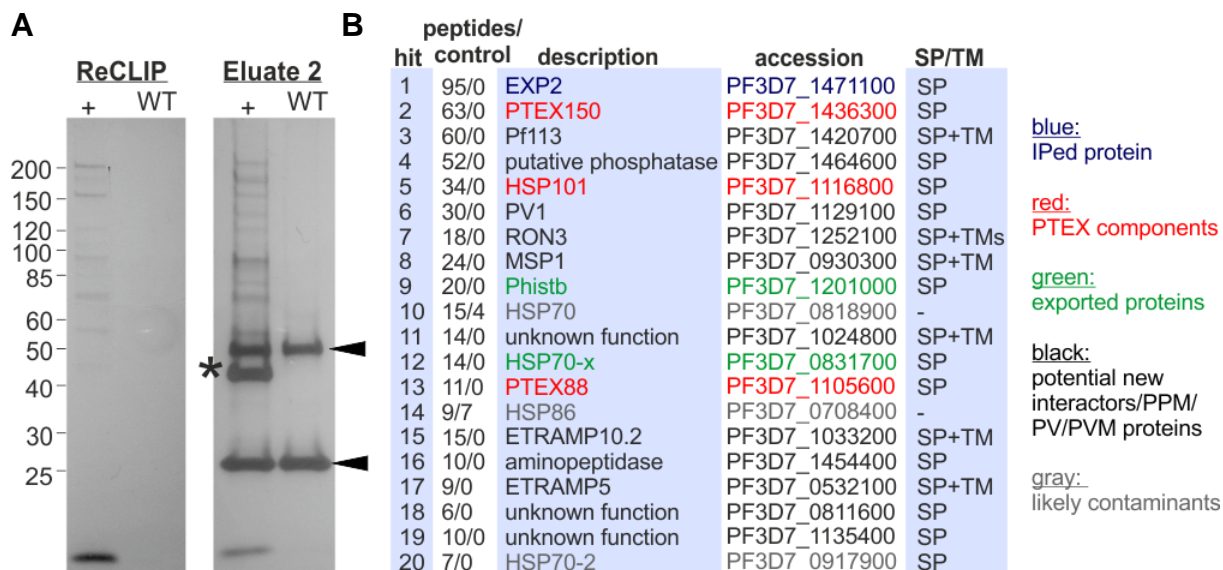


Figure 4. 22 | ReCLIP of endogenous EXP2 purifies known PTEX components and potential further interacting partners (A) Silver staining of IP samples from DSP-treated EXP2-3xHA^{endo} parasites (+) using HA binding beads compared to 3D7 parasites (WT). Released crosslinked eluates (ReCLIP) and NaOH eluates (Eluate2) were separated by SDS-PAGE and silver stained. Asterisk, shows IPed EXP2-3HA (bait); Arrow heads show antibody chains released by the chemical elution. **(B)** The table shows the 20 top hits after MS analysis of a ReCLIP and an Eluate 2. Peptides/control show peptide counts of the indicated protein over 3D7 (ReCLIP and Eluate 2 peptide counts pooled). SP, signal peptide; TM transmembrane domain.

4.4.2 Translocation intermediates stuck in translocation at the PVM are in a complex with EXP2

The translocation intermediates described in section 4.2 represent a useful approach to identify components of the export machinery that interact with the blocked substrates during translocation. Taking advantage of these intermediates it was investigated whether EXP2 is present at the site of arrest where these constructs are stuck in translocation.

To this end, the cell line EXP2-3XHA^{endo} was further transfected with translocation mDHFR substrates to gain information about their interaction with EXP2 during export. First, EXP2-3XHA^{endo} was transfected with SBP1-mDHFR-GFP. In the resulting cell line, SBP1 was correctly trafficked to the Maurer's clefts and after addition of WR the construct was arrested in the PV where it co-localized with EXP2-3XHA (Figure 4.23 A-B).

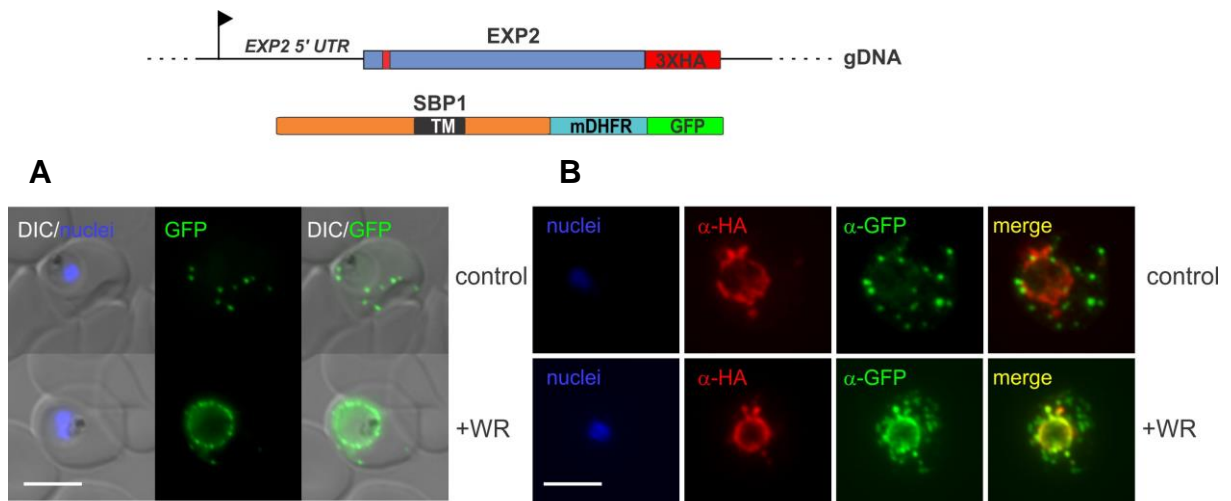


Figure 4. 23 | mDHFR intermediates arrested in translocation co-localized with EXP2. (A-B) Representative live fluorescence (A) or co-localization IFA (B) images of the cell line expressing endogenous EXP2 fused to 3xHA (EXP2-3xHA^{endo}) and SBP1-mDHFR-GFP (episomal) grown with (+WR) and without WR (control). DIC, differential interference contrast. Nuclei were stained with DAPI. Size bars: 5µm.

Next, this cell line (EXP2-3XHA^{endo} + SBP1-mDHFR-GFP) was grown in presence or absence of WR, parasites were lysed and EXP2-3xHA was immunoprecipitated (IPed) with anti HA -beads. The samples were analyzed by Western blot and SBP1-mDHFR-GFP (via GFP) and EXP2-3XHA (via HA) were detected in input, post binding lysate (unbound) and eluates (bound). EXP2-3xHA co-IPed the substrate SBP1-mDHFR-GFP only in presence of WR (when the SBP1-mDHFR-GFP is stuck in the translocon), whereas in the control the substrate was not detectable in the eluate (Figure 4.24 A).

The band intensities for the experiments without crosslinker were quantified to estimate the enrichment of both the IPed molecule (bait) and the co-IPed molecule (prey) over the control. As shown in Figure 4.24 A, the enrichment of the co IPed substrate was significant (n=3). SERA5 (a soluble molecule of the PV) and ETRAMP4 (a TM PVM resident protein) were detected to control for non-specific interactions. None of them was co-pulled down (Figure 4.24 A). These experiments were performed without crosslinker but reproducible results were obtained using cross-linker (DSP) to preserve labile interactions (4.24 C).

This indicates that substrates arrested during translocation interact specifically with EXP2 at the PVM. If the substrate (SBP1-mDHFR-GFP) is arrested in the translocon, it should also be able to co-immunoprecipitate the proposed translocon EXP2. To confirm these findings such reciprocal IP experiments were performed where SBP1-mDHFR-GFP was pulled down with anti-GFP beads. Consistent with an interaction of EXP2 with the substrate, SBP1 co-IPed EXP2-3XHA and the HA tagged protein was enriched in WR treated parasites if compared to control parasites without WR (Figure 4.24 B).

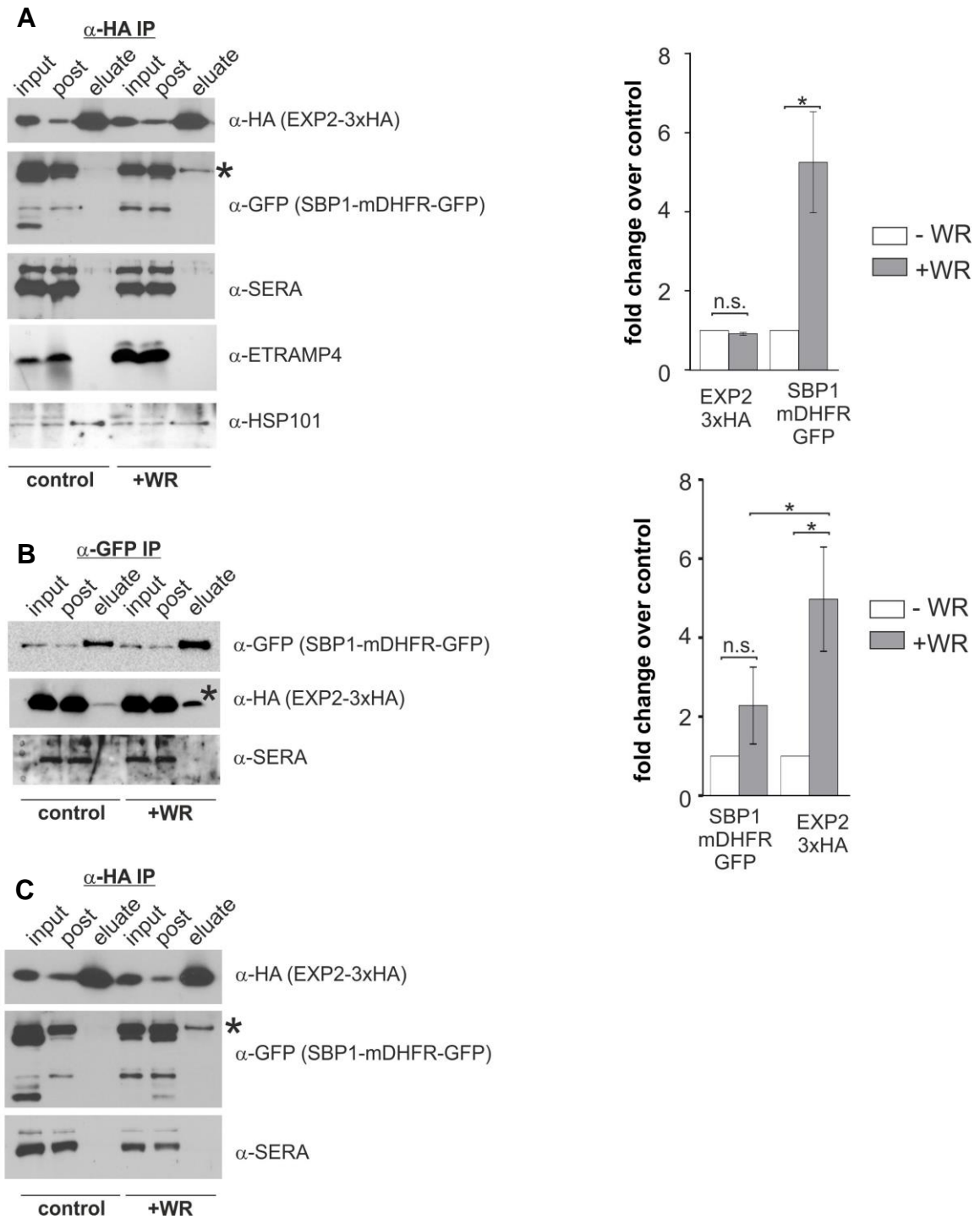


Figure 4. 24 | mDHFR intermediates arrested in translocation are in a complex with EXP2. (A) Left, Western blot of a representative co-IP experiment using anti -HA shows co-pull-down of SBP1-mDHFR-GFP (asterisk) in parasites grown with WR but not in untreated controls. Input, total lysate before IP; post, lysate after IP. Right, quantification of the signal intensity of the IPed EXP2-3XHA and the co-IPed SBP1-mDHFR-GFP in parasites grown with WR over the control ($n=3$). Asterisk comparing the intensity of IPed SBP1-mDHFR-GFP in WR+ over its control: $p=0,0288$; paired, two-tailed t test. **(B)** Left, Western blot of a representative co-IP experiment as in (A) but using anti GFP beads (reciprocal co-IP) to bind SBP1-mDHFR-GFP. Asterisk: enrichment of co-pulled down EXP2-3xHA in parasites grown with (+WR) compared to control (no WR). Right, quantification of the signal intensity of the IPed SBP1-mDHFR-GFP and the co-purified EXP2-3xHA in parasites grown with (WR+) over

control (n=3). Asterisk comparing EXP2-3xHA in WR+ over its control: p=0,035; paired, two-tailed t test. Asterisk comparing EXP2-3xHA enrichment with SBP1-mDHFR-GFP enrichment: p=0,047; unpaired, two-tailed t test. Error bars show S.D.; n.s., not significant. **(C)** Western blot of a representative experiment as in (A) but performed with parasites treated with DSP to preserve labile protein-protein interactions showed reproducibility of the results obtained in A. SERA5 (a soluble resident PV protein) and ETRAMP4 (a TM resident PVM protein) were detected with specific antibodies to exclude unspecific interactions. HSP101 was detected to verify integrity of the PTEX complex.

SBP1-mDHFR-GFP showed some enrichment in WR+ over control after the IP (potentially due to greater stability of the mDHFR folded molecule). The band intensities were therefore also quantified. This analysis revealed that this enrichment was not significant. In contrast the enrichment of the co-IPed EXP2-3xHA compared to the control was significant (n=3) (Figure 4.24 B). This indicates that the observed enrichment of the co-IPed molecule under WR is not because of the stabilization of the bait.

To elucidate the interaction of the arrested substrate with other components of the PTEX complex when trapped in the translocon, the proposed PTEX unfoldase HSP101 was detected in the experiment described in 4.24 A using specific antibodies. HSP101 was co-IPed by pulling down EXP2-3XHA in presence and absence of WR, consistent with its known interaction with EXP2 as bona fide component of PTEX. To exclude that the observed enrichment of the blocked substrate (SBP1-mDHFR-GFP) is not an indirect enrichment through HSP101 but it is because of a direct interaction with EXP2, an integrant cell line was generated that expresses HSP101-3XHA from the endogenous promoter using the strategy as described in 4.20 A. The resulting transgenic parasites were analyzed by PCR and Western blot. This verified the correct genomic integration and revealed a band of the expected size in the Western blot using antibodies anti HA (Figure 4.25 A-B).

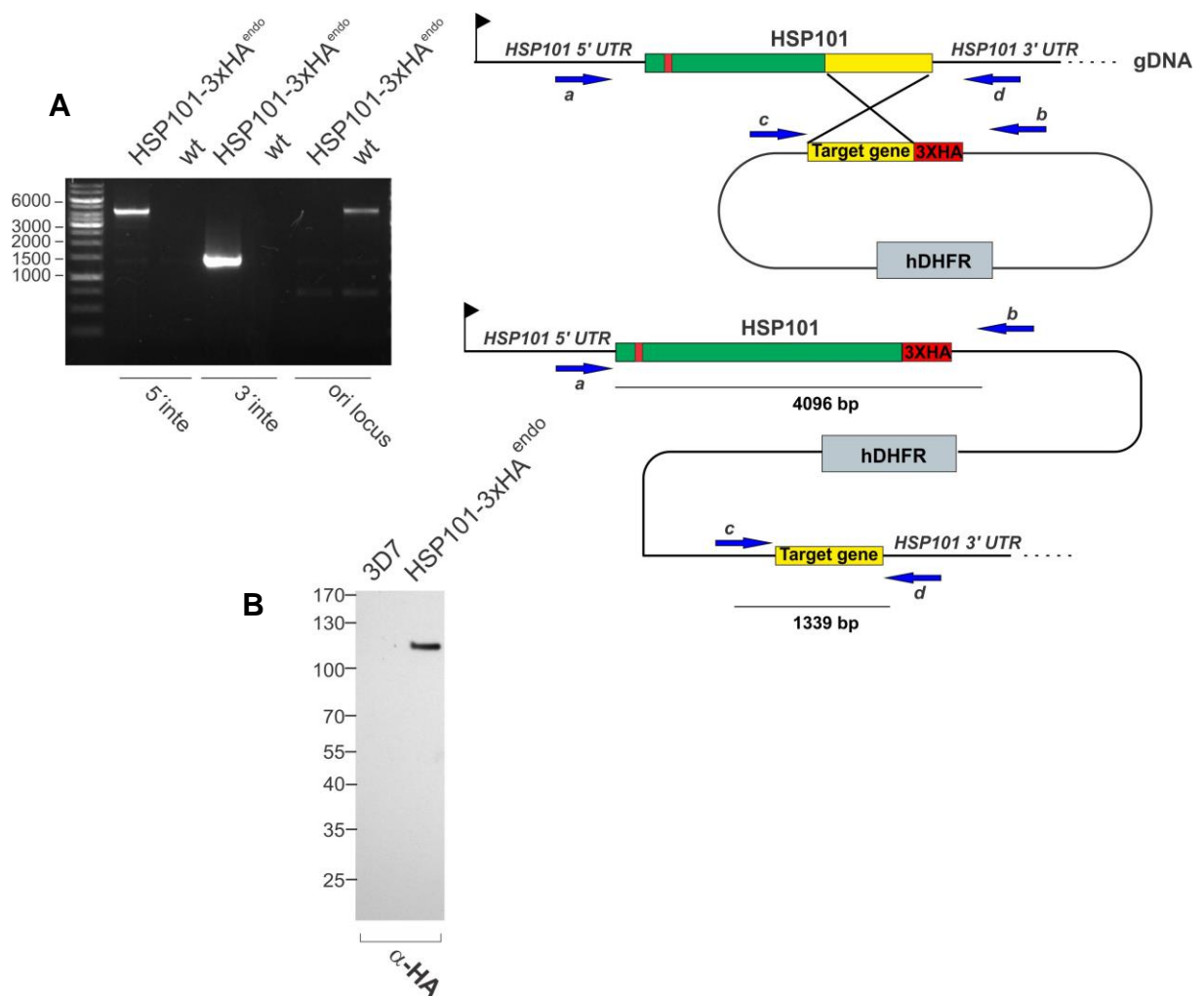


Figure 4. 25 | Endogenous tagging of HSP101 in *P. falciparum*. (A) Right, schematics of genomic integration approach for endogenous tagging of HSP101. After integration the parasites will express HSP101 tagged with 3XHA under the HSP101 promoter. Left, PCR on genomic DNA of HSP101-3xHA^{endo} and 3D7 (wt) parasites (as indicated) shows correct integration of the plasmid into the genome, leading to fusion of the endogenous *hsp101* gene with a sequence coding for 3 HA tags. A genome (blue arrows a and d) and a plasmid-specific primer (blue arrows c and b) were used each to confirm correct 5' and 3' integration. Primers were 5'HSP101fw (a) (473 bp upstream of start ATG) with pARL_1_40rv (b) to demonstrate 5' integration (5'inte, 4096 bp) and 3'HSP101 rv (d) (284 bp downstream of stop) with pARL55sense (c) to demonstrate 3' integration (3'inte, 1339 bp). Primers 5'HSP101fw (a) and 3'HSP101rv (d) were used to detect the unmodified original locus (4175 bp) in 3D7. (B) Western blot analysis using anti-HA antibodies detects triple HA tagged HSP101 in HSP101-3xHA^{endo} but not in WT parasites. Expected molecular weight of HSP101-3xHA is 109,1 kDa. Molecular weight standard is indicated in kDa.

This cell line was further transfected with SBP1-mDHFR-GFP. SBP1 was arrested in the parasite periphery upon addition of the ligand where it co-localized with the tagged HSP101 (Figure 4.26 A-B). Co-IP assays to pull down HSP101-3XHA were performed in presence and absence of WR. In comparison to the EXP2-3XHA, the substrate was not co-purified in WR treated parasites (Figure 4.26 C). These results thus suggest that HSP101 remains associated to PTEX but it is not interacting with the arrested mDHFR substrates. This further favours the idea that the observed enrichment is because of the interaction with EXP2, although indirect interactions via other components of PTEX can not be excluded.

Taken together these findings provide strong evidence that mDHFR substrates arrested in the translocon by prevention of unfolding are in close contact with the proposed membrane-spanning pore EXP2 at the PVM and demonstrate for the first time a link between translocation activity and PTEX.

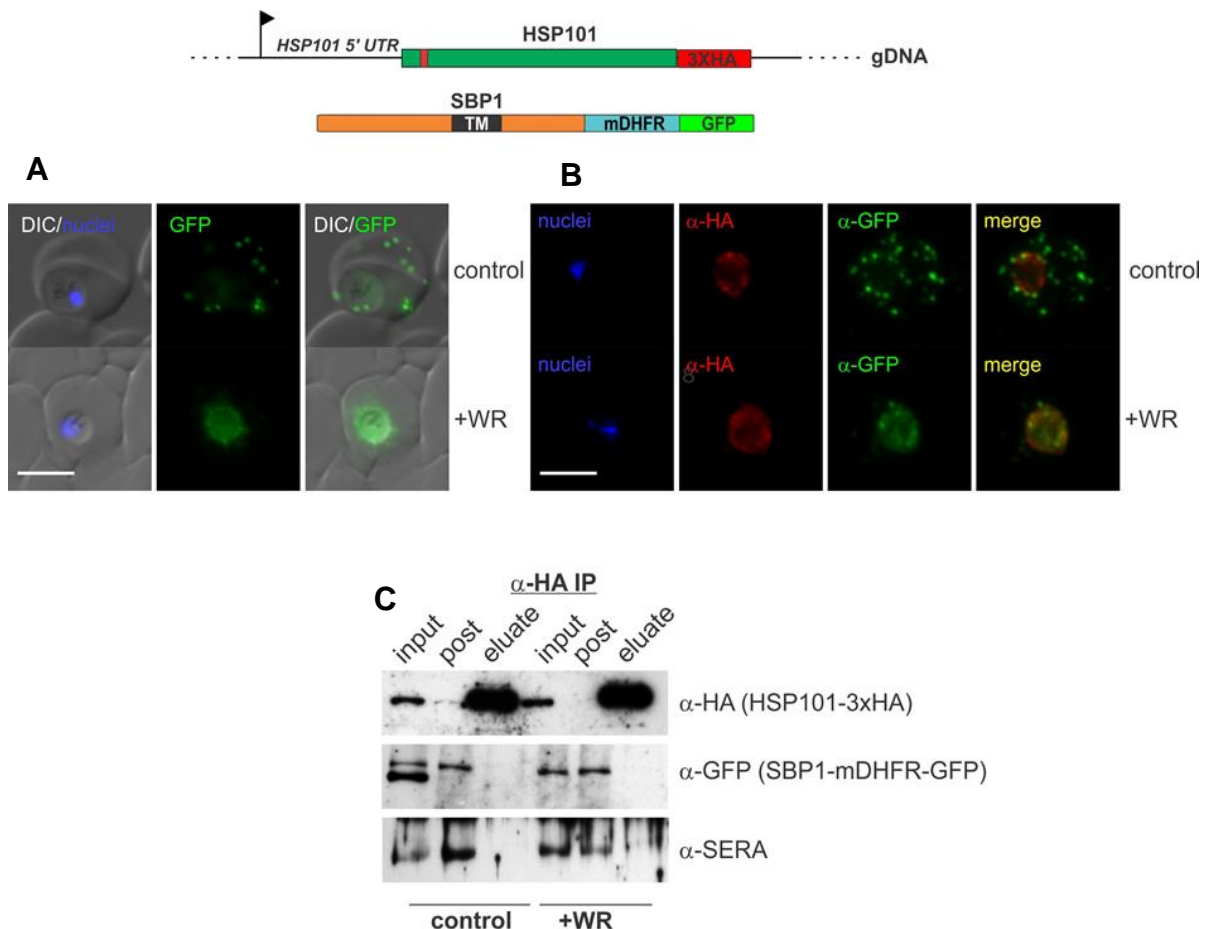


Figure 4. 26 | mDHFR intermediates arrested in translocation are not in direct contact with HSP101. (A-B) Representative live fluorescence (A) or co-localization IFA (B) images of the cell line expressing endogenous HSP101 fused to 3xHA (HSP101-3xHA^{endo}) and SBP1-mDHFR-GFP (episomal) grown with (+WR) and without WR (control). DIC, differential interference contrast. Nuclei were stained with DAPI. Size bars: 5 μ m. (C) Western blot of a representative co-IP experiment using anti -HA to pull down HSP101, shows that in

parasites grown with WR there is no enrichment of the mDHFR fused substrate. Input, total lysate before IP; post, lysate after IP. SERA5 (a soluble resident PV protein) was detected to exclude unspecific interactions.

4.4.3 PPM arrested mDHFR constructs do not interact with EXP2

The integrant cell line EXP2-3XHA^{endo} was also transfected with two further constructs: REX2-mDHFR-GFP (the construct arrested at the PPM that did not cause co-block) and REX2-GFP-mDHFR (the construct with the swapped fusion domains that is able to induce a co-block).

Co-IP assays were performed as described above (section 4.4.2). EXP2-3XHA was IPed with anti HA beads from parasites cultured with WR and in absence of WR. The co-blocking substrate REX2-GFP-mDHFR was co-IPed in presence of WR (Figure 4.27 B) but not in the control whereas REX2-mDHFR-GFP was not co-pulled down and was not detected in the eluted fraction (Figure 4.27 A).

These findings correlate with the results in section 4.2 and suggest that only those constructs that interact with EXP2 at the PVM (i.e SBP1-mDHFR-GFP and REX2-GFP-mDHFR), when they are arrested by prevention of unfolding, are able to induce a co-block, consistent with jamming of a common translocon at the PVM. REX2-mDHFR-GFP, which is arrested at the PPM extraction step preceding PTEX, does not form a complex with the proposed translocon pore EXP2 and therefore does not prevent the passage of other proteins.

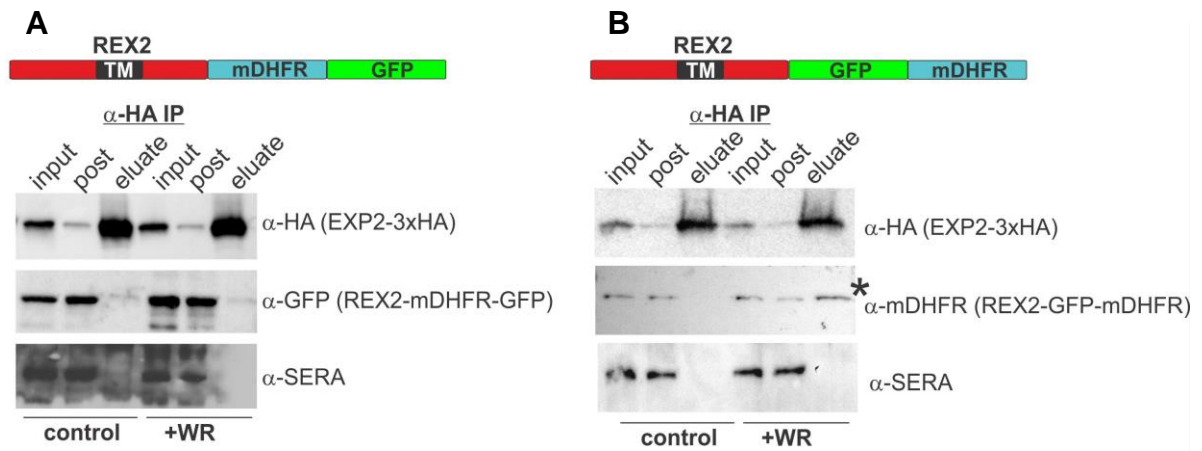


Figure 4. 27 | Only co-blocking mDHFR intermediates arrested in translocation are in a complex with EXP2. (A) Western blots of a representative co-IP experiment using HA beads with EXP2-3XHA^{endo} parasites expressing REX2-mDHFR-GFP grown with (WR+) and without WR (control) showed no enrichment of the mDHFR substrate. The mDHFR construct was detected using anti-GFP. **(B)** Western blot of a representative co-IP experiment using HA beads with EXP2-3XHA^{endo} parasites expressing REX2-GFP-mDHFR shows co-pull down of REX2-GFP-mDHFR substrate (asterisk) only when parasites were grown in presence of WR and not in untreated control. SERA5 (a soluble resident PV protein) was detected to exclude unspecific interactions. EXP2-3XHA was detected with anti HA antibodies and the mDHFR construct was detected with anti-mDHFR. Input, total lysate before IP; post, lysate after IP.

Chapter 5. Discussion

The infection of a fully differentiated cell such as the erythrocyte represented a step in the evolution of apicomplexan parasites that conferred advantages to survive in the host. However, at the same time the parasite had to develop a series of molecular adaptations that induces elaborate structural and physiological changes to the host cells to ensure survival and propagation in this unique niche.

Multiplication of asexual malaria parasites in the bloodstream involves an extensive remodelling of the host erythrocytes. These modifications rely entirely on self-encoded proteins that parasites need to export beyond their confines and recruit to specific localizations to bestow new properties on the infected erythrocyte. Protein export has been described in all *Plasmodium* species and the conservation of plasmepsin V and the components of PTEX throughout the genus indicate that the same protein export machinery is used by all *Plasmodium* species (De Koning Ward et al., 2009; Boddey et al., 2010). The predicted *P. falciparum* exportome seems to be 5–10 times larger than that of other *Plasmodium* species (Maier et al., 2009) and this was attributed to the requirements imposed by the export of PfEMP1 (Sargeant et al., 2006), a protein family only found in *P. falciparum* that mediates cytoadherence (Su et al., 1995; Baruch et al., 1996), a property associated with virulence and a more severe pathology in this species (Miller et al., 2002). Nevertheless, non-falciparum species induce host cell modifications such as Schüffner's dots in *P. vivax* (Akinyi et al., 2012) or intra-erythrocytic *P. berghei*-induced structures (IBIS) (Ingmundson et al., 2012) and may as well induce cytoadherence (Bernabeu et al., 2012; El-Assaad et al., 2013). This indicates that other species export a large and diverse set of proteins into the host cell (Cunningham et al., 2010; Sijwal and Rosenthal, 2010; Pasini et al., 2013) and current predictions based on the presence of the PEXEL motif underestimate the actual number of exported proteins. This argues for a prominent role of PEXEL-negative exported proteins (PNEPs) (Spielmann and Gilberger, 2010) or a different consensus of the PEXEL motif in *Plasmodium* taxa (Pick et al., 2011; Siau et al., 2014). For instance, *pir* (*Plasmodium* interspersed repeat) are multigene families present in all *Plasmodium* genomes so far sequenced; these proteins are thought to be destined to the host cell surface and have been involved in antigenic variation and immune evasion (Del Portillo et al., 2001; Janssen et al., 2004; Cunningham et al., 2010). Overall it can be concluded that protein export and host cell modifications are crucial processes for all *Plasmodium* species.

The parasite grows and replicates within a parasitophorous vacuole (PV) (Lingelbach and Joiner, 1998) enclosed by a membrane (PVM) that isolates it from the RBC cytosol.

Consequently proteins targeted to the host cell need to cross this membrane to reach their final localization. The requirement of all proteins for unfolding to be exported (Gehde et al., 2009; Grüning et al., 2012; Heiber et al., 2013), together with the discovery of the protein complex PTEX at the PVM that might function as a protein translocon (De Koning-Ward et al., 2009; Bullen et al., 2012; Beck et al., 2014; Elsworth et al., 2014a), were key advances to understand the molecular mechanism by which all proteins reach the iRBC. The data generated in this thesis shed light on the pathway malaria proteins take as they traffic from the parasite plasma membrane to the RBC cytosol with a particular focus on the translocation events for the different classes of exported proteins during this critical phase in export.

5.1 Major findings

5.1.1 Translocation pathway for TM proteins at the parasite periphery

The export pathway of soluble exported proteins in *P. falciparum* has been partially elucidated. Soluble proteins are trafficked along the classical secretory pathway via vesicles and exocytosed into the PV, which is considered the default compartment of the secretory pathway (Ansorge et al., 1996; Deponste et al., 2012). Once in the vacuole these proteins are potentially unfolded by HSP101 to become translocation-competent and fed through a protein-conducting channel at the PVM (Ansorge et al., 1996, Gehde et al., 2009; Spielmann and Marti; 2013; Heiber et al., 2013; Beck et al., 2014) (See Figure 5.1).

In contrast, the export pathway of TM proteins is still largely unclear. TM proteins enter to the secretory pathway, as evident from their sensitivity to treatment with BFA (Wickham et al., 2001; Haase et al., 2009; Saridaki et al., 2009; Grüning et al., 2012) and they are usually co-translationally inserted into the lipid bilayer of the ER via a signal peptide or a TM domain. Thereafter, they are trafficked by vesicles as membrane-associated proteins and finally are thought to be delivered into the PPM as integral membrane proteins, preserving the topology with which they were inserted into the ER membrane (Lodish et al., 2000; Lingelbach and Przyborski, 2006; Nilsson et al., 2012). For TM PNEPs this has been predicted to be a type Ib topology (Saridaki et al., 2009) and there is evidence that these proteins are indeed found in the PPM with their N-terminus facing the PV lumen (Grüning et al., 2012).

Since TM proteins end up integral in the PPM after fusion of the transport vesicle (Figure 5.1), it was originally thought that these proteins use vesicles to reach the PVM where they diffuse laterally (Haldar and Holder, 1993) to regions that will become Maurer's clefts and are then carried into the host cell with the nascent clefts (Spycher et al., 2006; Tilley et al., 2008). Recent data using time-lapse imaging indicated however that export is independent of

Maurer's clefts formation (Grüning et al., 2011). Other models proposed a continuous membrane flow mechanism through budding of vesicles from the PPM, subsequent fusion with the PVM and export beyond to the different membrane compartments in the RBC (Howard et al., 1987; Günther et al., 1991; Trelka et al., 2000; Taraschi et al., 2001; Lingelbach and Przyborski, 2006). There is currently experimental proof that supports the requirement of PNEPs TM proteins for unfolding to be exported (Grüning et al., 2012). This is consistent with translocation across membranes and excludes vesicular trafficking from the PPM to the destination in the host cell (Grüning et al., 2012). The evidence of a solubility shift for TM proteins in the host cell (Papakrivos et al., 2005; Grüning et al., 2012) and the hitherto not visualized presence of vesicles in the PV further speak against a vesicular pathway.

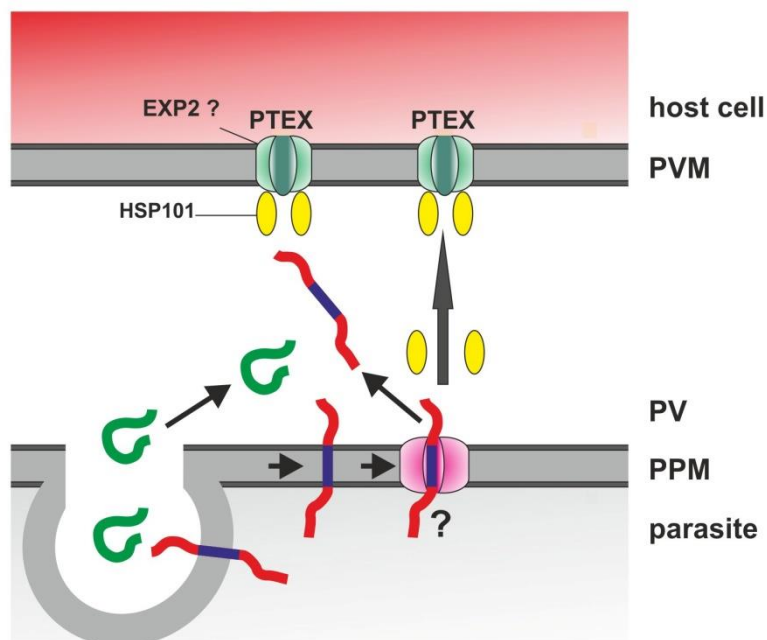


Figure 5. 1 | Model of translocation events for exported proteins at the parasite host-cell interface.

Soluble proteins (green line) are released into the parasitophorous vacuole (PV) after fusion of the transport vesicle arriving from the secretory pathway. Soluble proteins are next unfolded potentially by HSP101 (PTEX component) and translocated across the PVM through the putative protein-conducting channel EXP2 to be delivered into the host cell. Transmembrane proteins (red line) with a transmembrane region (blue) are delivered into the PPM as integral proteins and an extraction mechanism mediated by a hitherto unknown export machinery at the PPM must exist to free them from the membrane and render them translocation competent. One of the hypothetical models proposes that HSP101 dissociates from the PTEX complex and assist extraction out of the PPM. TM proteins converge on the translocation step at the PVM with soluble proteins, where both types of proteins depend on the same PTEX components.

As TM proteins are embedded in the PPM, a sequential mechanism must therefore exist to free them from the membrane, to render them translocation competent and to hand them over to the PVM translocon. It was recently demonstrated that TM proteins converge with soluble proteins in an export step at the PVM, where the components of PTEX, HSP101 and PTEX150 (Figure 5.1), are known to be mandatory for export into the host cell, as the inactivation of these components led to accumulation of exported proteins at the parasite periphery (Beck et al., 2014, Elsworth et al., 2014a). Nevertheless, these studies did not provide indications where TM proteins are arrested and whether these proteins actually are translocated at the PVM.

Thus, the sequence of events that TM proteins follow between the PPM and the PVM is still poorly understood. The prevention of unfolding of REX2 arrested the protein at the PPM (Grüring et al., 2012) and this established the precedent that TM proteins need to undergo a first unfolding-dependent translocation step at the PPM. Although *in vitro* studies using isolated mitochondria (Eilers et al., 1988) or isolated lysosomes (Salvador et al., 2000) as well as *in vivo* experiments using intact yeasts, restored import of arrested mDHFR intermediates by withdrawal of the folate analogue (methotrexate or aminopterin) (Wienhues et al., 1991), the arrested intermediates in *P. falciparum* could not be chased upon removal of the ligand and remained irreversibly blocked (Gehde et al., 2009). Fitting with these data, REX2-mDHFR-GFP was also irreversibly blocked at the PPM (Grüring et al., 2012), which impeded the characterization of the translocation steps of TM proteins beyond the PPM.

To overcome this failure of the system, different modifications of the original construct were tested, however no successful results were obtained, as the construct remained blocked and only newly synthesized protein was further exported. The irreversibility does not seem to be consequence of the C-terminal folded GFP after the mDHFR domain (Gehde et al., 2009; Deponte, 2012), since a myc tagged (not foldable domain) and a swapped construct (REX2-GFP-mDHFR) accumulated also irreversibly. The interaction between the ligand (WR) and the stabilized mDHFR domain appears thus to be not reversible in *P. falciparum*. This may be explained by the low dissociation constant of the folate analogue, which in the case of methotrexate ($K_d < 10$ nM) is two orders of magnitude smaller than that of the natural dihydrofolate (Appleman et al., 1988; Ainaravaru et al., 2005). In comparison to living yeast or isolated organelles, *P. falciparum* is an intracellular parasite surrounded by two membranes; thorough washes of the cells likely may not be sufficient to reduce the concentration of the ligand inside the PVM/ PPM below the K_d to cause the dissociation of the complex. This drawback reduced the flexibility of the system but offered on the other hand the possibility of generating stable translocation intermediates as discussed in the next section.

To investigate the mechanistic aspects of the export of TM proteins beyond the PPM and to dissect the individual steps of translocation, this study took advantage of the redox sensitive folding state of BPTI and tested this system for the first time in *P. falciparum*. The rationale was that BPTI fused C-terminally to a parasite protein would become folded only if the protein reaches the PV, a compartment thought to be oxidizing, in contrast to the reducing conditions in the cytoplasm (Kehr et al., 2010; Kasozi et al., 2013; Wither-Martinez et al., 2014) (Figure 5.2 A). The system proved to be effective to generate translocation incompetent substrates, unable to cross the PVM due to the stabilization of the BPTI intramolecular disulfide bridges under the oxidizing conditions in the PV. The findings *in vivo* in *P. falciparum* were comparable with the original application *in vitro* of BPTI, where an imported precursor fused to the domain became stuck across the mitochondrial membranes (Vestweber and Schatz, 1988). This indicates that even small proteins (BPTI is only 6 kDa) need to be in fully loose conformation to pass through the protein-conducting channel at the PVM and reinforces the requirement of unfolding for export in malaria parasites. In mitochondria even the introduction of a single disulfide bridge into an import precursor inhibited import to a significant extent (Schwartz et al., 1999; Matouschek, 2003). Retention of small proteins by oxidative folding has been described in the mitochondrial intermembrane space (IMS) (Mesecke et al., 2005). In this natural import pathway, termed disulfide relay system, proteins destined to the IMS are first translocated into the IMS with the help of the translocase of the outer membrane (TOM) complex in a reduced, unfolded and import-competent state. Subsequently, the incoming target proteins are oxidized by Mia40 and this leads to the formation of disulfide bridges and trapping in the IMS (Mesecke et al., 2005; Stengel et al., 2010).

The data obtained by fusing BPTI to REX2, showed first that TM proteins indeed are extracted out of the PPM and released transiently into the PV, likely comparable to a soluble protein (Figure 5.1), as demonstrated by protease protection assays that localize the arrested constructs entirely in the PV. Secondly, the BPTI fusion confirmed that TM proteins are also translocated at the PVM, as the oxidation-mediated folding in the vacuole prevented the export of the reporter. Hence, these findings are supportive of a two-step translocation process for TM proteins and speak further against a vesicular pathway between the PPM and the PVM. A similar sequential import process that operates in tandem between two translocation channels in the outer and inner mitochondrial membranes was described using a modified version of the BPTI (Hwang et al., 1991; Jascur et al., 1992).

The mechanism by which membrane proteins are freed from or ripped out of the PPM is still an unresolved question. There are precedents of membrane extraction that renders this as a plausible mechanism for export of TM proteins at the parasite-host cell interface. A well-

characterized example of 'retro-translocation' or 'dislocation' of integral membrane proteins is the ERAD (ER-associated degradation) pathway (Nakatsukasa and Brodsky 2008; Bagola et al., 2011; Zattas and Hochstrasser, 2015; Ruggiano et al., 2014) where defective or misfolded membrane-integral ER proteins are recognized and retro-translocated across the ER membrane back into the cytosol, where they are polyubiquitylated and degraded (Hiller et al., 1996, Wiertz et al., 1996). A related protein complex termed Asi involved in degradation of mislocalised integral membrane proteins was recently identified in the yeast inner nuclear membrane (Foresti et al., 2014; Khmelinskii et al., 2014).

These systems requires signal recognition, a driving force to ensure directionality which is conferred by chaperones or cytosolic factors (Stolz and Wolf, 2010) and a proteinaceous membrane channel to mediate extraction across the membrane bilayer (Schnell and Hebert, 2003; Ploegh, 2007; Bagola et al., 2011). Extraction of TM proteins out of the ER membrane has been proposed to be involved in the degradation of even polytopic membrane proteins (Nakatsukasa and Brodsky 2008; Nakatsukasa et al., 2008). Experiments with the 12 TM domain ERAD substrate Ste6p* showed that its TM domains became solvent exposed (Nakatsukasa et al., 2008). Some integral membrane ERAD substrates, such as MHC I (Wiertz et al., 1996) and cystic fibrosis transmembrane conductance regulator (CFTR) (Johnston et al., 1998), have been observed to reside in the cytoplasm, which suggested that membrane-spanning segments might be solubilized by removal from the lipid bilayer of the ER prior to proteasome-mediated degradation (Nakatsukasa and Brodsky, 2008; Vembar and Brodsky, 2008). The ERAD extraction of intact TM proteins is influenced by TM segment hydrophobicity (Carlson et al., 2006) and is an energy-dependent chaperone-assisted process. It is in this respect noteworthy that the export of PNEPs depends on specific types of TM domains (Haase et al., 2009; Saridaki et al., 2009; Grüring et al., 2012) and extractability of this domain out of the PPM might explain their further trafficking into the host cell. Intriguingly, and in contrast to the data available in *P. falciparum*, ERAD extraction is not dependent on unfolding for some substrates (Tirosh et al., 2003).

Components of the ERAD pathway interestingly were found in plastids of chromoalveolates (Sommer et al., 2007), including *P. falciparum*, where ERAD homologues have been identified and localized to the apicoplast (Agrawal et al., 2009; Spork et al., 2009; Kalanon et al., 2009). These proteins are thought to play a role in the transport of nuclear-encoded proteins across the plastid membranes (Sommer et al., 2007) and this led to speculate that the parasite has 'rewired' these components to other compartments to perform different transport functions (Spork et al., 2009).

The export machinery or trafficking factors that may perform this first extraction step in *P. falciparum* still remain enigmatic. Different unknown trafficking factors in the PV or at the

PPM can be involved at the first extraction and some may be also shared with the known translocation machinery at the PVM. Chaperones present in the PV may keep the extracted protein in a translocation competent state (Nyalwidhe and Lingelbach, 2006). It can also be speculated that PTEX components (i.e. HSP101) might dissociate from the PVM complex (Beck et al., 2014) and interact with PPM factors to assist extraction from the PPM (Figure 5.1). HSP101 can be involved in pulling the TM proteins out of the membrane, similar to the role of the cytosolic ERAD AAA-ATPase p97/cdc48, which generates the driving force that is required for membrane extraction (Rabinovich et al., 2002; Ravid et al., 2006; Carlson et al., 2006).

A still open question also is how PVM- resident TM proteins, such as ETRAMPs (Spielmann et al., 2003) or EXP1 (Simmons et al. 1987; Kara et al., 1988), become inserted into the PVM, as after fusion of the transport vesicle, these proteins should also require extraction out of the PPM and insertion into the PVM. However, to distinguish them from exported proteins that are translocated through the PVM into the host cell, these proteins would then require to be laterally released from the translocon into the PVM, for instance by a stop transfer signal, similar to proteins resident in the mitochondrial inner membrane (Chacinska et al., 2009; Botelho et al., 2011) or by a signal-anchor sequence analogous to the ER insertion via the Sec 61 translocon (Lodish et al., 2000; Rapoport, 2007). If the same translocation machinery is also involved in this step remains to be investigated.

Different exported proteins fused to BPTI showed contrasting phenotypes in terms of oxidation-mediated export arrest when expressed in the parasite. The fact that not all TM proteins were sensitive to the redox sensitive folding suggested that integral proteins may be translocated in different fashions at the parasite periphery. The data here shown indicate that the distance between the TM domain and the foldable moiety (in this thesis referred to as 'spacer') appears to affect the way a protein is handed over to the PVM translocon and so affects whether the protein is further translocated or not. As it was not the full region from the N-terminus to the blocking domain but only the region after the TM, this indicates that the TM domain may be involved in this hand over. The TM domain contains information critical for a protein to be exported (Haase et al., 2009; Saridaki et al., 2009; Grüning et al., 2012) and is thought to be determinant for protein sorting and localization in a specific membrane (Sharpe et al., 2010; Cosson et al., 2013). A model proposed is depicted in Figure 5.2.

According to this model, during PPM extraction, the TM domain emerges from the PPM into the PV and in the case of proteins with a short C-terminus or spacer (i.e. REX2 and PTP1), it cannot reach directly the PVM and thus these proteins are released transiently as a soluble intermediate into the PV, which leads to oxidative folding of BPTI and to export arrest in the PV (Figure 5.2 B). In contrast, in proteins with a long spacer such as SBP1 and MAHRP1 (or

the artificial constructs with an extended C-terminus), as the longer spacer emerges out of the PPM, it enables the TM domain to engage directly the PVM translocon and the protein crosses the membranes without exposing the C-terminus to the oxidizing environment in the PV (Figure 5.2 C), potentially by a transient interaction of PPM and PVM trafficking factors.

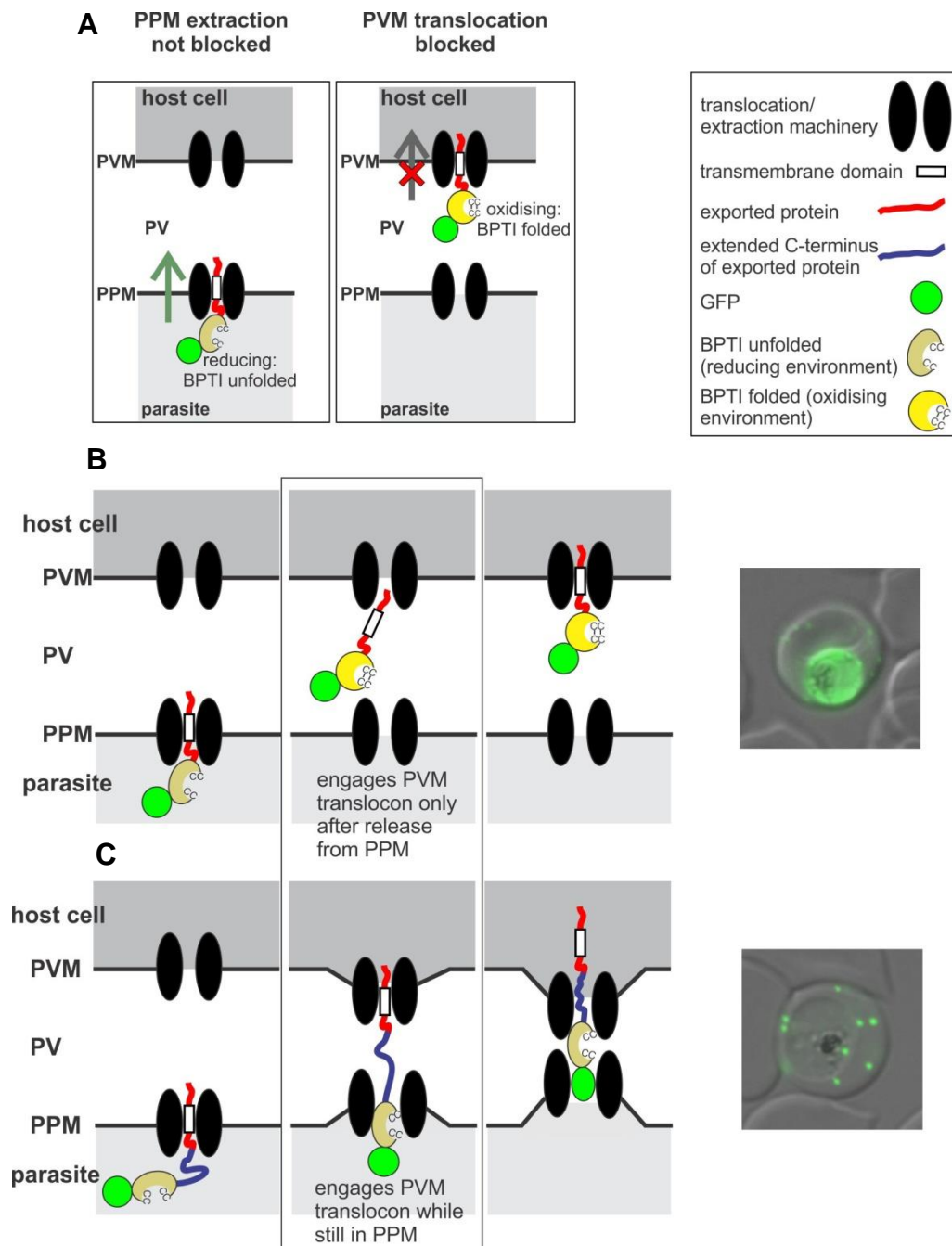


Figure 5. 2 | Model of translocation for TM proteins at the parasite periphery based on BPTI redox sensitive folding. (A) Schematic of the rationale for characterization of the translocation events of TM proteins beyond the PPM based on the redox dependent folding of BPTI. Only if TM proteins are released into the oxidising environment of the PV, the C-terminally fused BPTI would arrest export at the second translocation step **(B)** Model of translocation for protein with a short spacer (defined in this thesis as the distance between the TM

and the blocking domain), which are sensitive to folding since they are exposed to and arrested in the PV. **(C)** Model for translocation for TM BPTI fusions with long spacer, which are directly handed over to the PVM translocon during extraction out of the PPM and exported without PV intermediate. Features indicated in box on the top right. Live cell fluorescent images of *P. falciparum* parasites expressing BPTI constructs with short or long spacer right to the corresponding model in B and C.

One version of the proposed export models assumes that the membrane-spanning pore may span both membranes (Crabb et al., 2010; Spielmann and Marti, 2013). This situation seems however to be unlikely in our system, since BPTI fusion proteins with a short spacer otherwise would not traverse the oxidizing PV and would not become folded.

These findings thus sustain a model where translocation machineries at the PPM and the PVM may interact dynamically to mediate the export of parasite effectors, similar to the translocases in the outer and inner mitochondrial membranes (Hwang et al., 1989; Hwang et al., 1991; Horst et al., 1995). The scenario at the parasite boundary may also be comparable with protein import into plastids in euglenids and dinoflagellates, where proteins are first delivered by vesicles into the outermost plastid membrane upon fusion and further translocated through protein channels (Sulli et al., 1999; van Dooren et al., 2001; Sheiner and Striepen, 2012).

The leakiness observed in the BPTI constructs may indicate incomplete blockage of the PVM translocons by the arrested fusion protein. Consistently, the REX2-BPTI-GFP construct was not able to co-block the export of an internal control (data not shown). One explanation for this could be that the saturation of the translocons achieved by the BPTI fusion was not absolute. It is known that high saturation is needed to achieve efficient block of the transport of other proteins (Rassow et al., 1989). An alternative, not mutually exclusive, explanation could be the spatial arrangement of BPTI at the translocon. BPTI is a small protein (6 kDa) and has the shape of a 30-Å-long cylindrical particle with a diameter of 12–19 Å (Schwartz and Matouschek, 1999). The failure to co-block could therefore also arise from the shape of BPTI fusion, which might be not large enough to occlude the translocons and affect passage of other substrates. If this leads to a more rapid disassociation of the BPTI-fusion from the translocon, it could also affect the saturation of the translocons. A further alternative explanation can be the presence of thioredoxins in the PV (De Koning Ward et al., 2009; Kehr et al., 2010; Sharma et al., 2011) that might reduce the disulfide bonds and allow the protein to be translocated.

Since the BPTI- induced export arrest is not inducible, a global export arrest at the PVM would have deleterious effects on growth, as observed with arrested mDHFR constructs. Parasites may sense this and increase the efficiency of reduction in the PV to overcome this

blockade or there may be passive selection of parasites with an increasingly reducing PV in parasites carrying BPTI fusion constructs. Chloroplasts and mitochondria use redox signals to regulate protein translocation. The redox state of the chloroplast stroma is sensed by the translocon at the inner chloroplast membrane and the efficiency of translocation is adjusted accordingly (Stengel et al., 2010).

5.1.2 Evidence of translocation based export for other TM proteins

Although it is demonstrated that TM PNEPs require an unfolding-dependent translocation step to reach the host cell (Grüning et al., 2012) it was still unclear whether PEXEL TM proteins need also translocation to be exported. PNEP and PEXEL TM proteins are dependent in their export on the same PTEX factors at the PVM and can be co-blocked by an arrested translocation intermediate, however direct evidence of unfolding-dependent translocation for PEXEL proteins was still lacking. The parasite cell lines expressing PTP1- and STEVOR-mDHFR constructs demonstrated that indeed PEXEL TM proteins undergo translocation at the PVM, similar to PNEPs such as REX2, SBP1 and MAHRP1. Furthermore, PEXEL TM proteins appear to follow the same two-step export mechanism, as PTP1 (a protein with short spacer) was blocked in the PV when fused with BPTI and its C-terminally extended version was exported. The site of arrest for PEXEL mDHFR constructs was not investigated in the present work but based on the structural similarities of the tested constructs and the results obtained with the BPTI and PNEPs-mDHFR constructs, it may be assumed that PTP1-mDHFR was arrested at the PPM, comparable with REX2.

It is noteworthy that exported proteins with more than two TM domains have not been described in the exportome (Sargeant et al., 2006; Heiber et al., 2013). This may indicate restrictions imposed by the membrane translocation/extraction steps during export (Spielmann and Gilberger, 2015).

PfEMP1 is a TM PNEP displayed on the erythrocyte membrane and its trafficking is dependent on PTEX components (Beck et al., 2014; Elsworth et al., 2014a). The delivery of PfEMP1 is dependent on different proteins along the export pathway (Maier et al., 2008; Boddey and Cowman, 2013; McMillan et al., 2013) and these studies could not exclude that the block observed after inactivation of the PTEX is an indirect result of a failure to export other proteins required for PfEMP1 trafficking rather than a direct effect of PTEX inactivation. It might be assumed that this protein family exhibit the translocation mechanism here described for a TM PNEPs at the parasite boundary, nevertheless there is so far no proof that PfEMP1 variants are also translocated like other PNEPs. The translocation of these

proteins across the PVM has to date not been characterized, since most *var* genes average 8-10 kb in length, making it technically challenging to express the full-length sequences as mDHFR fusions from episomal expression plasmids (Melcher et al., 2010). Attempts to fuse the mDHFR domain to an endogenous PfEMP1 variant have so far been unsuccessful (data not shown).

5.1.3 Exported proteins are translocated through the same type of protein-conducting channels at the PVM

mDHFR intermediates have been a useful tool for the dissection of translocation mechanisms across membranes. The folding requirements of several *P. falciparum* exported proteins have been analysed using mDHFR fusion proteins (Gehde et al., 2009, Grüning et al., 2012; Heiber et al., 2013). In this work, the set of tested proteins was extended, including an entire repertoire of full length PEXEL and PNEP TM and soluble proteins. The data shown here strengthen the principle that the export of all proteins is dependent on unfolding and further support that translocation is the actual mechanism of trafficking to reach the RBC.

With aim to scrutinize the translocation events at the parasite boundary, mDHFR translocation intermediates that can be stably and conditionally arrested during translocation into the host cell were obtained in the present thesis. The requirement for unfolding of a protein to be transported indicates that exported proteins cross the PVM as linear polypeptides potentially through a protein-conducting channel (Gehde et al., 2009). The resistance of a cargo protein to unfolding during translocation hence prevents the passage of the polypeptide across the PVM. This resistance of the substrate correlates with its physical stability, which in case of mDHFR increases after ligand binding (Ainavarapu et al., 2005). In mitochondria, the extent of unfolding required during translocation is determined by the size of the protein channel (Matouschek et al., 2000). Protein channel diameters range between 10-27 Å (Schwartz and Matouschek, 1999; Ainavarapu et al., 2005) and the presence of a globular folded domain such as mDHFR is expected to clog the membrane pores.

To obtain stable translocation substrates an effective 'plug' must be fused to the cargo protein, thereby creating an efficient block for protein transport across the membrane (Schülke et al., 1997). Studies in mitochondria have demonstrated the ability of mDHFR intermediates to clog protein translocons and prevent the import of proteins (Rassow et al., 1989; Wienhues et al., 1991; Schülke et al., 1999) and the effect observed at the PVM may be comparable with that observed in mitochondrial import, where a limited number of import contact sites may be jammed with a translocation intermediate (Rassow et al., 1989). Fusion

of DHFR to secreted substrates in *Y. enterocolitica* led to a blockade of the type III secretion system (T3SS) and bacteria failed to secrete effectors into the host cell (Sorg et al., 2006; Riordan et al., 2008). High saturation is nevertheless required to achieve an absolute export blockade (Rassow et al., 1989). To generate stable translocation intermediates, studies of translocation using GFP have shown that potential clogging of transport machineries requires a presequence or TM domain able to either span the translocation pore or to insert into the surrounding membrane. Additionally, the length of the linker sequence, if two complexes or membranes are joined by the construct, may influence the transport kinetics and the stability of the fusion construct (Deponce, 2012). It is possible that such factors influenced the different properties (leakiness, induction of co-block, fluorescence pattern in the parasite periphery) of the different constructs analyzed in this work.

The series of double transfectant cell lines expressing different combinations of translocation arrested mDHFR intermediates together with other exported proteins showed that a PNEP TM precursor (SBP1-mDHFR-GFP) trapped by prevention of unfolding within a shared translocon interferes with the export of all types of exported proteins, including soluble and TM PNEPs and PEXEL proteins. The jamming of this common type of protein-conducting channels at the PVM led to the accumulation of further molecules of the intermediate itself and other exported proteins in the PV. Furthermore, soluble mDHFR intermediates arrested *en route* co-blocked export of TM proteins by jamming the PVM translocon; this indicates hence that the point where TM and soluble proteins of the different groups converge is the translocation through the same type of pore at the PVM.

These data support the principle that the different types of exported proteins cross the PVM through a single kind of protein-conducting channels. The present results are in accordance with two recent studies that revealed that all proteins converge on an export step at the PVM, involving PTEX components (Beck et al., 2014; Elsworth et al., 2014a), nevertheless these studies did not provide a direct evidence of translocation activity but the requirement of common trafficking factors in the PV that may fulfill the criteria of a protein translocon.

It is still puzzling how a single membrane-spanning pore can translocate hundreds of proteins with different export signals and domain organizations and what determines the specificity and substrate recognition to discriminate between protein destined to host cell and resident PV or PVM proteins that are not exported. HSP101 fulfills the features of the component that mediates substrate recognition based on structural similarities with other ATPases. Activity of HSP101 may be comparable to InVC in type III secretion systems (T3SS) in Gram negative bacteria (Akeda and Galán, 2005) and other AAA+ ATPase disassembly machines, able to recognize and unfold protein substrates (Ogura and Wilkinson, 2001).

The specificity for recognition of an exported protein is thought to be conferred by N-terminal sequences (Spielmann and Marti, 2013; Spillman et al., 2015) comparable to trafficking to organelles such as mitochondria or apicoplast (Schulz et al., 2015; Heiny et al., 2014). In *P. falciparum*, the mature PEXEL N-termini and in the case of PNEPs, sequences or structural signals present in PNEP N-termini and/ or the TM domain may determine this specificity (Spielmann and Gilberger, 2010; Grüring et al., 2012; Spielmann and Gilberger, 2013). It can be hypothesized that the PVM translocon may behave in a similar way to the translocase of the outer mitochondrial membrane (TOM), a versatile pore with a broad specificity against a range of presequences without a recognizable specific consensus sequence motif but that has the ability to distinguish between mitochondrial and non-mitochondrial proteins (Muto et al., 2001, Obita et al., 2003; Murcha et al., 2014).

One of the most intriguing questions raised from the mDHFR constructs was the ability and failure of some TM constructs to induce a co-block. The data obtained in this thesis revealed that this feature seems to depend on the capacity of the construct to reach and jam the translocons at the PVM and this is directly related with the length of the spacer between the TM region and the foldable mDHFR domain. Similar to the situation with the BPTI constructs, a special role must be taken by the TM domain, as it was not the entire region from the N-terminus to the blocking domain but the region between the TM and the blocking domain. Hence, the emergence of the TM out of the membrane seems to crucially affect translocation.

Experiments in mitochondria showed that the length of the linker between the signal sequence and the foldable domain determines the spanning of both membranes (Rassow et al., 1990). Assuming that the TM domain in the parasite periphery is analogous to the signal sequence in mitochondria, it could be hypothesized that TM export incompetent substrates with a long spacer span both membranes and engage components of both translocon machineries in transit across the membranes, resulting in the clogging of the translocation apparatus and the co-block of other exported proteins. A comparable phenomenon termed zippering has been observed *in vivo* in yeast mitochondria when an appropriate precursor becomes trapped *en route* to the matrix, spanning both outer and inner membranes and holding together translocation factors at both membranes (Schülke et al., 1997). The blocking of the translocation sites with this stuck intermediate inhibited the mitochondrial protein import (Schülke et al., 1999).

A model proposed for the co-block effect is shown in Figure 5.3. The behavior of different constructs appears to be related to the way they are translocated at the parasite periphery. mDHFR constructs with a short spacer did not interfere with the PVM translocation (failure to co-block) since these proteins are arrested at the PPM (Figure 5.3 A), where they are not

able to clog the protein-conducting channels at the PVM. The same proteins fused to BPTI are exposed to the oxidizing PV after PPM extraction, leading to oxidative folding of BPTI and retention of the protein in the PV (Figure 5.2 B).

In comparison, in mDHFR intermediates with a long spacer the TM emerge far enough from the PPM, to engage irreversibly the PVM translocon while being extracted out of the membrane, leading to the blockade of other proteins (Figure 5.3 B). Consistently, the BPTI fused constructs with a long spacer are directly handed over to the PVM translocon during PPM extraction, likely by transient interaction between the export machineries at both membranes. These proteins are thus not released into the vacuole, which avoids the oxidation-mediated folding (Figure 5.2 C).

From the data obtained in this thesis with protease protection assays, it seems that the TM mDHFR intermediates are however not spanning both membranes, as the blocking construct was found entirely in the PV (Figure 5.3 B). Previous studies in mitochondrial import have shown that a folded mDHFR domain on the mitochondrial surface can be unfolded and transported across the outer membrane, when the targeting sequence (a TM domain or presequence) is long enough to reach the import unfolding machinery, namely the ATPase mHSP70, in the inner mitochondrial membrane or matrix (Matouschek et al., 1997; Huang et al., 1999; Matouschek et al., 2000; Matouschek, 2003). This unfolding machinery potentially pulls the polypeptide chain at a distance into the matrix and unfolds the folded domain. A linker of at least 50 amino acids in front of a folded protein domain was sufficient to span both mitochondrial membranes and allow the interaction with proteins in the matrix (Rassow et al., 1990; Matouschek et al., 1997; Gaume et al., 1998). Matouschek et al., 1997 found that using a presequence length of 75 amino acids, a folded translocation-arrested DHFR fusion protein can interact with mHSP70 in the matrix. This critical length coincides with a sharp increase of the import rate of the folded precursor.

It can be thus hypothesized that in constructs with a long spacer between the TM domain and the mDHFR moiety, which reach and interact with the translocon at the PVM, the pulling force is high enough to pull the folded mDHFR out of the PPM and the intermediates are pulled into the PV, where they cannot be further translocated through the PVM translocon due the clogging effect. Hence, the fraction of the precursor spanning both membranes trapped in the translocons is considerably smaller than the co-blocked fraction present in the PV, assuming a limited number of translocation sites at the PVM and a continuous rapid transit of molecules across both membranes. For instance, previous studies quantitated around 270 import contact import sites per single mitochondrion (Rassow et al., 1989).

In the present study, the smallest spacer of a co-blocking exported protein was 100 amino acids (C-terminus of SBP1). In contrast the non co-blocking exported protein with the longest

spacer was REX2 (34 amino acids). From these results it can be estimated that a spacer as short as 99 amino acids but longer than 34 amino acids enables the TM of the substrate to emerge sufficiently from the PPM to engage PTEX at the PVM and to induce a direct hand over and jam the translocon at the PVM. However, the exact length of the spacer required to induce a co-block was not investigated in this thesis.

It was noteworthy that the PPM extraction is independent of the co-blocking effect and seems to be not affected by substrates arrested in translocation at the PVM. TM proteins were found co-blocked in the PV after jamming the PVM translocon either by soluble or TM mDHFR intermediates, indicating that the extraction step was not hampered and the TM proteins completed the passage across the PPM. This suggests that export machineries may operate independently or cooperatively depending on the exported substrate similar to mitochondrial import (Chacinska et al., 2003).

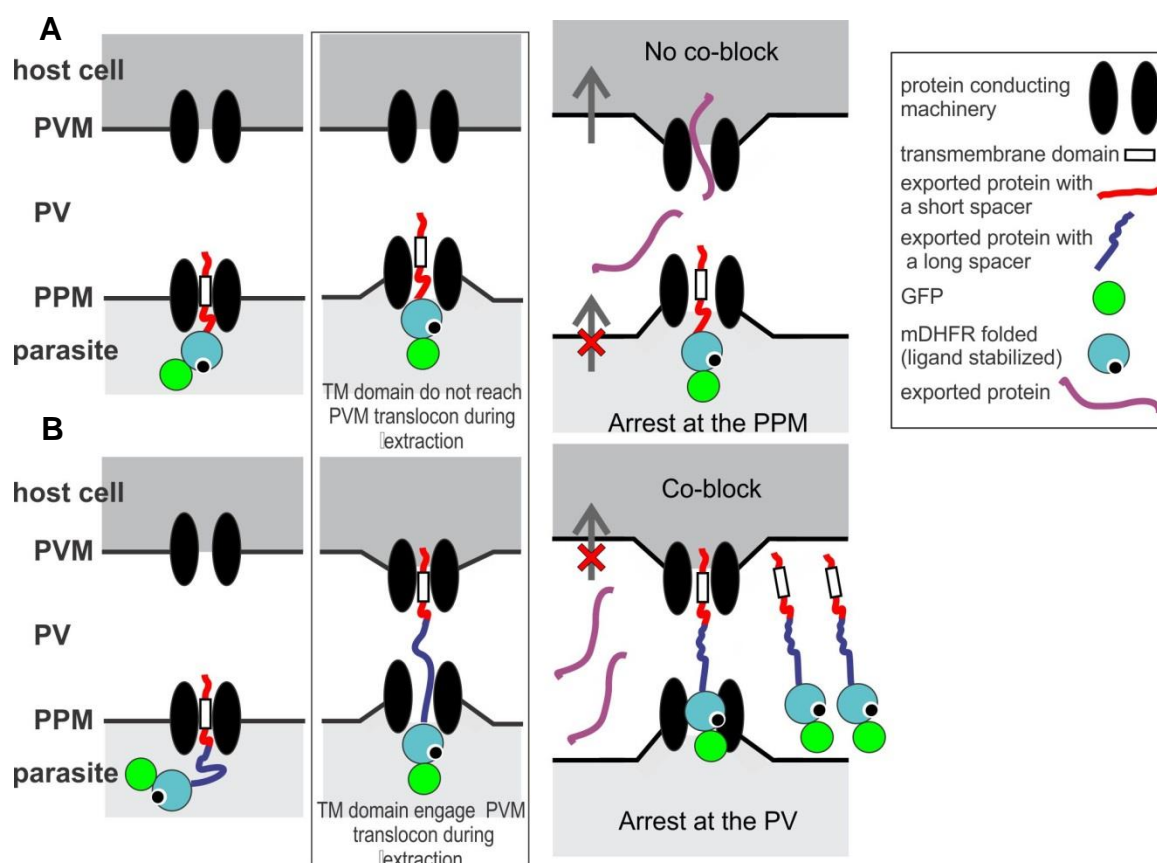


Figure 5. 3 | Model of co-block induced by arrested mDHFR TM intermediates at the parasite periphery.

(A) Model of translocation for TM mDHFR substrates with a short spacer (region between TM and blocking domain) unable to cause a co-block since they are arrested at the PPM. **(B)** Model of translocation for TM mDHFR intermediates with long spacers that are able to co-block the export of other proteins. The long spacer enables the TM of the protein to reach PVM translocon, which makes possible a direct hand over to the PVM translocon during extraction out of the PPM. Engagement with the PVM translocon leads to an arrest in this pore and prevents translocation of other proteins. Features are indicated in the box shown to the right.

5.1.4 Essentiality of protein export on parasite development

Taking advantage of the ability of the designed translocation substrates to prevent all exported proteins from reaching the infected RBC, this study analyzed the importance of global protein export on parasite growth. Remarkably, by stalling a folded intermediate in the translocation machinery, a profound growth defect was observed. The effect does not appear to be lethal over the time frame analysed, but parasites were unable to progress through the intraerythrocytic cycle and were arrested as young trophozoites, delaying the onset of schizogony. This phenotype is comparable with the inhibition of growth observed by knocking down of HSP101 and PTEX150 (Beck et al. 2014; Elsworth et al., 2014a). In contrast to these studies, in the here presented experiments, the PTEX components are still functional but the translocation of exported proteins is prevented by means of a translocation incompetent substrate. The exported proteins not delivered into the RBC must include proteins essential to complete the blood stage cycle *in vitro*, as evident from the impaired parasite development.

Similar effects were previously observed in other systems. Folded DHFR fusion proteins interfered with growth *in vivo* of *Legionella pneumophila* by occluding the type 4B secretion system and impairing delivery into the host cell of critical factors for intracellular replication and vacuole formation (Amyot et al., 2013). In yeast, a translocation intermediate in transit fused to protein A was able to join both translocases in the outer and inner mitochondrial membranes, inhibiting protein import and cell growth (Schülke et al., 1999). In *Shigella flexneri*, fusion of a folded domain to a secreted protein IpaB that obstructs T3SS prevented the secretion of IpaB itself and other T3SS effectors, which led to an attenuated invasion phenotype (Dohlich et al., 2014). Exported proteins in *P. falciparum* may function like the secretion systems seen in Gram negative bacteria, in which survival depends on, and pathogenicity arises from, a complex repertoire of secreted proteins that interact with host cell membranes or are present in the extracellular milieu, after crossing several membranes (Coburn et al., 2007; Maier et al., 2008; Diepold et al., 2015).

The outcome observed in WR-blocked parasites may be explained from a poorer nutrient uptake, since parasite-encoded exported proteins seem to be necessary for the activity of the PSAC (Beck et al., 2014; Spillman et al., 2015). According to this scenario, parasites incapable to export proteins and arrested at the transition to the trophozoite stage therefore would not be able to access to serum nutrients or precursors. Although most of the best characterized *P. falciparum*-specific members of the exportome play roles in the export and display of virulence proteins on the RBC surface (Cooke et al., 2006; Maier et al., 2007; Maier et al., 2008; Spycher et al., 2008; Rug et al., 2014), in the establishment of the

Maurer's clefts (Spycher et al., 2008; Dixon et al., 2008) and in the formation of the knobs, these proteins likely are not necessary for parasite growth under culture conditions (Maier et al., 2009). A large-scale knockout study estimated that around 25% of the *P. falciparum* exported proteins are essential for parasite erythrocytic development *in vitro* (Maier et al., 2008). These essential proteins might comprise effectors involved in restoration of the RBC membrane after the invasion process, in maintenance of ion gradients, in waste disposal, or in parasite egress. They may also function as chaperones of other crucial exported proteins or in the repair of the host cell membrane skeleton after oxidative damage (Maier et al., 2009).

It can be expected that a more pronounced effect of the export block would be seen *in vivo*, as arrested parasites would not traffic virulence factors such as PfEMP1 and knob components and in consequence will be more rapidly eliminated by the spleen. The data here indeed showed that some of these endogenous proteins such as KAHRP and REX1, required for the formation of knobs and the Maurer's clefts stability, respectively, were not exported due to clogging of the common translocon. Although not tested in this work, it would be interesting to further analyze the effect on cytoadherence, Maurer's clefts architecture and RBC deformability that these arrested parasites may exhibit.

A growth delay similar to that observed here upon blocking general protein export has been observed in the murine malaria parasite *P. berghei* by knocking out of *trx2*. Δ PbTRX2 parasites took longer to progress through the parasite cycle (Matthews et al., 2013) and the resulting defect may be consequence of loss of effector functions from a subset of exported proteins containing disulfide bridges that cannot be properly unfolded or from a partially clogged pore when such proteins are stuck in an unreduced state (Spillman et al., 2015). Nonetheless, in this study the effect on protein export was not investigated and the role of this PTEX constituent in protein export still remains conflicting (Matz et al., 2013), especially as unrelated phenotypes can equally lead to a slowed development in the mouse.

In comparison to the here shown global disruption of protein export by jamming the shared translocon, early ablation of protein export through chemical inhibition of the PM5 protease (Chang et al., 2008; Boddey et al., 2010; Russo et al., 2010), using a PEXEL-mimetic statin (RxVxLstatin), killed parasites at the transition from ring to trophozoite and led to a decrease in PEXEL processing and in binding to endothelial cells *in vitro* (Sleebs et al., 2014). However, accumulation of exported proteins in the parasite's ER or in the parasite periphery was not evident. The failure to detect an accumulation in the ER or other parts of the secretory pathway may indicate that already small amounts of precursors in the ER have a more detrimental effect than in the PV, potentially through dominant negative effects or by

disturbing other, unrelated processes of the secretory pathway (Spielmann and Gilberger, 2015).

The phenotype observed after abolition of PTEX function, either by inactivation of its components or modification of the exported substrate, may indicate that the putative translocon complex is not the most optimal of drug targets, unless lack of virulence factors *in vivo* potentiates the effect (Spielmann and Gilberger, 2015). Parasites were arrested in the transition between ring and trophozoite and its disruption neither killed the parasites nor affect late schizont stages. Moreover, the effect was reversible, when activity of the inactivated components was restored (Beck et al., 2014). Specific inhibitors thus would require pharmacokinetic properties or treatment regimens to uphold drug levels past the 48 h. Potential drugs acting on protein export would also benefit if they acted also on other live phases of the parasite life cycle. However, protein export during hepatic development remains still conflicting and the PTEX components expressed in liver stages appear to perform different roles than protein export (Matz et al., 2015), raising questions whether drugs acting on the blood stage export pathway may be effective against liver stages (Kalanon et al., 2016). In contrast, sexual stages export proteins into the host cell (Silvestrini et al., 2011; Morahan et al., 2011; Tiburcio et al., 2015) and appear to at least in part express components of the protein export pathway (Matthews et al., 2013; Beck et al., 2014); this may render gametocytogenesis partially susceptible to drugs targeting the export pathway.

5.1.5 Conditionally arrested substrates link PTEX with translocation activity

Although the findings in section 4.2 demonstrate that translocation across a protein-conducting channel is the actual mechanism of export at the PVM, there is so far no experimental evidence that links the PTEX components with translocation or unfolding activity.

EXP2 is the PTEX component suspected to be the membrane-spanning pore at the PVM. Despite the lack of a predicted TM domain, EXP2 is tightly associated with the membrane, resisting carbonate extraction (Johnson et al., 1994; De Koning-Ward et al., 2009). The protein is thought to oligomerize in a 600 KDa complex and insert into membranes, opening high conductance pores (Bullen et al., 2012). The structural homology of EXP2 with *Escherichia coli*, HlyE (De Koning-Ward et al., 2009), a toxin predicted to form homo-oligomeric pores within host cell membranes (Ludwig et al., 1999; Wallace et al., 2000), also supported this hypothesis.

Functional data of EXP2 in *P. falciparum* are to date still missing and no formal proof of its function in protein export and translocation is available. In a recent study, *P. falciparum* EXP2 was shown to complement the function of GRA17 in *Toxoplasma* GRA17-deficient parasites (Gold et al., 2015). However, GRA17 appears to play a role in nutrient access through the *T. gondii* PVM rather than in protein export (Gold et al., 2015). Exogenous expression of EXP2 and GRA17 in *Xenopus* oocytes revealed that the membrane conduction in the oocytes was altered by generation of non-selective pores (Gold et al., 2015). Together, these data suggested that EXP2 is involved in the solute channel activity at the PVM originally detected by patch clamp experiments (Desai et al., 1993; Desai and Rosenberg, 1997).

The expression in other parasite stages suggests that EXP2 may perform different functions across the life cycle (Matz et al., 2015) In liver stages the protein appear to carry out functions not related with protein export, as its partner HSP101 was not detectable at the PVM and reporters destined to be exported accumulated in the PV or PVM (Kalanon et al., 2016). It can be hypothesized that EXP2 is a high conductance channel at the PVM that interacts with different accessory factors such as PTEX150 and HSP101 to mediate protein export and with other components to perform function as solute pore channel for nutrient uptake or to insert PVM resident proteins (Kalanon et al., 2016) such as ETRAMPs and EXP1.

To gain insights into the function of EXP2 in *P. falciparum*, in the present thesis the endogenous protein was tagged. The organization of the PTEX complex was discovered originally by pulling down 3XHA tagged PTEX150 and HSP101 and confirming their interaction with EXP2 using specific antibodies against the endogenous protein (De Koning Ward et al., 2009; Bullen et al., 2012). Nevertheless, the endogenous EXP2 has so far not been tagged in this parasite. IP assays via a C-terminal HA tag may provide better results in affinity purification assays than IP assays performed with antibodies raised against EXP2 itself for two reasons: firstly, epitopes on EXP2 might be obscured through interactions with other proteins and may lead to false negative results (Dunham et al., 2012). Secondly, commercial monoclonal antibodies to HA may be of superior quality, in terms of avidity and specificity, in contrast to polyclonal sera, where false positives and background contaminants would be expected. In addition, endogenous tagging by genomic integration has the advantage that the endogenous protein is partaking in its natural physiological role and the entire population of the bait protein in the parasite is tagged, in contrast to episomal expression where the native protein can compete for association with interaction partners. This assumption applies particularly for essential proteins, which EXP2 is thought to be (de Koning-Ward et al., 2009; Matthews et al., 2013; Matz et al., 2013; Matz et al., 2015). Hence,

the endogenous HA tagging approach was chosen for EXP2 in this thesis. In accordance with the previous studies that characterized the complex, the PTEX core EXP2-HSP101-PTEX150 was isolated from the proteomic analyses when EXP2-3XHA was pulled down. Interestingly, several additional potential interacting partners of EXP2 were identified, that may be involved in functions different than protein export, may be further components of PTEX or may be unspecific interactors. Validation of these candidates requires further investigation and is currently ongoing. Consistent with the MS results obtained in the present work, a very recent study co-pulled down by immunoprecipitating 3XHA tagged PTEX150 two of the proteins (Pf113 and PV1) here identified, and through reciprocal IPs assumed them to be bona fide PTEX components (Elsworth et al., 2016). Further experiments, in particular functional assays, will be needed to further confirm this assumption.

Based on the observation that a trapped stable mDHFR intermediate clogs a common protein-conducting channel, it was assumed that it remains in contact with the translocon. These arrested substrates were therefore used in the present study to investigate their interaction with the export machinery and to potentially reveal the identity of the translocon in which they are stuck. Riglar et al., 2013 co-localized EXP2 by IFA with an mDHFR reporter arrested in export, nevertheless co-localization with substrates on the fluorescence microscope level is not sufficient to postulate interaction and validate PTEX as a bona fide translocon (Spielmann and Marti, 2013).

From the set of co-IP experiments performed in this work, it can be concluded that substrates arrested in transit by prevention of unfolding were found in a complex with the PTEX component EXP2. These data thus give clear evidence for an association between PTEX and translocation activity. Moreover, these findings represent strong evidence that EXP2 is part of a translocation entity and support its role in protein export. This adds weight to the hypothesis that EXP2 may be the PTEX component functioning as a protein-conducting channel at the PVM, which delivers parasite effectors into the infected cell. Nevertheless, from this series of experiments it cannot be ruled out that EXP2 is only structural part of the PTEX complex and has functions not necessarily related to that of a membrane pore through which proteins are translocated. The fact that the translocation incompetent substrate was found interacting only with EXP2 but not with other PTEX components tested (HSP101) supports that EXP2 is the site within which the arrested substrate is found when threaded and speaks against an indirect enrichment. Evidence that folded substrates are trapped within the channels of bacterial secretion systems (Amyoth et al. 2011; Dohlich et al., 2014), or within translocation machineries in mitochondria (Schülke et al., 1999), give support to these results.

HSP101–destabilization caused dissociation of HSP101 from EXP2 and PTEX150, whereas association with the exported protein RESA was enhanced, suggesting that HSP101 can interact with exported cargo independently of the EXP2–PTEX150 subcomplex (Beck et al., 2014). In contrast, in the present experiments, HSP101 was found as part of the complex when a translocation incompetent substrate was trapped within the complex but it was not found in close contact with the arrested substrate, since both were not co-purified in IP experiments. This might indicate that the putative ATPase dissociates from the substrate as it cannot unfold it, although it still appears to remain attached to the overall translocation complex. Dissociation of stabilized mDHFR substrates upon failed unfolding has been observed with AAA+ proteases such as ClpXP and ClpAP, ATP driven unfoldases involved in protein degradation and able to unfold multidomain proteins (Lee et al., 2001; Kenniston et al., 2005; Baker and Sauer, 2011).

A further confirmation of the model proposed in Figure 5.3 was the fact that only those constructs able to induce a co-block (SBP1-mDHFR-GFP and REX2-GFP-mDHFR) were found in close association with EXP2. This further supports the idea that a longer spacer enabled these constructs to reach the export machinery at the PVM where they remain attached and prevent the export of other proteins. In comparison, REX2-mDHFR-GFP, the non-co-blocking construct with a short spacer known to be arrested at the PPM (Grüring et al., 2012) was not found in a complex with EXP2. This might indicate that in absence of PPM extraction, the TM region of REX2-mDHFR remains arrested at the PPM and its short spacer does not allow the protein to engage and clog the PTEX component. This was in accordance with previous experiments that did not co-purified PTEX components by immunoprecipitation of the arrested REX2-mDHFR-GFP (Grüring et al., 2012).

5.1.6 Conclusions

Conditionally foldable intermediates shed light on the sequence of translocation events during protein export that take place at the parasite boundary for the different types of exported parasite proteins. The stable translocation substrates obtained in this work revealed and validated unifying principles in the protein export pathway and will be potentially useful to further unravel unknown mechanisms in malaria protein export.

The effectors involved in protein export are parasite specific and have demonstrated to be critical for parasite growth and pathogenicity. Hence, a comprehensive understanding of the protein export pathway in malaria parasites will help to identify potential targets to inhibit parasite development and modulate parasite induced pathology. The results presented in

this thesis propose several mechanistic models which will be the basis for future work about the complex series of translocation mechanisms that proteins undergo to find their final destination and exert its function in the host cell.

In spite of great advances to understand protein export, many questions remain to be addressed. PTEX is essential for the export of all proteins and fulfills the features of a translocation machinery at the PVM. Although the findings of this work link PTEX with translocation activity, conditional studies to abrogate the function of EXP2 will be crucial to clarify its role in protein export as protein-conducting channel and/or as solute pore at the PVM.

Many exported proteins, including the major virulence factor PfEMP1, contain TM domains and the uncovering of the export pathway for this kind of proteins is still an exciting field in parasite cell biology. The parasite-encoded effectors that mediate the extraction of TM proteins out of the PPM are still enigmatic and which role play the PTEX components in this step, wait to be elucidated. This extraction machinery also may be likely involved in extraction of PVM resident proteins on their way from the PPM to their final destination. As no vesicular pathway has been so far demonstrated, it is still also challenging to understand how RBC membrane and Maurer's clefts resident TM proteins reach their destination after crossing the PVM and how are inserted into the respective final membrane. The complexity of the translocation systems in other systems such as the mitochondria or the chloroplast may indicate that also in the malaria parasite a lot remains to be discovered for the protein trafficking steps at the PPM and PVM. New approaches will be necessary to resolve the intricate series of mechanisms that this parasite has evolved to conquer its host cell.

References

1. Abu Bakar, N., Klonis, N., Hanssen, E., Chan, C., and Tilley, L. (2010). Digestive-vacuole genesis and endocytic processes in the early intraerythrocytic stages of *Plasmodium falciparum*. *Journal of cell science* *123*, 441-450.
2. Adisa, A., Frankland, S., Rug, M., Jackson, K., Maier, A.G., Walsh, P., Lithgow, T., Klonis, N., Gilson, P.R., Cowman, A.F., *et al.* (2007). Re-assessing the locations of components of the classical vesicle-mediated trafficking machinery in transfected *Plasmodium falciparum*. *Int J Parasitol* *37*, 1127-1141.
3. Adl, S.M., Simpson, A.G., Farmer, M.A., Andersen, R.A., Anderson, O.R., Barta, J.R., Bowser, S.S., Brugerolle, G., Fensome, R.A., Fredericq, S., *et al.* (2005). The new higher level classification of eukaryotes with emphasis on the taxonomy of protists. *The Journal of eukaryotic microbiology* *52*, 399-451.
4. Adl, S.M., Simpson, A.G., Lane, C.E., Lukes, J., Bass, D., Bowser, S.S., Brown, M.W., Burki, F., Dunthorn, M., Hampl, V., *et al.* (2012). The revised classification of eukaryotes. *The Journal of eukaryotic microbiology* *59*, 429-493.
5. Agrawal, S., van Dooren, G.G., Beatty, W.L., and Striepen, B. (2009). Genetic evidence that an endosymbiont-derived endoplasmic reticulum-associated protein degradation (ERAD) system functions in import of apicoplast proteins. *The Journal of biological chemistry* *284*, 33683-33691.
6. Aikawa, M., Uni, Y., Andrutis, A.T., and Howard, R.J. (1986). Membrane-associated electron-dense material of the asexual stages of *Plasmodium falciparum*: evidence for movement from the intracellular parasite to the erythrocyte membrane. *Am J Trop Med Hyg* *35*, 30-36.
7. Ainarapu, S.R., Li, L., Badilla, C.L., and Fernandez, J.M. (2005). Ligand binding modulates the mechanical stability of dihydrofolate reductase. *Biophys J* *89*, 3337-3344.
8. Akeda, Y., and Galan, J.E. (2005). Chaperone release and unfolding of substrates in type III secretion. *Nature* *437*, 911-915.
9. Akinyi, S., Hanssen, E., Meyer, E.V., Jiang, J., Korir, C.C., Singh, B., Lapp, S., Barnwell, J.W., Tilley, L., and Galinski, M.R. (2012). A 95 kDa protein of *Plasmodium vivax* and *P. cynomolgi* visualized by three-dimensional tomography in the caveola-vesicle complexes (Schuffner's dots) of infected erythrocytes is a member of the PHIST family. *Molecular microbiology* *84*, 816-831.
10. Aley, S.B., Sherwood, J.A., Marsh, K., Eidelman, O., and Howard, R.J. (1986). Identification of isolate-specific proteins on sorbitol-enriched *Plasmodium falciparum* infected erythrocytes from Gambian patients. *Parasitology* *92* (Pt 3), 511-525.
11. Alkhalil, A., Cohn, J.V., Wagner, M.A., Cabrera, J.S., Rajapandi, T., and Desai, S.A. (2004). *Plasmodium falciparum* likely encodes the principal anion channel on infected human erythrocytes. *Blood* *104*, 4279-4286.
12. Alonso, P.L., Brown, G., Arevalo-Herrera, M., Binka, F., Chitnis, C., Collins, F., Doumbo, O.K., Greenwood, B., Hall, B.F., Levine, M.M., *et al.* (2011). A research agenda to underpin malaria eradication. *PLoS medicine* *8*, e1000406.
13. Amino, R., Giovannini, D., Thiberge, S., Gueirard, P., Boisson, B., Dubremetz, J.F., Prevost, M.C., Ishino, T., Yuda, M., and Menard, R. (2008). Host cell traversal is important for progression of the malaria parasite through the dermis to the liver. *Cell host & microbe* *3*, 88-96.
14. Amino, R., Thiberge, S., Shorte, S., Frischknecht, F., and Menard, R. (2006). Quantitative imaging of *Plasmodium* sporozoites in the mammalian host. *C R Biol* *329*, 858-862.
15. Ammelburg, M., Frickey, T., and Lupas, A.N. (2006). Classification of AAA+ proteins. *Journal of structural biology* *156*, 2-11.
16. Amyot, W.M., deJesus, D., and Isberg, R.R. (2013). Poison domains block transit of translocated substrates via the *Legionella pneumophila* Icm/Dot system. *Infect Immun* *81*, 3239-3252.
17. Anson, I., Bente, J., Bhakdi, S., and Lingelbach, K. (1996). Protein sorting in *Plasmodium falciparum*-infected red blood cells permeabilized with the pore-forming protein streptolysin O. *Biochem J* *315* (Pt 1), 307-314.
18. Anstey, N.M., Russell, B., Yeo, T.W., and Price, R.N. (2009). The pathophysiology of vivax malaria. *Trends in parasitology* *25*, 220-227.
19. Appleman, J.R., Prendergast, N., Delcamp, T.J., Freisheim, J.H., and Blakley, R.L. (1988). Kinetics of the formation and isomerization of methotrexate complexes of recombinant human dihydrofolate reductase. *The Journal of biological chemistry* *263*, 10304-10313.
20. Arie, F., Witkowski, B., Amaratunga, C., Beghain, J., Langlois, A.C., Khim, N., Kim, S., Duru, V., Bouchier, C., Ma, L., *et al.* (2014). A molecular marker of artemisinin-resistant *Plasmodium falciparum* malaria. *Nature* *505*, 50-55.
21. Arolas, J.L., Aviles, F.X., Chang, J.Y., and Ventura, S. (2006). Folding of small disulfide-rich proteins: clarifying the puzzle. *Trends Biochem Sci* *31*, 292-301.
22. Ayong, L., Pagnotti, G., Tobon, A.B., and Chakrabarti, D. (2007). Identification of *Plasmodium falciparum* family of SNAREs. *Molecular and biochemical parasitology* *152*, 113-122.
23. Backhaus, R., Zehe, C., Wegehingel, S., Kehlenbach, A., Schwappach, B., and Nickel, W. (2004). Unconventional protein secretion: membrane translocation of FGF-2 does not require protein unfolding. *Journal of cell science* *117*, 1727-1736.
24. Baer, K., Klotz, C., Kappe, S.H., Schnieder, T., and Frevert, U. (2007). Release of hepatic *Plasmodium*

- yoelii merozoites into the pulmonary microvasculature. *PLoS Pathog* 3, e171.
25. Bagola, K., Mehnert, M., Jarosch, E., and Sommer, T. (2011). Protein dislocation from the ER. *Biochimica et biophysica acta* 1808, 925-936.
 26. Baker, T.A., and Sauer, R.T. (2012). ClpXP, an ATP-powered unfolding and protein-degradation machine. *Biochimica et biophysica acta* 1823, 15-28.
 27. Bannister, L.H., Hopkins, J.M., Fowler, R.E., Krishna, S., and Mitchell, G.H. (2000). A brief illustrated guide to the ultrastructure of *Plasmodium falciparum* asexual blood stages. *Parasitology today* 16, 427-433.
 28. Bannister, L.H., Hopkins, J.M., Margos, G., Dluzewski, A.R., and Mitchell, G.H. (2004). Three-dimensional ultrastructure of the ring stage of *Plasmodium falciparum*: evidence for export pathways. *Microscopy and microanalysis : the official journal of Microscopy Society of America, Microbeam Analysis Society, Microscopical Society of Canada* 10, 551-562.
 29. Banumathy, G., Singh, V., and Tatu, U. (2002). Host chaperones are recruited in membrane-bound complexes by *Plasmodium falciparum*. *The Journal of biological chemistry* 277, 3902-3912.
 30. Barnwell, J.W. (1989). Cytoadherence and sequestration in *falciparum* malaria. *Experimental parasitology* 69, 407-412.
 31. Bartoloni, A., and Zammarchi, L. (2012). Clinical aspects of uncomplicated and severe malaria. *Mediterr J Hematol Infect Dis* 4, e2012026.
 32. Baruch, D.I., Gormely, J.A., Ma, C., Howard, R.J., and Pasloske, B.L. (1996). *Plasmodium falciparum* erythrocyte membrane protein 1 is a parasitized erythrocyte receptor for adherence to CD36, thrombospondin, and intercellular adhesion molecule 1. *Proc Natl Acad Sci U S A* 93, 3497-3502.
 33. Baum, J., Richard, D., Healer, J., Rug, M., Krnajski, Z., Gilberger, T.W., Green, J.L., Holder, A.A., and Cowman, A.F. (2006). A conserved molecular motor drives cell invasion and gliding motility across malaria life cycle stages and other apicomplexan parasites. *The Journal of biological chemistry* 281, 5197-5208.
 34. Beck, J.R., Muralidharan, V., Oksman, A., and Goldberg, D.E. (2014). PTEX component HSP101 mediates export of diverse malaria effectors into host erythrocytes. *Nature* 511, 592-595.
 35. Benting, J., Mattei, D., and Lingelbach, K. (1994). Brefeldin A inhibits transport of the glycophorin-binding protein from *Plasmodium falciparum* into the host erythrocyte. *Biochem J* 300 (Pt 3), 821-826.
 36. Bernabeu, M., Lopez, F.J., Ferrer, M., Martin-Jaular, L., Razaname, A., Corradin, G., Maier, A.G., Del Portillo, H.A., and Fernandez-Becerra, C. (2012). Functional analysis of *Plasmodium vivax* VIR proteins reveals different subcellular localizations and cytoadherence to the ICAM-1 endothelial receptor. *Cellular microbiology* 14, 386-400.
 37. Besteiro, S., Dubremetz, J.F., and Lebrun, M. (2011). The moving junction of apicomplexan parasites: a key structure for invasion. *Cellular microbiology* 13, 797-805.
 38. Bhatt, S., Weiss, D.J., Cameron, E., Bisanzio, D., Mappin, B., Dalrymple, U., Battle, K.E., Moyes, C.L., Henry, A., Eckhoff, P.A., *et al.* (2015). The effect of malaria control on *Plasmodium falciparum* in Africa between 2000 and 2015. *Nature* 526, 207-211.
 39. Bhattacharjee, S., Speicher, K.D., Stahelin, R.V., Speicher, D.W., and Haldar, K. (2012). PI(3)P-independent and -dependent pathways function together in a vacuolar translocation sequence to target malarial proteins to the host erythrocyte. *Molecular and biochemical parasitology* 185, 106-113.
 40. Bhattacharjee, S., Stahelin, R.V., Speicher, K.D., Speicher, D.W., and Haldar, K. (2012). Endoplasmic reticulum PI(3)P lipid binding targets malaria proteins to the host cell. *Cell* 148, 201-212.
 41. Billker, O., Lindo, V., Panico, M., Etienne, A.E., Paxton, T., Dell, A., Rogers, M., Sinden, R.E., and Morris, H.R. (1998). Identification of xanthurenic acid as the putative inducer of malaria development in the mosquito. *Nature* 392, 289-292.
 42. Billker, O., Shaw, M.K., Margos, G., and Sinden, R.E. (1997). The roles of temperature, pH and mosquito factors as triggers of male and female gametogenesis of *Plasmodium berghei* in vitro. *Parasitology* 115 (Pt 1), 1-7.
 43. Blackman, M.J., and Bannister, L.H. (2001). Apical organelles of Apicomplexa: biology and isolation by subcellular fractionation. *Molecular and biochemical parasitology* 117, 11-25.
 44. Blackman, M.J., Heidrich, H.G., Donachie, S., McBride, J.S., and Holder, A.A. (1990). A single fragment of a malaria merozoite surface protein remains on the parasite during red cell invasion and is the target of invasion-inhibiting antibodies. *The Journal of experimental medicine* 172, 379-382.
 45. Blisnick, T., Morales Betoulle, M.E., Barale, J.C., Uzureau, P., Berry, L., Desroses, S., Fujioka, H., Mattei, D., and Braun Breton, C. (2000). Pfsbp1, a Maurer's cleft *Plasmodium falciparum* protein, is associated with the erythrocyte skeleton. *Molecular and biochemical parasitology* 111, 107-121.
 46. Blobel, G., and Dobberstein, B. (1975). Transfer of proteins across membranes. I. Presence of proteolytically processed and unprocessed nascent immunoglobulin light chains on membrane-bound ribosomes of murine myeloma. *The Journal of cell biology* 67, 835-851.
 47. Boddey, J.A., and Cowman, A.F. (2013). *Plasmodium* nesting: remaking the erythrocyte from the inside out. *Annu Rev Microbiol* 67, 243-269.
 48. Boddey, J.A., Hodder, A.N., Gunther, S., Gilson, P.R., Patsiouras, H., Kapp, E.A., Pearce, J.A., de Koning-Ward, T.F., Simpson, R.J., Crabb, B.S., *et al.* (2010). An aspartyl protease directs malaria effector proteins to the host cell. *Nature* 463, 627-631.
 49. Boddey, J.A., Moritz, R.L., Simpson, R.J., and Cowman, A.F. (2009). Role of the *Plasmodium* export element in trafficking parasite proteins to the infected erythrocyte. *Traffic* 10, 285-299.
 50. Bonifacino, J.S., and Glick, B.S. (2004). The mechanisms of vesicle budding and fusion. *Cell* 116, 153-

- 166.
51. Botelho, S.C., Osterberg, M., Reichert, A.S., Yamano, K., Bjorkholm, P., Endo, T., von Heijne, G., and Kim, H. (2011). TIM23-mediated insertion of transmembrane alpha-helices into the mitochondrial inner membrane. *The EMBO journal* *30*, 1003-1011.
 52. Boucher, I.W., McMillan, P.J., Gabrielsen, M., Akerman, S.E., Brannigan, J.A., Schnick, C., Brzozowski, A.M., Wilkinson, A.J., and Muller, S. (2006). Structural and biochemical characterization of a mitochondrial peroxiredoxin from *Plasmodium falciparum*. *Molecular microbiology* *61*, 948-959.
 53. Bray, P.G., Ward, S.A., and O'Neill, P.M. (2005). Quinolines and artemisinin: chemistry, biology and history. *Current topics in microbiology and immunology* *295*, 3-38.
 54. Bruce-Chwatt, L.J., (1988) History of malaria from prehistory to eradication. In W. Wernsdorfer and I. McGregor (ed.) *Malaria. Principles and Practice of Malariology*, *1*, 1-59
 55. Bruce, M.C., Alano, P., Duthie, S., and Carter, R. (1990). Commitment of the malaria parasite *Plasmodium falciparum* to sexual and asexual development. *Parasitology* *100 Pt 2*, 191-200.
 56. Buffet, P.A., Safeukui, I., Deplaine, G., Brousse, V., Prendki, V., Thellier, M., Turner, G.D., and Mercereau-Pujalon, O. (2011). The pathogenesis of *Plasmodium falciparum* malaria in humans: insights from splenic physiology. *Blood* *117*, 381-392.
 57. Bullen, H.E., Charnaud, S.C., Kalanon, M., Riglar, D.T., Dekiwadia, C., Kangwanrangsan, N., Torii, M., Tsuboi, T., Baum, J., Ralph, S.A., *et al.* (2012). Biosynthesis, localization, and macromolecular arrangement of the *Plasmodium falciparum* translocon of exported proteins (PTEX). *The Journal of biological chemistry* *287*, 7871-7884.
 58. Campo, B., Vandal, O., Wesche, D.L., and Burrows, J.N. (2015). Killing the hypnozoite--drug discovery approaches to prevent relapse in *Plasmodium vivax*. *Pathogens and global health* *109*, 107-122.
 59. Cao, J., Kaneko, O., Thongkukiakul, A., Tachibana, M., Otsuki, H., Gao, Q., Tsuboi, T., and Torii, M. (2009). Rhoptry neck protein RON2 forms a complex with microneme protein AMA1 in *Plasmodium falciparum* merozoites. *Parasitology international* *58*, 29-35.
 60. Carlson, E.J., Pitonzo, D., and Skach, W.R. (2006). p97 functions as an auxiliary factor to facilitate TM domain extraction during CFTR ER-associated degradation. *The EMBO journal* *25*, 4557-4566.
 61. Carruthers, V.B., and Tomley, F.M. (2008). Microneme proteins in apicomplexans. *Subcell Biochem* *47*, 33-45.
 62. Chacinska, A., Koehler, C.M., Milenkovic, D., Lithgow, T., and Pfanner, N. (2009). Importing mitochondrial proteins: machineries and mechanisms. *Cell* *138*, 628-644.
 63. Chacinska, A., Rehling, P., Guiard, B., Frazier, A.E., Schulze-Specking, A., Pfanner, N., Voos, W., and Meisinger, C. (2003). Mitochondrial translocation contact sites: separation of dynamic and stabilizing elements in formation of a TOM-TIM-preprotein supercomplex. *The EMBO journal* *22*, 5370-5381.
 64. Chang, H.H., Falick, A.M., Carlton, P.M., Sedat, J.W., DeRisi, J.L., and Marletta, M.A. (2008). N-terminal processing of proteins exported by malaria parasites. *Molecular and biochemical parasitology* *160*, 107-115.
 65. Chu, T., Lingelbach, K., and Przyborski, J.M. (2011). Genetic evidence strongly support an essential role for PfPV1 in intra-erythrocytic growth of *P. falciparum*. *PloS one* *6*, e18396.
 66. Clark, S.A., and Theg, S.M. (1997). A folded protein can be transported across the chloroplast envelope and thylakoid membranes. *Molecular biology of the cell* *8*, 923-934.
 67. Clyde, D.F., Most, H., McCarthy, V.C., and Vanderberg, J.P. (1973). Immunization of man against sporozite-induced falciparum malaria. *Am J Med Sci* *266*, 169-177.
 68. Coburn, B., Sekirov, I., and Finlay, B.B. (2007). Type III secretion systems and disease. *Clinical microbiology reviews* *20*, 535-549.
 69. Collins, W.E., Contacos, P.G., Skinner, J.C., and Guinn, E.G. (1971). Studies on the transmission of simian malaria. IV. Further studies on the transmission of *Plasmodium knowlesi* by *Anopheles balabacensis balabacensis* mosquitoes. *J Parasitol* *57*, 961-966.
 70. Collins, W.E., and Jeffery, G.M. (2005). *Plasmodium ovale*: parasite and disease. *Clinical microbiology reviews* *18*, 570-581.
 71. Collins, W.E., and Jeffery, G.M. (2007). *Plasmodium malariae*: parasite and disease. *Clinical microbiology reviews* *20*, 579-592.
 72. Collins, W.E., Skinner, J.C., Broderson, J.R., Richardson, B.B., and Stanfill, P.S. (1989). The Uganda I/CDC strain of *Plasmodium malariae* in *Saimiri sciureus boliviensis*. *J Parasitol* *75*, 310-313.
 73. Combes, V., El-Assaad, F., Faille, D., Jambou, R., Hunt, N.H., and Grau, G.E. (2010). Microvesiculation and cell interactions at the brain-endothelial interface in cerebral malaria pathogenesis. *Prog Neurobiol* *91*, 140-151.
 74. Cooke, B.M., Buckingham, D.W., Glenister, F.K., Fernandez, K.M., Bannister, L.H., Marti, M., Mohandas, N., and Coppel, R.L. (2006). A Maurer's cleft-associated protein is essential for expression of the major malaria virulence antigen on the surface of infected red blood cells. *The Journal of cell biology* *172*, 899-908.
 75. Coppi, A., Natarajan, R., Pradel, G., Bennett, B.L., James, E.R., Roggero, M.A., Corradin, G., Persson, C., Tewari, R., and Sinnis, P. (2011). The malaria circumsporozoite protein has two functional domains, each with distinct roles as sporozoites journey from mosquito to mammalian host. *The Journal of experimental medicine* *208*, 341-356.
 76. Coppi, A., Tewari, R., Bishop, J.R., Bennett, B.L., Lawrence, R., Esko, J.D., Billker, O., and Sinnis, P. (2007). Heparan sulfate proteoglycans provide a signal to *Plasmodium* sporozoites to stop migrating and productively invade host cells. *Cell host & microbe* *2*, 316-327.

77. Cosson, P., Perrin, J., and Bonifacino, J.S. (2013). Anchors aweigh: protein localization and transport mediated by transmembrane domains. *Trends in cell biology* 23, 511-517.
78. Couffin, S., Hernandez-Rivas, R., Blisnick, T., and Mattei, D. (1998). Characterisation of PfSec61, a Plasmodium falciparum homologue of a component of the translocation machinery at the endoplasmic reticulum membrane of eukaryotic cells. *Molecular and biochemical parasitology* 92, 89-98.
79. Counihan, N.A., Kalanon, M., Coppel, R.L., and de Koning-Ward, T.F. (2013). Plasmodium rhostry proteins: why order is important. *Trends in parasitology* 29, 228-236.
80. Cowman, A.F., Berry, D., and Baum, J. (2012). The cellular and molecular basis for malaria parasite invasion of the human red blood cell. *The Journal of cell biology* 198, 961-971.
81. Cox-Singh, J., Davis, T.M., Lee, K.S., Shamsul, S.S., Matusop, A., Ratnam, S., Rahman, H.A., Conway, D.J., and Singh, B. (2008). Plasmodium knowlesi malaria in humans is widely distributed and potentially life threatening. *Clinical infectious diseases : an official publication of the Infectious Diseases Society of America* 46, 165-171.
82. Crabb, B.S., Cooke, B.M., Reeder, J.C., Waller, R.F., Caruana, S.R., Davern, K.M., Wickham, M.E., Brown, G.V., Coppel, R.L., and Cowman, A.F. (1997). Targeted gene disruption shows that knobs enable malaria-infected red cells to cytoadhere under physiological shear stress. *Cell* 89, 287-296.
83. Crabb, B.S., de Koning-Ward, T.F., and Gilson, P.R. (2010). Protein export in Plasmodium parasites: from the endoplasmic reticulum to the vacuolar export machine. *Int J Parasitol* 40, 509-513.
84. Cranston, H.A., Boylan, C.W., Carroll, G.L., Suter, S.P., Williamson, J.R., Gluzman, I.Y., and Krogstad, D.J. (1984). Plasmodium falciparum maturation abolishes physiologic red cell deformability. *Science* 223, 400-403.
85. Crosnier, C., Bustamante, L.Y., Bartholdson, S.J., Bei, A.K., Theron, M., Uchikawa, M., Mboup, S., Ndir, O., Kwiatkowski, D.P., Duraisingh, M.T., et al. (2011). Basigin is a receptor essential for erythrocyte invasion by Plasmodium falciparum. *Nature* 480, 534-537.
86. Cunningham, D., Lawton, J., Jarra, W., Preiser, P., and Langhorne, J. (2010). The pir multigene family of Plasmodium: antigenic variation and beyond. *Molecular and biochemical parasitology* 170, 65-73.
87. Curra, C., Pace, T., Franke-Fayard, B.M., Picci, L., Bertuccini, L., and Ponzi, M. (2012). Erythrocyte remodeling in Plasmodium berghei infection: the contribution of SEP family members. *Traffic* 13, 388-399.
88. Curt-Varesano, A., Braun, L., Ranquet, C., Hakimi, M.A., and Bougdour, A. (2016). The aspartyl protease TgASP5 mediates the export of the Toxoplasma GRA16 and GRA24 effectors into host cells. *Cellular microbiology* 18, 151-167.
89. Cyrklaff, M., Sanchez, C.P., Kilian, N., Bisseye, C., Simporé, J., Frischknecht, F., and Lanzer, M. (2011). Hemoglobins S and C interfere with actin remodeling in Plasmodium falciparum-infected erythrocytes. *Science* 334, 1283-1286.
90. Dacks, J.B., Davis, L.A., Sjogren, A.M., Andersson, J.O., Roger, A.J., and Doolittle, W.F. (2003). Evidence for Golgi bodies in proposed 'Golgi-lacking' lineages. *Proceedings Biological sciences / The Royal Society* 270 Suppl 2, S168-171.
91. Das, S., Hertrich, N., Perrin, A.J., Withers-Martinez, C., Collins, C.R., Jones, M.L., Watermeyer, J.M., Fobes, E.T., Martin, S.R., Saibil, H.R., et al. (2015). Processing of Plasmodium falciparum Merozoite Surface Protein MSP1 Activates a Spectrin-Binding Function Enabling Parasite Egress from RBCs. *Cell host & microbe* 18, 433-444.
92. Dasgupta, S., Auth, T., Gov, N.S., Satchwell, T.J., Hanssen, E., Zuccala, E.S., Riglar, D.T., Toye, A.M., Betz, T., Baum, J., et al. (2014). Membrane-wrapping contributions to malaria parasite invasion of the human erythrocyte. *Biophys J* 107, 43-54.
93. Davies, T.G., Field, L.M., Usherwood, P.N., and Williamson, M.S. (2007). DDT, pyrethrins, pyrethroids and insect sodium channels. *IUBMB Life* 59, 151-162.
94. de Castro, F.A., Ward, G.E., Jambou, R., Attal, G., Mayau, V., Jaureguiberry, G., Braun-Breton, C., Chakrabarti, D., and Langsley, G. (1996). Identification of a family of Rab G-proteins in Plasmodium falciparum and a detailed characterisation of pfrab6. *Molecular and biochemical parasitology* 80, 77-88.
95. de Keyzer, J., van der Does, C., and Driessen, A.J. (2003). The bacterial translocase: a dynamic protein channel complex. *Cell Mol Life Sci* 60, 2034-2052.
96. de Koning-Ward, T.F., Gilson, P.R., Boddey, J.A., Rug, M., Smith, B.J., Papenfuss, A.T., Sanders, P.R., Lundie, R.J., Maier, A.G., Cowman, A.F., et al. (2009). A newly discovered protein export machine in malaria parasites. *Nature* 459, 945-949.
97. del Portillo, H.A., Fernandez-Becerra, C., Bowman, S., Oliver, K., Preuss, M., Sanchez, C.P., Schneider, N.K., Villalobos, J.M., Rajandream, M.A., Harris, D., et al. (2001). A superfamily of variant genes encoded in the subtelomeric region of Plasmodium vivax. *Nature* 410, 839-842.
98. Delves, M., Plouffe, D., Scheurer, C., Meister, S., Wittlin, S., Winzeler, E.A., Sinden, R.E., and Leroy, D. (2012). The activities of current antimalarial drugs on the life cycle stages of Plasmodium: a comparative study with human and rodent parasites. *PLoS medicine* 9, e1001169.
99. Denzer, A.J., Nabholz, C.E., and Spiess, M. (1995). Transmembrane orientation of signal-anchor proteins is affected by the folding state but not the size of the N-terminal domain. *The EMBO journal* 14, 6311-6317.
100. Deponte, M. (2012). GFP tagging sheds light on protein translocation: implications for key methods in cell biology. *Cell Mol Life Sci* 69, 1025-1033.
101. Deponte, M., Hoppe, H.C., Lee, M.C., Maier, A.G., Richard, D., Rug, M., Spielmann, T., and Przyborski, J.M. (2012). Wherever I may roam: protein and membrane trafficking in P. falciparum-infected red blood

- cells. *Molecular and biochemical parasitology* 186, 95-116.
102. Desai, M., ter Kuile, F.O., Nosten, F., McGready, R., Asamo, K., Brabin, B., and Newman, R.D. (2007). Epidemiology and burden of malaria in pregnancy. *The Lancet Infectious diseases* 7, 93-104.
 103. Desai, S.A., Bezrukov, S.M., and Zimmerberg, J. (2000). A voltage-dependent channel involved in nutrient uptake by red blood cells infected with the malaria parasite. *Nature* 406, 1001-1005.
 104. Desai, S.A., Krogstad, D.J., and McCleskey, E.W. (1993). A nutrient-permeable channel on the intraerythrocytic malaria parasite. *Nature* 362, 643-646.
 105. Desai, S.A., and Rosenberg, R.L. (1997). Pore size of the malaria parasite's nutrient channel. *Proc Natl Acad Sci U S A* 94, 2045-2049.
 106. Diepold, A., and Armitage, J.P. (2015). Type III secretion systems: the bacterial flagellum and the injectisome. *Philos Trans R Soc Lond B Biol Sci* 370.
 107. Dixon, M.W., Hawthorne, P.L., Spielmann, T., Anderson, K.L., Trenholme, K.R., and Gardiner, D.L. (2008). Targeting of the ring exported protein 1 to the Maurer's clefts is mediated by a two-phase process. *Traffic* 9, 1316-1326.
 108. Djouaka, R.F., Bakare, A.A., Coulibaly, O.N., Akogbeto, M.C., Ranson, H., Hemingway, J., and Strode, C. (2008). Expression of the cytochrome P450s, CYP6P3 and CYP6M2 are significantly elevated in multiple pyrethroid resistant populations of *Anopheles gambiae* s.s. from Southern Benin and Nigeria. *BMC Genomics* 9, 538.
 109. Dohlich, K., Zumsteg, A.B., Goosmann, C., and Kolbe, M. (2014). A substrate-fusion protein is trapped inside the Type III Secretion System channel in *Shigella flexneri*. *PLoS Pathog* 10, e1003881.
 110. Dondorp, A.M., Nosten, F., Yi, P., Das, D., Phyto, A.P., Tarning, J., Lwin, K.M., Ariey, F., Hanpithakpong, W., Lee, S.J., *et al.* (2009). Artemisinin resistance in *Plasmodium falciparum* malaria. *The New England journal of medicine* 361, 455-467.
 111. Doumbo, O.K., Thera, M.A., Kone, A.K., Raza, A., Tempest, L.J., Lyke, K.E., Plowe, C.V., and Rowe, J.A. (2009). High levels of *Plasmodium falciparum* rosetting in all clinical forms of severe malaria in African children. *Am J Trop Med Hyg* 81, 987-993.
 112. Duffy, M.F., Maier, A.G., Byrne, T.J., Marty, A.J., Elliott, S.R., O'Neill, M.T., Payne, P.D., Rogerson, S.J., Cowman, A.F., Crabb, B.S., *et al.* (2006). VAR2CSA is the principal ligand for chondroitin sulfate A in two allogeneic isolates of *Plasmodium falciparum*. *Molecular and biochemical parasitology* 148, 117-124.
 113. Dunham, W.H., Mullin, M., and Gingras, A.C. (2012). Affinity-purification coupled to mass spectrometry: basic principles and strategies. *Proteomics* 12, 1576-1590.
 114. Ecker, A., Lehane, A.M., Clain, J., and Fidock, D.A. (2012). PfCRT and its role in antimalarial drug resistance. *Trends in parasitology* 28, 504-514.
 115. Egan, T.J. (2008). Recent advances in understanding the mechanism of hemozoin (malaria pigment) formation. *J Inorg Biochem* 102, 1288-1299.
 116. Ehlgren, F., Pham, J.S., de Koning-Ward, T., Cowman, A.F., and Ralph, S.A. (2012). Investigation of the *Plasmodium falciparum* food vacuole through inducible expression of the chloroquine resistance transporter (PfCRT). *PLoS one* 7, e38781.
 117. Eilers, M., Hwang, S., and Schatz, G. (1988). Unfolding and refolding of a purified precursor protein during import into isolated mitochondria. *The EMBO journal* 7, 1139-1145.
 118. Eilers, M., and Schatz, G. (1986). Binding of a specific ligand inhibits import of a purified precursor protein into mitochondria. *Nature* 322, 228-232.
 119. Ejigiri, I., and Sinnis, P. (2009). *Plasmodium* sporozoite-host interactions from the dermis to the hepatocyte. *Curr Opin Microbiol* 12, 401-407.
 120. El Bakkouri, M., Pow, A., Mulichak, A., Cheung, K.L., Artz, J.D., Amani, M., Fell, S., de Koning-Ward, T.F., Goodman, C.D., McFadden, G.I., *et al.* (2010). The Clp chaperones and proteases of the human malaria parasite *Plasmodium falciparum*. *J Mol Biol* 404, 456-477.
 121. El-Assaad, F., Wheway, J., Mitchell, A.J., Lou, J., Hunt, N.H., Combes, V., and Grau, G.E. (2013). Cytoadherence of *Plasmodium berghei*-infected red blood cells to murine brain and lung microvascular endothelial cells in vitro. *Infect Immun* 81, 3984-3991.
 122. Elford, B.C., and Ferguson, D.J. (1993). Secretory processes in *Plasmodium*. *Parasitology today* 9, 80-81.
 123. Elliott, D.A., McIntosh, M.T., Hosgood, H.D., 3rd, Chen, S., Zhang, G., Baevova, P., and Joiner, K.A. (2008). Four distinct pathways of hemoglobin uptake in the malaria parasite *Plasmodium falciparum*. *Proc Natl Acad Sci U S A* 105, 2463-2468.
 124. Elmendorf, H.G., and Haldar, K. (1994). *Plasmodium falciparum* exports the Golgi marker sphingomyelin synthase into a tubovesicular network in the cytoplasm of mature erythrocytes. *The Journal of cell biology* 124, 449-462.
 125. Elsworth, B., Matthews, K., Nie, C.Q., Kalanon, M., Charnaud, S.C., Sanders, P.R., Chisholm, S.A., Counihan, N.A., Shaw, P.J., Pino, P., *et al.* (2014). PTEX is an essential nexus for protein export in malaria parasites. *Nature* 511, 587-591.
 126. Elsworth, B., Crabb, B.S., and Gilson, P.R. (2014). Protein export in malaria parasites: an update. *Cellular microbiology* 16, 355-363.
 127. Elsworth, B., Sanders, P.R., Nebl, T., Batinovic, S., Kalanon, M., Nie, C.Q., Charnaud, S.C., Bullen, H.E., de Koning Ward, T.F., Tilley, L., *et al.* (2016). Proteomic analysis reveals novel proteins associated with the *Plasmodium* protein exporter PTEX and a loss of complex stability upon truncation of the core PTEX component, PTEX150. *Cellular microbiology*.
 128. Endo, T., Kawakami, M., Goto, A., America, T., Weisbeek, P., and Nakai, M. (1994). Chloroplast protein

- import. Chloroplast envelopes and thylakoids have different abilities to unfold proteins. *Eur J Biochem* 225, 403-409.
129. Ewer, K.J., O'Hara, G.A., Duncan, C.J., Collins, K.A., Sheehy, S.H., Reyes-Sandoval, A., Goodman, A.L., Edwards, N.J., Elias, S.C., Halstead, F.D., *et al.* (2013). Protective CD8+ T-cell immunity to human malaria induced by chimpanzee adenovirus-MVA immunisation. *Nature communications* 4, 2836.
130. Fidock, D.A., Nomura, T., Talley, A.K., Cooper, R.A., Dzekunov, S.M., Ferdig, M.T., Ursos, L.M., Sidhu, A.B., Naude, B., Deitsch, K.W., *et al.* (2000). Mutations in the *P. falciparum* digestive vacuole transmembrane protein PfCRT and evidence for their role in chloroquine resistance. *Mol Cell* 6, 861-871.
131. Fischer, K., Marti, T., Rick, B., Johnson, D., Benting, J., Baumeister, S., Helmbrecht, C., Lanzer, M., and Lingelbach, K. (1998). Characterization and cloning of the gene encoding the vacuolar membrane protein EXP-2 from *Plasmodium falciparum*. *Molecular and biochemical parasitology* 92, 47-57.
132. Foley, M., and Tilley, L. (1998). Quinoline antimalarials: mechanisms of action and resistance and prospects for new agents. *Pharmacology & therapeutics* 79, 55-87.
133. Foresti, O., Rodriguez-Vaello, V., Funaya, C., and Carvalho, P. (2014). Quality control of inner nuclear membrane proteins by the Asi complex. *Science* 346, 751-755.
134. Fried, M., and Duffy, P.E. (1996). Adherence of *Plasmodium falciparum* to chondroitin sulfate A in the human placenta. *Science* 272, 1502-1504.
135. Galinski, M.R., Meyer, E.V., and Barnwell, J.W. (2013). *Plasmodium vivax*: modern strategies to study a persistent parasite's life cycle. *Adv Parasitol* 81, 1-26.
136. Gardner, J.P., Pinches, R.A., Roberts, D.J., and Newbold, C.I. (1996). Variant antigens and endothelial receptor adhesion in *Plasmodium falciparum*. *Proc Natl Acad Sci U S A* 93, 3503-3508.
137. Gardner, M.J., Hall, N., Fung, E., White, O., Berriman, M., Hyman, R.W., Carlton, J.M., Pain, A., Nelson, K.E., Bowman, S., *et al.* (2002). Genome sequence of the human malaria parasite *Plasmodium falciparum*. *Nature* 419, 498-511.
138. Garoff, H., and Ansoerge, W. (1981). Improvements of DNA sequencing gels. *Anal Biochem* 115, 450-457.
139. Gaume, B., Klaus, C., Ungermann, C., Guiard, B., Neupert, W., and Brunner, M. (1998). Unfolding of preproteins upon import into mitochondria. *The EMBO journal* 17, 6497-6507.
140. Gehde, N., Hinrichs, C., Montilla, I., Charpian, S., Lingelbach, K., and Przyborski, J.M. (2009). Protein unfolding is an essential requirement for transport across the parasitophorous vacuolar membrane of *Plasmodium falciparum*. *Molecular microbiology* 71, 613-628.
141. Gerald, N., Mahajan, B., and Kumar, S. (2011). Mitosis in the human malaria parasite *Plasmodium falciparum*. *Eukaryotic cell* 10, 474-482.
142. Gething, P.W., Patil, A.P., Smith, D.L., Guerra, C.A., Elyazar, I.R., Johnston, G.L., Tatem, A.J., and Hay, S.I. (2011). A new world malaria map: *Plasmodium falciparum* endemicity in 2010. *Malaria journal* 10, 378.
143. Glushakova, S., Lizunov, V., Blank, P.S., Melikov, K., Humphrey, G., and Zimmerberg, J. (2013). Cytoplasmic free Ca²⁺ is essential for multiple steps in malaria parasite egress from infected erythrocytes. *Malaria journal* 12, 41.
144. Gold, D.A., Kaplan, A.D., Lis, A., Bett, G.C., Rosowski, E.E., Cirelli, K.M., Bougdour, A., Sidik, S.M., Beck, J.R., Lourido, S., *et al.* (2015). The *Toxoplasma* Dense Granule Proteins GRA17 and GRA23 Mediate the Movement of Small Molecules between the Host and the Parasitophorous Vacuole. *Cell host & microbe* 17, 642-652.
145. Goldberg, D.E. (2013). Complex nature of malaria parasite hemoglobin degradation [corrected]. *Proc Natl Acad Sci U S A* 110, 5283-5284.
146. Gratzer, W.B., and Dluzewski, A.R. (1993). The red blood cell and malaria parasite invasion. *Semin Hematol* 30, 232-247.
147. Greenwood, B.M., Fidock, D.A., Kyle, D.E., Kappe, S.H., Alonso, P.L., Collins, F.H., and Duffy, P.E. (2008). Malaria: progress, perils, and prospects for eradication. *The Journal of clinical investigation* 118, 1266-1276.
148. Gregson, A., and Plowe, C.V. (2005). Mechanisms of resistance of malaria parasites to antifolates. *Pharmacological reviews* 57, 117-145.
149. Grüring, C., Heiber, A., Kruse, F., Flemming, S., Franci, G., Colombo, S.F., Fasana, E., Schoeler, H., Borgese, N., Stunnenberg, H.G., *et al.* (2012). Uncovering common principles in protein export of malaria parasites. *Cell host & microbe* 12, 717-729.
150. Grüring, C., Heiber, A., Kruse, F., Ungefehr, J., Gilberger, T.W., and Spielmann, T. (2011). Development and host cell modifications of *Plasmodium falciparum* blood stages in four dimensions. *Nature communications* 2, 165.
151. Grüring, C., and Spielmann, T. (2012). Imaging of live malaria blood stage parasites. *Methods Enzymol* 506, 81-92.
152. Grützke, J., Rindte, K., Goosmann, C., Silvie, O., Rauch, C., Heuer, D., Lehmann, M.J., Mueller, A.K., Brinkmann, V., Matuschewski, K., *et al.* (2014). The spatiotemporal dynamics and membranous features of the *Plasmodium* liver stage tubovesicular network. *Traffic* 15, 362-382.
153. Guerra, C.A., Gikandi, P.W., Tatem, A.J., Noor, A.M., Smith, D.L., Hay, S.I., and Snow, R.W. (2008). The limits and intensity of *Plasmodium falciparum* transmission: implications for malaria control and elimination worldwide. *PLoS medicine* 5, e38.
154. Gunther, K., Tummler, M., Arnold, H.H., Ridley, R., Goman, M., Scaife, J.G., and Lingelbach, K. (1991). An exported protein of *Plasmodium falciparum* is synthesized as an integral membrane protein.

- Molecular and biochemical parasitology 46, 149-157.
155. Haase, S., Herrmann, S., Gruring, C., Heiber, A., Jansen, P.W., Langer, C., Treeck, M., Cabrera, A., Bruns, C., Struck, N.S., *et al.* (2009). Sequence requirements for the export of the Plasmodium falciparum Maurer's clefts protein REX2. *Molecular microbiology* 71, 1003-1017.
 156. Haldar, K. (1998). Intracellular trafficking in Plasmodium-infected erythrocytes. *Curr Opin Microbiol* 1, 466-471.
 157. Haldar, K., and Holder, A.A. (1993). Export of parasite proteins to the erythrocyte in Plasmodium falciparum-infected cells. *Semin Cell Biol* 4, 345-353.
 158. Haldar, K., Samuel, B.U., Mohandas, N., Harrison, T., and Hiller, N.L. (2001). Erythrocytic vacuolar rafts induced by malaria parasites. *Curr Opin Hematol* 8, 92-97.
 159. Hammoudi, P.M., Jacot, D., Mueller, C., Di Cristina, M., Dogga, S.K., Marq, J.B., Romano, J., Tosetti, N., Dubrot, J., Emre, Y., *et al.* (2015). Fundamental Roles of the Golgi-Associated Toxoplasma Aspartyl Protease, ASP5, at the Host-Parasite Interface. *PLoS Pathog* 11, e1005211.
 160. Hanahan, D. (1983). Studies on transformation of Escherichia coli with plasmids. *J Mol Biol* 166, 557-580.
 161. Hanssen, E., Hawthorne, P., Dixon, M.W., Trenholme, K.R., McMillan, P.J., Spielmann, T., Gardiner, D.L., and Tilley, L. (2008). Targeted mutagenesis of the ring-exported protein-1 of Plasmodium falciparum disrupts the architecture of Maurer's cleft organelles. *Molecular microbiology* 69, 938-953.
 162. Hanssen, E., Sougrat, R., Frankland, S., Deed, S., Klonis, N., Lippincott-Schwartz, J., and Tilley, L. (2008). Electron tomography of the Maurer's cleft organelles of Plasmodium falciparum-infected erythrocytes reveals novel structural features. *Molecular microbiology* 67, 703-718.
 163. Hausler, T., Stierhof, Y.D., Wirtz, E., and Clayton, C. (1996). Import of a DHFR hybrid protein into glycosomes in vivo is not inhibited by the folate-analogue aminopterin. *The Journal of cell biology* 132, 311-324.
 164. Hawthorne, P.L., Trenholme, K.R., Skinner-Adams, T.S., Spielmann, T., Fischer, K., Dixon, M.W., Ortega, M.R., Anderson, K.L., Kemp, D.J., and Gardiner, D.L. (2004). A novel Plasmodium falciparum ring stage protein, REX, is located in Maurer's clefts. *Molecular and biochemical parasitology* 136, 181-189.
 165. Hay, S.I., Smith, D.L., and Snow, R.W. (2008). Measuring malaria endemicity from intense to interrupted transmission. *The Lancet Infectious diseases* 8, 369-378.
 166. Heiber, A., Kruse, F., Pick, C., Gruring, C., Flemming, S., Oberli, A., Schoeler, H., Retzlaff, S., Mesen-Ramirez, P., Hiss, J.A., *et al.* (2013). Identification of new PNEPs indicates a substantial non-PEXEL exportome and underpins common features in Plasmodium falciparum protein export. *PLoS Pathog* 9, e1003546.
 167. Heiny, S.R., Pautz, S., Recker, M., and Przyborski, J.M. (2014). Protein Traffic to the Plasmodium falciparum apicoplast: evidence for a sorting branch point at the Golgi. *Traffic* 15, 1290-1304.
 168. Hemingway, J. (2014). The role of vector control in stopping the transmission of malaria: threats and opportunities. *Philos Trans R Soc Lond B Biol Sci* 369, 20130431.
 169. Hemingway, J., and Ranson, H. (2000). Insecticide resistance in insect vectors of human disease. *Annu Rev Entomol* 45, 371-391.
 170. Hiller, M.M., Finger, A., Schweiger, M., and Wolf, D.H. (1996). ER degradation of a misfolded luminal protein by the cytosolic ubiquitin-proteasome pathway. *Science* 273, 1725-1728.
 171. Hoffman, S.L., Vekemans, J., Richie, T.L., and Duffy, P.E. (2015). The March Toward Malaria Vaccines. *Am J Prev Med* 49, S319-333.
 172. Holder, A.A. (1988). The precursor to major merozoite surface antigens: structure and role in immunity. *Prog Allergy* 41, 72-97.
 173. Howard, R.J., Lyon, J.A., Uni, S., Saul, A.J., Aley, S.B., Klotz, F., Panton, L.J., Sherwood, J.A., Marsh, K., Aikawa, M., *et al.* (1987). Transport of an Mr approximately 300,000 Plasmodium falciparum protein (Pf EMP 2) from the intraerythrocytic asexual parasite to the cytoplasmic face of the host cell membrane. *The Journal of cell biology* 104, 1269-1280.
 174. Hsiao, C.H., Luisa Hiller, N., Haldar, K., and Knoll, L.J. (2013). A HT/PEXEL motif in Toxoplasma dense granule proteins is a signal for protein cleavage but not export into the host cell. *Traffic* 14, 519-531.
 175. Huang, S., Ratliff, K.S., Schwartz, M.P., Spenner, J.M., and Matouschek, A. (1999). Mitochondria unfold precursor proteins by unraveling them from their N-termini. *Nat Struct Biol* 6, 1132-1138.
 176. Hulden, L., and Hulden, L. (2011). Activation of the hypnozoite: a part of Plasmodium vivax life cycle and survival. *Malaria journal* 10, 90.
 177. Hunt, N.H., Golenser, J., Chan-Ling, T., Parekh, S., Rae, C., Potter, S., Medana, I.M., Miu, J., and Ball, H.J. (2006). Immunopathogenesis of cerebral malaria. *Int J Parasitol* 36, 569-582.
 178. Hunt, N.H., and Grau, G.E. (2003). Cytokines: accelerators and brakes in the pathogenesis of cerebral malaria. *Trends Immunol* 24, 491-499.
 179. Hwang, S.T., Wachter, C., and Schatz, G. (1991). Protein import into the yeast mitochondrial matrix. A new translocation intermediate between the two mitochondrial membranes. *The Journal of biological chemistry* 266, 21083-21089.
 180. Ingmundson, A., Alano, P., Matuschewski, K., and Silvestrini, F. (2014). Feeling at home from arrival to departure: protein export and host cell remodelling during Plasmodium liver stage and gametocyte maturation. *Cellular microbiology* 16, 324-333.
 181. Ingmundson, A., Nahar, C., Brinkmann, V., Lehmann, M.J., and Matuschewski, K. (2012). The exported Plasmodium berghei protein IBIS1 delineates membranous structures in infected red blood cells.

- Molecular microbiology 83, 1229-1243.
182. Janouskovec, J., Horak, A., Obornik, M., Lukes, J., and Keeling, P.J. (2010). A common red algal origin of the apicomplexan, dinoflagellate, and heterokont plastids. *Proc Natl Acad Sci U S A* 107, 10949-10954.
 183. Janssen, C.S., Phillips, R.S., Turner, C.M., and Barrett, M.P. (2004). Plasmodium interspersed repeats: the major multigene superfamily of malaria parasites. *Nucleic Acids Res* 32, 5712-5720.
 184. Jascur, T., Goldenberg, D.P., Vestweber, D., and Schatz, G. (1992). Sequential translocation of an artificial precursor protein across the two mitochondrial membranes. *The Journal of biological chemistry* 267, 13636-13641.
 185. Jin, Y., Kebaier, C., and Vanderberg, J. (2007). Direct microscopic quantification of dynamics of Plasmodium berghei sporozoite transmission from mosquitoes to mice. *Infect Immun* 75, 5532-5539.
 186. Johnson, D., Gunther, K., Ansorge, I., Benting, J., Kent, A., Bannister, L., Ridley, R., and Lingelbach, K. (1994). Characterization of membrane proteins exported from Plasmodium falciparum into the host erythrocyte. *Parasitology* 109 (Pt 1), 1-9.
 187. Johnston, J.A., Ward, C.L., and Kopito, R.R. (1998). Aggresomes: a cellular response to misfolded proteins. *The Journal of cell biology* 143, 1883-1898.
 188. Jones, R.M., Chichester, J.A., Mett, V., Jaje, J., Tottey, S., Manceva, S., Casta, L.J., Gibbs, S.K., Musiychuk, K., Shamloul, M., *et al.* (2013). A plant-produced Pfs25 VLP malaria vaccine candidate induces persistent transmission blocking antibodies against Plasmodium falciparum in immunized mice. *PLoS one* 8, e79538.
 189. Josling, G.A., and Llinas, M. (2015). Sexual development in Plasmodium parasites: knowing when it's time to commit. *Nature reviews Microbiology* 13, 573-587.
 190. Kalanon, M., Bargieri, D., Sturm, A., Matthews, K., Ghosh, S., Goodman, C.D., Thiberge, S., Mollard, V., McFadden, G.I., Menard, R., *et al.* (2016). The Plasmodium translocon of exported proteins component EXP2 is critical for establishing a patent malaria infection in mice. *Cellular microbiology* 18, 399-412.
 191. Kalanon, M., Tonkin, C.J., and McFadden, G.I. (2009). Characterization of two putative protein translocation components in the apicoplast of Plasmodium falciparum. *Eukaryotic cell* 8, 1146-1154.
 192. Kara, U.A., Stenzel, D.J., Ingram, L.T., Bushell, G.R., Lopez, J.A., and Kidson, C. (1988). Inhibitory monoclonal antibody against a (myristylated) small-molecular-weight antigen from Plasmodium falciparum associated with the parasitophorous vacuole membrane. *Infect Immun* 56, 903-909.
 193. Kasozi, D., Mohring, F., Rahlfs, S., Meyer, A.J., and Becker, K. (2013). Real-time imaging of the intracellular glutathione redox potential in the malaria parasite Plasmodium falciparum. *PLoS Pathog* 9, e1003782.
 194. Kats, L.M., Cooke, B.M., Coppel, R.L., and Black, C.G. (2008). Protein trafficking to apical organelles of malaria parasites - building an invasion machine. *Traffic* 9, 176-186.
 195. Kaviratne, M., Khan, S.M., Jarra, W., and Preiser, P.R. (2002). Small variant STEVOR antigen is uniquely located within Maurer's clefts in Plasmodium falciparum-infected red blood cells. *Eukaryotic cell* 1, 926-935.
 196. Keeling, P.J. (2008). Evolutionary biology: bridge over troublesome plastids. *Nature* 451, 896-897.
 197. Keeling, P.J. (2010). The endosymbiotic origin, diversification and fate of plastids. *Philos Trans R Soc Lond B Biol Sci* 365, 729-748.
 198. Kehr, S., Sturm, N., Rahlfs, S., Przyborski, J.M., and Becker, K. (2010). Compartmentation of redox metabolism in malaria parasites. *PLoS Pathog* 6, e1001242.
 199. Kenniston, J.A., Baker, T.A., and Sauer, R.T. (2005). Partitioning between unfolding and release of native domains during ClpXP degradation determines substrate selectivity and partial processing. *Proc Natl Acad Sci U S A* 102, 1390-1395.
 200. Khatlab, A., and Klinkert, M.Q. (2006). Maurer's clefts-restricted localization, orientation and export of a Plasmodium falciparum RIFIN. *Traffic* 7, 1654-1665.
 201. Khmelinskii, A., Blaszcak, E., Pantazopoulou, M., Fischer, B., Omnus, D.J., Le Dez, G., Brossard, A., Gunnarsson, A., Barry, J.D., Meurer, M., *et al.* (2014). Protein quality control at the inner nuclear membrane. *Nature* 516, 410-413.
 202. Kilejian, A., Rashid, M.A., Aikawa, M., Aji, T., and Yang, Y.F. (1991). Selective association of a fragment of the knob protein with spectrin, actin and the red cell membrane. *Molecular and biochemical parasitology* 44, 175-181.
 203. Kilian, N., Dittmer, M., Cyrklaff, M., Ouermi, D., Bisseye, C., Simporé, J., Frischknecht, F., Sanchez, C.P., and Lanzer, M. (2013). Haemoglobin S and C affect the motion of Maurer's clefts in Plasmodium falciparum-infected erythrocytes. *Cellular microbiology* 15, 1111-1126.
 204. Klemba, M., Beatty, W., Gluzman, I., and Goldberg, D.E. (2004). Trafficking of plasmepsin II to the food vacuole of the malaria parasite Plasmodium falciparum. *The Journal of cell biology* 164, 47-56.
 205. Koch, M., and Baum, J. (2016). The mechanics of malaria parasite invasion of the human erythrocyte - towards a reassessment of the host cell contribution. *Cellular microbiology* 18, 319-329.
 206. Kolakovich, K.A., Gluzman, I.Y., Duffin, K.L., and Goldberg, D.E. (1997). Generation of hemoglobin peptides in the acidic digestive vacuole of Plasmodium falciparum implicates peptide transport in amino acid production. *Molecular and biochemical parasitology* 87, 123-135.
 207. Kono, M., Herrmann, S., Loughran, N.B., Cabrera, A., Engelberg, K., Lehmann, C., Sinha, D., Prinz, B., Ruch, U., Heussler, V., *et al.* (2012). Evolution and architecture of the inner membrane complex in asexual and sexual stages of the malaria parasite. *Molecular biology and evolution* 29, 2113-2132.
 208. Kostaropoulos, I., Papadopoulos, A.I., Metaxakis, A., Boukouvala, E., and Papadopoulou-Mourkidou, E.

- (2001). Glutathione S-transferase in the defence against pyrethroids in insects. *Insect Biochem Mol Biol* 31, 313-319.
209. Kriek, N., Tilley, L., Horrocks, P., Pinches, R., Elford, B.C., Ferguson, D.J., Lingelbach, K., and Newbold, C.I. (2003). Characterization of the pathway for transport of the cytoadherence-mediating protein, PfEMP1, to the host cell surface in malaria parasite-infected erythrocytes. *Molecular microbiology* 50, 1215-1227.
210. Kulzer, S., Charnaud, S., Dagan, T., Riedel, J., Mandal, P., Pesce, E.R., Blatch, G.L., Crabb, B.S., Gilson, P.R., and Przyborski, J.M. (2012). Plasmodium falciparum-encoded exported hsp70/hsp40 chaperone/co-chaperone complexes within the host erythrocyte. *Cellular microbiology* 14, 1784-1795.
211. Kulzer, S., Rug, M., Brinkmann, K., Cannon, P., Cowman, A., Lingelbach, K., Blatch, G.L., Maier, A.G., and Przyborski, J.M. (2010). Parasite-encoded Hsp40 proteins define novel mobile structures in the cytosol of the P. falciparum-infected erythrocyte. *Cellular microbiology* 12, 1398-1420.
212. Kyes, S.A., Kraemer, S.M., and Smith, J.D. (2007). Antigenic variation in Plasmodium falciparum: gene organization and regulation of the var multigene family. *Eukaryotic cell* 6, 1511-1520.
213. Lal, K., Prieto, J.H., Bromley, E., Sanderson, S.J., Yates, J.R., 3rd, Wastling, J.M., Tomley, F.M., and Sinden, R.E. (2009). Characterisation of Plasmodium invasive organelles; an ookinete microneme proteome. *Proteomics* 9, 1142-1151.
214. Lambros, C., and Vanderberg, J.P. (1979). Synchronization of Plasmodium falciparum erythrocytic stages in culture. *J Parasitol* 65, 418-420.
215. Lauer, S., VanWye, J., Harrison, T., McManus, H., Samuel, B.U., Hiller, N.L., Mohandas, N., and Haldar, K. (2000). Vacuolar uptake of host components, and a role for cholesterol and sphingomyelin in malarial infection. *The EMBO journal* 19, 3556-3564.
216. Lauer, S.A., Rathod, P.K., Ghorri, N., and Haldar, K. (1997). A membrane network for nutrient import in red cells infected with the malaria parasite. *Science* 276, 1122-1125.
217. Laveran, A. (1881). Nature parasitaire des accidents de l'impaludisme : description d'un nouveau parasite trouvé dans le sang des malades atteints de fièvre palustre (Paris: J.-B. Baillière).
218. Lazarus, M.D., Schneider, T.G., and Taraschi, T.F. (2008). A new model for hemoglobin ingestion and transport by the human malaria parasite Plasmodium falciparum. *Journal of cell science* 121, 1937-1949.
219. Lee, C., Schwartz, M.P., Prakash, S., Iwakura, M., and Matouschek, A. (2001). ATP-dependent proteases degrade their substrates by processively unraveling them from the degradation signal. *Mol Cell* 7, 627-637.
220. Lee, M.C., and Miller, E.A. (2007). Molecular mechanisms of COPII vesicle formation. *Semin Cell Dev Biol* 18, 424-434.
221. Lee, M.C., Moura, P.A., Miller, E.A., and Fidock, D.A. (2008). Plasmodium falciparum Sec24 marks transitional ER that exports a model cargo via a diacidic motif. *Molecular microbiology* 68, 1535-1546.
222. Lee, P.A., Tullman-Ercek, D., and Georgiou, G. (2006). The bacterial twin-arginine translocation pathway. *Annu Rev Microbiol* 60, 373-395.
223. Leech, J.H., Barnwell, J.W., Aikawa, M., Miller, L.H., and Howard, R.J. (1984). Plasmodium falciparum malaria: association of knobs on the surface of infected erythrocytes with a histidine-rich protein and the erythrocyte skeleton. *The Journal of cell biology* 98, 1256-1264.
224. Leiriao, P., Rodrigues, C.D., Albuquerque, S.S., and Mota, M.M. (2004). Survival of protozoan intracellular parasites in host cells. *EMBO reports* 5, 1142-1147.
225. Lin, C.S., Uboldi, A.D., Marapana, D., Czabotar, P.E., Epp, C., Bujard, H., Taylor, N.L., Perugini, M.A., Hodder, A.N., and Cowman, A.F. (2014). The merozoite surface protein 1 complex is a platform for binding to human erythrocytes by Plasmodium falciparum. *The Journal of biological chemistry* 289, 25655-25669.
226. Lingelbach, K., and Joiner, K.A. (1998). The parasitophorous vacuole membrane surrounding Plasmodium and Toxoplasma: an unusual compartment in infected cells. *Journal of cell science* 111 (Pt 11), 1467-1475.
227. Lingelbach, K., and Przyborski, J.M. (2006). The long and winding road: protein trafficking mechanisms in the Plasmodium falciparum infected erythrocyte. *Molecular and biochemical parasitology* 147, 1-8.
228. Lisewski, A.M., Quiros, J.P., Ng, C.L., Adikesavan, A.K., Miura, K., Putluri, N., Eastman, R.T., Scandfeld, D., Regenbogen, S.J., Altenhofen, L., et al. (2014). Super-genomic network compression and the discovery of EXP1 as a glutathione transferase inhibited by artesunate. *Cell* 158, 916-928.
229. Lodish, H. (2000) Protein structure and function. In H Lodish (ed), *Molecular Cell Biology*. WH Freeman
230. Ludwig, A., Bauer, S., Benz, R., Bergmann, B., and Goebel, W. (1999). Analysis of the SlyA-controlled expression, subcellular localization and pore-forming activity of a 34 kDa haemolysin (ClyA) from Escherichia coli K-12. *Molecular microbiology* 31, 557-567.
231. Luse, S.A., and Miller, L.H. (1971). Plasmodium falciparum malaria. Ultrastructure of parasitized erythrocytes in cardiac vessels. *Am J Trop Med Hyg* 20, 655-660.
232. Lysenko, A.J., and Beljaev, A.E. (1969). An analysis of the geographical distribution of Plasmodium ovale. *Bulletin of the World Health Organization* 40, 383-394.
233. Maier, A.G., Cooke, B.M., Cowman, A.F., and Tilley, L. (2009). Malaria parasite proteins that remodel the host erythrocyte. *Nature reviews Microbiology* 7, 341-354.
234. Maier, A.G., Rug, M., O'Neill, M.T., Beeson, J.G., Marti, M., Reeder, J., and Cowman, A.F. (2007). Skeleton-binding protein 1 functions at the parasitophorous vacuole membrane to traffic PfEMP1 to the Plasmodium falciparum-infected erythrocyte surface. *Blood* 109, 1289-1297.
235. Maier, A.G., Rug, M., O'Neill, M.T., Brown, M., Chakravorty, S., Szeszak, T., Chesson, J., Wu, Y.,

- Hughes, K., Coppel, R.L., *et al.* (2008). Exported proteins required for virulence and rigidity of *Plasmodium falciparum*-infected human erythrocytes. *Cell* 134, 48-61.
236. Malkin, E.M., Durbin, A.P., Diemert, D.J., Sattabongkot, J., Wu, Y., Miura, K., Long, C.A., Lambert, L., Miles, A.P., Wang, J., *et al.* (2005). Phase 1 vaccine trial of Pvs25H: a transmission blocking vaccine for *Plasmodium vivax* malaria. *Vaccine* 23, 3131-3138.
237. Marti, M., Good, R.T., Rug, M., Knuepfer, E., and Cowman, A.F. (2004). Targeting malaria virulence and remodeling proteins to the host erythrocyte. *Science* 306, 1930-1933.
238. Marti, M., and Spielmann, T. (2013). Protein export in malaria parasites: many membranes to cross. *Curr Opin Microbiol* 16, 445-451.
239. Matouschek, A. (2003). Protein unfolding--an important process in vivo? *Curr Opin Struct Biol* 13, 98-109.
240. Matouschek, A., Azem, A., Ratliff, K., Glick, B.S., Schmid, K., and Schatz, G. (1997). Active unfolding of precursor proteins during mitochondrial protein import. *The EMBO journal* 16, 6727-6736.
241. Matouschek, A., Pfanner, N., and Voos, W. (2000). Protein unfolding by mitochondria. The Hsp70 import motor. *EMBO reports* 1, 404-410.
242. Matthews, K., Kalanon, M., Chisholm, S.A., Sturm, A., Goodman, C.D., Dixon, M.W., Sanders, P.R., Nebl, T., Fraser, F., Haase, S., *et al.* (2013). The *Plasmodium* translocon of exported proteins (PTEX) component thioredoxin-2 is important for maintaining normal blood-stage growth. *Molecular microbiology* 89, 1167-1186.
243. Matz, J.M., Goosmann, C., Brinkmann, V., Grutzke, J., Ingmundson, A., Matuschewski, K., and Kooij, T.W. (2015). The *Plasmodium berghei* translocon of exported proteins reveals spatiotemporal dynamics of tubular extensions. *Scientific reports* 5, 12532.
244. Matz, J.M., Ingmundson, A., Costa Nunes, J., Stenzel, W., Matuschewski, K., and Kooij, T.W. (2015). In Vivo Function of PTEX88 in Malaria Parasite Sequestration and Virulence. *Eukaryotic cell* 14, 528-534.
245. Matz, J.M., Matuschewski, K., and Kooij, T.W. (2013). Two putative protein export regulators promote *Plasmodium* blood stage development in vivo. *Molecular and biochemical parasitology* 191, 44-52.
246. Maund, S.J., Campbell, P.J., Giddings, J.M., Hamer, M.J., Henry, K., Pilling, E.D., Warinton, J.S., and Wheeler, J.R. (2012). Ecotoxicology of synthetic pyrethroids. *Top Curr Chem* 314, 137-165.
247. McMillan, P.J., Millet, C., Batinovic, S., Maiorca, M., Hanssen, E., Kenny, S., Muhle, R.A., Melcher, M., Fidock, D.A., Smith, J.D., *et al.* (2013). Spatial and temporal mapping of the PfEMP1 export pathway in *Plasmodium falciparum*. *Cellular microbiology* 15, 1401-1418.
248. Medana, I.M., and Turner, G.D. (2006). Human cerebral malaria and the blood-brain barrier. *Int J Parasitol* 36, 555-568.
249. Melcher, M., Muhle, R.A., Henrich, P.P., Kraemer, S.M., Avril, M., Vigan-Womas, I., Mercereau-Puijalon, O., Smith, J.D., and Fidock, D.A. (2010). Identification of a role for the PfEMP1 semi-conserved head structure in protein trafficking to the surface of *Plasmodium falciparum* infected red blood cells. *Cellular microbiology* 12, 1446-1462.
250. Mesecke, N., Terziyska, N., Kozany, C., Baumann, F., Neupert, W., Hell, K., and Herrmann, J.M. (2005). A disulfide relay system in the intermembrane space of mitochondria that mediates protein import. *Cell* 121, 1059-1069.
251. Miller, L.H., Ackerman, H.C., Su, X.Z., and Wellems, T.E. (2013). Malaria biology and disease pathogenesis: insights for new treatments. *Nature medicine* 19, 156-167.
252. Miller, L.H., Baruch, D.I., Marsh, K., and Doumbo, O.K. (2002). The pathogenic basis of malaria. *Nature* 415, 673-679.
253. Mills, J.P., Diez-Silva, M., Quinn, D.J., Dao, M., Lang, M.J., Tan, K.S., Lim, C.T., Milon, G., David, P.H., Mercereau-Puijalon, O., *et al.* (2007). Effect of plasmoidal RESA protein on deformability of human red blood cells harboring *Plasmodium falciparum*. *Proc Natl Acad Sci U S A* 104, 9213-9217.
254. Moon, R.W., Hall, J., Ranguti, F., Ho, Y.S., Almond, N., Mitchell, G.H., Pain, A., Holder, A.A., and Blackman, M.J. (2013). Adaptation of the genetically tractable malaria pathogen *Plasmodium knowlesi* to continuous culture in human erythrocytes. *Proc Natl Acad Sci U S A* 110, 531-536.
255. Morahan, B.J., Strobel, C., Hasan, U., Czesny, B., Mantel, P.Y., Marti, M., Eksi, S., and Williamson, K.C. (2011). Functional analysis of the exported type IV HSP40 protein PfGECO in *Plasmodium falciparum* gametocytes. *Eukaryotic cell* 10, 1492-1503.
256. Mordue, D.G., Desai, N., Dustin, M., and Sibley, L.D. (1999). Invasion by *Toxoplasma gondii* establishes a moving junction that selectively excludes host cell plasma membrane proteins on the basis of their membrane anchoring. *The Journal of experimental medicine* 190, 1783-1792.
257. Morrison, D.A. (2008). Prospects for elucidating the phylogeny of the Apicomplexa. *Parasite* 15, 191-196.
258. Mota, M.M., Hafalla, J.C., and Rodriguez, A. (2002). Migration through host cells activates *Plasmodium* sporozoites for infection. *Nature medicine* 8, 1318-1322.
259. Mueller, A.K., Labaied, M., Kappe, S.H., and Matuschewski, K. (2005). Genetically modified *Plasmodium* parasites as a protective experimental malaria vaccine. *Nature* 433, 164-167.
260. Muller, I.B., and Hyde, J.E. (2010). Antimalarial drugs: modes of action and mechanisms of parasite resistance. *Future Microbiol* 5, 1857-1873.
261. Mundwiler-Pachlatko, E., and Beck, H.P. (2013). Maurer's clefts, the enigma of *Plasmodium falciparum*. *Proc Natl Acad Sci U S A* 110, 19987-19994.
262. Murcha, M.W., Kmiec, B., Kubiszewski-Jakubiak, S., Teixeira, P.F., Glaser, E., and Whelan, J. (2014). Protein import into plant mitochondria: signals, machinery, processing, and regulation. *J Exp Bot* 65,

- 6301-6335.
263. Muto, T., Obita, T., Abe, Y., Shodai, T., Endo, T., and Kohda, D. (2001). NMR identification of the Tom20 binding segment in mitochondrial presequences. *J Mol Biol* 306, 137-143.
264. Naik, R.S., Branch, O.H., Woods, A.S., Vijaykumar, M., Perkins, D.J., Nahlen, B.L., Lal, A.A., Cotter, R.J., Costello, C.E., Ockenhouse, C.F., *et al.* (2000). Glycosylphosphatidylinositol anchors of *Plasmodium falciparum*: molecular characterization and naturally elicited antibody response that may provide immunity to malaria pathogenesis. *The Journal of experimental medicine* 192, 1563-1576.
265. Nakatsukasa, K., and Brodsky, J.L. (2008). The recognition and retrotranslocation of misfolded proteins from the endoplasmic reticulum. *Traffic* 9, 861-870.
266. Nakatsukasa, K., Huyer, G., Michaelis, S., and Brodsky, J.L. (2008). Dissecting the ER-associated degradation of a misfolded polytopic membrane protein. *Cell* 132, 101-112.
267. Nguitragool, W., Bokhari, A.A., Pillai, A.D., Rayavara, K., Sharma, P., Turpin, B., Aravind, L., and Desai, S.A. (2011). Malaria parasite clag3 genes determine channel-mediated nutrient uptake by infected red blood cells. *Cell* 145, 665-677.
268. Nilsson, S., Angeletti, D., Wahlgren, M., Chen, Q., and Moll, K. (2012). *Plasmodium falciparum* antigen 332 is a resident peripheral membrane protein of Maurer's clefts. *PloS one* 7, e46980.
269. Nussenzweig, R.S., Vanderberg, J., Most, H., and Orton, C. (1967). Protective immunity produced by the injection of x-irradiated sporozoites of *plasmodium berghei*. *Nature* 216, 160-162.
270. Nyalwidhe, J., and Lingelbach, K. (2006). Proteases and chaperones are the most abundant proteins in the parasitophorous vacuole of *Plasmodium falciparum*-infected erythrocytes. *Proteomics* 6, 1563-1573.
271. Nzila, A. (2006). The past, present and future of antifolates in the treatment of *Plasmodium falciparum* infection. *The Journal of antimicrobial chemotherapy* 57, 1043-1054.
272. Oberli, A., Slater, L.M., Cutts, E., Brand, F., Mundwiler-Pachlatko, E., Rusch, S., Masik, M.F., Erat, M.C., Beck, H.P., and Vakonakis, I. (2014). A *Plasmodium falciparum* PHIST protein binds the virulence factor PfEMP1 and comigrates to knobs on the host cell surface. *FASEB journal : official publication of the Federation of American Societies for Experimental Biology* 28, 4420-4433.
273. Oberli, A., Zurbrugg, L., Rusch, S., Brand, F., Butler, M.E., Day, J.L., Cutts, E.E., Lavstsen, T., Vakonakis, I., and Beck, H.P. (2016). *Plasmodium falciparum* PHIST Proteins Contribute to Cytoadherence and Anchor PfEMP1 to the Host Cell Cytoskeleton. *Cellular microbiology*.
274. Obita, T., Muto, T., Endo, T., and Kohda, D. (2003). Peptide library approach with a disulfide tether to refine the Tom20 recognition motif in mitochondrial presequences. *J Mol Biol* 328, 495-504.
275. Ogura, T., and Wilkinson, A.J. (2001). AAA+ superfamily ATPases: common structure--diverse function. *Genes Cells* 6, 575-597.
276. Oh, S.S., Voigt, S., Fisher, D., Yi, S.J., LeRoy, P.J., Derick, L.H., Liu, S., and Chishti, A.H. (2000). *Plasmodium falciparum* erythrocyte membrane protein 1 is anchored to the actin-spectrin junction and knob-associated histidine-rich protein in the erythrocyte skeleton. *Molecular and biochemical parasitology* 108, 237-247.
277. Olliaro, P. (2001). Mode of action and mechanisms of resistance for antimalarial drugs. *Pharmacology & therapeutics* 89, 207-219.
278. Orito, Y., Ishino, T., Iwanaga, S., Kaneko, I., Kato, T., Menard, R., Chinzei, Y., and Yuda, M. (2013). Liver-specific protein 2: a *Plasmodium* protein exported to the hepatocyte cytoplasm and required for merozoite formation. *Molecular microbiology* 87, 66-79.
279. Pachlatko, E., Rusch, S., Muller, A., Hemphill, A., Tilley, L., Hanssen, E., and Beck, H.P. (2010). MAHRP2, an exported protein of *Plasmodium falciparum*, is an essential component of Maurer's cleft tethers. *Molecular microbiology* 77, 1136-1152.
280. Painter, H.J., Morrissey, J.M., Mather, M.W., and Vaidya, A.B. (2007). Specific role of mitochondrial electron transport in blood-stage *Plasmodium falciparum*. *Nature* 446, 88-91.
281. Papakrivov, J., Newbold, C.I., and Lingelbach, K. (2005). A potential novel mechanism for the insertion of a membrane protein revealed by a biochemical analysis of the *Plasmodium falciparum* cytoadherence molecule PfEMP-1. *Molecular microbiology* 55, 1272-1284.
282. Pasini, E.M., Braks, J.A., Fonager, J., Klop, O., Aime, E., Spaccapelo, R., Otto, T.D., Berriman, M., Hiss, J.A., Thomas, A.W., *et al.* (2013). Proteomic and genetic analyses demonstrate that *Plasmodium berghei* blood stages export a large and diverse repertoire of proteins. *Mol Cell Proteomics* 12, 426-448.
283. Pei, X., An, X., Guo, X., Tarnawski, M., Coppel, R., and Mohandas, N. (2005). Structural and functional studies of interaction between *Plasmodium falciparum* knob-associated histidine-rich protein (KAHRP) and erythrocyte spectrin. *The Journal of biological chemistry* 280, 31166-31171.
284. Pelle, K.G., Jiang, R.H., Mantel, P.Y., Xiao, Y.P., Hjelmqvist, D., Gallego-Lopez, G.M., A, O.T.L., Kang, B.H., Allred, D.R., and Marti, M. (2015). Shared elements of host-targeting pathways among apicomplexan parasites of differing lifestyles. *Cellular microbiology* 17, 1618-1639.
285. Petersen, I., Eastman, R., and Lanzer, M. (2011). Drug-resistant malaria: molecular mechanisms and implications for public health. *FEBS letters* 585, 1551-1562.
286. Phyto, A.P., Nkhoma, S., Stepniewska, K., Ashley, E.A., Nair, S., McGready, R., ler Moo, C., Al-Saai, S., Dondorp, A.M., Lwin, K.M., *et al.* (2012). Emergence of artemisinin-resistant malaria on the western border of Thailand: a longitudinal study. *Lancet* 379, 1960-1966.
287. Pick, C., Ebersberger, I., Spielmann, T., Bruchhaus, I., and Burmester, T. (2011). Phylogenomic analyses of malaria parasites and evolution of their exported proteins. *BMC Evol Biol* 11, 167.
288. Ponsford, M.J., Medana, I.M., Prapansilp, P., Hien, T.T., Lee, S.J., Dondorp, A.M., Esiri, M.M., Day, N.P., White, N.J., and Turner, G.D. (2012). Sequestration and microvascular congestion are associated

- with coma in human cerebral malaria. *J Infect Dis* 205, 663-671.
289. Pradel, G. (2007). Proteins of the malaria parasite sexual stages: expression, function and potential for transmission blocking strategies. *Parasitology* 134, 1911-1929.
 290. Proellocks, N.I., Herrmann, S., Buckingham, D.W., Hanssen, E., Hodges, E.K., Elsworth, B., Morahan, B.J., Coppel, R.L., and Cooke, B.M. (2014). A lysine-rich membrane-associated PHISTb protein involved in alteration of the cytoadhesive properties of Plasmodium falciparum-infected red blood cells. *FASEB journal : official publication of the Federation of American Societies for Experimental Biology* 28, 3103-3113.
 291. Prudencio, M., Rodrigues, C.D., Ataíde, R., and Mota, M.M. (2008). Dissecting in vitro host cell infection by Plasmodium sporozoites using flow cytometry. *Cellular microbiology* 10, 218-224.
 292. Prudencio, M., Rodriguez, A., and Mota, M.M. (2006). The silent path to thousands of merozoites: the Plasmodium liver stage. *Nature reviews Microbiology* 4, 849-856.
 293. Przyborski, J.M., Miller, S.K., Pfahler, J.M., Henrich, P.P., Rohrbach, P., Crabb, B.S., and Lanzer, M. (2005). Trafficking of STEVOR to the Maurer's clefts in Plasmodium falciparum-infected erythrocytes. *The EMBO journal* 24, 2306-2317.
 294. Pulcini, S., Staines, H.M., Lee, A.H., Shafik, S.H., Bouyer, G., Moore, C.M., Daley, D.A., Hoke, M.J., Altenhofen, L.M., Painter, H.J., et al. (2015). Mutations in the Plasmodium falciparum chloroquine resistance transporter, PfCRT, enlarge the parasite's food vacuole and alter drug sensitivities. *Scientific reports* 5, 14552.
 295. Rabinovich, E., Kerem, A., Frohlich, K.U., Diamant, N., and Bar-Nun, S. (2002). AAA-ATPase p97/Cdc48p, a cytosolic chaperone required for endoplasmic reticulum-associated protein degradation. *Mol Cell Biol* 22, 626-634.
 296. Ralph, S.A., van Dooren, G.G., Waller, R.F., Crawford, M.J., Fraunholz, M.J., Foth, B.J., Tonkin, C.J., Roos, D.S., and McFadden, G.I. (2004). Tropical infectious diseases: metabolic maps and functions of the Plasmodium falciparum apicoplast. *Nature reviews Microbiology* 2, 203-216.
 297. Ranson, H., N'Guessan, R., Lines, J., Moiroux, N., Nkuni, Z., and Corbel, V. (2011). Pyrethroid resistance in African anopheline mosquitoes: what are the implications for malaria control? *Trends in parasitology* 27, 91-98.
 298. Rapaport, D., Neupert, W., and Lill, R. (1997). Mitochondrial protein import. Tom40 plays a major role in targeting and translocation of preproteins by forming a specific binding site for the presequence. *The Journal of biological chemistry* 272, 18725-18731.
 299. Rapoport, T.A. (2007). Protein translocation across the eukaryotic endoplasmic reticulum and bacterial plasma membranes. *Nature* 450, 663-669.
 300. Rassow, J., Guiard, B., Wienhues, U., Herzog, V., Hartl, F.U., and Neupert, W. (1989). Translocation arrest by reversible folding of a precursor protein imported into mitochondria. A means to quantitate translocation contact sites. *The Journal of cell biology* 109, 1421-1428.
 301. Rassow, J., Hartl, F.U., Guiard, B., Pfanner, N., and Neupert, W. (1990). Polypeptides traverse the mitochondrial envelope in an extended state. *FEBS letters* 275, 190-194.
 302. Rathore, D., Sacci, J.B., de la Vega, P., and McCutchan, T.F. (2002). Binding and invasion of liver cells by Plasmodium falciparum sporozoites. Essential involvement of the amino terminus of circumsporozoite protein. *The Journal of biological chemistry* 277, 7092-7098.
 303. Ravid, T., Kreft, S.G., and Hochstrasser, M. (2006). Membrane and soluble substrates of the Doa10 ubiquitin ligase are degraded by distinct pathways. *The EMBO journal* 25, 533-543.
 304. Repnik, U., Gangopadhyay, P., Bietz, S., Przyborski, J.M., Griffiths, G., and Lingelbach, K. (2015). The apicomplexan parasite Babesia divergens internalizes band 3, glycophorin A and spectrin during invasion of human red blood cells. *Cellular microbiology* 17, 1052-1068.
 305. Richie, T.L., Billingsley, P.F., Sim, B.K., James, E.R., Chakravarty, S., Epstein, J.E., Lyke, K.E., Mordmuller, B., Alonso, P., Duffy, P.E., et al. (2015). Progress with Plasmodium falciparum sporozoite (PfSPZ)-based malaria vaccines. *Vaccine* 33, 7452-7461.
 306. Richie, T.L., Charoenvit, Y., Wang, R., Epstein, J.E., Hedstrom, R.C., Kumar, S., Luke, T.C., Freilich, D.A., Aguiar, J.C., Sacci, J.B., Jr., et al. (2012). Clinical trial in healthy malaria-naive adults to evaluate the safety, tolerability, immunogenicity and efficacy of MuStDO5, a five-gene, sporozoite/hepatic stage Plasmodium falciparum DNA vaccine combined with escalating dose human GM-CSF DNA. *Hum Vaccin Immunother* 8, 1564-1584.
 307. Riglar, D.T., Richard, D., Wilson, D.W., Boyle, M.J., Dekiwadia, C., Turnbull, L., Angrisano, F., Marapana, D.S., Rogers, K.L., Whitchurch, C.B., et al. (2011). Super-resolution dissection of coordinated events during malaria parasite invasion of the human erythrocyte. *Cell host & microbe* 9, 9-20.
 308. Riglar, D.T., Rogers, K.L., Hanssen, E., Turnbull, L., Bullen, H.E., Charnaud, S.C., Przyborski, J., Gilson, P.R., Whitchurch, C.B., Crabb, B.S., et al. (2013). Spatial association with PTEX complexes defines regions for effector export into Plasmodium falciparum-infected erythrocytes. *Nature communications* 4, 1415.
 309. Riordan, K.E., Sorg, J.A., Berube, B.J., and Schneewind, O. (2008). Impassable YscP substrates and their impact on the Yersinia enterocolitica type III secretion pathway. *J Bacteriol* 190, 6204-6216.
 310. Risco-Castillo, V., Topcu, S., Marinach, C., Manzoni, G., Bigorgne, A.E., Briquet, S., Baudin, X., Lebrun, M., Dubremetz, J.F., and Silvie, O. (2015). Malaria Sporozoites Traverse Host Cells within Transient Vacuoles. *Cell host & microbe* 18, 593-603.
 311. Rogerson, S.J., Grau, G.E., and Hunt, N.H. (2004). The microcirculation in severe malaria. *Microcirculation* 11, 559-576.

312. Rottmann, M., McNamara, C., Yeung, B.K., Lee, M.C., Zou, B., Russell, B., Seitz, P., Plouffe, D.M., Dharia, N.V., Tan, J., *et al.* (2010). Spiroindolones, a potent compound class for the treatment of malaria. *Science* 329, 1175-1180.
313. Rowe, J.A., Moulds, J.M., Newbold, C.I., and Miller, L.H. (1997). *P. falciparum* rosetting mediated by a parasite-variant erythrocyte membrane protein and complement-receptor 1. *Nature* 388, 292-295.
314. Rucktaschel, R., Girzalsky, W., and Erdmann, R. (2011). Protein import machineries of peroxisomes. *Biochimica et biophysica acta* 1808, 892-900.
315. Rudzinska, M.A., Trager, W., Lewengrub, S.J., and Gubert, E. (1976). An electron microscopic study of *Babesia microti* invading erythrocytes. *Cell and tissue research* 169, 323-334.
316. Rug, M., Cyrklaff, M., Mikkonen, A., Lemgruber, L., Kuelzer, S., Sanchez, C.P., Thompson, J., Hanssen, E., O'Neill, M., Langer, C., *et al.* (2014). Export of virulence proteins by malaria-infected erythrocytes involves remodeling of host actin cytoskeleton. *Blood* 124, 3459-3468.
317. Ruggiano, A., Foresti, O., and Carvalho, P. (2014). Quality control: ER-associated degradation: protein quality control and beyond. *The Journal of cell biology* 204, 869-879.
318. Russo, I., Babbitt, S., Muralidharan, V., Butler, T., Oksman, A., and Goldberg, D.E. (2010). Plasmeprin V licenses *Plasmodium* proteins for export into the host erythrocyte. *Nature* 463, 632-636.
319. Sachs, J., and Malaney, P. (2002). The economic and social burden of malaria. *Nature* 415, 680-685.
320. Salmon, B.L., Oksman, A., and Goldberg, D.E. (2001). Malaria parasite exit from the host erythrocyte: a two-step process requiring extraerythrocytic proteolysis. *Proc Natl Acad Sci U S A* 98, 271-276.
321. Salvador, N., Aguado, C., Horst, M., and Knecht, E. (2000). Import of a cytosolic protein into lysosomes by chaperone-mediated autophagy depends on its folding state. *The Journal of biological chemistry* 275, 27447-27456.
322. Sam-Yellowe, T.Y., Florens, L., Johnson, J.R., Wang, T., Drazba, J.A., Le Roch, K.G., Zhou, Y., Batalov, S., Carucci, D.J., Winzeler, E.A., *et al.* (2004). A *Plasmodium* gene family encoding Maurer's cleft membrane proteins: structural properties and expression profiling. *Genome research* 14, 1052-1059.
323. Sargeant, T.J., Marti, M., Caler, E., Carlton, J.M., Simpson, K., Speed, T.P., and Cowman, A.F. (2006). Lineage-specific expansion of proteins exported to erythrocytes in malaria parasites. *Genome Biol* 7, R12.
324. Saridaki, T., Frohlich, K.S., Braun-Breton, C., and Lanzer, M. (2009). Export of PfSBP1 to the *Plasmodium falciparum* Maurer's clefts. *Traffic* 10, 137-152.
325. Schatz, G., and Dobberstein, B. (1996). Common principles of protein translocation across membranes. *Science* 271, 1519-1526.
326. Scherf, A., Hernandez-Rivas, R., Buffet, P., Bottius, E., Benatar, C., Pouvelle, B., Gysin, J., and Lanzer, M. (1998). Antigenic variation in malaria: in situ switching, relaxed and mutually exclusive transcription of var genes during intra-erythrocytic development in *Plasmodium falciparum*. *The EMBO journal* 17, 5418-5426.
327. Scherf, A., Lopez-Rubio, J.J., and Riviere, L. (2008). Antigenic variation in *Plasmodium falciparum*. *Annu Rev Microbiol* 62, 445-470.
328. Schluter, A., Fourcade, S., Ripp, R., Mandel, J.L., Poch, O., and Pujol, A. (2006). The evolutionary origin of peroxisomes: an ER-peroxisome connection. *Molecular biology and evolution* 23, 838-845.
329. Schnell, D.J., and Hebert, D.N. (2003). Protein translocons: multifunctional mediators of protein translocation across membranes. *Cell* 112, 491-505.
330. Schnell, J.R., Dyson, H.J., and Wright, P.E. (2004). Structure, dynamics, and catalytic function of dihydrofolate reductase. *Annu Rev Biophys Biomol Struct* 33, 119-140.
331. Schofield, L., and Grau, G.E. (2005). Immunological processes in malaria pathogenesis. *Nature reviews Immunology* 5, 722-735.
332. Schulke, N., Sepuri, N.B., Gordon, D.M., Saxena, S., Dancis, A., and Pain, D. (1999). A multisubunit complex of outer and inner mitochondrial membrane protein translocases stabilized in vivo by translocation intermediates. *The Journal of biological chemistry* 274, 22847-22854.
333. Schulke, N., Sepuri, N.B., and Pain, D. (1997). In vivo zippering of inner and outer mitochondrial membranes by a stable translocation intermediate. *Proc Natl Acad Sci U S A* 94, 7314-7319.
334. Schulz, C., Schendzielorz, A., and Rehling, P. (2015). Unlocking the presequence import pathway. *Trends in cell biology* 25, 265-275.
335. Schulze, J., Kwiatkowski, M., Borner, J., Schluter, H., Bruchhaus, I., Burmester, T., Spielmann, T., and Pick, C. (2015). The *Plasmodium falciparum* exportome contains non-canonical PEXEL/HT proteins. *Molecular microbiology* 97, 301-314.
336. Schwartz, M.P., Huang, S., and Matouschek, A. (1999). The structure of precursor proteins during import into mitochondria. *The Journal of biological chemistry* 274, 12759-12764.
337. Schwartz, M.P., and Matouschek, A. (1999). The dimensions of the protein import channels in the outer and inner mitochondrial membranes. *Proc Natl Acad Sci U S A* 96, 13086-13090.
338. Sedegah, M., Hollingdale, M.R., Farooq, F., Ganeshan, H., Belmonte, M., Kim, Y., Peters, B., Sette, A., Huang, J., McGrath, S., *et al.* (2014). Sterile immunity to malaria after DNA prime/adenovirus boost immunization is associated with effector memory CD8+T cells targeting AMA1 class I epitopes. *PloS one* 9, e106241.
339. Seder, R.A., Chang, L.J., Enama, M.E., Zephir, K.L., Sarwar, U.N., Gordon, I.J., Holman, L.A., James, E.R., Billingsley, P.F., Gunasekera, A., *et al.* (2013). Protection against malaria by intravenous immunization with a nonreplicating sporozoite vaccine. *Science* 341, 1359-1365.
340. Seeber, F., and Soldati-Favre, D. (2010). Metabolic pathways in the apicoplast of apicomplexa. *Int Rev*

- Cell Mol Biol 281, 161-228.
341. Sharma, A., Sharma, A., Dixit, S., and Sharma, A. (2011). Structural insights into thioredoxin-2: a component of malaria parasite protein secretion machinery. *Scientific reports* 1, 179.
 342. Sharma, S., Pradhan, A., Chauhan, V.S., and Tuteja, R. (2005). Isolation and characterization of type I signal peptidase of different malaria parasites. *Journal of biomedicine & biotechnology* 2005, 301-309.
 343. Sharpe, H.J., Stevens, T.J., and Munro, S. (2010). A comprehensive comparison of transmembrane domains reveals organelle-specific properties. *Cell* 142, 158-169.
 344. Sheiner, L., and Striepen, B. (2013). Protein sorting in complex plastids. *Biochimica et biophysica acta* 1833, 352-359.
 345. Sherman I.W. (1998). A brief history of Malaria and discovery of the parasite's life cycle. In IW Sherman (ed.), *Malaria Parasite Biology, Pathogenesis and Protection*. American Society for Microbiology, 557 pp.
 346. Sherry, B.A., Alava, G., Tracey, K.J., Martiney, J., Cerami, A., and Slater, A.F. (1995). Malaria-specific metabolite hemozoin mediates the release of several potent endogenous pyrogens (TNF, MIP-1 alpha, and MIP-1 beta) in vitro, and altered thermoregulation in vivo. *Journal of inflammation* 45, 85-96.
 347. Siau, A., Huang, X., Yam, X.Y., Bob, N.S., Sun, H., Rajapakse, J.C., Renia, L., and Preiser, P.R. (2014). Identification of a new export signal in *Plasmodium yoelii*: identification of a new exportome. *Cellular microbiology* 16, 673-686.
 348. Sijwali, P.S., and Rosenthal, P.J. (2010). Functional evaluation of *Plasmodium* export signals in *Plasmodium berghei* suggests multiple modes of protein export. *PloS one* 5, e10227.
 349. Silvestrini, M., Altamura, C., Cerqua, R., Pedone, C., Balucani, C., Luzzi, S., Bartolini, M., Provinciali, L., and Vernieri, F. (2011). Early activation of intracranial collateral vessels influences the outcome of spontaneous internal carotid artery dissection. *Stroke* 42, 139-143.
 350. Sim, B.K., Toyoshima, T., Haynes, J.D., and Aikawa, M. (1992). Localization of the 175-kilodalton erythrocyte binding antigen in micronemes of *Plasmodium falciparum* merozoites. *Molecular and biochemical parasitology* 51, 157-159.
 351. Simmons, D., Woollett, G., Bergin-Cartwright, M., Kay, D., and Scaife, J. (1987). A malaria protein exported into a new compartment within the host erythrocyte. *The EMBO journal* 6, 485-491.
 352. Sinden, R.E. (2009). Malaria, sexual development and transmission: retrospect and prospect. *Parasitology* 136, 1427-1434.
 353. Sinden, R.E., Hartley, R.H., and Winger, L. (1985). The development of *Plasmodium* ookinetes in vitro: an ultrastructural study including a description of meiotic division. *Parasitology* 91 (Pt 2), 227-244.
 354. Singh, A.P., Buscaglia, C.A., Wang, Q., Levay, A., Nussenzweig, D.R., Walker, J.R., Winzeler, E.A., Fujii, H., Fontoura, B.M., and Nussenzweig, V. (2007). *Plasmodium* circumsporozoite protein promotes the development of the liver stages of the parasite. *Cell* 131, 492-504.
 355. Singh, B., and Daneshvar, C. (2013). Human infections and detection of *Plasmodium knowlesi*. *Clinical microbiology reviews* 26, 165-184.
 356. Singh, B., Kim Sung, L., Matusop, A., Radhakrishnan, A., Shamsul, S.S., Cox-Singh, J., Thomas, A., and Conway, D.J. (2004). A large focus of naturally acquired *Plasmodium knowlesi* infections in human beings. *Lancet* 363, 1017-1024.
 357. Sleebs, B.E., Lopaticki, S., Marapana, D.S., O'Neill, M.T., Rajasekaran, P., Gazdik, M., Gunther, S., Whitehead, L.W., Lowes, K.N., Barford, L., et al. (2014). Inhibition of Plasmeprin V activity demonstrates its essential role in protein export, PfEMP1 display, and survival of malaria parasites. *PLoS Biol* 12, e1001897.
 358. Smith, A.L., Friedman, D.B., Yu, H., Carnahan, R.H., and Reynolds, A.B. (2011). ReCLIP (reversible cross-link immuno-precipitation): an efficient method for interrogation of labile protein complexes. *PloS one* 6, e16206.
 359. Smith, T.G., Lourenco, P., Carter, R., Walliker, D., and Ranford-Cartwright, L.C. (2000). Commitment to sexual differentiation in the human malaria parasite, *Plasmodium falciparum*. *Parasitology* 121 (Pt 2), 127-133.
 360. Snow, R.W., Guerra, C.A., Noor, A.M., Myint, H.Y., and Hay, S.I. (2005). The global distribution of clinical episodes of *Plasmodium falciparum* malaria. *Nature* 434, 214-217.
 361. Sommer, M.S., Gould, S.B., Lehmann, P., Gruber, A., Przyborski, J.M., and Maier, U.G. (2007). Der1-mediated preprotein import into the periplastid compartment of chromalveolates? *Molecular biology and evolution* 24, 918-928.
 362. Spielmann, T., and Beck, H.P. (2000). Analysis of stage-specific transcription in *Plasmodium falciparum* reveals a set of genes exclusively transcribed in ring stage parasites. *Molecular and biochemical parasitology* 111, 453-458.
 363. Spielmann, T., Dixon, M.W., Hernandez-Valladares, M., Hannemann, M., Trenholme, K.R., and Gardiner, D.L. (2006). Reliable transfection of *Plasmodium falciparum* using non-commercial plasmid mini preparations. *Int J Parasitol* 36, 1245-1248.
 364. Spielmann, T., Ferguson, D.J., and Beck, H.P. (2003). etramps, a new *Plasmodium falciparum* gene family coding for developmentally regulated and highly charged membrane proteins located at the parasite-host cell interface. *Molecular biology of the cell* 14, 1529-1544.
 365. Spielmann, T., Gardiner, D.L., Beck, H.P., Trenholme, K.R., and Kemp, D.J. (2006). Organization of ETRAMPs and EXP-1 at the parasite-host cell interface of malaria parasites. *Molecular microbiology* 59, 779-794.
 366. Spielmann, T., and Gilberger, T.W. (2010). Protein export in malaria parasites: do multiple export motifs

- add up to multiple export pathways? *Trends in parasitology* 26, 6-10.
367. Spielmann, T., Hawthorne, P.L., Dixon, M.W., Hannemann, M., Klotz, K., Kemp, D.J., Klonis, N., Tilley, L., Trenholme, K.R., and Gardiner, D.L. (2006). A cluster of ring stage-specific genes linked to a locus implicated in cytoadherence in *Plasmodium falciparum* codes for PEXEL-negative and PEXEL-positive proteins exported into the host cell. *Molecular biology of the cell* 17, 3613-3624.
368. Spielmann, T., Montagna, G.N., Hecht, L., and Matuschewski, K. (2012). Molecular make-up of the *Plasmodium parasitophorous* vacuolar membrane. *Int J Med Microbiol* 302, 179-186.
369. Spielmann, T., and Gilberger, T.W. (2015). Critical Steps in Protein Export of *Plasmodium falciparum* Blood Stages. *Trends Parasitol* 31, 514-525.
370. Spillman, N.J., Allen, R.J., McNamara, C.W., Yeung, B.K., Winzeler, E.A., Diagana, T.T., and Kirk, K. (2013). Na(+) regulation in the malaria parasite *Plasmodium falciparum* involves the cation ATPase PfATP4 and is a target of the spiroindolone antimalarials. *Cell host & microbe* 13, 227-237.
371. Spillman, N.J., Beck, J.R., and Goldberg, D.E. (2015). Protein export into malaria parasite-infected erythrocytes: mechanisms and functional consequences. *Annu Rev Biochem* 84, 813-841.
372. Spork, S., Hiss, J.A., Mandel, K., Sommer, M., Kooij, T.W., Chu, T., Schneider, G., Maier, U.G., and Przyborski, J.M. (2009). An unusual ERAD-like complex is targeted to the apicoplast of *Plasmodium falciparum*. *Eukaryotic cell* 8, 1134-1145.
373. Spring, M., Murphy, J., Nielsen, R., Dowler, M., Bennett, J.W., Zirling, S., Williams, J., de la Vega, P., Ware, L., Komisar, J., *et al.* (2013). First-in-human evaluation of genetically attenuated *Plasmodium falciparum* sporozoites administered by bite of *Anopheles* mosquitoes to adult volunteers. *Vaccine* 31, 4975-4983.
374. Spycher, C., Klonis, N., Spielmann, T., Kump, E., Steiger, S., Tilley, L., and Beck, H.P. (2003). MAHRP-1, a novel *Plasmodium falciparum* histidine-rich protein, binds ferriprotoporphyrin IX and localizes to the Maurer's clefts. *The Journal of biological chemistry* 278, 35373-35383.
375. Spycher, C., Rug, M., Klonis, N., Ferguson, D.J., Cowman, A.F., Beck, H.P., and Tilley, L. (2006). Genesis of and trafficking to the Maurer's clefts of *Plasmodium falciparum*-infected erythrocytes. *Mol Cell Biol* 26, 4074-4085.
376. Spycher, C., Rug, M., Pachlatko, E., Hanssen, E., Ferguson, D., Cowman, A.F., Tilley, L., and Beck, H.P. (2008). The Maurer's cleft protein MAHRP1 is essential for trafficking of PfEMP1 to the surface of *Plasmodium falciparum*-infected erythrocytes. *Molecular microbiology* 68, 1300-1314.
377. Staines, H.M., Alkhalil, A., Allen, R.J., De Jonge, H.R., Derbyshire, E., Egee, S., Ginsburg, H., Hill, D.A., Huber, S.M., Kirk, K., *et al.* (2007). Electrophysiological studies of malaria parasite-infected erythrocytes: current status. *Int J Parasitol* 37, 475-482.
378. Staines, H.M., Ashmore, S., Felgate, H., Moore, J., Powell, T., and Ellory, J.C. (2006). Solute transport via the new permeability pathways in *Plasmodium falciparum*-infected human red blood cells is not consistent with a simple single-channel model. *Blood* 108, 3187-3194.
379. Stengel, A., Benz, J.P., Soll, J., and Bolter, B. (2010). Redox-regulation of protein import into chloroplasts and mitochondria: similarities and differences. *Plant Signal Behav* 5, 105-109.
380. Straimer, J., Gnadig, N.F., Witkowski, B., Amaratunga, C., Duru, V., Ramadani, A.P., Dacheux, M., Khim, N., Zhang, L., Lam, S., *et al.* (2015). Drug resistance. K13-propeller mutations confer artemisinin resistance in *Plasmodium falciparum* clinical isolates. *Science* 347, 428-431.
381. Straimer, J., Lee, M.C., Lee, A.H., Zeitler, B., Williams, A.E., Pearl, J.R., Zhang, L., Rebar, E.J., Gregory, P.D., Llinas, M., *et al.* (2012). Site-specific genome editing in *Plasmodium falciparum* using engineered zinc-finger nucleases. *Nature methods* 9, 993-998.
382. Struck, N.S., de Souza Dias, S., Langer, C., Marti, M., Pearce, J.A., Cowman, A.F., and Gilberger, T.W. (2005). Re-defining the Golgi complex in *Plasmodium falciparum* using the novel Golgi marker PfGRASP. *Journal of cell science* 118, 5603-5613.
383. Struck, N.S., Herrmann, S., Schmuck-Barkmann, I., de Souza Dias, S., Haase, S., Cabrera, A.L., Treeck, M., Bruns, C., Langer, C., Cowman, A.F., *et al.* (2008). Spatial dissection of the cis- and trans-Golgi compartments in the malaria parasite *Plasmodium falciparum*. *Molecular microbiology* 67, 1320-1330.
384. Sturm, A., Amino, R., van de Sand, C., Regen, T., Retzlaff, S., Rennenberg, A., Krueger, A., Pollok, J.M., Menard, R., and Heussler, V.T. (2006). Manipulation of host hepatocytes by the malaria parasite for delivery into liver sinusoids. *Science* 313, 1287-1290.
385. Su, X.Z., Heatwole, V.M., Wertheimer, S.P., Guinet, F., Herrfeldt, J.A., Peterson, D.S., Ravetch, J.A., and Wellems, T.E. (1995). The large diverse gene family var encodes proteins involved in cytoadherence and antigenic variation of *Plasmodium falciparum*-infected erythrocytes. *Cell* 82, 89-100.
386. Sulli, C., Fang, Z., Muchhal, U., and Schwartzbach, S.D. (1999). Topology of *Euglena* chloroplast protein precursors within endoplasmic reticulum to Golgi to chloroplast transport vesicles. *The Journal of biological chemistry* 274, 457-463.
387. Szymczak, A.L., Workman, C.J., Wang, Y., Vignali, K.M., Dilioglou, S., Vanin, E.F., and Vignali, D.A. (2004). Correction of multi-gene deficiency in vivo using a single 'self-cleaving' 2A peptide-based retroviral vector. *Nature biotechnology* 22, 589-594.
388. Tan, C.H., Vythilingam, I., Matusop, A., Chan, S.T., and Singh, B. (2008). Bionomics of *Anopheles latens* in Kapit, Sarawak, Malaysian Borneo in relation to the transmission of zoonotic simian malaria parasite *Plasmodium knowlesi*. *Malaria journal* 7, 52.
389. Tan, K.R., Magill, A.J., Parise, M.E., Arguin, P.M., Centers for Disease, C., and Prevention (2011). Doxycycline for malaria chemoprophylaxis and treatment: report from the CDC expert meeting on malaria chemoprophylaxis. *Am J Trop Med Hyg* 84, 517-531.

390. Taraschi, T.F., Trelka, D., Martinez, S., Schneider, T., and O'Donnell, M.E. (2001). Vesicle-mediated trafficking of parasite proteins to the host cell cytosol and erythrocyte surface membrane in *Plasmodium falciparum* infected erythrocytes. *Int J Parasitol* 31, 1381-1391.
391. Tarr, S.J., Cryar, A., Thalassinou, K., Haldar, K., and Osborne, A.R. (2013). The C-terminal portion of the cleaved HT motif is necessary and sufficient to mediate export of proteins from the malaria parasite into its host cell. *Molecular microbiology* 87, 835-850.
392. Tarr, S.J., and Osborne, A.R. (2015). Experimental determination of the membrane topology of the *Plasmodium* protease Plasmeprin V. *PLoS one* 10, e0121786.
393. Tawk, L., Chicanne, G., Dubremetz, J.F., Richard, V., Payrastre, B., Vial, H.J., Roy, C., and Wengelnik, K. (2010). Phosphatidylinositol 3-phosphate, an essential lipid in *Plasmodium*, localizes to the food vacuole membrane and the apicoplast. *Eukaryotic cell* 9, 1519-1530.
394. Taylor, D.W., Parra, M., Chapman, G.B., Stearns, M.E., Rener, J., Aikawa, M., Uni, S., Aley, S.B., Panton, L.J., and Howard, R.J. (1987). Localization of *Plasmodium falciparum* histidine-rich protein 1 in the erythrocyte skeleton under knobs. *Molecular and biochemical parasitology* 25, 165-174.
395. Templeton, T.J., and Pain, A. (2016). Diversity of extracellular proteins during the transition from the 'proto-apicomplexan' alveolates to the apicomplexan obligate parasites. *Parasitology* 143, 1-17.
396. Tham, W.H., Wilson, D.W., Lopatnicki, S., Schmidt, C.Q., Tetteh-Quarcoo, P.B., Barlow, P.N., Richard, D., Corbin, J.E., Beeson, J.G., and Cowman, A.F. (2010). Complement receptor 1 is the host erythrocyte receptor for *Plasmodium falciparum* PfRh4 invasion ligand. *Proc Natl Acad Sci U S A* 107, 17327-17332.
397. Tiburcio, M., Sauerwein, R., Lavazec, C., and Alano, P. (2015). Erythrocyte remodeling by *Plasmodium falciparum* gametocytes in the human host interplay. *Trends in parasitology* 31, 270-278.
398. Tilley, L., Sougrat, R., Lithgow, T., and Hanssen, E. (2008). The twists and turns of Maurer's cleft trafficking in *P. falciparum*-infected erythrocytes. *Traffic* 9, 187-197.
399. Tirosh, B., Furman, M.H., Tortorella, D., and Ploegh, H.L. (2003). Protein unfolding is not a prerequisite for endoplasmic reticulum-to-cytosol dislocation. *The Journal of biological chemistry* 278, 6664-6672.
400. Tomkiewicz, D., Nouwen, N., and Driessen, A.J. (2007). Pushing, pulling and trapping--modes of motor protein supported protein translocation. *FEBS letters* 581, 2820-2828.
401. Tonkin, C.J., Pearce, J.A., McFadden, G.I., and Cowman, A.F. (2006). Protein targeting to destinations of the secretory pathway in the malaria parasite *Plasmodium falciparum*. *Curr Opin Microbiol* 9, 381-387.
402. Towbin, H., Staehelin, T., and Gordon, J. (1979). Electrophoretic transfer of proteins from polyacrylamide gels to nitrocellulose sheets: procedure and some applications. *Proc Natl Acad Sci U S A* 76, 4350-4354.
403. Trager, W., and Jensen, J.B. (1976). Human malaria parasites in continuous culture. *Science* 193, 673-675.
404. Trelka, D.P., Schneider, T.G., Reeder, J.C., and Taraschi, T.F. (2000). Evidence for vesicle-mediated trafficking of parasite proteins to the host cell cytosol and erythrocyte surface membrane in *Plasmodium falciparum* infected erythrocytes. *Molecular and biochemical parasitology* 106, 131-145.
405. Trenholme, K.R., Gardiner, D.L., Holt, D.C., Thomas, E.A., Cowman, A.F., and Kemp, D.J. (2000). *clag9*: A cytoadherence gene in *Plasmodium falciparum* essential for binding of parasitized erythrocytes to CD36. *Proc Natl Acad Sci U S A* 97, 4029-4033.
406. Triglia, T., Thompson, J., Caruana, S.R., Delorenzi, M., Speed, T., and Cowman, A.F. (2001). Identification of proteins from *Plasmodium falciparum* that are homologous to reticulocyte binding proteins in *Plasmodium vivax*. *Infect Immun* 69, 1084-1092.
407. Turusov, V., Rakitsky, V., and Tomatis, L. (2002). Dichlorodiphenyltrichloroethane (DDT): ubiquity, persistence, and risks. *Environ Health Perspect* 110, 125-128.
408. Ulmschneider, M.B., Koehler Leman, J., Fennell, H., and Beckstein, O. (2015). Peptide Folding in Translocon-Like Pores. *The Journal of membrane biology* 248, 407-417.
409. Umlas, J., and Fallon, J.N. (1971). New thick-film technique for malaria diagnosis. Use of saponin stratomalytic solution for lysis. *Am J Trop Med Hyg* 20, 527-529.
410. Ungermann, C., Neupert, W., and Cyr, D.M. (1994). The role of Hsp70 in conferring unidirectionality on protein translocation into mitochondria. *Science* 266, 1250-1253.
411. Vaidya, A.B., and Mather, M.W. (2009). Mitochondrial evolution and functions in malaria parasites. *Annu Rev Microbiol* 63, 249-267.
412. van den Berg, H. (2009). Global status of DDT and its alternatives for use in vector control to prevent disease. *Environ Health Perspect* 117, 1656-1663.
413. van Dooren, G.G., Marti, M., Tonkin, C.J., Stimmer, L.M., Cowman, A.F., and McFadden, G.I. (2005). Development of the endoplasmic reticulum, mitochondrion and apicoplast during the asexual life cycle of *Plasmodium falciparum*. *Molecular microbiology* 57, 405-419.
414. van Dooren, G.G., Schwartzbach, S.D., Osafune, T., and McFadden, G.I. (2001). Translocation of proteins across the multiple membranes of complex plastids. *Biochimica et biophysica acta* 1541, 34-53.
415. van Dooren, G.G., and Striepen, B. (2013). The algal past and parasite present of the apicoplast. *Annu Rev Microbiol* 67, 271-289.
416. van Ooij, C., Tamez, P., Bhattacharjee, S., Hiller, N.L., Harrison, T., Liolios, K., Kooij, T., Ramesar, J., Balu, B., Adams, J., *et al.* (2008). The malaria secretome: from algorithms to essential function in blood stage infection. *PLoS Pathog* 4, e1000084.
417. van Schaijk, B.C., Kumar, T.R., Vos, M.W., Richman, A., van Gemert, G.J., Li, T., Eappen, A.G., Williamson, K.C., Morahan, B.J., Fishbaugher, M., *et al.* (2014). Type II fatty acid biosynthesis is essential for *Plasmodium falciparum* sporozoite development in the midgut of *Anopheles* mosquitoes. *Eukaryotic cell* 13, 550-559.

418. VanBuskirk, K.M., O'Neill, M.T., De La Vega, P., Maier, A.G., Krzych, U., Williams, J., Dowler, M.G., Sacci, J.B., Jr., Kangwanransan, N., Tsuboi, T., *et al.* (2009). Preerythrocytic, live-attenuated *Plasmodium falciparum* vaccine candidates by design. *Proc Natl Acad Sci U S A* *106*, 13004-13009.
419. Varnai, P., and Balla, T. (1998). Visualization of phosphoinositides that bind pleckstrin homology domains: calcium- and agonist-induced dynamic changes and relationship to myo-[3H]inositol-labeled phosphoinositide pools. *The Journal of cell biology* *143*, 501-510.
420. Vaughan, A.M., Kappe, S.H., Ploss, A., and Mikolajczak, S.A. (2012). Development of humanized mouse models to study human malaria parasite infection. *Future Microbiol* *7*, 657-665.
421. Vembar, S.S., and Brodsky, J.L. (2008). One step at a time: endoplasmic reticulum-associated degradation. *Nat Rev Mol Cell Biol* *9*, 944-957.
422. Vestweber, D., Brunner, J., Baker, A., and Schatz, G. (1989). A 42K outer-membrane protein is a component of the yeast mitochondrial protein import site. *Nature* *341*, 205-209.
423. Vestweber, D., and Schatz, G. (1988). A chimeric mitochondrial precursor protein with internal disulfide bridges blocks import of authentic precursors into mitochondria and allows quantitation of import sites. *The Journal of cell biology* *107*, 2037-2043.
424. Viebig, N.K., Gamain, B., Scheidig, C., Lepolard, C., Przyborski, J., Lanzer, M., Gysin, J., and Scherf, A. (2005). A single member of the *Plasmodium falciparum* var multigene family determines cytoadhesion to the placental receptor chondroitin sulphate A. *EMBO reports* *6*, 775-781.
425. Vinetz, J.M., Li, J., McCutchan, T.F., and Kaslow, D.C. (1998). *Plasmodium malariae* infection in an asymptomatic 74-year-old Greek woman with splenomegaly. *The New England journal of medicine* *338*, 367-371.
426. Voss, T.S., Healer, J., Marty, A.J., Duffy, M.F., Thompson, J.K., Beeson, J.G., Reeder, J.C., Crabb, B.S., and Cowman, A.F. (2006). A var gene promoter controls allelic exclusion of virulence genes in *Plasmodium falciparum* malaria. *Nature* *439*, 1004-1008.
427. Wallace, A.J., Stillman, T.J., Atkins, A., Jamieson, S.J., Bullough, P.A., Green, J., and Artymiuk, P.J. (2000). *E. coli* hemolysin E (HlyE, ClyA, SheA): X-ray crystal structure of the toxin and observation of membrane pores by electron microscopy. *Cell* *100*, 265-276.
428. Waller, K.L., Cooke, B.M., Nunomura, W., Mohandas, N., and Coppel, R.L. (1999). Mapping the binding domains involved in the interaction between the *Plasmodium falciparum* knob-associated histidine-rich protein (KAHRP) and the cytoadherence ligand *P. falciparum* erythrocyte membrane protein 1 (PfEMP1). *The Journal of biological chemistry* *274*, 23808-23813.
429. Wang, J., Zhang, C.J., Chia, W.N., Loh, C.C., Li, Z., Lee, Y.M., He, Y., Yuan, L.X., Lim, T.K., Liu, M., *et al.* (2015). Haem-activated promiscuous targeting of artemisinin in *Plasmodium falciparum*. *Nature communications* *6*, 10111.
430. Ward, G.E., Tilney, L.G., and Langsley, G. (1997). Rab GTPases and the unusual secretory pathway of plasmodium. *Parasitology today* *13*, 57-62.
431. Waterkeyn, J.G., Wickham, M.E., Davern, K.M., Cooke, B.M., Coppel, R.L., Reeder, J.C., Culvenor, J.G., Waller, R.F., and Cowman, A.F. (2000). Targeted mutagenesis of *Plasmodium falciparum* erythrocyte membrane protein 3 (PfEMP3) disrupts cytoadherence of malaria-infected red blood cells. *The EMBO journal* *19*, 2813-2823.
432. Wells, T.N., Burrows, J.N., and Baird, J.K. (2010). Targeting the hypnozoite reservoir of *Plasmodium vivax*: the hidden obstacle to malaria elimination. *Trends in parasitology* *26*, 145-151.
433. White, M.T., Bejon, P., Olotu, A., Griffin, J.T., Bojang, K., Lusingu, J., Salim, N., Abdulla, S., Otsyula, N., Agnandji, S.T., *et al.* (2014). A combined analysis of immunogenicity, antibody kinetics and vaccine efficacy from phase 2 trials of the RTS,S malaria vaccine. *BMC Med* *12*, 117.
434. White, N.J. (2011). Determinants of relapse periodicity in *Plasmodium vivax* malaria. *Malaria journal* *10*, 297.
435. White, N.J., Pukrittayakamee, S., Hien, T.T., Faiz, M.A., Mokuolu, O.A., and Dondorp, A.M. (2014). Malaria. *Lancet* *383*, 723-735.
436. White, N.J., Pukrittayakamee, S., Phyto, A.P., Rueangweerayut, R., Nosten, F., Jittamala, P., Jeeyapant, A., Jain, J.P., Lefevre, G., Li, R., *et al.* (2014). Spiroindolone KAE609 for falciparum and vivax malaria. *The New England journal of medicine* *371*, 403-410.
437. Wickert, H., Gottler, W., Krohne, G., and Lanzer, M. (2004). Maurer's cleft organization in the cytoplasm of plasmodium falciparum-infected erythrocytes: new insights from three-dimensional reconstruction of serial ultrathin sections. *European journal of cell biology* *83*, 567-582.
438. Wickham, M.E., Rug, M., Ralph, S.A., Klonis, N., McFadden, G.I., Tilley, L., and Cowman, A.F. (2001). Trafficking and assembly of the cytoadherence complex in *Plasmodium falciparum*-infected human erythrocytes. *The EMBO journal* *20*, 5636-5649.
439. Wickner, W., and Schekman, R. (2005). Protein translocation across biological membranes. *Science* *310*, 1452-1456.
440. Wienhues, U., Becker, K., Schleyer, M., Guiard, B., Tropschug, M., Horwich, A.L., Pfanner, N., and Neupert, W. (1991). Protein folding causes an arrest of preprotein translocation into mitochondria in vivo. *The Journal of cell biology* *115*, 1601-1609.
441. Wiertz, E.J., Jones, T.R., Sun, L., Bogyo, M., Geuze, H.J., and Ploegh, H.L. (1996). The human cytomegalovirus US11 gene product dislocates MHC class I heavy chains from the endoplasmic reticulum to the cytosol. *Cell* *84*, 769-779.
442. Withers-Martinez, C., Strath, M., Hackett, F., Haire, L.F., Howell, S.A., Walker, P.A., Christodoulou, E., Dodson, G.G., and Blackman, M.J. (2014). The malaria parasite egress protease SUB1 is a calcium-

- dependent redox switch subtilisin. *Nature communications* 5, 3726.
443. World Health Organization (2011) The use of DDT in malaria vector control http://www.who.int/malaria/publications/atoz/who_htm_gmp_2011/en/
444. World Health Organization (2015) World Malaria Report 2015 <http://www.who.int/malaria/publications/world-malaria-report-2015/report/en/>
445. World Health Organization (2015) Guidelines for the treatment of malaria apps.who.int/iris/bitstream/10665/162441/1/9789241549127_eng.pdf
446. Wu, Y., Sifri, C.D., Lei, H.H., Su, X.Z., and Wellems, T.E. (1995). Transfection of *Plasmodium falciparum* within human red blood cells. *Proc Natl Acad Sci U S A* 92, 973-977.
447. Yeh, E., and DeRisi, J.L. (2011). Chemical rescue of malaria parasites lacking an apicoplast defines organelle function in blood-stage *Plasmodium falciparum*. *PLoS Biol* 9, e1001138.
448. Zattas, D., and Hochstrasser, M. (2015). Ubiquitin-dependent protein degradation at the yeast endoplasmic reticulum and nuclear envelope. *Crit Rev Biochem Mol Biol* 50, 1-17.
449. Zilversmit M., Hartl DL. (2005). Evolutionary history and population genetics of human malaria parasites. In IW Sherman (ed.), *Molecular approaches to malaria*, , 542 pp.
450. Zimmermann, R., Eyrisch, S., Ahmad, M., and Helms, V. (2011). Protein translocation across the ER membrane. *Biochimica et biophysica acta* 1808, 912-924.
451. Zuccala, E.S., Gout, A.M., Dekiwadia, C., Marapana, D.S., Angrisano, F., Turnbull, L., Riglar, D.T., Rogers, K.L., Whitchurch, C.B., Ralph, S.A., *et al.* (2012). Subcompartmentalisation of proteins in the rhoptries correlates with ordered events of erythrocyte invasion by the blood stage malaria parasite. *PloS one* 7, e46160.
452. Zucker, J.R. (1996). Changing patterns of autochthonous malaria transmission in the United States: a review of recent outbreaks. *Emerging infectious diseases* 2, 37-43.

Acknowledgements

My first and most earnest gratitude is to my supervisor Dr. Tobias Spielmann for supervising this PhD thesis and for giving me the opportunity to move abroad and work at his research group. Thanks a lot for the encouragement, helpful advices and ingenious ideas when the experiments did not work out.

Thanks to former and present colleagues and laboratory mates I worked with during the last years in both Spielmann and Gilberger research groups. Special thanks to Bärbel Bergmann, not only for the technical assistance and critical reading of this thesis but also for always taking the time to help me out when needed. Thanks to Ferdinand Reinsch for the generation of the parasite cell lines expressing PEXEL BPTI and mDHFR constructs. Thanks to Alexandra Blancke-Soares for providing the integrant cell line SBP1-mDHFR-GFP. Also to Sogol Gachkar who assisted with cloning of deletion constructs.

Thanks to Prof. Stefan Tenzer in Institute for Immunology, University Medical Center, Johannes Gutenberg University, Mainz for the mass spectrometry analysis. Thanks to supervisors and readers at the University of Hamburg and Bernhard Nocht Institut for Tropical Medicine.

Last but not least I would like to thank all my friends and people standing next to me during these years in Germany, to my family in Hamburg who opened the doors to me as I came here and to my mother and brother in Costa Rica.

List of publications and manuscripts

Heiber, A., Kruse, F., Pick, C., Grüning, C., Flemming, S., Oberli, A., Schoeler, H., Retzlaff, S., **Mesén-Ramírez, P.**, Hiss, J.A., Kadekoppala, M., Hecht, L., Holder, A.A., Gilberger, T.-W. & Spielmann, T. **(2013)** *Identification of new PNEPs indicates a substantial non-PEXEL exportome and underpins common features in Plasmodium falciparum protein export.* PLoS Pathog, Vol. 9(8), pp. e1003546

Mesén-Ramírez, P., Reinsch, F., Blancke-Soares A, Bergmann B., Ullrich A.K., Tenzer S., Spielmann, T. **(2016)** *Stable translocation intermediates jam global protein export in Plasmodium falciparum parasites and link the PTEX component EXP2 with translocation activity* 2015 (In revision)

Appendix 1

Table S1. Cloning strategies for constructs in this study

Construct	Primers	Enzymes	Template	Backbone Vector
SBP-1mDHFRGFP	SBP-1fw(XhoI) SBP-1rv(AvrII)	XhoI-AvrII	cDNA	pARL2- REX2mDHFRGFP (Grüning et. al 2012)
SBP-1-mDHFR-GFP PH mut	GFP-PH mut fw BstBI PH mut rv XmaI	BstBI-XmaI	GFP PH mut (Kruse et al, unpublished data)	pARL2 SBP-1mDHFRGFP
REX2-GFP-mDHFR	REX2XhoI fw GFPrv Nhe-XmaI mDHFR Nhe fw mDHFR Spe-XmaI	XhoI-XmaI NheI-XmaI	REX2-GFP (Haase et al.,2009) REX2mDHFRGFP (Grüning et. al 2012)	pARL2- REX2mDHFRGFP (Grüning et. al 2012)
REX2-(N-mDHFR)-GFP	mDHFR Nhe fw mDHFRrv Spe		REX2mDHFRGFP (Grüning et. al 2012)	pARL2_GFP
REX2-ZnFwt-GFP	REX2 ZnFwt fw REX2 ZnFwt rv		REX2-GFP (Haase et al.,2009)	pARL1_GFP
REX2-ZnFmut-GFP	REX2 ZnFmut rv REX2 ZnFmutfw		REX2-GFP (Haase et al.,2009)	pARL1_GFP
REX2-5XZnFwt-GFP	REX2 Kpn fw REX2 AvrII rv		Synthesized gen	pARL1_GFP
REX2-5XZnFmut-GFP	REX2 Kpn fw REX2 AvrII rv		Synthesized gen	pARL1_GFP
REX2+3C-mDHFR- GFP	REX2XhoI fw REX2rvAvrII Ext C-t	XhoI-AvrII	Synthesized gen	pARL2- REX2mDHFRGFP (Grüning et. al 2012)
MAHRP1mDHFRGFP	MAHRP1 Xho fw MAHRP1 AvrII rv	XhoI-AvrII	cDNA	pARL2- REX2mDHFRGFP (Grüning et. al 2012)
REX3-mDHFRGFP	REX3 XhoI fw REX3 AvrII rv	XhoI-AvrII	cDNA	pARL2- REX2mDHFRGFP (Grüning et. al 2012)
KAHRP-mDHFRGFP	KAHRP Xho fw KAHRP AvrII rv	XhoI-AvrII	cDNA	pARL2- REX2mDHFRGFP (Grüning et. al 2012)
PTP1-mDHFRGFP	PTP1 XhoI fw PTP1 rv AvrII	XhoI-AvrII	3D7 genomic DNA	pARL2- REX2mDHFRGFP (Grüning et. al 2012)
PTP1-(3C) mDHFRGFP	PTP1 XhoI fw PTP1 rv SpeI	XhoI-SpeI	3D7 genomic DNA	pARL2-REX2(3C) mDHFRGFP
STEVORmDHFRGFP	STEVOR_0900900 XhoI fw STEVOR_0900900 AvrII rv	XhoI-AvrII	3D7 genomic DNA	pARL2- REX2mDHFRGFP (Grüning et. al 2012)
REX2-BPTIwt-GFP	BPTI fwAvrII BPTI rv KpnI	AvrII-KpnI	BPTI synthesized gen	pARL2- REX2mDHFRGFP (Grüning et. al 2012)
REX2-BPTImut-GFP	BPTI fwAvrII BPTI rv KpnI	AvrII-KpnI	BPTI-mut synthesized gen	pARL2- REX2mDHFRGFP (Grüning et. al 2012)
SBP1-BPTIwt-GFP	SBP-1fw(XhoI) SBP-1rv(AvrII)	XhoI-AvrII	cDNA	REX2-BPTIwt-GFP
REX3-BPTI-GFP	REX3 XhoI fw REX3 AvrII rv	XhoI-AvrII	cDNA	REX2-BPTIwt-GFP
MAHRP1-BPTI-GFP	MAHRP1 Xho fw MAHRP1 AvrII rv	XhoI-AvrII	cDNA	REX2-BPTIwt-GFP
REX3-BPTImut-GFP	REX3 XhoI fw REX3 AvrII rv	XhoI-AvrII	cDNA	REX2-BPTImut-GFP
ΔCSBP1-BPTIwt-GFP	SBP-1fw(XhoI) SBP259AvrIIrv	XhoI-AvrII	cDNA	REX2-BPTIwt-GFP

Construct	Primers	Enzymes	Template	Backbone Vector
ΔCSBP1-BPTImut-GFP	SBP-1fw(XhoI) SBP259AvrIIrv	XhoI-AvrII	cDNA	REX2-BPTImut-GFP
ΔNSBP1-BPTIwt-GFP	SBP-1fw(XhoI) /SBP1 40rv (Product1a) SBP1 211fw/ SBP- 259rv(AvrII)(Product1b) SBP-1fw(XhoI) /SBP259rv(AvrII)	XhoI-AvrII	cDNA cDNA Product1a + Product1b	REX2-BPTIwt-GFP
REX2+3C-BPTIwtGFP	REX2XhoI fw REX2rvAvrII Ext C-t	XhoI-AvrII	Synthesized gen	REX2-BPTIwt-GFP
PTP1 BPTI-GFP	PTP1 XhoI fw PTP1 rv AvrII	XhoI-AvrII	3D7 genomic DNA	REX2-BPTIwt-GFP
PTP1 (3C) BPTI-GFP	PTP1 XhoI fw PTP1 rv SpeI	XhoI-SpeI	3D7 genomic DNA	REX2-(3C) BPTIwt-GFP
MSRP6-mCherry	MSRP6 fw KpnI MSRP6 rv AvrII	XhoI-AvrII	MSRP6-GFP (Heiber et al., 2013)	REX2-mCherry (Grüning et. al 2012)
REX3-mCherry	REX3KpnI fw REX3AvrIIrv	KpnI-AvrII	cDNA	REX2-mCherry (Grüning et. al 2012)
STEVOR-mCherry	STEVOR KpnI fw STEVOR AvrII rv	KpnI-AvrII	3D7 genomic DNA	REX2-mCherry (Grüning et. al 2012)
pARL2-T2A-mCherry	pARL2 XhoI fw pARL2-2A-AvrIIrv	XhoI-AvrII	Vector	pARL2 GFP-mCherry
SBP-1mDHFRGFP2A REX3mCherry	SBP- 1fw(XhoI)/GFPrvSpe REX3 fw AvrII/ REX3 rv KpnI	XhoI-SpeI AvrII-KpnI	SBP-1mDHFRGFP cDNA	pARL2 -T2AmCherry
SBP1-mDHFR-GFP-2A KAHRP-mCherry	SBP-1fw(XhoI)/ GFPrvSpe KAHRPfwAvrII/ KAHRPrvKpnI	XhoI-SpeI AvrII-KpnI	SBP-1mDHFRGFP cDNA	pARL2 -T2AmCherry
SBP1-mDHFR-GFP-2A STEVOR-mCherry	SBP-1fw(XhoI)/ GFPrvSpe STEVOR fw1/STEVOR fw2 AvrII STEVOR rv KpnI	XhoI-SpeI AvrII-KpnI	SBP-1mDHFRGFP 3D7 genomic DNA	pARL2 -T2AmCherry
SBP1-mDHFR-GFP-2A MSRP6mCherry	SBP-1fw(XhoI)/ GFPrvSpe MSRP6 fw AvrII/MSRP6 rv KpnI	XhoI-SpeI AvrII-KpnI	SBP-1mDHFRGFP MSRP6-GFP	pARL2 -T2AmCherry
REX2-GFP-mDHFR-2A KAHRP-mCherry	REX2XhoI fw/ mDHFR Spe-Xma rv KAHRP fw AvrII/ KAHRP rv KpnI	XhoI-AvrII	REX2GFPmDHFR cDNA	pARL2 -T2AmCherry
EXP2-3XHA	EXP2 Not fw/ EXP2 HA rv1 (Product 1) EXP2 Not fw/ 3xHA Sall rv2	NotI-Sall	3D7 genomic DNA Product 1	SLI in pARL1
EXP2-GFP	EXP2 Not fw/ EXP2 AvrII HA rv1	NotI-AvrII	3D7 genomic DNA	SLI in pARL1
HSP101-3XHA	HSP101NotI fw/ HSP101KpnI	NotI-KpnI	3D7 genomic DNA	SLI in pARL1

Appendix 2

Table S2. MS Analysis of IP assays from EXP2-3XHA

description	IEP	mw	max score	accession	reported peptides	sequence coverage	FDR level	entry
Exported protein 2 OS=Plasmodium falciparum (isolate 3D7) GN=EXP-2 PE=4 SV=1	4,91	33639,87	14962,63	Q8IKC8	11	58,54	0	Q8IKC8_PLAF7
Uncharacterized protein OS=Plasmodium falciparum (isolate 3D7) GN=PF11_0302 PE=4 SV=1	4,79	52179,70	11165,02	Q8II72	17	62,39	0	Q8II72_PLAF7
Surface protein, Pf113 OS=Plasmodium falciparum (isolate 3D7) GN=PF113 PE=4 SV=1	4,29	113601,01	5094,79	Q8ILP3	27	47,68	0	Q8ILP3_PLAF7
Uncharacterized protein OS=Plasmodium falciparum (isolate 3D7) GN=PF14_0344 PE=4 SV=1	4,03	112580,03	6084,10	Q8ILA1	39	58,31	0	Q8ILA1_PLAF7
Circumsporozoite-related antigen OS=Plasmodium falciparum (isolate 3D7) GN=PF11_0224 PE=4 SV=1	5,55	17295,54	7143,94	Q8IIF0	5	54,94	0	Q8IIF0_PLAF7
Early transcribed membrane protein 5, ETRAMP5 OS=Plasmodium falciparum (isolate 3D7) GN=ETRAMP5 PE=4 SV=1	5,08	19143,80	8279,37	Q8I3F3	5	38,67	0	Q8I3F3_PLAF7
Phosphatase, putative OS=Plasmodium falciparum (isolate 3D7) GN=PF14_0614 PE=4 SV=2	5,38	171164,56	1507,24	Q8IKJ1	35	34,74	0	Q8IKJ1_PLAF7
Heat shock protein 101, putative OS=Plasmodium falciparum (isolate 3D7) GN=PF11_0175 PE=1 SV=1	9,48	103102,13	1868,57	Q8IIJ8	26	44,70	0	Q8IIJ8_PLAF7
Conserved Plasmodium protein OS=Plasmodium falciparum (isolate 3D7) GN=PF11_0067 PE=4 SV=2	7,92	91300,58	931,34	Q8IIU7	14	26,13	0	Q8IIU7_PLAF7
Conserved Plasmodium protein OS=Plasmodium falciparum (isolate 3D7) GN=PF10_0242 PE=4 SV=2	4,12	171628,76	494,11	Q8IJF6	18	13,93	0	Q8IJF6_PLAF7
Heat shock 70 kDa protein OS=Plasmodium falciparum (isolate 3D7) GN=PF08_0054 PE=3 SV=1	5,34	74428,30	1040,59	Q8IB24	11	26,14	0	Q8IB24_PLAF7
Uncharacterized protein OS=Plasmodium falciparum (isolate 3D7) GN=PF07_0087 PE=4 SV=1	8,66	29649,43	3646,62	Q8IBP0	7	39,34	0	Q8IBP0_PLAF7
Uncharacterized protein OS=Plasmodium falciparum (isolate 3D7) GN=PFL0050c PE=4 SV=1	4,20	77572,41	957,31	Q8I635	14	31,70	0	Q8I635_PLAF7
Merozoite surface protein 1 OS=Plasmodium falciparum (isolate 3D7) GN=MSP1 PE=4 SV=1	6,07	196866,74	449,23	Q8IOU8	18	17,50	0	Q8IOU8_PLAF7
Conserved Plasmodium protein OS=Plasmodium falciparum (isolate 3D7) GN=PF11_0364	9,00	28667,07	2110,54	Q8II11	8	36,33	0	Q8II11_PLAF7
Uncharacterized protein OS=Plasmodium falciparum (isolate 3D7) GN=PF10_0323 PE=4 SV=1	9,85	39096,78	1178,93	Q8IJ76	6	42,82	0	Q8IJ76_PLAF7
GTP-binding nuclear protein ran/tc4 OS=Plasmodium falciparum (isolate 3D7) GN=PF11_0183 PE=4 SV=1	8,15	24989,41	3284,44	Q7KQK6	7	47,66	0	Q7KQK6_PLAF7
Hsp70-x OS=Plasmodium falciparum (isolate 3D7) PE=2 SV=1	5,44	75623,24	765,92	K7NTP5	11	24,01	0	K7NTP5_PLAF7
Elongation factor 1-alpha OS=Plasmodium falciparum (isolate 3D7) GN=PF13_0304 PE=3 SV=1	9,43	49186,86	635,44	Q8I0P6	7	30,25	0	Q8I0P6_PLAF7
Heat shock protein 70 (HSP70)	5,00	72501,66	843,86	Q8I2X4	5	22,24	0	Q8I2X4_PLAF7

description	IEP	mw	max score	accession	reported peptides	sequence coverage	FDR level	entry
homologue OS=Plasmodium falciparum (isolate 3D7) GN=PF10875w PE=3 SV=1								
Uncharacterized protein OS=Plasmodium falciparum (isolate 3D7) GN=MAL8P1.95 PE=4 SV=1	3,91	36540,70	1014,40	C0H4U4	6	16,83	0	C0H4U4_PLAF7
Heat shock protein 86 OS=Plasmodium falciparum (isolate 3D7) GN=PF07_0029 PE=1 SV=1	4,74	86565,71	400,27	Q8IC05	8	12,48	0	Q8IC05_PLAF7
Rhoptry neck protein 3, putative OS=Plasmodium falciparum (isolate 3D7) GN=PFL2505c PE=4 SV=1	9,45	264125,09	296,25	Q8I4R5	20	10,70	0	Q8I4R5_PLAF7
40S ribosomal protein S11, putative OS=Plasmodium falciparum (isolate 3D7) GN=PFC0775w PE=1 SV=2	10,5 8	19045,23	954,60	O77381	4	26,71	0	O77381_PLAF7
Peptidase, putative OS=Plasmodium falciparum (isolate 3D7) GN=PF14_0517 PE=3 SV=1	6,36	88787,90	503,49	Q8IKT5	13	18,06	0	Q8IKT5_PLAF7
Serine repeat antigen 6 (SERA-6) OS=Plasmodium falciparum (isolate 3D7) GN=SERA-6 PE=1 SV=3	5,84	120489,71	363,29	Q9TY96	7	7,66	0	Q9TY96_PLAF7
60S ribosomal protein L32, putative OS=Plasmodium falciparum (isolate 3D7) GN=PF10190w PE=1 SV=1	11,4 9	15640,71	1376,13	Q8I3B0	2	23,66	0	Q8I3B0_PLAF7
Uncharacterized protein OS=Plasmodium falciparum (isolate 3D7) GN=PFD0090c PE=4 SV=1	9,90	50142,69	317,62	Q8I206	2	2,80	0	Q8I206_PLAF7
Glycophorin-binding protein OS=Plasmodium falciparum (isolate 3D7) GN=GBP PE=3 SV=1	4,84	95958,30	316,02	Q8I6U8	4	9,10	0	GBP_PLAF7
Serine-repeat antigen protein OS=Plasmodium falciparum (isolate 3D7) GN=SERA PE=1 SV=1	5,09	113365,07	281,50	Q9TY95	9	10,73	0	SERA_PLAF7
Uncharacterized protein OS=Plasmodium falciparum (isolate 3D7) GN=PF08_0004 PE=4 SV=1	10,5 2	15901,73	1021,87	Q8IBD0	2	13,87	0	Q8IBD0_PLAF7
Chaperonin, cpn60 OS=Plasmodium falciparum (isolate 3D7) GN=PFL1545c PE=3 SV=2	4,77	81826,29	262,18	Q8I0V3	2	4,60	0	Q8I0V3_PLAF7
Ribosomal protein L3, putative OS=Plasmodium falciparum (isolate 3D7) GN=PF10_0272 PE=1 SV=1	10,6 2	44677,26	612,37	Q8IJC6	7	31,35	0	Q8IJC6_PLAF7
Serine repeat antigen 9 (SERA-9) OS=Plasmodium falciparum (isolate 3D7) GN=SERA9 PE=3 SV=1	4,97	107197,87	220,55	Q8I3C0	3	3,11	0	Q8I3C0_PLAF7
Plasmodium exported protein OS=Plasmodium falciparum (isolate 3D7) GN=PF11_0508 PE=4 SV=1	5,49	53097,16	372,07	Q8IHN2	2	4,44	0	Q8IHN2_PLAF7
DNA/RNA-binding protein Alba, putative OS=Plasmodium falciparum (isolate 3D7) GN=PF08_0074 PE=4 SV=1	10,9 2	27315,67	518,05	Q8IAX8	3	11,69	0	Q8IAX8_PLAF7
Sexual stage-specific protein OS=Plasmodium falciparum (isolate 3D7) GN=PFD0310w PE=4 SV=1	5,75	16625,97	588,66	Q6ZMA7	2	26,75	0	Q6ZMA7_PLAF7
L-lactate dehydrogenase OS=Plasmodium falciparum (isolate 3D7) GN=PfLDH PE=1 SV=1	7,34	34335,94	552,86	Q76NM3	2	11,08	0	Q76NM3_PLAF7
Hypoxanthine phosphoribosyltransferase OS=Plasmodium falciparum (isolate 3D7) GN=PF10_0121 PE=4 SV=1	7,61	26761,71	490,20	Q8IJS1	2	6,93	0	Q8IJS1_PLAF7
Uncharacterized protein OS=Plasmodium falciparum (isolate 3D7) GN=PFD0080c PE=4 SV=1	8,70	60726,45	223,51	Q8I207	2	3,39	0	Q8I207_PLAF7
60S ribosomal protein L4, putative OS=Plasmodium falciparum (isolate	10,9 3	46553,67	445,81	Q8I431	4	16,79	0	Q8I431_PLAF7

description	IEP	mw	max score	accession	reported peptides	sequence coverage	FDR level	entry
3D7) GN=PFE0350c PE=1 SV=1								
V-type H(+)-translocating pyrophosphatase, putative OS=Plasmodium falciparum (isolate 3D7) GN=PF14_0541 PE=3 SV=1	6,11	77272,06	582,43	Q8IKR1	3	5,44	0	Q8IKR1_PLAF7
Actin-1 OS=Plasmodium falciparum (isolate 3D7) GN=PFL2215w PE=3 SV=1	5,04	42098,84	267,54	Q8I4X0	2	5,59	0	ACT1_PLAF7
Trypsin OS=Sus scrofa PE=1 SV=1	6,91	25093,83	7391,11	P00761	4	25,11	0	TRYP_PIG
Igh protein OS=Mus musculus GN=Igh PE=2 SV=1	7,80	52717,41	17196,18	I6L985	11	34,33	0	I6L985_MOUSE
Anti-acid phosphatase variable light chain 11 (Fragment) OS=Mus musculus PE=2 SV=1	8,22	12570,14	12885,44	A2MY50	5	50,88	0	A2MY50_MOUSE
Igk protein OS=Mus musculus GN=Igk PE=2 SV=1	5,88	25986,72	32931,50	I6L958	7	32,48	0	I6L958_MOUSE
Ig kappa chain V-III region PC 7043 OS=Mus musculus PE=1 SV=1	4,25	12116,27	21006,64	P01665	3	53,15	0	KV3AD_MOUSE
Igk protein OS=Mus musculus GN=Igkv3-7 PE=1 SV=1	5,22	26602,41	30849,71	Q66JS7	7	30,67	0	Q66JS7_MOUSE
Igh protein OS=Mus musculus GN=Ighg2c PE=2 SV=1	7,43	52906,66	310,96	Q58E56	5	10,48	0	Q58E56_MOUSE
Igk protein OS=Mus musculus GN=Igk PE=1 SV=1	7,58	26101,95	31020,17	I6L978	8	51,71	0	I6L978_MOUSE
Anti-colorectal carcinoma light chain OS=Mus musculus GN=Gm16939 PE=1 SV=1	6,93	26796,95	31193,57	Q7TS98	8	40,25	0	Q7TS98_MOUSE
Ig gamma-2A chain C region, A allele OS=Mus musculus GN=Ighg	7,14	36959,78	2834,80	P01863	8	33,33	0	GCAA_MOUSE
Igh protein OS=Mus musculus GN=Ighg1 PE=1 SV=1	6,62	51692,03	16112,89	Q99LC4	12	36,72	0	Q99LC4_MOUSE
Ighg protein OS=Mus musculus GN=Ighg PE=1 SV=1	7,58	52744,52	1244,43	Q91Z05	9	30,87	0	Q91Z05_MOUSE
Igh protein OS=Mus musculus GN=Igh PE=1 SV=1	7,65	52983,76	2155,92	Q6PJA7	10	33,69	0	Q6PJA7_MOUSE
Ig kappa chain V-V region MOPC 41 OS=Mus musculus GN=Gm5571 PE=1 SV=1	5,13	14482,21	6464,95	P01639	2	27,69	0	KV5A7_MOUSE
LOC207685 protein (Fragment) OS=Mus musculus GN=Iglv2 PE=2 SV=1	5,92	25217,14	3960,36	A4FU62	5	30,04	0	A4FU62_MOUSE
ENSMUSG00000076577 protein OS=Mus musculus GN=Igkv8-30 PE=1 SV=1	5,89	26950,93	30370,08	Q52L64	8	35,42	0	Q52L64_MOUSE
Igh protein OS=Mus musculus GN=Igh-1a PE=1 SV=1	8,20	51837,75	2135,51	Q6PF95	8	32,54	0	Q6PF95_MOUSE
Igk protein OS=Mus musculus GN=Igkv1-133 PE=2 SV=1	7,12	26586,82	30978,58	Q58EU8	8	57,74	0	Q58EU8_MOUSE
Keratin, type I cytoskeletal 9 (Cytokeratin-9) (CK-9) (Keratin-9) (K9)	5,01	62357,66	17209,93	P35527	28	63,08	0	K1C9_HUMAN
Keratin, type II cytoskeletal 1 OS=Homo sapiens GN=KRT1 PE=1 SV=6	8,27	66209,90	10582,58	P04264	22	48,14	0	K2C1_HUMAN
Keratin, type I cytoskeletal 10 (Cytokeratin-10) (CK-10) (Keratin-10) (K10)	4,96	59738,86	10065,20	P13645	22	48,74	0	K1C10_HUMAN
Keratin, type II cytoskeletal 2 epidermal OS=Homo sapiens GN=KRT2 PE=1 SV=2	8,05	65718,10	7721,56	P35908	30	74,02	0	K22E_HUMAN
Hemoglobin subunit beta OS=Homo sapiens GN=HBB PE=1 SV=2	6,88	16112,48	14267,40	P68871	9	85,03	0	HBB_HUMAN
Hemoglobin subunit alpha OS=Homo sapiens GN=HBA1 PE=1 SV=2	9,18	15314,60	7529,77	P69905	5	72,54	0	HBA_HUMAN

description	IEP	mw	max score	accession	reported peptides	sequence coverage	FDR level	entry
Keratin, type I cytoskeletal 14 (Cytokeratin-14) (CK-14) (Keratin-14) (K14)	4,90	51906,76	2565,06	P02533	12	41,95	0	K1C14_HUMAN
Dynein heavy chain 1, axonemal OS=Homo sapiens GN=DNAH1 PE=2 SV=4	5,55	498002,79	403,36	Q9P2D7	2	1,11	0	DYH1_HUMAN
Band 3 anion transport protein OS=Homo sapiens GN=SLC4A1 PE=1 SV=3	4,90	102077,65	703,02	P02730	7	10,10	0	B3AT_HUMAN
Keratin, type II cytoskeletal 5 OS=Homo sapiens GN=KRT5 PE=1 SV=3	7,79	62606,56	2615,35	P13647	19	47,97	0	K2C5_HUMAN
Keratin, type II cytoskeletal 6A OS=Homo sapiens GN=KRT6A PE=1 SV=3	8,05	60330,16	4060,25	P02538	16	45,74	0	K2C6A_HUMAN
Keratin, type II cytoskeletal 71 OS=Homo sapiens GN=KRT71 PE=1 SV=3	6,23	57804,87	320,06	Q3SY84	4	7,07	0	K2C71_HUMAN
Serum albumin OS=Homo sapiens GN=ALB PE=1 SV=2	5,86	71362,71	323,62	P02768	4	7,55	0	ALBU_HUMAN
Ig kappa chain V-l region Lay OS=Homo sapiens PE=1 SV=1	8,20	11948,22	1904,87	P01605	2	25,00	0	KV113_HUMAN
Dermcidin OS=Homo sapiens GN=DCD PE=1 SV=2	6,11	11397,93	1520,60	P81605	4	47,27	0	DCD_HUMAN
Actin, cytoplasmic 1 OS=Homo sapiens GN=ACTB PE=1 SV=1	5,14	42079,02	575,82	P60709	4	12,80	0	ACTB_HUMAN
Keratin, type II cytoskeletal 1b OS=Homo sapiens GN=KRT77	5,63	62186,65	2013,68	Q7Z794	7	21,88	0	K2C1B_HUMAN
Keratin, type I cytoskeletal 17 (Cytokeratin-17) (CK-17) (Keratin-17) (K17) (39.1)	4,78	48390,88	1651,75	Q04695	7	19,21	0	K1C17_HUMAN
Hemoglobin subunit delta OS=Homo sapiens GN=HBD PE=1 SV=2	8,24	16169,56	5825,90	P02042	8	70,75	0	HBD_HUMAN
Desmoglein-1 OS=Homo sapiens GN=DSG1 PE=1 SV=2	4,72	114774,31	358,86	Q02413	3	4,58	0	DSG1_HUMAN
Keratin, type II cytoskeletal 6B OS=Homo sapiens GN=KRT6B PE=1 SV=5	8,05	60352,17	4571,21	P04259	18	49,11	0	K2C6B_HUMAN
Cystatin-A OS=Homo sapiens GN=CSTA PE=1 SV=1	5,21	11006,51	2088,64	P01040	3	68,37	0	CYTA_HUMAN
Keratin, type I cytoskeletal 27 OS=Homo sapiens GN=KRT27 PE=1 SV=2	4,79	50449,71	1433,54	Q7Z3Y8	3	11,33	0	K1C27_HUMAN
Ubiquitin-60S ribosomal protein L40 OS=Homo sapiens GN=UBA52 PE=1 SV=2	10,26	15013,47	422,03	P62987	2	30,47	0	RL40_HUMAN
Heat shock cognate 71 kDa protein OS=Homo sapiens GN=HSPA8 PE=1 SV=1	5,20	71126,31	349,98	P11142	2	5,42	0	HSP7C_HUMAN
Keratin, type I cytoskeletal 16 (Cytokeratin-16) (CK-16) (Keratin-16) (K16)	4,79	51610,07	1313,47	P08779	8	27,27	0	K1C16_HUMAN
Keratin, type II cytoskeletal 8 OS=Homo sapiens GN=KRT8 PE=1 SV=7	5,34	53704,36	694,66	P05787	4	9,32	0	K2C8_HUMAN
Keratin, type II cytoskeletal 4 OS=Homo sapiens GN=KRT4 PE=1 SV=4	6,22	57684,52	1456,28	P19013	5	13,67	0	K2C4_HUMAN
Keratin, type I cytoskeletal 25 OS=Homo sapiens GN=KRT25 PE=1 SV=1	4,81	49888,27	1433,54	Q7Z3Z0	3	8,00	0	K1C25_HUMAN
Keratin, type II cytoskeletal 3 OS=Homo sapiens GN=KRT3 PE=1 SV=3	6,07	64588,18	844,22	P12035	7	16,08	0	K2C3_HUMAN
Serum albumin OS=Bos taurus GN=ALB PE=1 SV=4	5,76	71289,43	1461,07	P02769	17	32,45	0	ALBU_BOVIN

description	IEP	mw	max score	accession	reported peptides	sequence coverage	FDR level	entry
Enolase 1 OS=Saccharomyces cerevisiae GN=ENO1 PE=1 SV=2	6,15	46859,19	26980,25	P00924	23	79,18	0	ENO1_YEAST
Enolase 2 OS=Saccharomyces cerevisiae GN=ENO2 PE=1 SV=2	5,59	46971,28	19916,72	P00925	14	68,65	0	ENO2_YEAST
Uncharacterized protein OS=Plasmodium falciparum (isolate 3D7) GN=PFL1300c PE=4 SV=1	9,40	57789,66	203,80	Q8I5E9	2	4,04	0	Q8I5E9_PLAF7
Probable cathepsin C OS=Plasmodium falciparum (isolate 3D7) GN=PF11_0174 PE=1 SV=1	5,76	81381,49	190,14	Q8IIJ9	2	5,57	0	CATC_PLAF7

Column descriptions

Column Title Description

- A description Protein description as parsed from source database
- B IEP Calculated isoelectric point
- C mw Calculated molecular weight (Da)
- D max score Maximum identification score provided by PLGS database searching
- E accession Database accession number (as parsed from source database)
- F reported peptides Number of peptides after ISOQuant processing
- G sequence coverage Sequence coverage as calculated for reported peptides (column F)
- H FDR level Estimated FDR level
- I entry Protein entry as parsed from source database
- J species Source species of each protein
- K-V Calculated quantification value (fmol on colum) for each technical replicate run
- W-Z AVERAGE Averaged values intensity over technical replicates for each sample

